
Minimum Detectable Concentrations with Typical Radiation Survey Instruments for Various Contaminants and Field Conditions

Draft Report for Comment

U.S. Nuclear Regulatory Commission

Office of Nuclear Regulatory Research

A. M. Huffert/NRC
E. W. Abelquist/ORISE
W. S. Brown/BNL



9509200367 950831
PDR NUREG
1507 R PDR

AVAILABILITY NOTICE

Availability of Reference Materials Cited in NRC Publications

Most documents cited in NRC publications will be available from one of the following sources:

1. The NRC Public Document Room, 2120 L Street, NW., Lower Level, Washington, DC 20555-0001
2. The Superintendent of Documents, U.S. Government Printing Office, P. O. Box 37082, Washington, DC 20402-9328
3. The National Technical Information Service, Springfield, VA 22161-0002

Although the listing that follows represents the majority of documents cited in NRC publications, it is not intended to be exhaustive.

Referenced documents available for inspection and copying for a fee from the NRC Public Document Room include NRC correspondence and internal NRC memoranda; NRC bulletins, circulars, information notices, inspection and investigation notices; licensee event reports; vendor reports and correspondence; Commission papers; and applicant and licensee documents and correspondence.

The following documents in the NUREG series are available for purchase from the Government Printing Office: formal NRC staff and contractor reports, NRC-sponsored conference proceedings, international agreement reports, grantee reports, and NRC booklets and brochures. Also available are regulatory guides, NRC regulations in the *Code of Federal Regulations*, and *Nuclear Regulatory Commission Issuances*.

Documents available from the National Technical Information Service include NUREG-series reports and technical reports prepared by other Federal agencies and reports prepared by the Atomic Energy Commission, forerunner agency to the Nuclear Regulatory Commission.

Documents available from public and special technical libraries include all open literature items, such as books, journal articles, and transactions. *Federal Register* notices, Federal and State legislation, and congressional reports can usually be obtained from these libraries.

Documents such as theses, dissertations, foreign reports and translations, and non-NRC conference proceedings are available for purchase from the organization sponsoring the publication cited.

Single copies of NRC draft reports are available free, to the extent of supply, upon written request to the Office of Administration, Distribution and Mail Services Section, U.S. Nuclear Regulatory Commission, Washington DC 20555-0001.

Copies of industry codes and standards used in a substantive manner in the NRC regulatory process are maintained at the NRC Library, Two White Flint North, 11545 Rockville Pike, Rockville, MD 20852-2738, for use by the public. Codes and standards are usually copyrighted and may be purchased from the originating organization or, if they are American National Standards, from the American National Standards Institute, 1430 Broadway, New York, NY 10018-3308.

Minimum Detectable Concentrations with Typical Radiation Survey Instruments for Various Contaminants and Field Conditions

Draft Report for Comment

Manuscript Completed: July 1995
Date Published: August 1995

A. M. Huffert, E. W. Abelquist¹, W. S. Brown²

Division of Regulatory Applications
Office of Nuclear Regulatory Research
U.S. Nuclear Regulatory Commission
Washington, DC 20555-0001



¹Environmental Survey and Site Assessment Program, Energy/Environment System Division, Oak Ridge Institute for Science and Education, Oak Ridge, TN 37831-0117

²Human Factors and Performance Analysis Group, Brookhaven National Laboratory, Upton, NY 11973-5000

1 **ABSTRACT**

2 This report describes and quantitatively evaluates the effects of various factors on the detection
3 sensitivity of commercially available portable field instruments being used to conduct radiological
4 surveys in support of decommissioning. The U.S. Nuclear Regulatory Commission (NRC) is
5 currently involved in a rulemaking effort to establish residual contamination criteria for release of
6 facilities for restricted or unrestricted use. In support of that rulemaking, the Commission has
7 prepared a draft Generic Environmental Impact Statement (GEIS), consistent with the National
8 Environmental Policy Act (NEPA). The effects of this new rulemaking on the overall cost of
9 decommissioning are among the many factors considered in the GEIS. The overall cost includes
10 the costs of decontamination, waste disposal, and radiological surveys to demonstrate compliance
11 with the applicable guidelines. An important factor affecting the costs of such radiological
12 surveys is the minimum detectable concentrations (MDCs) of field survey instruments in relation
13 to the residual contamination guidelines. The purpose of this study was two-fold. First, the data
14 were used to determine the validity of the theoretical MDCs used in the NRC draft GEIS.
15 Second, the results of the study, published herein, provide guidance to licensees for (a) selection
16 and proper use of portable survey instruments and (b) understanding the field conditions and the
17 extent to which the capabilities of those instruments can be limited. The types of instruments
18 commonly used in field radiological surveys were evaluated, such as gas proportional, Geiger-
19 Mueller (GM), zinc sulfide (ZnS), and sodium iodide (NaI) detectors.

1 **CONTENTS**

2		<u>Page</u>
3	ABSTRACT	iii
4	ABBREVIATIONS	xi
5	ACKNOWLEDGMENTS	xii
6	FOREWORD	xiii
7	1 INTRODUCTION	1-1
8	1.1 Background	1-1
9	1.2 Need for This Report	1-1
10	1.3 Scope	1-2
11	1.4 Methodology	1-2
12	2 INSTRUMENTATION	2-1
13	2.1 Gas Proportional Detectors	2-1
14	2.2 Geiger-Mueller Detectors	2-1
15	2.3 Zinc Sulfide Scintillation Detectors	2-1
16	2.4 Sodium Iodide Scintillation Detectors	2-2
17	2.5 Ratemeters-Scalers	2-2
18	2.6 Pressurized Ionization Chamber	2-2
19	2.7 Portable Gamma Spectrometer	2-2
20	2.8 Laboratory Instrumentation	2-2
21	3 STATISTICAL INTERPRETATIONS OF MINIMUM DETECTABLE	
22	CONCENTRATIONS	3-1
23	3.1 MDC Fundamental Concepts	3-1
24	3.2 Review of MDC Expressions	3-6
25	4 VARIABLES AFFECTING INSTRUMENT MINIMUM DETECTABLE	
26	CONCENTRATIONS	4-1
27	4.1 Radionuclide Sources for Calibration	4-2
28	4.2 Source-to-Detector Distance	4-3
29	4.3 Window Density Thickness	4-4
30	4.4 Source Geometry Factors	4-5
31	4.5 Ambient Background Count Rate	4-6
32	5 VARIABLES AFFECTING MINIMUM DETECTABLE CONCENTRATIONS	
33	IN THE FIELD	5-1
34	5.1 Background Count Rates for Various Materials	5-1
35	5.2 Effects of Surface Condition on Detection Sensitivity	5-2
36	5.2.1 Surface Preparation	5-3
37	5.2.2 Measurement Results for Various Surface Types	5-3

Contents

	<u>Page</u>
1	
2	
3	5.3 Attenuation Effects of Overlaying Material 5-5
4	5.3.1 Methodology 5-6
5	5.3.2 Measurement of Various Surface Coatings 5-7
6	
7	6 HUMAN PERFORMANCE AND SCANNING SENSITIVITY 6-1
8	6.1 Review of Scanning Sensitivity Expressions and Results 6-1
9	6.2 Scanning as a Signal Detection Problem 6-2
10	6.3 Influences on Surveyor Performance 6-3
11	6.4 Ideal Observer and Real Performance 6-4
12	6.4.1 The Ideal Poisson Observer 6-5
13	6.4.2 Actual Observer Performance 6-7
14	6.5 Actual Surveyor Performance—Field Tests 6-7
15	6.5.1 General Method 6-8
16	6.5.2 Indoor Scan Using GM Detector 6-9
17	6.5.3 Indoor Scan Using Gas Proportional Detector 6-10
18	6.5.4 Outdoor Scan Using NaI Scintillation Detector 6-11
19	6.5.5 General Discussion 6-11
20	
21	7 <i>IN SITU</i> GAMMA SPECTROMETRY AND EXPOSURE RATE MEASUREMENTS . . . 7-1
22	7.1 <i>In Situ</i> Gamma Spectrometry Measurements in Outdoor Test Area 7-1
23	7.2 Exposure Rate Measurements in Outdoor Test Area 7-4
24	8 LABORATORY INSTRUMENTATION DETECTION LIMITS 8-1
25	8.1 Review of Analytical Minimum Detectable Concentrations 8-1
26	8.2 Background Activities for Various Soil Types 8-1
27	8.3 Effects of Soil Condition on MDC 8-2
28	8.3.1 Effects of Soil Moisture on MDC 8-3
29	8.3.2 Effects of Soil Density on MDC 8-4
30	8.3.2 Effects of High-Z Materials on MDC 8-4
31	9 REFERENCES 9-1
32	TABLES
33	3.1 MDC Results for Data Obtained From Gas Proportional Detector Using
34	Various MDC Expressions 3-7
35	4.1 Characteristics of Radionuclide Sources Used for Calibration and
36	Measurements 4-7
37	4.2 Average Total Efficiencies for Various Detectors and Radionuclides 4-8
38	4.3 Minimum Detectable Concentrations for Various Detectors and Radionuclides 4-9
39	4.4 Source-to-Detector Distance Effects for β Emitters 4-10
40	4.5 Source-to-Detector Distance Effects for α Emitters 4-10
41	4.6 Minimum Detectable Concentrations for Various Source-to-Detector Distances
42	for β Emitters 4-11

1	TABLES (Continued)		Page
2			<u>Page</u>
3	4.7	Minimum Detectable Concentrations for Various Source-to-Detector Distances	
4		for α Emitters	4-12
5	4.8	Window Density Thickness Effects for β Emitters	4-13
6	4.9	Minimum Detectable Concentrations for Various Window Density Thicknesses	4-14
7	4.10	Source Geometry Effects on Instrument Efficiency	4-15
8	4.11	Ambient Background Effects	4-16
9	5.1	Background Count Rate for Various Materials	5-9
10	5.2	Minimum Detectable Concentrations for Various Materials	5-10
11	5.3	Surface Material Effects on Source Efficiency for Tc-99 Distributed on	
12		Various Surfaces	5-11
13	5.4	Surface Material Effects for Th-230 Distributed on Various Surfaces	5-12
14	5.5	Surface Material Effects on MDC for Tc-99 and Th-230 Distributed	
15		Various Surfaces	5-13
16	5.6	Effects of Oil Density Thickness on Source Efficiency and MDC	
17		(Gas Proportional— $\alpha + \beta$)	5-14
18	5.7	Effects of Paint Density Thickness on Source Efficiency and MDC	
19		(Gas Proportional— $\alpha + \beta$)	5-15
20	5.8	Effects of Paint Density Thickness on Source Efficiency and MDC	
21		(Gas Proportional— α -Only)	5-16
22	5.9	Effects of Paint Density Thickness on Source Efficiency and MDC	
23		(Gas Proportional— β -Only)	5-17
24	5.10	Effects of Paint Density Thickness on Source Efficiency and MDC	
25		(GM Detector)	5-18
26	5.11	Effects of Paint Density Thickness on Source Efficiency and MDC	
27		(ZnS Scintillation Detector)	5-19
28	5.12	Effects of Dust Density Thickness on Source Efficiency and MDC	
29		(Gas Proportional— $\alpha + \beta$)	5-20
30	5.13	Effects of Dust Density Thickness on Source Efficiency and MDC	
31		(Gas Proportional— α Only)	5-21
32	5.14	Effects of Dust Density Thickness on Source Efficiency and MDC	
33		(Gas Proportional— β Only)	5-22
34	5.15	Effects of Dust Density Thickness on Source Efficiency and MDC	
35		(GM Detector)	5-23
36	5.16	Effects of Dust Density Thickness on MDC for Various Sources	
37		(ZnS Scintillation Detector)	5--24
38	5.17	Effects of Water Density Thickness on Source Efficiency and MDC	
39		(Gas Proportional— $\alpha + \beta / C-14$	5-25
40	5.18	Effects of Water Density Thickness on Source Efficiency and MDC	
41		(Gas Proportional— $\alpha + \beta / Tc-99$)	5-26
42	5.19	Effects of Water Density Thickness on Source Efficiency and MDC	
43		(Gas Proportional— $\alpha + \beta / SrY-90$)	5-27
44	5.20	Effects of Water Density Thickness on Source Efficiency and MDC	
45		(Gas Proportional— α -Only)	5-28

Contents

1	TABLES (Continued)		
2			<u>Page</u>
3	5.21	Effects of Water Density Thickness on Source Efficiency and MDC	
4		(Gas Proportional— β -Only/C-14)	5-29
5	5.22:	Effects of Water Density Thickness on Source Efficiency and MDC	
6		(Gas Proportional— β -Only/Tc-99)	5-30
7	5.23	Effects of Water Density Thickness on Source Efficiency and MDC	
8		(Gas Proportional— β -Only/SrY-90)	5-31
9	5.24	Effects of Water Density Thickness on Source Efficiency and MDC	
10		(GM Detector/C-14)	5-32
11	5.25	Effects of Water Density Thickness on Source Efficiency and MDC	
12		(GM Detector/Tc-99)	5-33
13	5.26	Effects of Water Density Thickness on Source Efficiency and MDC	
14		(GM Detector/SrY-90)	5-34
15	5.27	Effects of Water Density Thickness on Source Efficiency and MDC	
16		(ZnS Scintillation Detector)	5-35
17	6.1	Cumulative Poisson Probabilities of Observed Values for Selected Average	
18		Numbers of Counts per Interval	6-6
19	6.2	Scanning Sensitivity of the Ideal Poisson Observer for Various Background Levels . .	6-6
20	7.1	<i>In Situ</i> Gamma Spectrometry Data From Outdoor Test Area	7-3
21	7.2	Exposure Rate Measurements From Outdoor Test Area	7-7
22	8.1	Typical Radionuclide Concentrations Found in Background Soil Samples	
23		in the United States	8-2
24	8.2	Effects of Moisture Content on Gamma Spectrometry Analyses	8-5
25	FIGURES		
26	3.1	Critical Level, L_C	3-8
27	3.2	Detection Limit, L_D	3-8
28	4.1	MDCs for Gas Proportional Detector ($\alpha+\beta$ Mode) for Various Radionuclides	4-17
29	4.2	MDCs for GM Detector for Various Radionuclides	4-18
30	4.3	Source-to-Detector Distance Effects on MDC for Higher Energy β Emitters	4-19
31	4.4	Source-to-Detector Distance Effects on MDC for Lower Energy β Emitters	4-20
32	4.5	Source-to-Detector Distance Effects on MDC for α Emitters	4-21
33	4.6	Effects of Window Density Thickness on Total Efficiency for Higher Energy β	
34		Emitters	4-22
35	4.7	Effects of Window Density Thickness on Total Efficiency for Lower Energy β	
36		Emitters	4-23
37	4.8	Effects of Window Density Thickness on MCD for Higher Energy β Emitters	4-24
38	4.9	Effects of Window Density Thickness on MCD for Lower Energy β Emitters	4-25
39	4.10	Effects of Ambient Background on MCD Calculation	4-26
40	5.1	Effect of Surface Material on Gas Proportional Detector (α -Only) MDC	5-36
41	5.2	Effect of Surface Material on Gas Proportional Detector (β -Only) MDC	5-37
42	5.3	Effects of Oil Density Thickness on Source Efficiency for Various Sources	5-38
43	5.4	Effects of Oil Density Thickness on MDC for Various Sources	5-39

1	FIGURES (Continued)	
2		<u>Page</u>
3	5.5 Effects of Paint Density Thickness on Source Efficiency for Various Sources	
4	Using the Gas Proportional Detector in $\alpha+\beta$ and α -Only Modes	5-40
5	5.6 Effects of Paint Density Thickness on MDC for Various Sources	
6	Using the Gas Proportional Detector in $\alpha+\beta$ and α -Only Modes	5-41
7	5.7 Effects of Paint Density Thickness on Source Efficiency for	
8	Various Sources using the Gas Proportional Detector in β Only Mode	5-42
9	5.8 Effects of Paint Density Thickness on MDC for Various Sources	
10	Using the Gas Proportional Detector in β -Only Mode	5-43
11	5.9 Effects of Paint Density Thickness on Source Efficiency for	
12	Various Sources Using the GM Detector	5-44
13	5.10 Effects of Paint Density Thickness on MDC for Various Sources	
14	Using the GM Detector	5-45
15	5.11 Effects of Paint Density Thickness on Source Efficiency for	
16	Alpha Sources Using the ZnS Scintillation Detector	5-46
17	5.12 Effects of Paint Density Thickness on MDC for Alpha Sources	
18	Using the ZnS Scintillation Detector	5-47
19	5.13 Effects of Dust Density Thickness on Source Efficiency for Various Sources	
20	using the Gas Proportional Detector in $\alpha+\beta$ and α -Only Modes	5-48
21	5.14 Effects of Dust Density Thickness on MDC for Various Sources	
22	Using the Gas Proportional Detector in $\alpha+\beta$ and α -Only Modes	5-49
23	5.15 Effects of Dust Density Thickness on Source Efficiency for	
24	Various Sources Using the Gas Proportional Detector in β -Only Mode	5-50
25	5.16 Effects of Dust Density Thickness on MDC for Various Sources Using	
26	the Gas Proportional Detector in β -Only Mode	5-51
27	5.17 Effects of Dust Density Thickness on Source Efficiency for	
28	Various Sources Using the GM Detector	5-52
29	5.18 Effects of Dust Density Thickness on MDC for Various Sources	
30	Using the GM Detector	5-53
31	5.19 Effects of Dust Density Thickness on Source Efficiency for an Alpha	
32	Source Using the ZnS Scintillation Detector	5-54
33	5.20 Effects of Dust Density Thickness on MDC for an Alpha Source Using	
34	the ZnS Scintillation Detector	5-55
35	5.21 Effects of Water Density Thickness on Source Efficiency for	
36	Various Sources Using the Gas Proportional Detector in $\alpha+\beta$ and α -Only Modes . .	5-56
37	5.22 Effects of Water Density Thickness on MDC for Various Sources	
38	Using the Gas Proportional Detector in $\alpha+\beta$ and α -Only Modes	5-57
39	5.23 Effects of Water Density Thickness on Source Efficiency for	
40	Various Sources Using the Gas Proportional Detector in β -Only Mode	5-58
41	5.24 Effects of Water Density Thickness on MDC for Various Sources	
42	Using the Gas Proportional Detector in β -Only Mode	5-59
43	5.25 Effects of Water Density Thickness on Source Efficiency for	
44	Various Sources Using the GM Detector	5-60

Contents

1	FIGURES (Continued)	
2		<u>Page</u>
3	5.26 Effects of Water Density Thickness on MDC for Various Sources	
4	Using the GM Detector	5-61
5	5.27 Effects of Water Density Thickness on Source Efficiency for	
6	Alpha Sources Using the ZnS Scintillation Detector	5-62
7	5.28 Effects of Water Density Thickness on MDC for Alpha Sources	
8	Using the ZnS Scintillation Detector	5-63
9	5.29 Overall Effects of Paint, Dust, and Water Density Thickness on	
10	Total Efficiency for Various Sources Using the Gas Proportional	
11	Detector in β -Only Mode	5-64
12	5.30 Overall Effects of Paint, Dust, and Water Density Thickness on	
13	Source Efficiency for Various Sources Using the Gas Proportional	
14	in β -Only Mode	5-65
15	6.1 A Signal Detection Theory View of the Detection of Signals in Noise	6-13
16	6.2 Scan Survey as a Series of Stages	6-14
17	6.3 Related Operating Characteristic (ROC) for Poisson Observer Detecting	
18	180 cpm in a 60-cpm Background	6-15
19	6.4 Instructions Provided to Field Survey Test Participants for Indoor GM Scans	6-16
20	6.5 Instructions Provided to Field Survey Test Participants for Outdoor NaI Scans	6-17
21	6.7 Scale Map of the Wall Showing Location, Extent, and Radiation Levels of Hidden	
22	Sources for Gas Proportional Scans	6-18
23	6.8 Scale Map of the Outdoor Scan Test Area Showing Location, Extent, and	
24	Radiation Levels of Hidden Sources for NaI Scans	6-19
25	6.9 Surveyor Performance in Indoor Scan Survey Using GM Detector	6-20
26	6.10 Surveyor Performance in Indoor Scan Survey Using Gas Proportional Detector	6-21
27	6.11 Surveyor Performance in Outdoor Scan Survey Using NaI Scintillation Detector	6-22
28	7.1 Co-60 <i>In Situ</i> Gamma Spectrometry Results in Outdoor Test Area	7-2
29	7.2 Exposure Rate Measurements in the Outdoor Test Area	7-6
30	8.1 Efficiency vs. Energy for Various Densities	8-6

1 ABBREVIATIONS

2	ANL	Argonne National Laboratory
3	ANSI	American National Standards Institute, Inc.
4	BNL	Brookhaven National Laboratory
5	CRT	cathode ray tube
6	dpm	disintegrations per minute
7	EML	Environmental Measurements Laboratory (U.S. Dept. of Energy)
8	EPA	Environmental Protection Agency
9	ESSAP	Environmental Survey and Site Assessment Program
10	GEIS	Generic Environmental Impact Statement
11	GM	Geiger-Mueller
12	MDC	minimum detectable concentration
13	NaI	sodium iodide
14	NCRP	National Council on Radiation Protection and Measurements
15	NEPA	National Environmental Policy Act
16	NIST	National Institute of Standards and Technology
17	NRC	Nuclear Regulatory Commission
18	ORISE	Oak Ridge Institute for Science and Education
19	ORNL	Oak Ridge National Laboratory
20	PNL	Pacific Northwest Laboratory
21	PIC	pressurized ionization chamber
22	ROC	relative operating characteristic
23	TEDE	total effective dose equivalent
24	ZnS	zinc sulfide

1 **ACKNOWLEDGEMENTS**

2 This report was a collaborative effort by the staff of the Environmental Survey and Site
3 Assessment Program (ESSAP) of the Oak Ridge Institute for Science and Education, Brookhaven
4 National Laboratory, and the Nuclear Regulatory Commission. In addition to writing certain
5 sections, Eric Abelquist, working closely with Tony Huffert of the NRC, was responsible for the
6 overall planning and management of this project. Dr. William Brown, Brookhaven National
7 Laboratory, provided input on the human factors associated with scanning and wrote the bulk of
8 Section 6. Many of the detection sensitivity experiments conducted in this report were designed
9 and performed by Elmer Bjelland and Lea Mashburn, while Jim Payne and Scott Potter performed
10 many measurements during development of the feasibility study. Other technical contributors
11 included Wade Adams, Armin Ansari, William L. (Jack) Beck, Dale Condra, Ann Payne, and Tim
12 Vitkus. Elaine Waters, Robyn Ellis, Tabatha Fox, and Debbie Adams provided much of the word
13 processing support, while Teresa Bright and Dean Herrera produced all of the graphics.

14 Special thanks to Jim Berger, George Chabot, Ken Swinth, and Ed Walker who performed
15 valuable reviews of the report and provided thoughtful comments, and to all the computer
16 simulation and field survey test participants.

1 **FOREWORD**

2 The NRC is amending its regulations to establish residual radioactivity criteria for decommissioning of licensed nuclear
3 facilities. As part of this initiative, the NRC staff has prepared a draft Generic Environmental Impact Statement (GEIS),
4 consistent with the National Environmental Policy Act (NEPA). The effects of this new rulemaking on the overall cost of
5 decommissioning are among the many factors considered in the GEIS. The overall cost includes the costs of
6 decontamination, waste disposal, and radiological surveys to demonstrate compliance with the applicable guidelines.

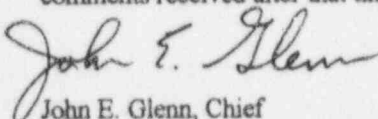
7 An important factor affecting the costs of such radiological surveys is the minimum detectable concentration (MDC) of
8 field survey instruments in relation to the residual contamination guidelines. This study was intended to provide
9 guidance to licensees for (a) selection and proper use of portable survey instruments and (b) understanding the field
10 conditions and the extent to which the capabilities of those instruments can be limited. The types of instruments
11 commonly used in field radiological surveys that were evaluated included, in part, gas proportional, Geiger-Mueller
12 (GM), zinc sulfide (ZnS), and sodium iodide (NaI) detectors.

13 This draft report describes and quantitatively evaluates the effects of various factors on the detection sensitivity of
14 commercially available portable field instruments being used to conduct radiological surveys in support of decommis-
15 sioning. The results, approaches, and methods described herein are provided for information only. The NRC staff plans
16 to prepare a final report based upon the commitments and suggestions obtained on this staff draft.

17 Written comments should be addressed to: Chief, Rules Review and Directives Branch, Division of Freedom of
18 Information and Publications Services, Office of Administration, U.S. Nuclear Regulatory Commission, Washington,
19 DC 20555-0001. Hand deliver comments to 11545 Rockville Pike, Rockville, Maryland, between 7:15 a.m. and 4:30
20 p.m. on Federal workdays.

21 Comments may be submitted electronically, in either ASCII text or WordPerfect format, by calling the NRC Enhanced
22 Participatory Rulemaking on Radiological Criteria for Decommissioning Electronic Bulletin Board, 1-800-880-6091
23 (see *Federal Register* Vol. 58, No.132, July 13, 1993). The bulletin board may be accessed using a personal computer,
24 a modem, and most commonly available communications software packages. Communication software parameters
25 should be set as follows: parity to none, data bits to 8, and stop bits to 1 (N,8,1). Use ANSI or VT-100 terminal
26 emulation. Background documents on the rulemaking are also available for downloading and viewing on the bulletin
27 board. For more information, contact Ms. Christine Daily, U.S. Nuclear Regulatory Commission, Washington, DC
28 20555-0001; phone (301)415-6026; FAX (301)415-5385.

29 Comments are sought specifically on the application of nonparametric statistics, the Data Quality Objectives process,
30 and the survey process. Comments on this draft report will be most useful if received 60 days from its publication, but
31 comments received after that time will also be considered.



32 John E. Glenn, Chief
33 Radiation Protection and
34 Health Effects Branch
35 Division of Regulatory Applications
36 Office of Nuclear Regulatory Research

1 INTRODUCTION

1.1 Background

Facilities licensed by the U.S. Nuclear Regulatory Commission (NRC) are required to demonstrate that residual radioactivity at their site meets the applicable guidelines before the associated license can be terminated. NRC is currently involved in a rulemaking effort to establish residual contamination criteria for release of facilities for restricted or unrestricted use. In support of that rulemaking, the Commission is preparing a Generic Environmental Impact Statement (GEIS), consistent with the National Environmental Policy Act (NEPA).

The effects of this new rulemaking on the overall cost of decommissioning are among the many factors considered in the GEIS. The overall cost includes the costs of decontamination, waste disposal, and radiological surveys to demonstrate compliance with the applicable guidelines. An important factor affecting the costs of such radiological surveys is the minimum detectable concentration (MDC) of field survey instruments in relation to the residual contamination guidelines. The MDC may apply to either the concentration of radioactivity present on a material surface or within a volume of material. If the guidelines are lower than the MDC of field survey instruments, extensive laboratory analysis would become necessary, significantly increasing the overall cost of decommissioning projects.

1.2 Need for This Report

Currently, comprehensive and well-controlled data on detection sensitivity of field survey instruments, under conditions typically encountered by licensees during decommissioning, are not available. A limited literature search was performed on the detection sensitivity capabilities of portable survey instruments. In general, the MDC information contained in the literature is for optimum capabilities under conditions of low background, smooth clean surfaces, and experienced survey personnel. Additional studies were determined to be necessary to develop comprehensive information, relative to instrument performance, under actual field conditions. Furthermore, many studies do not identify the method by which detector sensitivities were determined or defined (e.g., detection sensitivities may be calculated for various confidence levels, using ratemeter output as opposed to integrated counts or audible signal change), and as such, comparison of detection sensitivities reported in the literature may not be appropriate. A few notable studies that do specify the methodology to determine scanning sensitivities are summarized in Section 6.

The purpose of this study was two-fold. First, the data were used to determine the validity of the theoretical MDCs used in the draft GEIS. Second, the results of the study, published herein, will provide guidance to licensees for selection and proper use of portable survey instruments, and an understanding of the field conditions under which, and the extent to which, the capabilities of those instruments can be limited.

Introduction

1.3 Scope

The major emphasis of this study was the measure of detection sensitivity for field survey instruments. The parameters which were studied, for their effects on the detection sensitivity of field instruments, included variables that determine the instrument MDC (e.g., probe surface area, radionuclide energy, window density thickness, source-to-detector geometry) and variables that can affect the detection sensitivity of the instrument in the field (e.g., various surface types and coatings, including painted, scabbled, or wet surfaces). It was not anticipated that empirical data would be obtained for every possible combination of variables; rather, the emphasis was on establishing the necessary baseline data, so that accurate predictions could be made regarding an instrument's response under a variety of possible field conditions.

The types of instruments commonly used in field radiological surveys that were evaluated in this study included gas proportional, Geiger-Mueller (GM), zinc sulfide (ZnS) scintillation, and sodium iodide (NaI) scintillation detectors. Comparison of field survey instruments by different manufacturers (Ludlum, Eberline, Bicon, etc.) was not the intended purpose of this study. The specific instruments which were used for these measurements are, in general, representative; one notable exception is the pressurized ionization chamber described in Section 2. All instrumentation used in this study is described in Section 2.

The detection sensitivity of a number of commonly used laboratory procedures was also addressed in this study. Because most of the information on laboratory procedures and also on thermoluminescence dosimeters is already available, this information was provided in the form of a literature review. However, it was anticipated that some laboratory measurements would have to be made to address specific objectives of the study.

Finally, this report was not intended to be a complete evaluation of the performance of portable survey instrumentation. Several references are available that provide comprehensive information on the performance of health physics instrumentation. One such study involves the evaluation of ionization chambers, GM detectors, alpha survey meters, and neutron dose equivalent survey meters according to the draft ANSI standard N42.17 (Swinth & Kenoyer). These instruments were subjected to a broad array of testing, including general characteristics, electronic and mechanical requirements, radiation response, interfering responses, and environmental factors. An important result of the cited study was highlighting the susceptibility of air and gas-flow proportional counters to environmental factors such as humidity, elevations, and temperature. The study also concluded that the alpha scintillation detector is relatively stable under variable environmental conditions. Another study summarized the regulatory requirements and practices of NRC licensees regarding the use of accredited calibration laboratories. That report concluded that more definitive guidance was needed to describe how to perform and document calibration to demonstrate compliance with the regulatory requirements (NUREG/CR-6062).

1.4 Methodology

During radiological surveys in support of decommissioning, field instruments are generally used to scan the surface areas for elevated direct radiation, and to make direct measurements of total surface activity at a particular location. Although the surface scans and direct measurements can

1 be performed with the same instruments, the two procedures have very different MDCs.
2 Scanning can have a much higher MDC than a static count, depending on scanning speed,
3 distance of the probe to the surface, and other instrument factors. The scanning MDC is also
4 affected by the "human factor," described in Section 6. Therefore, when applicable, the MDC of
5 each instrument was determined for both the scanning and static modes of operation.

6 There are several statistical interpretations of the MDC concept that can result in different MDC
7 values for an instrument, using the same set of data. The specific approach for statistical
8 interpretation of the data, in this study, was selected after a thorough review of the relevant
9 literature. A sensitivity study, evaluating the quantitative effects of various statistical treatments
10 on the MDC, was also performed (Section 3).

11 Studies were performed primarily at Oak Ridge Institute for Science and Education (ORISE)
12 facilities in Oak Ridge, Tennessee. A measurement hood, constructed of Plexiglas, provided a
13 controlled environment in which to obtain measurements with minimal disturbances from ambient
14 airflow. The Plexiglas measurement hood measured 93 cm in length, 60 cm in height, and 47 cm
15 in depth, and was equipped with a barometer and thermometer to measure ambient pressure and
16 temperature within the chamber. Measurements were performed within the measurement hood
17 using a detector-source jig to ensure that the detector-to-source geometry was reproducible for
18 all parameters studied. Various field conditions were simulated, under well-controlled and
19 reproducible conditions. Special sources were constructed and characterized in ESSAP
20 laboratories to meet specific objectives of this study. On the basis of the empirical results
21 obtained from these studies, sets of normalized curves were constructed which would indicate
22 instrument response as a function of source energy, geometry, background radiation level, and
23 other parameters.

24 The quantitative data were treated and reported in accordance with Environmental Protection
25 Agency (EPA) guidance (HPSR-1/EPA 520/1-80-012). Data were reported with an
26 unambiguous statement of the uncertainty. The assessment of the uncertainty included an
27 estimate of the combined overall uncertainty. Random and systematic uncertainties associated
28 with measurement parameters (e.g., number of counts, weight, volume) were propagated to
29 determine an overall uncertainty. The basic laws governing the propagation of errors were
30 assumed to apply to both the random and systematic uncertainties in the same manner.
31 Specifically, the systematic uncertainties are treated as if they possess a random nature, in that
32 they are equally likely to be positive or negative (NCRP 112). Uncertainties were also
33 propagated in the MDC determination to provide a measure of the overall uncertainty in the MDC
34 from both counting errors and other sources of error (e.g., detector efficiency, source efficiency,
35 calibration source activity).

36 Experts at several other facilities were contacted to discuss various aspects of this study, such as
37 the statistical approaches to MDC measurements, methods for construction of calibration sources,
38 and to obtain calibration sources, already constructed, that could be used in this study. These
39 institutions included the National Institute of Standards and Technology (NIST), the Department
40 of Energy's Environmental Measurement Laboratory (EML), Argonne National Laboratory
41 (ANL), Pacific Northwest Laboratory (PNL), and Oak Ridge National Laboratory (ORNL).
42 ORISE also collaborated with Brookhaven National Laboratory (BNL) to address the "human
43 factor" in performing radiological scan surveys (Section 6).

1 2 INSTRUMENTATION

2 The types of instruments commonly used in field radiological surveys are briefly described in this
3 section. The instrumentation that was used in this study is specified by make and model. This
4 was necessary in the event that the data generated in this study are reviewed and/or compared to
5 the results obtained by other investigators. However, the use of these instruments does not, in
6 any way, represent an endorsement of a particular product, or a particular manufacturer, on the
7 part of Oak Ridge Institute for Science and Education (ORISE) or the NRC.

8 2.1 Gas Proportional Detectors

9 Gas proportional detectors are used for detecting both alpha and beta radiation. Ludlum 43-68
10 detectors, with an active probe area of 126 cm² (effective probe area is 100 cm², which accounts
11 for the fraction of the probe area covered by the protective screen), were used in this study. Gas
12 proportional detectors with larger probe surfaces, such as the Ludlum Model 43-37 detectors
13 with an active probe area of 573 cm², are suitable for scanning surface areas. The detector cavity
14 in these instruments is filled with P-10 gas (90% argon, 10% methane). Alpha or beta particles,
15 or both, enter this cavity through an aluminized Mylar window. The density thickness of this
16 window is one factor that can affect the detector efficiency, hence the MDC of the instrument.
17 The instrument can be used to detect (a) only alpha radiation by using a low operating voltage, (b)
18 alpha and beta radiation by using a higher operating voltage, or (c) only beta radiation by using a
19 Mylar shield to block the alpha particles in a mixed alpha/beta field. Instrument response was
20 evaluated using all three modes of operation.

21 2.2 Geiger-Mueller Detectors

22 "Pancake" detectors are used for detecting beta and gamma radiation. Eberline Model HP-260
23 detectors were used in this study. This instrument has an active probe area of approximately 20
24 cm² (15.5-cm² effective probe area). The detector tube is filled with readily ionizable inert gas,
25 which is a mixture of argon, helium, neon, and a halogen-quenching gas. Incident radiation enters
26 this cavity through a mica window. The density thickness of the window can vary between 1.4
27 and 2.0 mg/cm², affecting detection sensitivity. The output pulses are registered on a digital
28 scaler/ratemeter with a set threshold value.

29 2.3 Zinc Sulfide Scintillation Detectors

30 Alpha scintillation detectors use scintillators as detection media, instead of gas. A commonly used
31 detector is the zinc sulfide scintillation detector, which uses silver-activated zinc sulfide, ZnS(Ag).
32 The Eberline Model AC-3-7, with an active probe area of 74 cm² (59 cm² effective probe area),
33 was used in this study. Alpha particles enter the scintillator through an aluminized Mylar window.
34 The Mylar window prevents ambient light from activating the photomultiplier, but is still thin
35 enough to allow penetration by alpha radiation without significant energy degradation. The light
36 pulses are amplified by a photomultiplier, converted to voltage pulses, and counted on a digital
37 scaler/ratemeter with a set threshold value.

Instrumentation

1 2.4 Sodium Iodide Scintillation Detectors

2 For detection of gamma radiation, thallium-activated sodium iodide scintillation detectors are
3 widely used. Primarily, these detectors are useful for scanning surface areas for elevated gamma
4 radiation. In this study, the Victoreen Model 489-55 with a 3.2 cm by 3.8 cm NaI(Tl) crystal was
5 used. The output voltage pulse is recorded on a ratemeter.

6 2.5 Ratemeters-Scalers

7 The detectors that were described above are used in conjunction with ratemeter-scalers. The
8 detector response is recorded as an integrated count or it is noted as a count rate, or both. Both
9 modes of operation were evaluated in the study. The following instrument combinations were
10 used: Ludlum Model 2221 ratemeter-scaler was used with Ludlum 43-68, Eberline HP-260, and
11 Eberline AC-3-7 detectors; and Ludlum Model 12 ratemeter-scaler was used with the Victoreen
12 489-55 detector.

13 2.6 Pressurized Ionization Chamber

14 The pressurized ionization chamber (PIC) can be used to monitor "real time" direct gamma-ray
15 levels and record exposure rates. Ionization chambers operate by collecting ions within a cavity
16 chamber filled with pressurized argon gas. The current generated is proportional to the amount of
17 ionization produced in the chamber. Quantitative measurements of exposure rate are made and
18 recorded in micro-roentgen per hour. In this study, Reuter-Stokes Model RSS-112 was used.

19 2.7 Portable Gamma Spectrometer

20 Portable gamma spectrometers can be used to identify and quantitate gamma-emitting
21 radionuclides in the field. The Environmental Survey and Site Assessment Program (ESSAP) at
22 the Oak Ridge Institute for Science and Education (ORISE) has used the portable gamma-
23 spectrometry capability, mainly for qualitative analysis of contaminants in the field, but not to
24 obtain data for direct comparison with the guidelines. The system used by ESSAP is manufac-
25 tured by EG&G ORTEC, and includes a 13-percent relative efficiency, p-type germanium
26 detector.

27 2.8 Laboratory Instrumentation

28 The study of field survey instruments was extended to include a limited number of measurements
29 using laboratory instrumentation. The following laboratory instrumentation was used.

- 30 ● Canberra 3100 VAX workstation connected to intrinsic germanium detectors (Oxford
31 instruments and EG&G ORTEC) with extended range capability for low-energy x-rays
- 32 ● Canberra 3100 VAX workstation connected to solid-state alpha detectors (Canberra and
33 Oxford instruments)
- 34 ● Low background alpha/beta gas flow proportional counters (Oxford instruments)
- 35 ● Liquid scintillation counter (Packard instruments)

3 STATISTICAL INTERPRETATIONS OF MINIMUM DETECTABLE CONCENTRATIONS

Detection limits for field survey instrumentation are an important criterion in the selection of appropriate instrumentation and measurement procedures. For the most part, detection limits need to be determined in order to evaluate whether a particular instrument and measurement procedure is capable of detecting residual activity at a certain fraction of the regulatory guidelines. NUREG-1500 provides surface activity guidelines that correspond to both 3 and 15 millirem per year total effective dose equivalent (TEDE). Thus, one may demonstrate compliance with decommissioning criteria by performing surface activity measurements and directly comparing the results to the surface activity guidelines in NUREG-1500. However, before any measurements are performed, the survey instrument and measurement procedures to be used must be shown to possess sufficient detection capabilities relative to the surface activity guidelines; i.e., the detection limit of the survey instrument must be a certain fraction of this limit (e.g., 50%).

The measurement of residual radioactivity during surveys in support of decommissioning often involves measurement of residual radioactivity at near-background levels. Thus, the minimum amount of radioactivity that may be detected by a given survey instrument and measurement procedure must be determined. In general, the minimum detectable concentration (MDC) is the minimum activity concentration on a surface or within a material volume, that an instrument is expected to detect (e.g., activity expected to be detected 95% of the time). It is important to note, however, that this activity concentration, or the MDC, is determined *a priori*, that is, before survey measurements are conducted.

As generally defined, the detection limit, which may be a count or count rate, is independent of field conditions such as scabbled, wet, or dusty surfaces. These field conditions do, however, affect the instrument's "detection sensitivity" or MDC. Therefore, the terms MDC and detection limit should not be used interchangeably. For this study, the MDC corresponds to the smallest activity concentration measurement that is practically achievable with a given instrument and type of measurement procedure. That is, the MDC depends not only on the particular instrument characteristics (background, integration time, etc.), but also on the factors involved in the survey measurement process (HPSR-1/EPA 520/1-80-012), which may include source-to-detector geometry, efficiency, and other physical factors (backscatter and self-absorption).

3.1 MDC Fundamental Concepts

The scope of this report precludes a rigorous derivation of MDC concepts, yet sufficient theory is presented to acquaint the user of this manual with the fundamental concepts. The detection limits discussed in this report are based on counting statistics alone and do not include other sources of error (e.g., systematic uncertainties in the measurement process). Although the following statistical formulation assumes a normal distribution of net counts, between sample and blank, it should be recognized that this may not be the case for low blank total counts. However, in consideration of the advantage of having a single, simple MDC expression, and the fact that deviations from the normality assumption do not affect the MDC expression contained herein as

Statistical Interpretations of MDCs

1 severely as had been expected (Brodsky 1992), it was decided that the normality assumption was
2 proper for purposes of this report. That is, the MDC concepts discussed below should be
3 considered as providing information on the general detection capability of the measurement
4 system, and not as absolute levels of activity that can or cannot be detected (NCRP 58).

5 The MDC concepts discussed in this document derive from statistical hypothesis testing, in which
6 a decision is made on the presence of activity. Specifically, a choice is made between the null
7 hypothesis (H_0) and the alternative hypothesis (H_1). The null hypothesis is generally stated as "no
8 net activity is present in the sample" (i.e., observed counts are not greater than background),
9 while the alternative hypothesis states that the observed counts are greater than background, and
10 thus, that net activity is present. These statements are written:

11 H_0 : No net activity is present in the sample, and

12 H_1 : Net activity is present in the sample.

13 It should be noted that the term "sample" has a general meaning in this context, it may apply to
14 direct measurements of surface activity, laboratory analyses of samples, etc.

15 A first step in the understanding of the MDC concepts is to consider an appropriate blank
16 (background) distribution for the medium to be evaluated. Currie defines the blank as the signal
17 resulting from a sample which is identical, in principle, to the sample of interest, except that the
18 residual activity is absent. This determination must be made under the same geometry and
19 counting conditions as used for the sample (Brodsky & Gallagher). In the context of this report,
20 an example of this medium may be an unaffected concrete surface that is considered
21 representative of the surfaces to be measured in the remediated area. It should be noted that the
22 terms blank and background are used interchangeably in this report.

23 In this statistical framework, one must consider the distribution of counts obtained from
24 measurements of the blank, which may be characterized by a population mean (μ_B) and standard
25 deviation (σ_B). Now consider the measurement of a sample that is known to be free of residual
26 activity. This zero-activity (background) sample has a mean count (C_B) and standard deviation
27 (s_B). The net count (and, subsequently, residual activity) may be determined by subtracting the
28 blank counts from the sample counts. This results in a zero-mean count frequency distribution
29 that is approximately normally distributed (Figure 3.1). The standard deviation of this
30 distribution, σ_0 , is obtained by propagating the individual errors (standard deviations) associated
31 with both the blank (σ_B) and the zero-activity samples (s_B). That is,

$$\sigma_0 = \sqrt{\sigma_B^2 + s_B^2} \quad (3-1)$$

32 A critical level may then be determined from this distribution and used as a decision tool to decide
33 when activity is present. The critical level, L_C , is that net count in a zero-mean count distribution
34 having a probability, denoted by α , of being exceeded (Figure 3.1). It is a common practice to set
35 α equal to 0.05 and to accept a 5-percent probability of incorrectly concluding that activity is
36 present when it is not. That is, if the observed net count is less than the critical level, the surveyor
37 correctly concludes that no net activity is present. When the net count exceeds L_C , the null
38 hypothesis is rejected in favor of its alternative, and the surveyor falsely concludes that net activity

1 is present in the blank sample. It should also be noted that the critical level, L_C , is equivalent to a
 2 given probability (e.g., 5%) of committing a Type I error (false positive detection). The
 3 expression for L_C is generally given as:

$$L_C = k_\alpha \sigma_0 \quad (3-2)$$

4 where k_α is the value of the standard normal deviate corresponding to a one-tailed probability
 5 level of $1-\alpha$. As stated previously, the usual choice for α is 0.05, and the corresponding value for
 6 k_α is 1.645. For an appropriate blank counted under the same conditions as the sample, the
 7 assumption may be made that the standard deviations of the blank and zero-activity sample are
 8 equal (i.e., σ_B equals s_B). Thus, the critical level may be expressed as:

$$L_C = 1.645 \sqrt{2 s_B^2} = 2.33 s_B \quad (3-3)$$

9 The L_C value determined above is in terms of net counts, and as such, the L_C value should be
 10 added to the background count if comparisons are to be made to the directly observable
 11 instrument gross count.

12 The detection limit, L_D , is defined to be the number of mean net counts obtained from samples for
 13 which the observed net counts are almost always certain to exceed the critical level (Figure 3.2).
 14 It is important to recognize that L_D is the mean of a net count distribution. The detection limit is
 15 positioned far enough above zero so that there is a probability, denoted by β , that the L_D will
 16 result in a signal less than L_C . It is common practice to set β equal to 0.05 and to accept a 5-
 17 percent probability of incorrectly concluding that no activity is present, when it is indeed present
 18 (Type II error). That is, the surveyor has already agreed to conclude that no net activity is
 19 present for an observed net count that is less than the critical level, however, an amount of
 20 residual activity that would yield a mean net count of L_D is expected to produce a net count less
 21 than the critical level 5 percent of the time. This is equivalent to missing residual activity when it
 22 was present.

23 The expression for L_D is generally given as:

$$L_D = L_C + k_\beta \sigma_D \quad (3-4)$$

24 where k_β is the value of the standard normal deviate corresponding to a one-tailed probability
 25 level of $1-\beta$ for detecting the presence of net activity, and σ_D is the standard deviation of the net
 26 sample count (C_S) when C_S equals L_D . The quantity σ_D is propagated from the error in the gross
 27 count and from the background when the two are subtracted to obtain L_D :

$$\sigma_D = \sqrt{(L_D + \sigma_0^2)} \quad (3-5)$$

28 This expression for σ_D may be substituted into Equation 3-4 and the equation solved for L_D .

29 As stated previously, the usual choice for β is 0.05, and the corresponding value for k_β is 1.645.
 30 If the assumption is made that σ_D is approximately equal to the standard deviation of the
 31 background, then for the case of paired observations of the background and sample ($\sigma_0^2 = 2s_B^2$)

Statistical Interpretations of MDCs

1 the detection limit may be expressed as:

$$L_D = 2.71 + 4.65 s_B \quad (3-6)$$

2 The assumption that the standard deviation of the count (σ_D) is approximately equal to that of the
3 background greatly simplifies the expression for L_D , and is usually valid for total counts greater
4 than 70 for each sample and blank count (Brodsky 1992). Brodsky has also examined this
5 expression and determined that in the limit of very low background counts, s_B would be zero and
6 the constant 2.71 should be 3, based on a Poisson count distribution (Brodsky & Gallagher).
7 Thus, the expression for the detection limit becomes:

$$L_D = 3 + 4.65 s_B \quad (3-7)$$

8 The detection limit calculated above may be stated as the net count having a 95-percent
9 probability of being detected when a sample contains activity at L_D , and with a maximum 5-
10 percent probability of falsely interpreting sample activity as activity due to background (false
11 negative or Type II error).

12 The MDC of a sample follows directly from the detection limit concepts. It is a level of
13 radioactivity, either on a surface or within a volume of material, that is practically achievable by
14 an overall measurement process (HPSR-1/EPA 520/1-80-012). The expression for MDC may be
15 given as:

$$MDC = \frac{[3 + 4.65 s_B]}{KT} \quad (3-8)$$

16 where K is a proportionality constant that relates the detector response to the activity level in a
17 sample for a given set of measurement conditions and T is the counting time. This factor typically
18 encompasses the detector efficiency, self-absorption factors, probe area corrections, et cetera.
19

20 This expression of the MDC equation was derived assuming equivalent (paired) observations of
21 the sample and blank (i.e., equal counting intervals for the sample and background), in contrast to
22 the MDC expression that results when taking credit for repetitive observations of the blank (well-
23 known blank). There is some debate concerning the appropriateness of taking credit for repetitive
24 observations of the blank, considering the uncertainties associated with using a well-known blank
25 for many samples when there can be instrument instabilities or changes in the measurement
26 process that may be undetected by the surveyor (Brodsky 1991). Therefore, it is desirable to
27 obtain repetitive measurements of background, simply to provide a better estimate of the
28 background value that must be subtracted from each gross count in the determination of surface
29 activity. Thus, the background is typically well known for purposes other than reducing the
30 corresponding MDC, such as to improve the accuracy of the background value. The expression
31 for MDC that will be used throughout this report is given as:

$$MDC = \frac{3 + 4.65 \sqrt{C_B}}{KT} \quad (3-9)$$

1 where C_B is the background count in time, T , for paired observations of the sample and blank.
 2 For example, if ten 1-minute repetitive observations of background were performed, C_B would be
 3 equal to the average of the ten observations and T is equal to 1 minute. The quantities
 4 encompassed by the proportionality constant, K , such as the detection efficiency and probe
 5 geometry, should also be average, "well-known" values for the instrument. For making
 6 assessments of MDC for surface activity measurements, the MDC is given in units of
 7 disintegrations per minute per 100 square centimeters (dpm/100 cm²).

8 For cases in which the background and sample are counted for different time intervals, the MDC
 9 becomes (Strom & Stansbury 1992)

$$MDC = \frac{3 + 3.29 \sqrt{R_B T_{S+B} \left(1 + \frac{T_{S+B}}{T_B}\right)}}{K T_{S+B}} \quad (3-10)$$

10 where R_B is the background counting rate, and T_{S+B} and T_B are the sample and background
 11 counting times, respectively.

12 One difficulty with the MDC expression in Equation 3-9 is that all uncertainty is attributed to
 13 Poisson counting errors, which can result in an overestimate of the detection capabilities of a
 14 measurement process. The proportionality constant, K , embodies measurement parameters that
 15 may have associated uncertainties that may be significant as compared to the Poisson counting
 16 errors. A conservative solution to this problem has been to replace the parameter values
 17 (specifically the mean parameter values) that determine K with lower bound values that represent
 18 a 95-percent probability that the parameter values are higher than that bound (NUREG/CR-4007;
 19 ANSI N13.30). In this case, the MDC equation becomes

$$MDC = \frac{3 + 4.65 \sqrt{C_B}}{K_{0.05} T} \quad (3-11)$$

20 where $K_{0.05}$ is the lower bound value that represents a 95-percent probability that values of K are
 21 higher than that bound (ANSI N13.30). For example, if the detector efficiency in a specified
 22 measurement process was experimentally determined to be 0.20 ± 0.08 (2σ error), the value of
 23 the detector efficiency that would be used in Equation 3-9 is 0.12. This would have the effect of
 24 increasing the MDC by a factor of 1.7 (using 0.12 instead of 0.20). Therefore, it is important to
 25 have an understanding of the magnitude of the uncertainty associated with each of the
 26 parameters used in the MDC determination. In this context, errors associated with each
 27 measurement parameter were propagated in the MDC determination. The magnitude of the
 28 uncertainty in the MDC may then be used as a decision tool, allowing for determination of the
 29 need to implement some methodology for adjusting the MDC for uncertainties in K .

1 **3.2 Review of MDC Expressions**

2 A significant aspect of this study involved the review of the relevant literature on statistical
3 interpretations of MDC. One approach, suited for this application of the MDC concept, was
4 selected and used throughout the entire study, for consistency. However, other statistical
5 approaches were considered in a sensitivity study. That is, the same set of measurement results
6 were used to calculate the MDC, using several statistical treatments of the data. The tabulated
7 results provided the range of MDC values, calculated using the various approaches.

8 The data used to perform the MDC sensitivity analysis were obtained by performing static
9 measurements under ideal laboratory conditions with a gas proportional detector, operated in the
10 beta-only mode, on a SrY-90 source (the expressions for scanning sensitivity were not evaluated
11 in this part). For purposes of comparison, both the background and sample counting times were
12 one minute long, i.e., paired observations. Ten repetitive measurements of background were
13 obtained and the mean and standard deviation were calculated to be 354 and 18 counts,
14 respectively. The total efficiency of the detector was determined to be 0.34 count per
15 disintegration and probe area correction for 126-cm² detector was made.

16
17 Several expressions of MDC (or the various terms used to convey detection limit) were reviewed
18 in the literature. The measurement results determined above were used to determine the values
19 for the various expressions of MDC. The average background from the repetitive observations
20 was used in the MDC equations that required a background value, while the standard deviation of
21 the background distribution was used for others. Table 3.1 illustrates the variations in MDC that
22 may be calculated from the same set of measurement results. The MDC values ranged from 146
23 to 211 dpm/100 cm², for the gas proportional detectors calibrated to SrY-90.

24 The MDC sensitivity study demonstrates that the MDC expressions widely referenced in the
25 literature produce very consistent MDC results. The smallest value of MDC results from the
26 expression that allows credit to be taken for the "well-known" blank (Currie 1968). However,
27 there is no difference in the conclusion that would be reached concerning the demonstration that
28 the instrumentation possesses sufficient detection capabilities relative to the surface activity
29 guidelines.

Table 3.1 MDC Results for Data Obtained From Gas Proportional Detector Using Various MDC Expressions

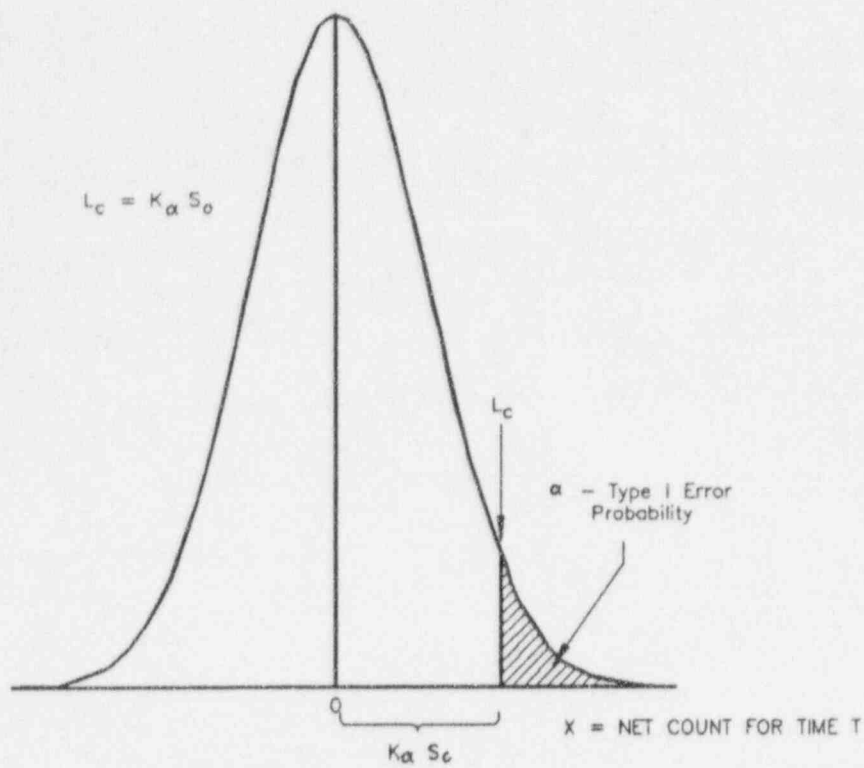
MDC Expression ^{a,b}	MDC Result ^c (dpm/100 cm ²)	Reference
$2.71 + 4.65 \sqrt{B}$	210	NCRP 58 EPA 1980
$2.71 + 4.65 \sigma_B$	204	Currie 1968
$2.71 + 3.29 \sigma_B$	146	Currie 1968
$3 + 4.65 \sqrt{B}$	211	Brodsky & Gallagher 1991
$\frac{+ 3.29 \sqrt{R_b t_g (1 + \frac{t_g}{t_b})^d}}{(Efficiency)(t_g)}$	211	Strom & Stansbury 1992

^aThe data used in each MDC expression were obtained from a 43-68 gas proportional detector and SrY-90 source. Average background counts (*B*) of 354 in 1 minute, standard deviation of 18, probe area correction for 126-cm² detector, and detector efficiency of 0.34 count per disintegration were obtained.

^bEach MDC expression is written using symbols that may be different from the ones that were presented in their respective references. However, the meaning of each has been preserved.

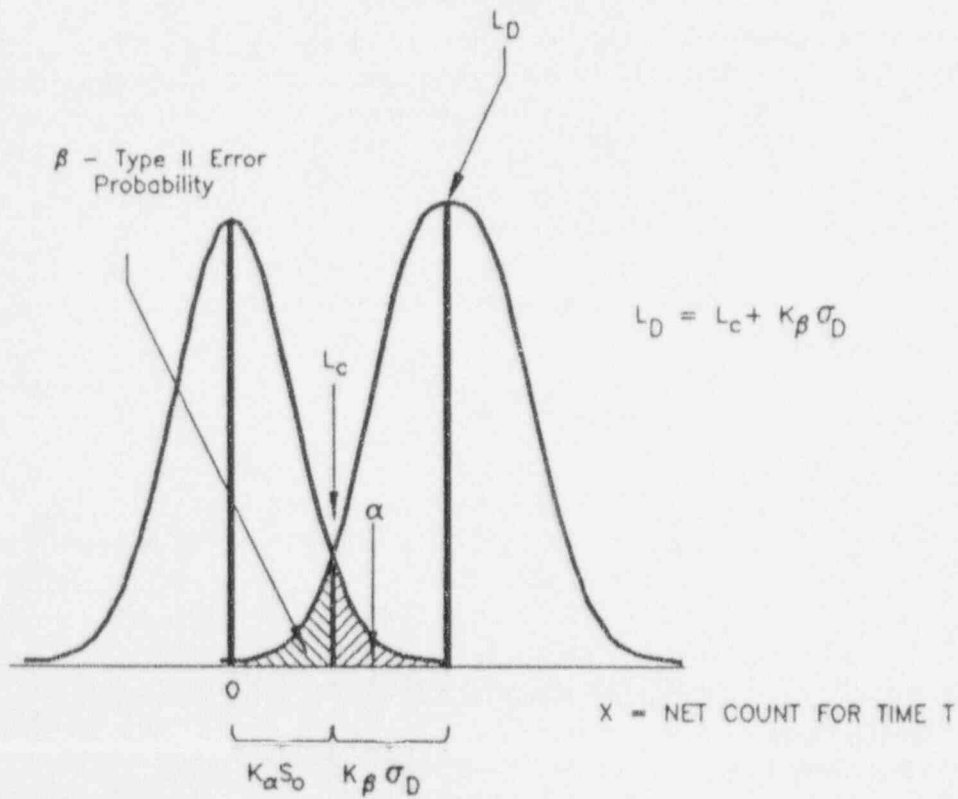
^cEach MDC result was presented in terms of dpm/100 cm² to facilitate comparison of the different MDC expressions. This involved correcting the MDC expression for probe area and detector efficiency.

^dThe terms *R_b*, *t_g*, and *t_b* refer to the background counting rate, gross count time, and background counting time, respectively. Using *t_g* equal to *t_b* (1 minute), resulted in the same expression as that of Brodsky and Gallagher (1991).



1

Figure 3.1 Critical Level, L_c



2

Figure 3.2 Detection Limit, L_D

4 VARIABLES AFFECTING INSTRUMENT MINIMUM DETECTABLE CONCENTRATIONS

Before the MDC for a particular instrument and survey procedure can be determined, it is necessary to introduce the expression for total alpha or beta surface activity per unit area. The International Standard ISO 7503-1, "Evaluation of Surface Contamination," recommends that the total surface activity, A_s , be calculated similarly to the following expression

$$A_s = \frac{R_{S+B} - R_B}{(\epsilon_i)(W)(\epsilon_s)} \quad (4-1)$$

where

R_{S+B} is the gross count rate of the measurement in cpm,

R_B is the background count rate in cpm,

ϵ_i is the instrument or detector efficiency (unitless),

ϵ_s is the efficiency of the contamination source (unitless), and

W is the area of the detector window (cm^2).

(For instances in which W does not equal 100 cm^2 , probe area corrections are necessary to convert the detector response to units of dpm per 100 cm^2 .)

This expression clearly distinguishes between instrument (detector) efficiency and source efficiency. The product of the instrument and source efficiency yields the total efficiency, ϵ_{tot} . Currently, surface contamination is assessed by converting the instrument response to surface activity using one overall total efficiency. This is not a problem provided that the calibration source exhibits similar characteristics as does the surface contamination—radiation energy, backscatter effects, source geometry, self-absorption, etc. In practice this is hardly the case; more likely, instrument efficiencies are determined with a clean, stainless steel source, and then those efficiencies are used to measure contamination on a dust-covered concrete surface. By separating the efficiency into two components, the surveyor has a greater ability to consider the actual characteristics of the surface contamination.

The instrument efficiency is defined as the ratio between the net count rate of the instrument and the surface emission rate of a source for a specified geometry. The surface emission rate, $q_{2\pi}$, is defined as the "number of particles of a given type above a given energy emerging from the front face of the source per unit time" (ISO 7503-1). The surface emission rate is the 2π particle fluence that embodies both the absorption and scattering processes that affect the radiation emitted from the source. Thus, the instrument efficiency is determined by

$$\epsilon_i = \frac{R_{s+b} - R_b}{q} \quad (4-2)$$

Variables Affecting Instrument MDCs

1 The instrument efficiency is determined during calibration by obtaining a static count with the
2 detector over a calibration source that has a traceable activity or surface emission rate or both. In
3 many cases, it is the source surface emission rate that is measured by the manufacturer and
4 certified as National Institutes of Standards and Technology (NIST) traceable. The source
5 activity is then calculated from the surface emission rate based on assumed backscatter and self-
6 absorption properties of the source. The maximum value of instrument efficiency is 1.

7 The source efficiency, ϵ_s , is defined as the ratio between the number of particles of a given type
8 emerging from the front face of a source and the number of particles of the same type created or
9 released within the source per unit time (ISO 7503-1). The source (or surface) efficiency takes
10 into account the increased particle emission due to backscatter effects, as well as the decreased
11 particle emission due to self-absorption losses. For an ideal source (no backscatter or self-
12 absorption), the value of ϵ_s is 0.5. Many real sources will exhibit values of ϵ_s less than 0.5,
13 although values greater than 0.5 are possible, depending on the relative importance of the
14 absorption and backscatter processes. Source efficiencies must be determined experimentally.

15 This current section considers some of the factors that affect the instrument efficiency, ϵ_i . These
16 detector-related factors include detector size (probe surface area), window density thickness,
17 geotropism, instrument response time, counting time (static mode), scan rate (scan mode), and
18 ambient conditions such as temperature, pressure, and humidity. The instrument efficiency also
19 depends on the solid angle effects, which include source-to-detector distance and source
20 geometry.

21 Section 5 covers some of the factors that affect the source efficiency, ϵ_s . Among these source-
22 related factors are the type of radiation and its energy, source uniformity, surface roughness and
23 coverings, and surface composition (e.g., wood, metal, concrete).

24 4.1 Radionuclide Sources for Calibration

26 For accurate measurements of total surface activity, it is essential that field instruments be
27 calibrated appropriately. The MDC of an instrument depends on a variety of parameters, one of
28 which involves the selection of calibration sources. Calibration sources should be selected that
29 emit alpha or beta radiation with energies similar to those expected of the contaminant in the field.
30 ISO-8769, "Reference Sources for the Calibration of Surface Contamination Monitors," provides
31 recommendations on calibration source characteristics.

32 An instrument's MDC depends on the type and energy of radiation. The radionuclides selected
33 for this study were chosen so that they represent the types or the range, or both, of energies
34 commonly encountered in decommissioned facilities. These radionuclides are C-14, Ni-63, SrY-
35 90, Tc-99, and Tl-204 for beta measurements, and Th-230 and Pu-239 for alpha measurements.
36 The calibration sources, available at ESSAP facilities, are traceable to NIST standards. Generally,
37 the sources are of three geometric shapes: "button" sources (simulating a point source,
38 approximately 5 cm²), disc sources that cover a standard area of approximately 15 cm², or
39 distributed sources that typically range from 126 to 150 cm². Table 4.1 summarizes the
40 calibration sources used in this study.

1 The efficiencies determined in this section are for ideal laboratory conditions, which include the
2 use of smooth, clean calibration source surfaces. Table 4.2 presents the average total efficiencies
3 for the gas proportional, GM, and ZnS detectors compiled from historical calibration data at
4 ESSAP. Table 4.3 provides MDCs that were calculated for the gas proportional detector ($\alpha + \beta$
5 mode) and the GM detector using the ambient background count rates provided in Table 5.1 and
6 the total efficiencies in Table 4.2. As expected, the MDCs decrease with increasing beta energy.
7 This is shown graphically in Figures 4.1 and 4.2 for the gas proportional and GM detectors,
8 respectively. For beta energies (beta endpoint energies are used in this report) ranging from 300
9 to 1400 keV, the calculated MDCs are generally constant. However, the MDCs increase rapidly
10 with decreasing beta energies below 300 keV.

11 4.2 Source-to-Detector Distance

12 The distance between a source and the detector is another factor that may affect the instrument
13 efficiency and, thus, the MDC. In this study, instrument MDC was evaluated as a function of
14 distance from the source. The range of distances was selected to be appropriate for the type of
15 radiation being measured, and in consideration of the typical detector-to-surface distances
16 encountered in the course of performing surveys in support of decommissioning. Counts of
17 1 minute in duration were made with the detector at various distances above the source.

18 The source-to-detector distance was evaluated using a Ludlum Model 43-68 gas proportional
19 detector with a 0.8 mg/cm² window for beta emitters, including C-14, Ni-63, SrY-90, Tc-99 (two
20 source geometries were used), and Tl-204, and for Pu-239 and Th-230 (alpha emitters). Five 1-
21 minute measurements were made at contact and at distances of 0.5 cm, 1 cm, and 2 cm. The
22 distances were obtained by cutting out the specified thicknesses of plastic and using them to
23 maintain the desired source-to-detector spacing. Tables 4.4 and 4.5 show the results of an
24 increasing source-to-detector distance on instrument response. Specifically, the net count rate
25 obtained at each distance was normalized to the net count rate obtained in contact with the
26 source. These results demonstrate the significant reduction in instrument response that occurred
27 when source-to-detector distance was increased by less than 1 cm.

28 As was expected, the greatest reduction in detector response per increased distance from the
29 source was obtained for the alpha and low-energy beta emitters, i.e., Ni-63 and C-14. The
30 modest reduction in instrument response for the alpha-emitting Pu-239 and Th-230 sources, from
31 being in contact with the source to 1 cm, was somewhat unexpected. The C-14 and Ni-63
32 exhibited equal or greater reductions in instrument response over this range compared to the alpha
33 emitters. Somewhat more anticipated was the dramatic reduction in instrument response from 1
34 to 2 cm for the Pu-239 and Th-230 sources. The instrument response to the Th-230 disc source
35 at 2 cm was only 4 percent of the response obtained in contact with the source. This was
36 contrasted to the Pu-239 disc source that exhibited 20 percent of the response at 2 cm relative to
37 the contact measurement. The greater instrument response of Pu-239 at 2 cm relative to Th-230
38 at the same distance was likely due to the higher energy of the Pu-239 alpha emission (i.e., 5.1
39 MeV for Pu-239 versus 4.7 MeV for Th-230).

Variables Affecting Instrument MDCs

1 The data presented in Tables 4.4 and 4.5 were used to determine total efficiencies as a function of
2 detector-to-source distance. It should be noted that although total efficiencies were determined
3 and reported at each distance, the detector-to-source distance influences the instrument efficiency,
4 ϵ_i (as opposed to ϵ_s). These total efficiencies were used to calculate the MDCs presented in
5 Tables 4.6 and 4.7. Figures 4.3 and 4.4 illustrate the effects of source-to-detector distance on the
6 MDC for the beta emitters. These figures show that the source-to-detector distance effect on
7 MDCs was relatively minor for the higher energy beta emitters (e.g., SrY-90 and Tl-204), but
8 considerable for the alpha and low to mid-energy beta emitters. Figure 4.5 shows the effects of
9 source-to-detector distance on the MDC for alpha emitters. For alpha emitters, the MDCs
10 gradually increased as the detector-to-source spacing increased from contact to 1 cm. At 2-cm
11 distance, consistent with the substantial reduction in total efficiency, the MDCs increased
12 significantly. The MDC determined for Ni-63 at a detector-to-source distance of 2 cm was
13 $52,000 \pm 56,000$ dpm/100 cm², with the relatively large uncertainty attributed to the error in the
14 total efficiency determination. This magnitude of uncertainty in the MDC term suggests that the
15 detection capability for the measurement process, i.e. detecting Ni-63 with a gas proportional
16 detector 2 cm from the surface, is likely overestimated. This particular example illustrates the
17 need for adjusting the MDC to account for uncertainties in the calibration factors (refer to Section
18 3.1.1 for discussion of MDC adjustment factor).

19 The practicality of these results may be realized by the deviation in instrument response that
20 results when the source-to-detector distance during calibration is only slightly different (i.e., less
21 than 1 cm for some radionuclides) from the detector-to-surface spacing maintained during field
22 measurements of surface activity. That is, small changes in detector-to-surface distance produce
23 significant changes in detector response, especially for alpha and low-energy beta radiation (1 to 2
24 cm spacing is not unusual for a roughly scabbled concrete surface). The effects on Tl-204 and
25 SrY-90, although less than those on lower energy beta emitters, were still appreciable.

26 To minimize the effects of source-to-detector distance on MDCs, it is recommended that the
27 detector be calibrated at a source-to-detector distance that is similar to the expected detector-to-
28 surface spacing in the field.

29 4.3 Window Density Thickness

30 The detector-related factors that may change the instrument MDC are detector size (probe
31 surface area), window density thickness, geotropism, instrument response time, counting time
32 (static mode), scan rate (scan mode), and ambient conditions such as temperature, pressure, and
33 humidity. In many instances, this information is already available. For example, the effects of
34 ambient conditions and geotropism are usually tested by users concerned about the instrument or
35 detector performance (Swinth & Kenoyer, LA-10729).

36 One detector-related factor evaluated in this report was the effect of window density thickness on
37 instrument response (using the Ludlum model 43-68) for C-14, Ni-63, Sr-90, Tc-99 (two source
38 geometries were used for Tc-99), and Tl-204. Window density thickness for gas proportional
39 detectors may be varied to provide a mechanism to control instrument response to various surface
40 activity conditions. For example, in the assessment of low-energy beta emitters, a relatively thin
41 window (e.g., 0.4 mg/cm²) provides greater sensitivity. Similarly, when beta radiation in the

1 presence of alpha radiation must be assessed, it is possible to selectively discriminate out the alpha
2 radiation using an alpha shield (i.e., using 3.8 mg/cm² window density thickness).

3 Measurements were performed for window density thicknesses of 0.3, 0.4, 0.8, and 3.8 mg/cm².
4 In addition, MDC measurements at window density thicknesses of 1.3, 1.8, 2.3, 2.8, and 3.3
5 mg/cm² were performed for the two Tc-99 source geometries. Window density thicknesses were
6 varied by adding sheets of 0.5-mg/cm² Mylar between the source and the detector. The results of
7 these measurements are in Table 4.8. Figures 4.6 and 4.7 illustrate the effects of window density
8 thickness on the total efficiency. The total efficiency was reduced more significantly for the lower
9 energy beta emitters as the window density thickness was increased.

10 The total efficiencies presented in Table 4.8 were used to determine MDCs as a function of
11 window density thickness (Table 4.9). Figures 4.8 and 4.9 illustrate the effects of window density
12 thickness on the MDC for the beta emitters. These figures show, as did the source-to-detector
13 distance evaluation, that the window density thickness over the range of 0.3 to 3.8 mg/cm² has a
14 trivial effect on MDCs for the higher energy beta emitters (e.g., SrY-90 and Tl-204), but was
15 considerable for the low to mid-energy beta emitters. These figures illustrate how the detector
16 MDC calibrated to lower energy beta emitters is significantly affected by the window density
17 thickness. As with the effects of source-to-detector distance on MDCs, it is essential that the
18 detector be calibrated with the same window density thickness that will be used for survey
19 measurements in the field. This concern may arise if the window is replaced in the field with one
20 of a different thickness and returned to service without recalibration.

21 4.4 Source Geometry Factors

22 The source geometry must be considered in determining the instrument MDC. The detector's
23 response may be influenced, in part, by the contaminant's distribution on the surface being
24 assessed. For example, if the contamination is characterized by relatively large uniform areas of
25 activity, then the detector should be calibrated to a distributed or extended source. Similarly, if
26 the surface can be characterized by localized spots of surface contamination, that may be
27 approximated by a point source, then the calibration source should be similar to a point source
28 geometry.

29 The source geometry effect on detector response was evaluated by determining the instrument
30 efficiencies (ϵ_i) for gas proportional, GM, and ZnS detectors placed in contact with both
31 distributed and disc sources. The radionuclide sources used in this evaluation were Tc-99 and Th-
32 230. The instrument efficiencies determined for each detector and geometry configuration are in
33 Table 4.10. The instrument efficiencies determined with the disc sources were 6 to 42 percent
34 greater than those obtained with the distributed sources. These results were expected because of
35 the solid angle of the measurement geometry. That is, for the smaller disc source, a larger
36 fraction of the radiation particles (α and β) emitted from the source intersect the detector probe
37 area. Walker provides further information on the effects of source-to-detector geometry.

38 During the course of performing field survey measurements, it would be a time-consuming task to
39 determine the contaminant geometry at each measurement location in an effort to select the most
40 appropriate instrument efficiency. The benefits of a better defined contaminant geometry should
41 be weighed against the increased labor expended in characterizing the contamination. It may be

Variables Affecting Instrument MDCs

1 appropriate (conservative) to use the instrument efficiency obtained from a distributed source
2 geometry for all surface activity measurement locations, except for those locations of elevated
3 direct radiation. Only for locations of elevated direct radiation would effort be warranted to
4 characterize the contaminant geometry in order to select the most appropriate instrument
5 efficiency.

6 4.5 Ambient Background Count Rate

7 The effects of ambient background (in particular, relatively high ambient background) on the
8 calculated MDC and measured activity concentration of a radioactive source using a GM detector
9 was evaluated. The procedure included collecting five 1-minute measurements of the ambient
10 background, followed by five 1-minute measurements of a NIST-traceable Tc-99 disc source
11 (activity concentration was 1,500 dpm within a 5-cm² active area). A jig was used to ensure that
12 a reproducible geometry was maintained for each measurement. The ambient background was
13 increased by placing Cs-137 sources at various distances from the GM detector. The ambient
14 background levels ranged from approximately 50 to 1,500 cpm. This procedure allowed a
15 comparison of the *a priori* MDC and the measured activity concentration of the Tc-99 source.
16 The measured activity concentration was calculated using a total efficiency of 0.17 count per
17 disintegration (from Table 4.2); no probe area correction was made since it was known that the
source activity was limited to a 5-cm² area. Results are tabulated in Table 4.11.

19 As expected, the calculated detection sensitivity (or MDC) of the GM detector increased directly
20 with the square root of the ambient background level (Figure 4.10). For ambient background
21 levels ranging from 50 to 145 cpm (consistent with background levels typically encountered
22 during final status surveys), the measured activity of the Tc-99 was very similar to the stated
23 activity of the source. As the ambient background levels were increased to 1,000 cpm, the
24 measured activity was, with one exception, consistently lower than the certified source activity.
25 As the ambient background was further increased to 1,500 cpm, the measured activity was less
26 than 60 percent of the certified source activity, with significant uncertainty at the 95-percent
27 confidence level.

28 In general, as the ambient background increases, and the ratio of the calculated MDC to the actual
29 activity concentration present approaches unity, the uncertainty in the measured activity increases.
30 However, only when the calculated MDC was approximately 70 percent of the actual activity
31 concentration (MDC equal to 1,070 dpm per 5 cm²), was there significant uncertainty and
32 inaccuracy in the measured activity. For the case in which the MDC is a small fraction of the
33 guideline value, significant uncertainty in the value is acceptable (e.g., ±100% uncertainty in a
34 value that is 20% of the guideline gives adequate assurance that the compliance with the guideline
35 has been achieved). If this is not the case, caution must be exercised when making measurements
36 that are close to the MDC, because substantial uncertainties may be associated with the
37 measurements.

1 **Table 4.1 Characteristics of Radionuclide Sources Used for Calibration and Static**
 2 **Measurements**

3	Radionuclide	Active Area (cm ²)	Activity (Emission Rate)	Source Backing Material	Surface Coating
4	C-14	13	12,860 cpm	stainless steel (S.S.)	0.9 mg/cm ² aluminized Mylar
5	C-14	13	959,000 cpm	S.S.	0.9 mg/cm ² aluminized Mylar
6	Ni-63	15	16,600 cpm	Ni	NA
7	SrY-90	15	36,800 cpm	S.S./Kapton/Al	NA
8	SrY-90	13	8,080 cpm	Ni	NA
9	Tc-99	4.9	940 cpm	S.S.	NA
10	Tc-99	4.9	83,400 cpm	S.S.	NA
11	Tc-99	126	26,300 cpm	S.S./Al	NA
12	Tc-99	150	14,400 cpm	S.S.	NA
13	Tl-204	15	6,920 cpm	S.S.	NA
14	Th-230	150	25,100 cpm	S.S.	NA
15	Th-230	126	28,200 cpm	S.S./Al	NA
16	Th-230	5.1	52,700 cpm	Ni	NA
17	Pu-239	5.1	46,300 cpm	Ni	NA

Table 4.2 Average Total Efficiencies for Various Detectors and Radionuclides

Radionuclide	Total Efficiency (Counts Per Disintegration) ^a				
	Gas Proportional			GM	ZnS
	α Only	β Only	$\alpha+\beta$		
Beta					
Ni-63	--- ^b	---	0.08 ^c , 0.06 ^d	0.0025	---
C-14	---	---	0.11 ^d	0.05	---
Tc-99	---	0.13 ^e	0.22 ^d	0.17	---
Tl-204	---	0.29 ^e	0.35 ^d	0.26	---
SrY-90	---	---	0.42 ^d	0.32	---
Alpha					
Th-230	0.19 ^d	---	---	---	0.18
Pu-239	---	---	---	---	0.19

^aThe total efficiencies represent average values compiled from historical instrument calibration data. These values should be considered as the ideal efficiencies obtained under laboratory conditions.

^bData not obtained.

^cFor window density thickness of 0.4 mg/cm².

^dFor window density thickness of 0.8 mg/cm².

^eFor window density thickness of 3.8 mg/cm².

1 **Table 4.3 Minimum Detectable Concentrations for Various Detectors and Radionuclides**

2 3 Radionuclide (Endpoint β Energy)	Minimum Detectable Concentration (dpm/100 cm ²) ^a	
	Gas Proportional ($\alpha+\beta$)	GM
4 Ni-63 (66 keV)	1,160 ^b	70,000
5 C-14 (156 keV)	630	3,500
6 Tc-99 (294 keV)	320	1,000
7 Tl-204 (763 keV)	200	670
8 SrY-90 (1415 keV)	170	550

9 ^aMDCs were calculated on the basis of the ambient background count rates presented in Table 5.1 for the gas
 10 proportional detector ($\alpha+\beta$ mode) and the GM detector, and the total efficiencies in Table 4.2. Probe area corrections
 11 of 126 and 20 cm², respectively, were made for the gas proportional and GM detectors. The following MDC equation
 12 was used for 1-minute counts:

$$MDC = \frac{3 + 4.65 \sqrt{C_B}}{KT}$$

13 ^bMDC calculated using total efficiency for window density thickness of 0.8 mg/cm² (0.06 count per disintegration
 14 (c/dis)).

Table 4.4 Source-to-Detector Distance Effects for β Emitters

Distance From Source (cm)	Normalized Net Count Rate ^{a,b}					
	Ni-63 (Disc)	C-14 (Disc)	Tc-99 (Disc)	Tc-99 (Distributed)	Tl-204 (Disc)	SrY-90 (Disc)
Contact	1	1	1	1	1	1
0.5	0.381 ± 0.064 ^c	0.786 ± 0.047	0.864 ± 0.016	0.803 ± 0.015	0.910 ± 0.024	0.9189 ± 0.0065
1	0.196 ± 0.053	0.648 ± 0.048	0.7779 ± 0.0085	0.701 ± 0.023	0.836 ± 0.026	0.8534 ± 0.0088
2	0.038 ± 0.041	0.431 ± 0.034	0.5920 ± 0.0090	0.503 ± 0.014	0.645 ± 0.033	0.6995 ± 0.0063

^aNormalized net count rate determined by dividing the net count rate at each distance by the net count rate at contact with the source.

^bGas proportional detector operated in the $\alpha + \beta$ mode was used for all measurements.

^cUncertainties represent the 95% confidence interval, based on propagating the counting errors in each measurement.

Table 4.5 Source-to-Detector Distance Effects for α Emitters

Distance From Source (cm)	Normalized Net Count Rate ^{a,b}		
	Pu-239 (Disc)	Th-230 (Disc)	Th-230 (Distributed)
Contact	1	1	1
0.5	0.808 ± 0.013 ^c	0.812 ± 0.010	0.761 ± 0.026
1	0.656 ± 0.015	0.606 ± 0.012	0.579 ± 0.021
2	0.1974 ± 0.0046	0.0423 ± 0.0027	0.0990 ± 0.0093

^aNormalized net count rate determined by dividing the net count rate at each distance by the net count rate at contact with the source.

^bGas proportional detectors operated in the α mode were used for all measurements.

^cUncertainties represent the 95% confidence interval, based on propagating the counting errors in each measurement.

Table 4.6 Minimum Detectable Concentrations for Various Source-to-Detector Distances for β Emitters

Distance From Source (cm)	Total Efficiency (c/dls) and Minimum Detectable Concentration (dpm/100 cm ²) ^{a,b}											
	Ni-63		C-14		Tc-99 (Disc)		Tc-99 (Distributed)		Tl-204		Sr-Y-90	
	EFF	MDC	EFF	MDC	EFF	MDC	EFF	MDC	EFF	MDC	EFF	MDC
Contact	0.0360 ± 0.0041*	2,000 ± 250	0.1006 ± 0.0051	715 ± 51	0.250 ± 0.010	287 ± 19	0.207 ± 0.016	347 ± 32	0.338 ± 0.015	213 ± 14	0.464 ± 0.016	154.9 ± 9.5
0.5	0.0137 ± 0.0019	5,250 ± 760	0.0790 ± 0.0034	910 ± 61	0.2164 ± 0.0090	332 ± 22	0.166 ± 0.013	433 ± 41	0.308 ± 0.013	234 ± 16	0.427 ± 0.014	169 ± 10
1	0.0071 ± 0.0018	10,200 ± 2,600	0.0652 ± 0.0040	1,103 ± 88	0.1947 ± 0.0076	369 ± 24	0.145 ± 0.012	496 ± 49	0.282 ± 0.013	255 ± 18	0.396 ± 0.014	181 ± 11
2	0.0014 ± 0.0015	52,000 ± 56,000	0.0434 ± 0.0029	1,660 ± 140	0.1482 ± 0.0060	485 ± 32	0.1042 ± 0.0086	690 ± 67	0.218 ± 0.014	330 ± 27	0.325 ± 0.011	221 ± 14

^aMeasurements performed with a gas proportional detector operated in the $\alpha + \beta$ mode with an 0.8-mg/cm² window density thickness.

^bThe instrument background was 355 counts and probe area corrections of 126 cm² were made for the gas proportional detectors. The following MDC equation was used for 1-minute counts:

$$MDC = \frac{3 + 4.65 \sqrt{C_B}}{KT}$$

^cUncertainties represent the 95% confidence interval, based on propagating the errors in the calibration source activity and in counting statistics.

Table 4.7 Minimum Detectable Concentrations for Various Source-to-Detector Distances for α Emitters

Distance From Source (cm)	Total Efficiency (c/dis) and Minimum Detectable Concentration (dpm/100 cm ²) ^{a,b}					
	Pu-239 (Disc)		Th-230 (Disc)		Th-230 (Distributed)	
	EFF	MDC	EFF	MDC	EFF	MDC
Contact	0.2549 ± 0.0053 ^c	24 ± 14	0.2495 ± 0.0044	24 ± 15	0.2002 ± 0.097	30 ± 18
0.5	0.2061 ± 0.0036	29 ± 18	0.1910 ± 0.0034	32 ± 19	0.1524 ± 0.0067	40 ± 24
1	0.1672 ± 0.0040	36 ± 22	0.1426 ± 0.0034	43 ± 26	0.1160 ± 0.0052	52 ± 32
2	0.0503 ± 0.0012	121 ± 73	0.00994 ± 0.00069	610 ± 370	0.0198 ± 0.0019	310 ± 190

^aMeasurements performed with a gas proportional detector operated in the α mode with a 0.8 mg/cm² window density thickness.

^bThe instrument background was 1 count and probe area corrections of 126 cm² were made for the gas proportional detectors. The following MDC equation was used for 1-minute counts:

$$MDC = \frac{3 + 4.65 \sqrt{C_B}}{KT}$$

^cUncertainties represent the 95% confidence interval, based on propagating the errors in the calibration source activity and in counting statistics.

Table 4.8 Window Density Thickness Effects for β Emitters

Window Density Thickness (mg/cm ²)	Total Efficiency (Counts Per Disintegration) ^a					
	Ni-63 (Disc)	C-14 (Disc)	Tc-99 (Disc)	Tc-99 (Distributed)	Tl-204 (Disc)	SrY-90 (Disc)
0.3	0.0695 ± 0.0041 ^b	0.1273 ± 0.0032	0.288 ± 0.011	0.227 ± 0.018	0.354 ± 0.018	0.477 ± 0.017
0.4	0.0699 ± 0.0032	0.1302 ± 0.0039	0.291 ± 0.011	0.224 ± 0.018	0.359 ± 0.015	0.482 ± 0.019
0.8	0.0409 ± 0.0020	0.1096 ± 0.0032	0.266 ± 0.011	0.209 ± 0.017	0.342 ± 0.015	0.474 ± 0.017
1.3	— ^c	—	0.247 ± 0.010	0.196 ± 0.016	—	—
1.8	—	—	0.2268 ± 0.0092	0.183 ± 0.015	—	—
2.3	—	—	0.2117 ± 0.0090	0.170 ± 0.013	—	—
2.8	—	—	0.1980 ± 0.0085	0.157 ± 0.012	—	—
3.3	—	—	0.1848 ± 0.0074	0.149 ± 0.012	—	—
3.8	0.0005 ± 0.0011	0.0383 ± 0.0018	0.1638 ± 0.0064	0.129 ± 0.010	0.275 ± 0.012	0.429 ± 0.015

^aGas proportional detectors operated in the $\alpha + \beta$ mode^b were used for all measurements.

^bUncertainties represent the 95% confidence interval, based on propagating the errors in the calibration source activity and in counting statistics.

^cMeasurement not performed.

1 **Table 4.9 Minimum Detectable Concentrations for Various Window Density Thicknesses**

2

3

Window Density Thickness (mg/cm ²)	Minimum Detectable Concentration (dpm/100 cm ²) ^{a,b}					
	Ni-63 (Disc)	C-14 (Disc)	Tc-99 (Disc)	Tc-99 (Distributed)	Tl-204 (Disc)	SrY-90 (Disc)
4 0.3	1,014 ± 80 ^c	554 ± 32	245 ± 16	311 ± 30	199 ± 14	147.9 ± 9.4
5 0.4	1,016 ± 71	546 ± 33	244 ± 16	317 ± 30	198 ± 13	147.3 ± 9.6
6 0.8	1,760 ± 120	656 ± 39	270 ± 18	344 ± 32	210 ± 14	151.8 ± 9.6
7 1.3	— ^d	—	291 ± 19	367 ± 34	—	—
8 1.8	—	—	317 ± 21	392 ± 38	—	—
9 2.3	—	—	340 ± 23	423 ± 40	—	—
10 2.8	—	—	363 ± 24	457 ± 43	—	—
11 3.3	—	—	389 ± 25	482 ± 46	—	—
12 3.8	130,000 ± 290,000	1,860 ± 130	435 ± 28	555 ± 52	259 ± 18	166 ± 10

13 ^aGas proportional detectors operated in the α + β mode were used for all measurements.

14 ^bBackground levels were determined for each window density thickness and efficiencies were used from Table 4.8. Probe area corrections of 126 cm² were made for the gas proportional detectors. The following MDC equation was used for 1-minute counts:

$$MDC = \frac{3 + 4.65 \sqrt{C_B}}{KT}$$

16 ^cUncertainties represent the 95% confidence interval, based on propagating the errors in the calibration source activity and in counting statistics.

17 ^dMeasurement not performed.

Table 4.10 Source Geometry Effects on Instrument Efficiency

Source Geometry	Instrument Efficiency ^a			
	Te-99		Th-230	
	$\alpha + \beta$	β only	GM	ZnS
Point (Disc) Source ^b	0.445 ± 0.017 ^c	0.253 ± 0.010	0.278 ± 0.012	0.3304 ± 0.0068
Distributed Source ^d	0.382 ± 0.030	0.199 ± 0.016	0.195 ± 0.023	0.313 ± 0.016
Ratio of Point-to-Distributed Source	1.16	1.27	1.42	1.25

^aThe instrument efficiency was determined by dividing the net count rate by the 2 π emission rate of the source.

^bThe point (disc) source area for both Te-99 and Th-230 was 5 cm².

^cUncertainties represent the 95% confidence interval, based on propagating the errors in the calibration source emission rate and in counting statistics.

^dThe distributed source area for both Te-99 and Th-230 was 126 cm².

1

2

3

4

5

6

7

8

9

Table 4.11 Ambient Background Effects

Variables Affecting Instrument MDCs

Background ^a (cpm)	Gross Counts (cpm)	Measured Activity ^b (dpm)	MDC ^c (dpm)
53.0 ± 9.2 ^d	295 ± 32	1,420 ± 190	220
117 ± 22	375 ± 26	1,520 ± 200	310
145 ± 20	413 ± 56	1,580 ± 350	350
192 ± 26	399 ± 38	1,220 ± 270	400
223 ± 26	458 ± 35	1,380 ± 280	430
291 ± 44	538 ± 54	1,450 ± 410	480
445 ± 46	725 ± 66	1,650 ± 480	590
594 ± 42	815 ± 38	1,300 ± 330	680
1,021 ± 38	1,223 ± 55	1,190 ± 390	890
1,490 ± 100	1,642 ± 91	880 ± 800	1,070

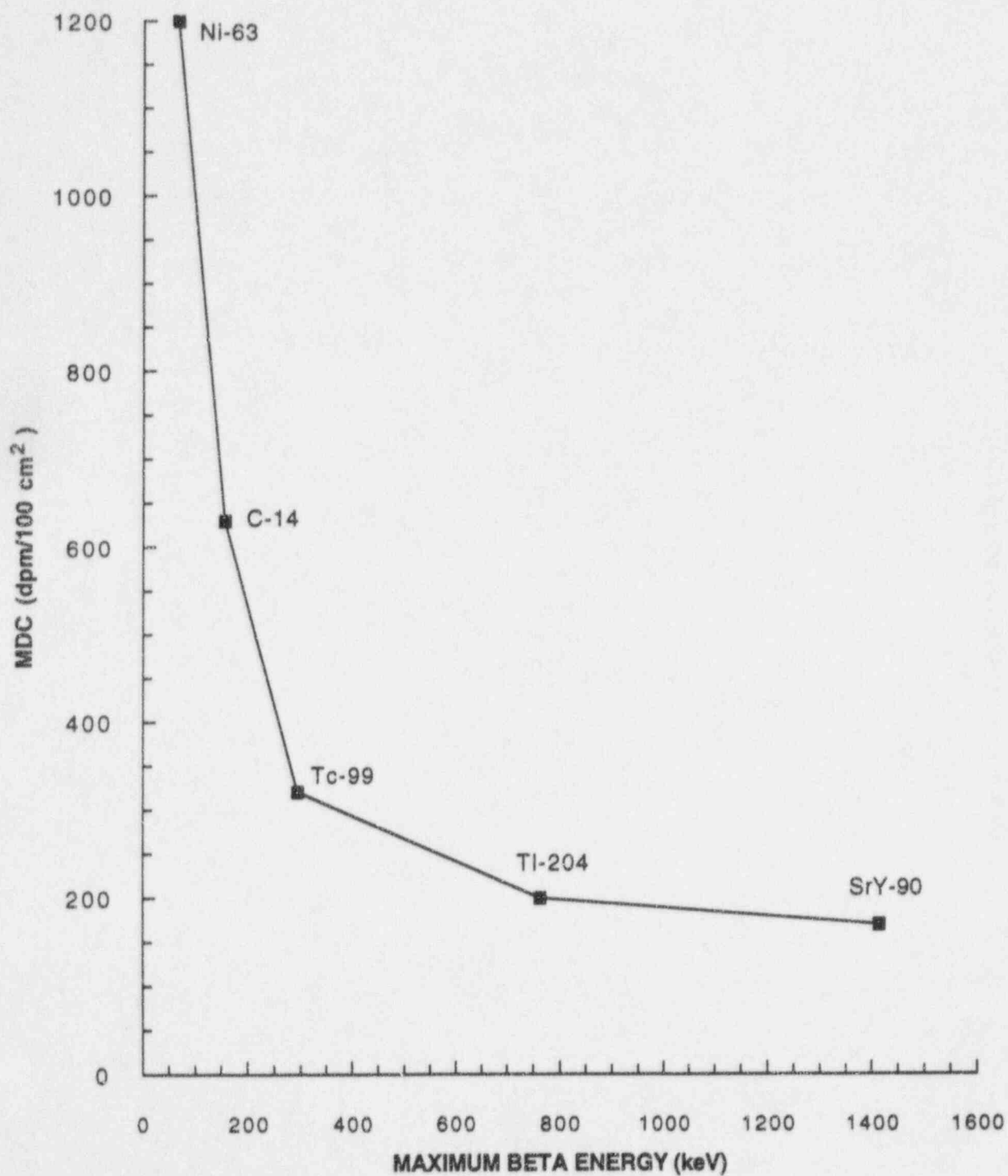
^aMeasurements performed with an Eberline HP-260 GM detector.

^bMeasured activity was calculated by subtracting the background from the gross counts and dividing by a total efficiency of 0.17 count per disintegration. Gross counts were determined by the average of five 1-minute measurements of a Tc-99 source.

^cThe following MDC equation was used for 1-minute counts and an assumed efficiency of 0.17 counts per disintegration:

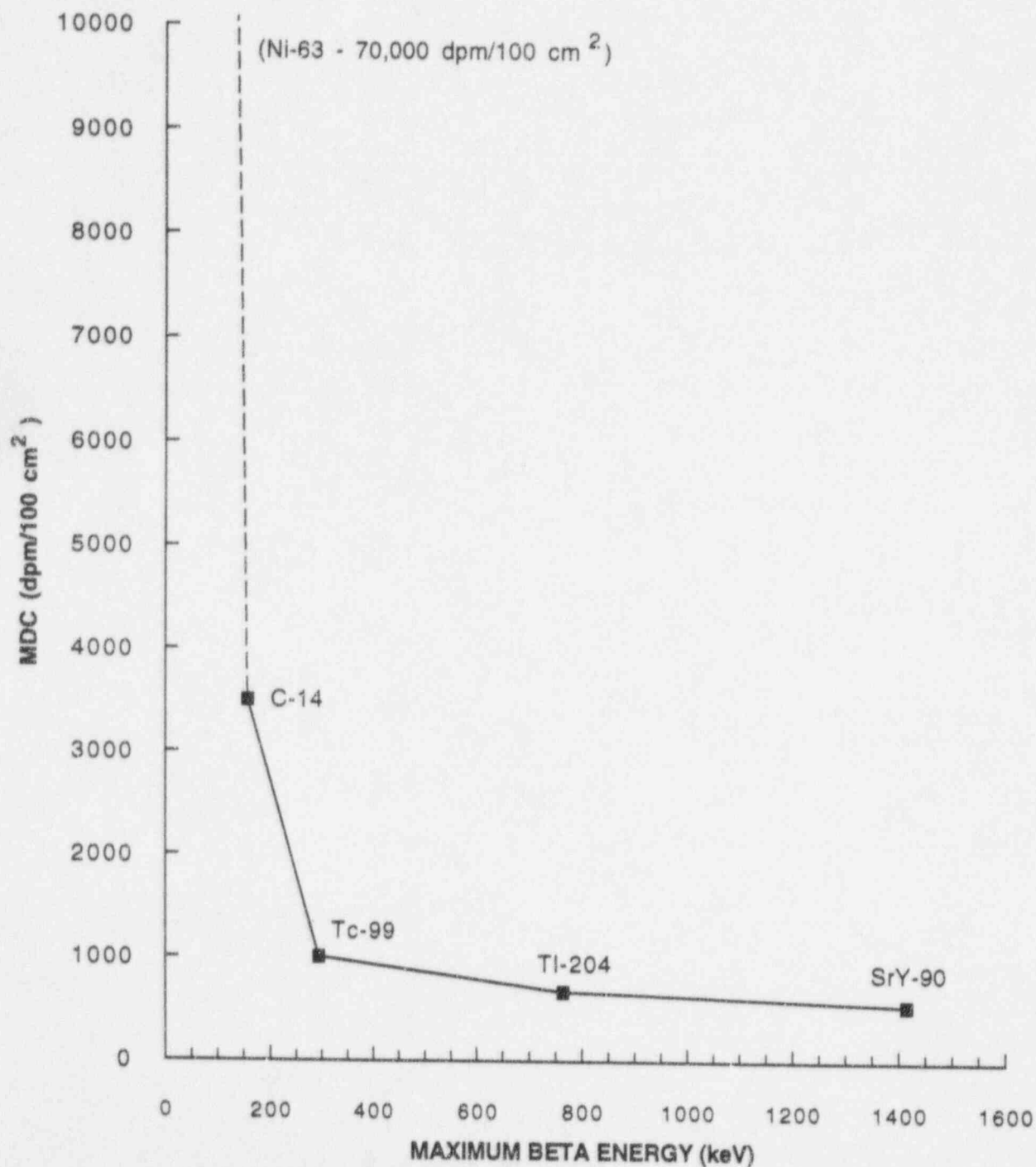
$$MDC = \frac{3 + 4.65 \sqrt{C_B}}{KT}$$

^dUncertainties represent the 95% confidence interval, based on propagating the counting errors in each measurement.

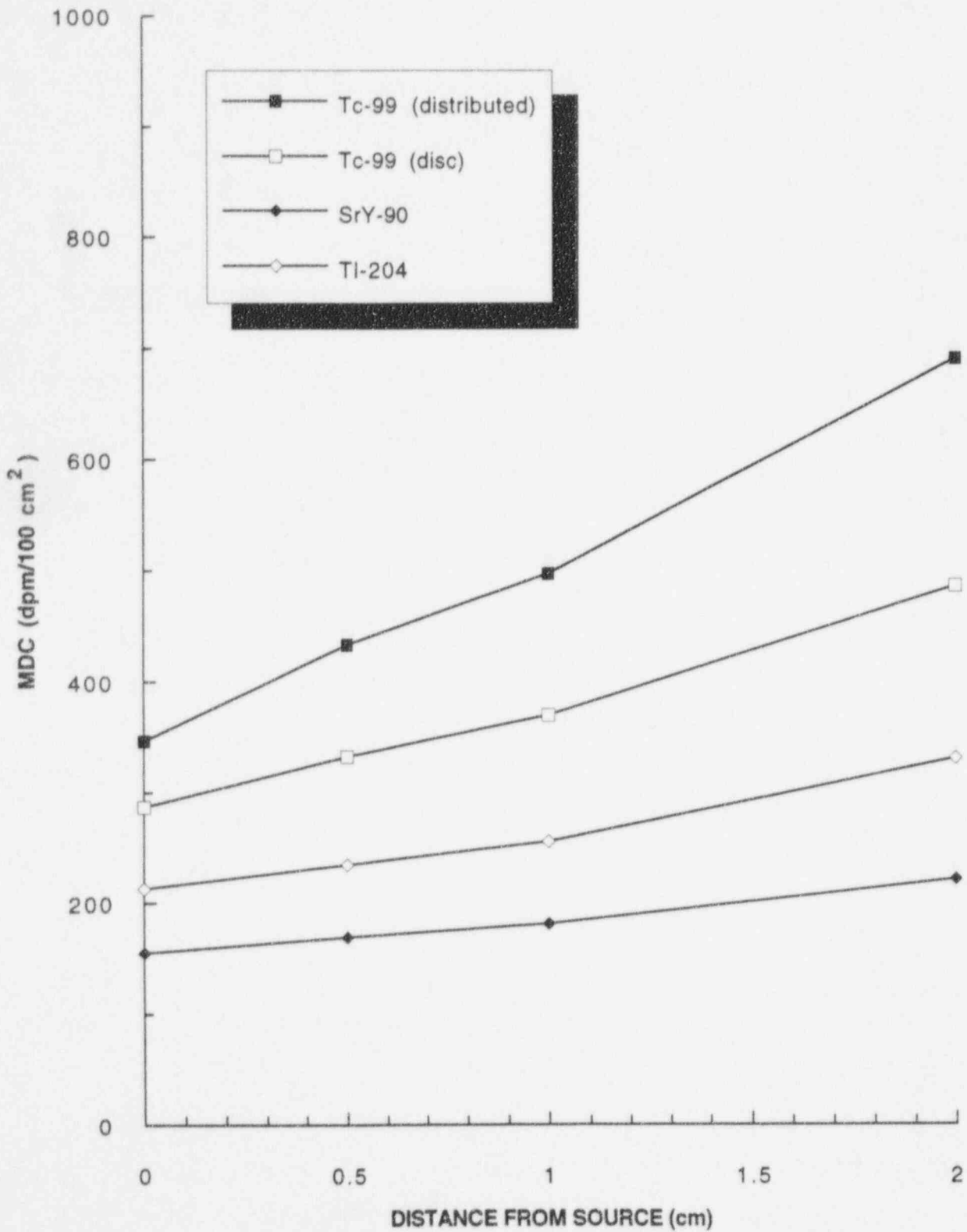


1 Figure 4.1 MDCs for Gas Proportional Detector ($\alpha+\beta$ Mode) for Various Radionuclides

Variables Affecting Instrument MDCs

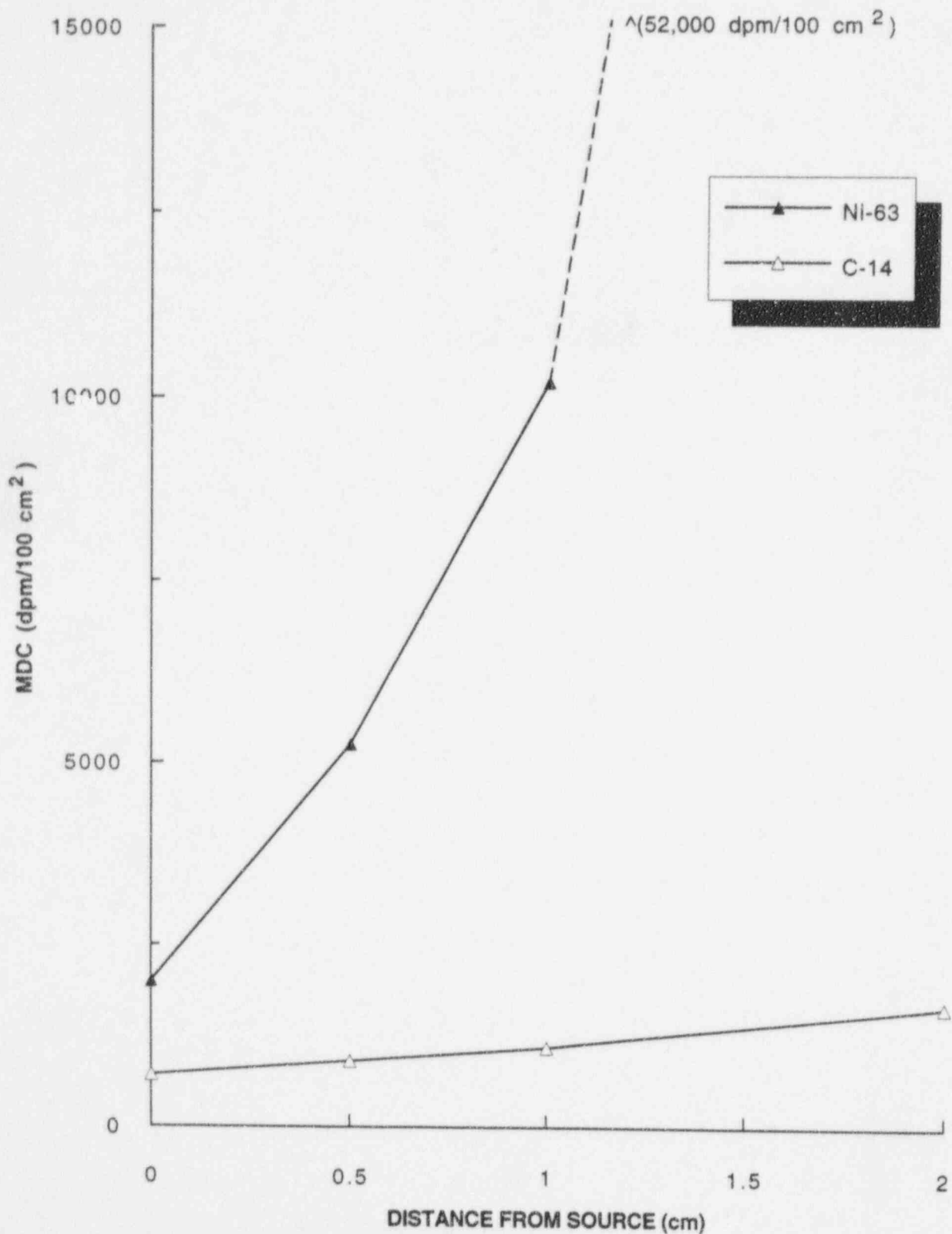


1 Figure 4.2 MDCs for GM Detector for Various Radionuclides

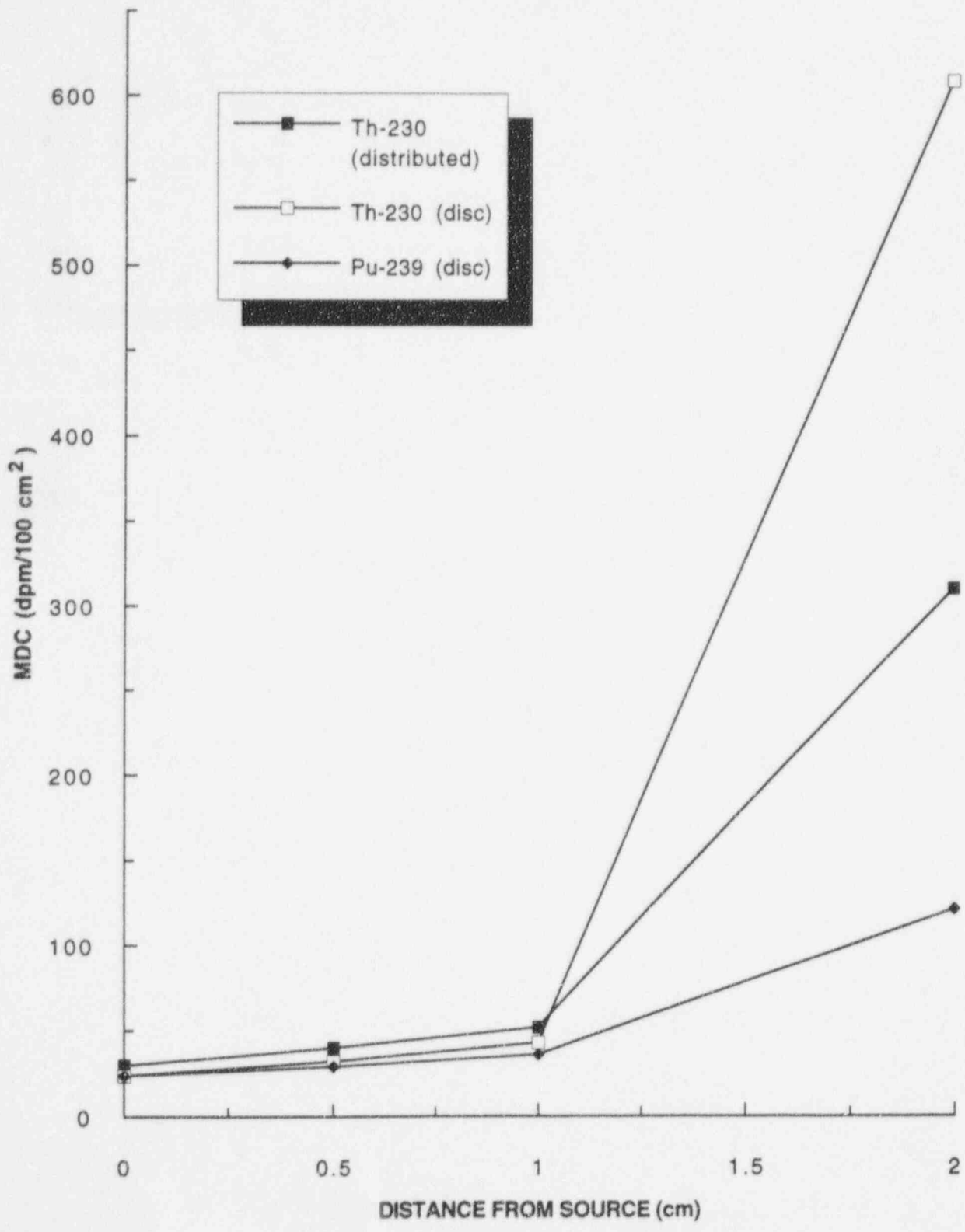


1 Figure 4.3 Source-to-Detector Distance Effects on MDC for Higher Energy β Emitters

Variables Affecting Instrument MDCs

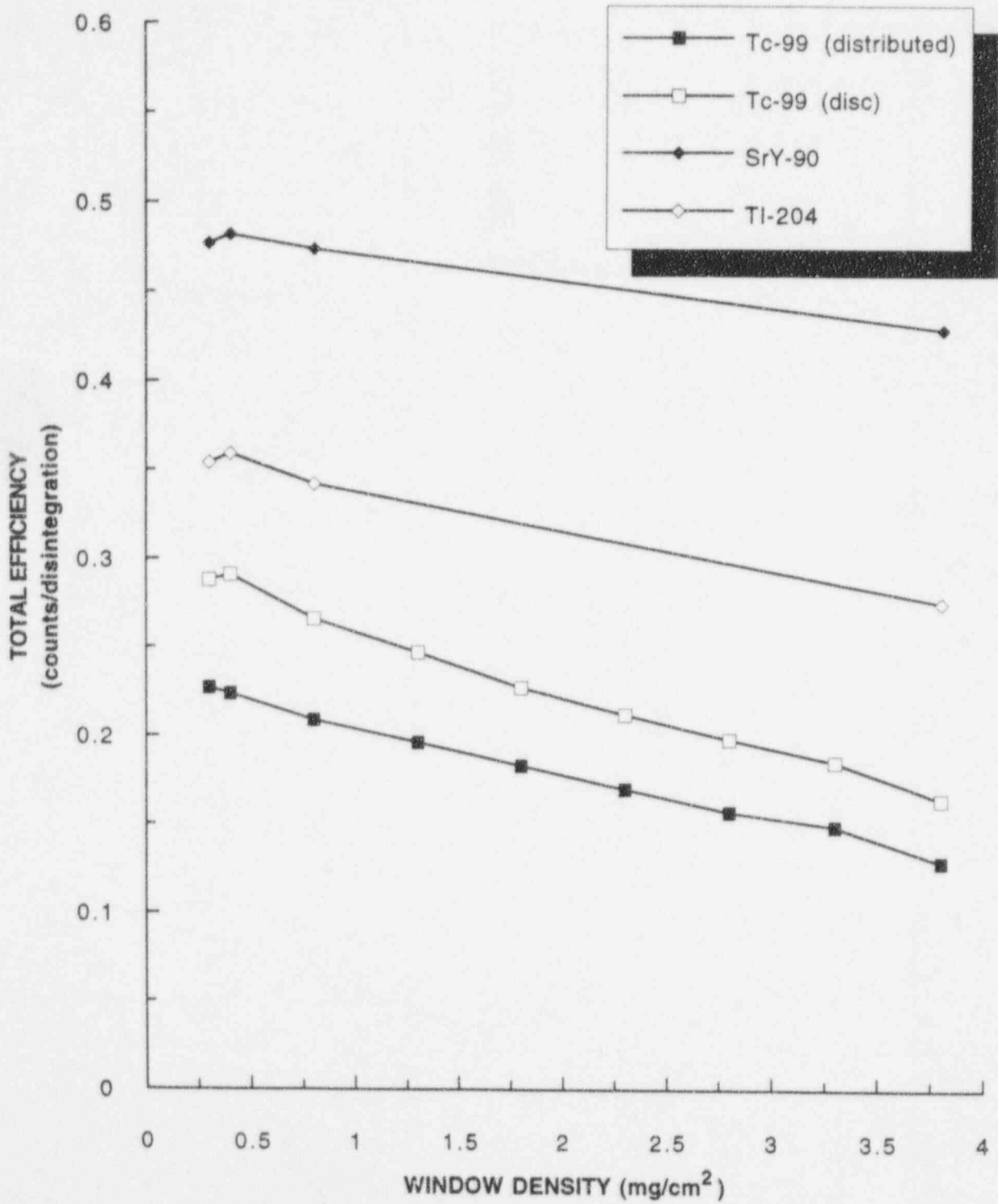


1 Figure 4.4 Source-to-Detector Distance Effects on MDC for Lower Energy β Emitters



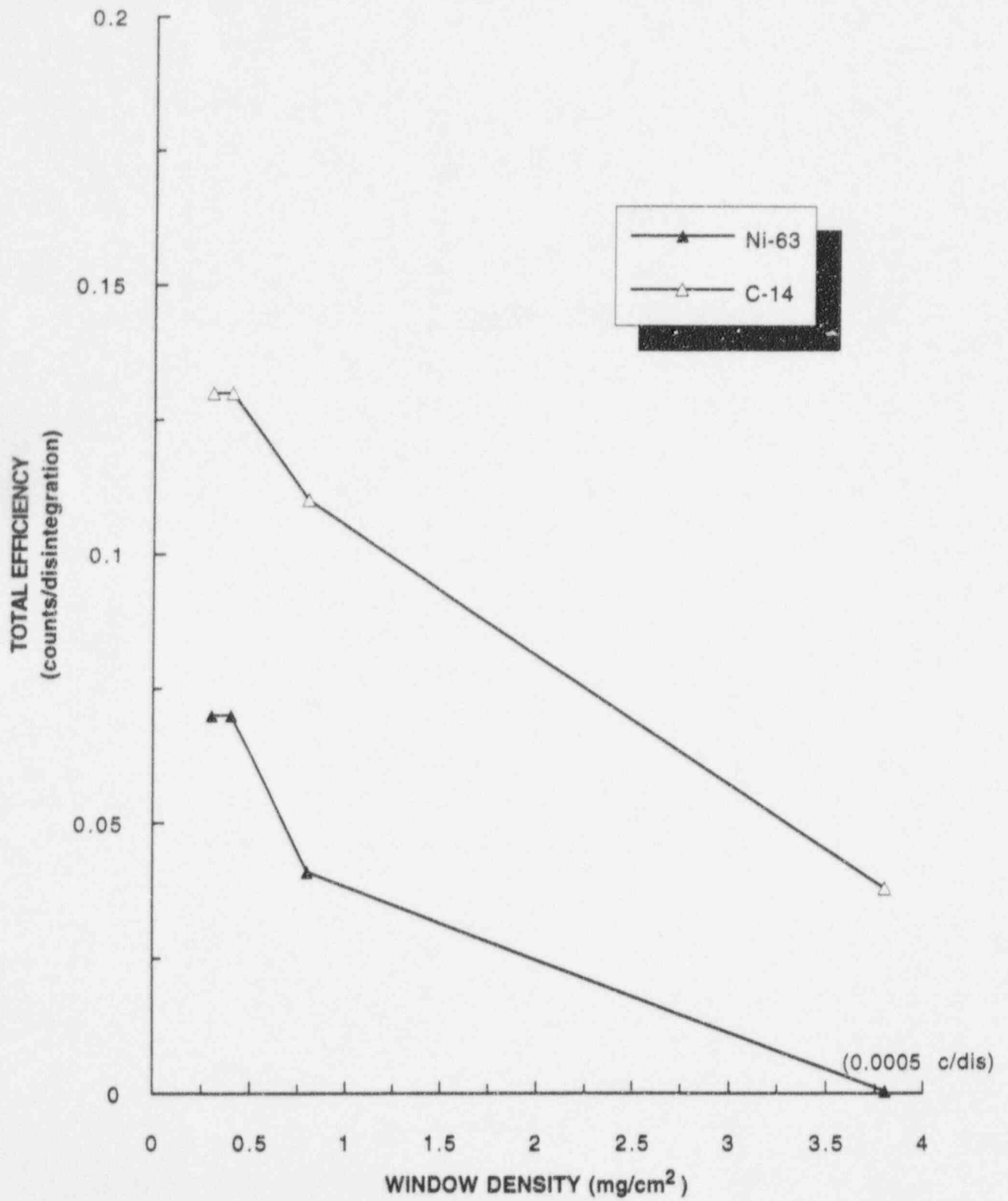
1 Figure 4.5 Source-to-Detector Distance Effects on MDC for α Emitters

Variables Affecting Instrument MDCs



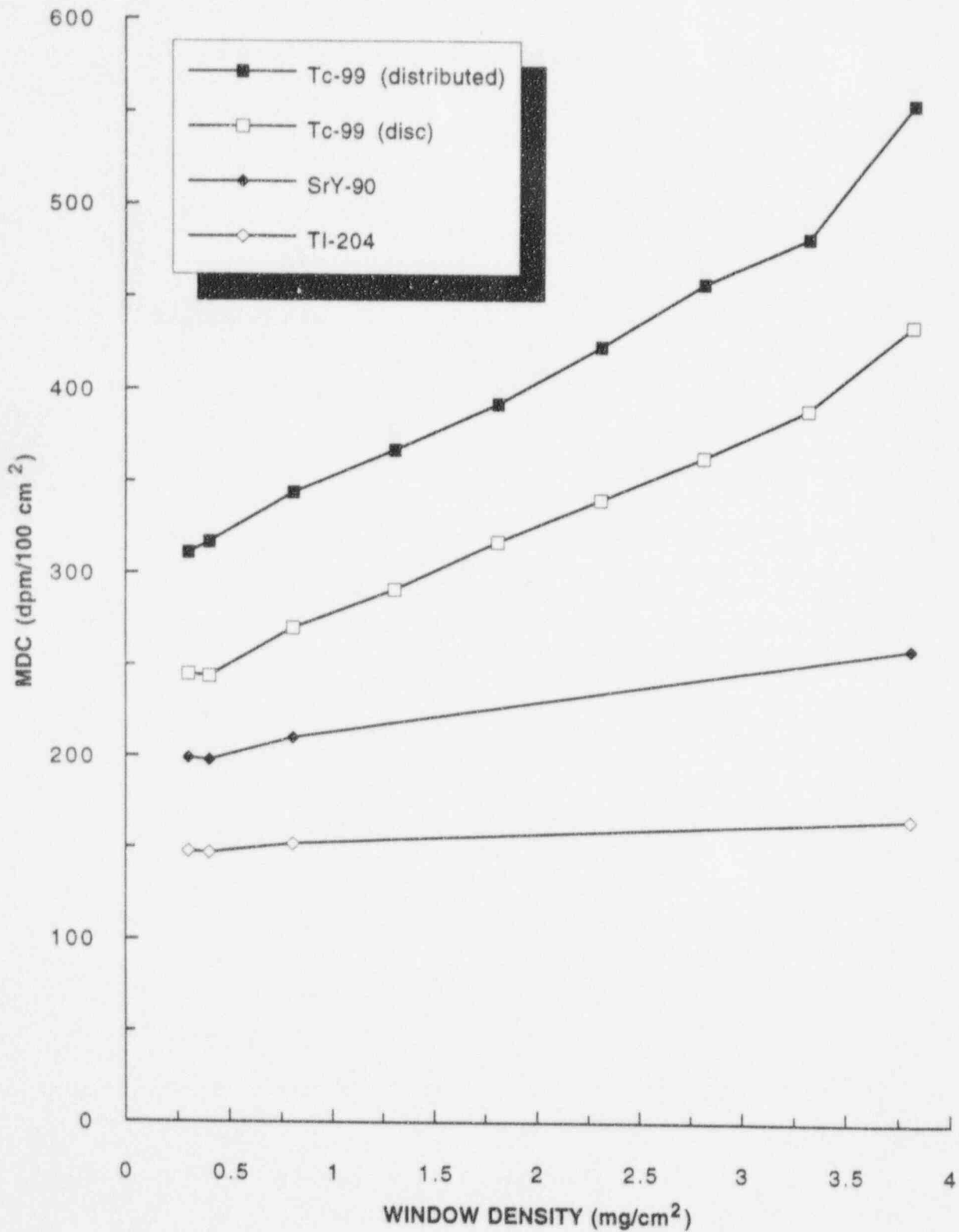
1
2

Figure 4.6 Effects of Window Density Thickness on Total Efficiency for Higher Energy β Emitters

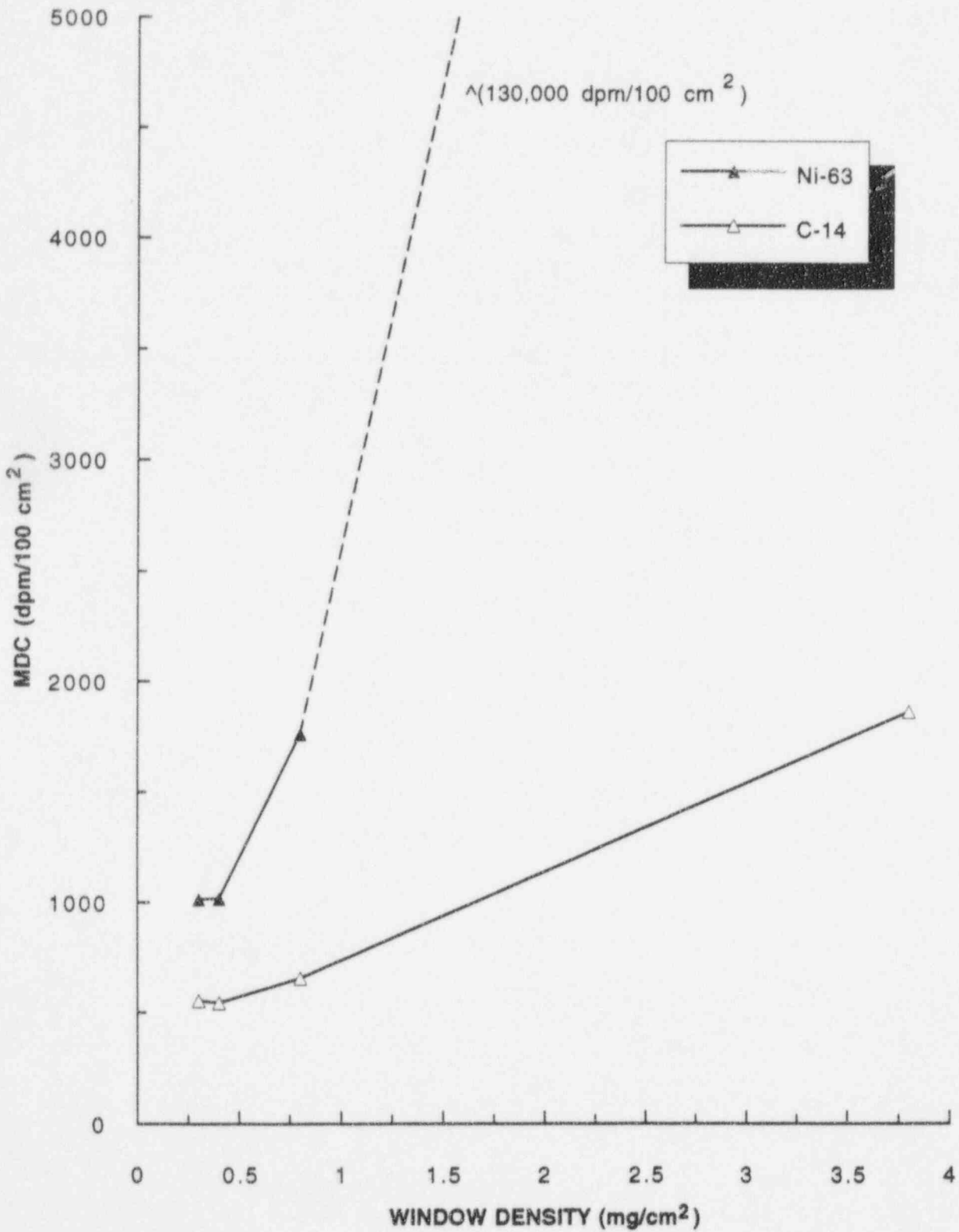


1 Figure 4.7 Effects of Window Density Thickness on Total Efficiency for Lower Energy β
 2 Emitters

Variables Affecting Instrument MDCs

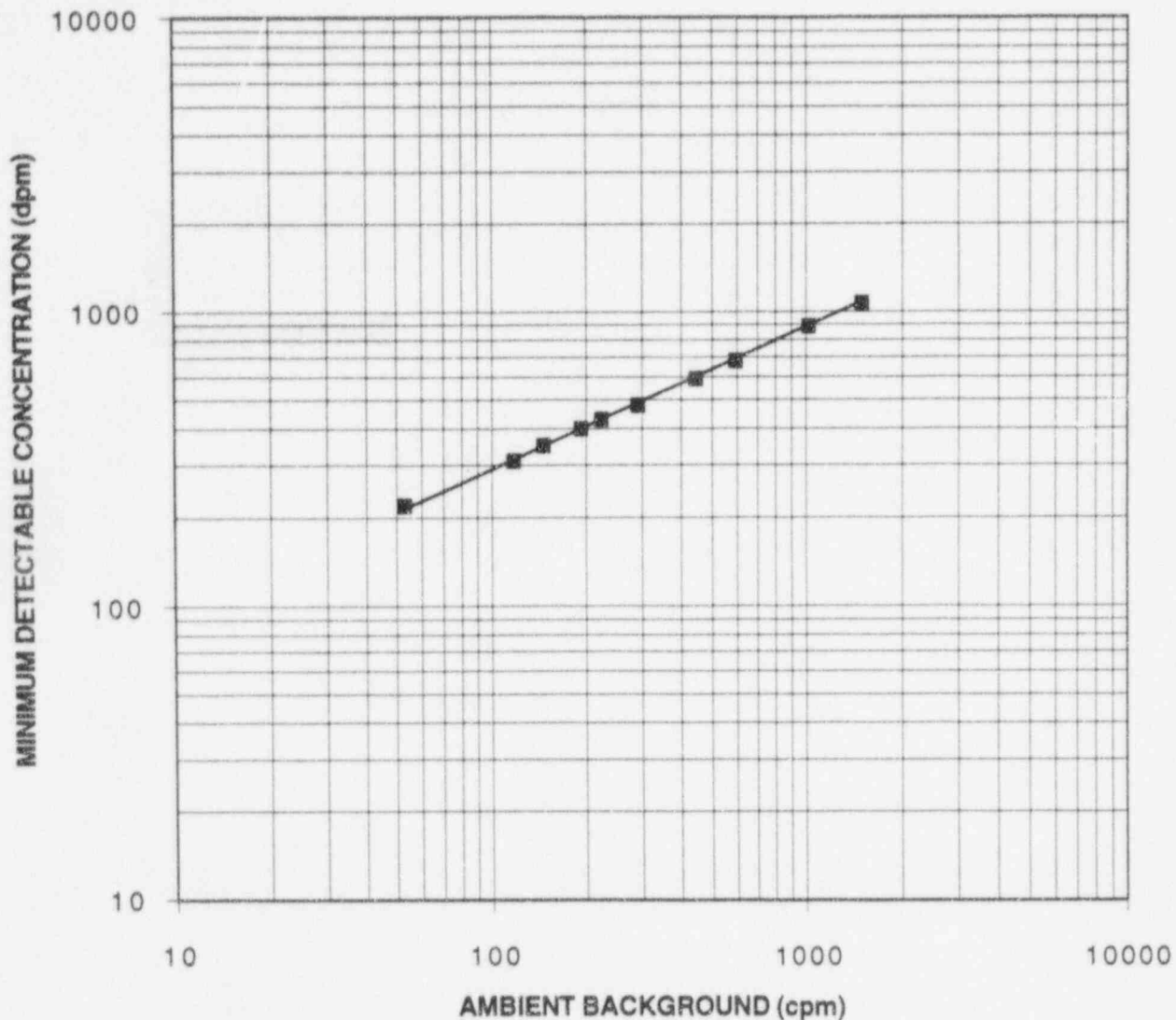


1 Figure 4.8 Effects of Window Density Thickness on MCD for Higher Energy β Emitters



1 Figure 4.9 Effects of Window Density Thickness on MCD for Lower Energy β Emitters

Variables Affecting Instrument MDCs



1 Figure 4.10 Effects of Ambient Background on MDC Calculation

5 VARIABLES AFFECTING MINIMUM DETECTABLE CONCENTRATIONS IN THE FIELD

Surface activity levels are assessed by converting detector response, through the use of a calibration factor, to radioactivity. Once the detector has been calibrated and an instrument efficiency (ϵ_i) established, several factors must still be carefully considered when using that instrument in the field. These factors involve the background count rate for the particular surface and the surface efficiency (ϵ_s), which include the physical composition of the surface and any surface coatings. Ideally, the surveyor should use experimentally determined surface efficiencies for the anticipated field conditions. The surveyor needs to know how and to what degree these different field conditions can affect the sensitivity of the instrument. A particular field condition may significantly affect the usefulness of a particular instrument (e.g., wet surfaces for alpha measurements or scabbled surfaces for low-energy beta measurements).

One of the more significant implicit assumptions made during instrument calibration and subsequent use of the instrument in the field is that the composition and geometry of contamination in the field is the same as that of the calibration source. This may not be the case, considering that many calibration sources are fabricated from materials different (e.g., activity plated on a metallic disc) from those that comprise the surfaces of interest in the field (Walker 1994). This difference usually manifests itself in the varying backscatter characteristics of the calibration and field surface materials.

Generally, it will be necessary to recalculate the instrument MDC to adjust for the field conditions. However, for most of the items discussed below, the detection limit (in net counts or net count rate) remains the same, but the MDC may be different. In this study, the effects of typically encountered surface types and field conditions were evaluated quantitatively. These are discussed in the following sections.

5.1 Background Count Rates for Various Materials

Several different types of surface materials may be encountered in a facility undergoing decommissioning. Among the typical surface materials that were evaluated in this study were (a) brick, (b) ceramic block, (c) ceramic tile, (d) concrete block, (e) unpainted drywall, (f) vinyl floor tile, (g) linoleum, (h) steel, (i) wood pine treated with a commercially available water sealant product, and (j) untreated pine. The main difference considered was the background activity associated with each of these types of surface materials. In most cases, the background count rate for that type of surface needs to be determined and a new MDC established, provided that the specific surface type was not considered in the initial evaluation of the instrument's MDC.

Ambient background count rates were initially determined for gas proportional, ZnS scintillation, GM, and NaI scintillation detectors. Three variations were used for the gas proportional detectors: (a) detection of alpha radiation only (using a high voltage setting that discriminated all beta pulses), (b) detection of beta radiation only (using sufficient window density thickness to block alpha radiation), and (c) detection of alpha and beta radiation. Results of ambient

Variables Affecting MDCs in the Field

1 background count rates are in Table 5.1. The ambient backgrounds were determined at the same
2 location for all the tested surface materials and, as such, the ambient background was sometimes
3 greater than a particular surface material background. This result was considered acceptable
4 because a primary objective of this study was to evaluate detector responses in as close to field
5 conditions as possible.

6 Background count rates were obtained for ten surface materials using the same instrument/
7 detector combinations that were used to determine the ambient background. In general,
8 background count rates were lowest for the linoleum, carbon steel, and wood, and highest for the
9 brick and ceramic materials (Table 5.1). These background count rates will vary depending on
10 the local area background radiation levels; however, the data provide information on the relative
11 backgrounds in common construction materials.

12 MDCs for the gas proportional detectors operated in both the alpha-only and beta-only modes
13 were calculated for each of the surface materials assuming a total efficiency (ϵ_{tot}) of 0.20 and
14 0.25 count per disintegration, for alpha and beta, respectively (Table 5.2). The MDCs were
15 calculated from Equation 3-9, using the background count rates presented in Table 5.1. The
16 MDCs in the alpha-only mode ranged from 28 to 83 dpm/100 cm², while the MDCs in the beta-
17 only mode ranged from 268 to 425 dpm/100 cm². Since the detector MDC varies directly with
18 the background count rate, the lowest MDCs were obtained for linoleum, carbon steel and wood,
19 and concrete block and drywall, while the highest MDCs were for brick and ceramic materials.
20 Figures 5.1 and 5.2 illustrate the effect of surface material background count rates on detector
21 MDC for the gas proportional detectors operated in both the alpha-only and beta-only modes,
22 respectively. These figures demonstrate the importance of carefully assessing the alpha
23 background for various surface materials due to the wide range of MDC values. This is in
24 contrast to the beta MDCs, which are fairly consistent for all materials examined, with the notable
25 exception of brick and ceramics. In application, it is important that the surveyor establish specific
26 material backgrounds that are representative of the surface types and field conditions.

27 The reader is referred to NUREG-1501, "Background as a Residual Radioactivity Criterion for
28 Decommissioning," for additional information on background radionuclide concentrations.

29 5.2 Effects of Surface Condition on Detection Sensitivity

30 The conversion of the surface emission rate to the activity of the contamination source is often a
31 complicated task that may result in significant uncertainty if there are deviations from the assumed
32 source geometry. For example, consider the measurement error associated with an alpha surface
33 activity measurement on a rough surface, such as scabbled concrete, where substantial attenuation
34 reduces the count rate as compared to the calibration performed on the smooth surface of a
35 National Institute of Standards and Technology (NIST) traceable source.

36 The effects of surface condition on detection sensitivity were evaluated for surfaces commonly
37 encountered during decommissioning surveys. The surfaces studied were abraded (scabbled)
38 concrete, finished (sealed) concrete, carbon steel, stainless steel, and wood. The results of this
39 study provide a quantitative range of how various surface conditions may affect the detectability
40 of various contaminants.

1 5.2.1 Surface Preparation

2 For this study, known quantities of NIST traceable Tc-99 and Th-230 standard sources, in
3 aqueous solutions, were dispensed on each of the surfaces. The preparation of the reference
4 sources from the traceable solution involved measurement uncertainties (e.g., pipetting errors,
5 volumetric determinations) that were propagated into the overall statement of uncertainty.

6 Background count rates were obtained for instrument/surface combinations that were used to
7 determine the surface activity measurements, so that the proper background could be subtracted
8 from the gross counts. For the surface materials studied, the Tc-99 and Th-230 were dispensed
9 to simulate both a point source and distributed source geometry (it should be noted that the Tc-99
10 and Th-230 were not mixed, but were dispensed on separate areas of each surface). The areal
11 extent of the point source activity ranged from approximately 5 to 10 cm², while the distributed
12 source geometry was fabricated by uniformly depositing droplets of the Tc-99 and Th-230 activity
13 over a larger area (126 cm²). The total Tc-99 activity dispensed in the point source geometry was
14 2828 ± 91 dpm, while 4595 ± 79 dpm of Th-230 was dispensed in a point source geometry. The
15 Tc-99 and Th-230 activity dispensed in the distributed source geometry was 2830 ± 100 dpm and
16 4600 ± 170 dpm, respectively. Once dispensed, the radioactive material was allowed to dry
17 overnight in a ventilated hood.

18 Uniformity measurements with a GM detector for distributed sources were performed to evaluate
19 how well the activity was spread over the surfaces (refer to Section 5.3.1 for a detailed
20 description of uniformity measurements). It was important that the activity was precisely
21 distributed the same for each of the materials. Because the instrument response is dependent on
22 the source geometry (Section 4.4), the instrument efficiencies (ϵ_i) determined by placing the
23 detectors in contact with the NIST-traceable plate sources were applicable to the measurements
24 performed on the Oak Ridge Institute for Science and Education (ORISE) fabricated sources
25 provided that the activity was uniformly deposited over the same active area (126 cm²) as the
26 NIST-traceable source. It should be noted that the preparation of a scabbled surface source by
27 deposition on a "pre-scabbled" surface may not be representative of the actual field surface
28 condition. That is, on a real scabbled surface the activity will likely be concentrated in the "peaks"
29 or undisturbed surface, and will be absent in the "valleys."

30 5.2.2 Measurement Results for Various Surface Types

31 Beta measurements were performed with gas proportional and GM detectors. Two variations
32 were used for the gas proportional detectors: detection of beta radiation only (using 3.8-mg/cm²
33 window density thickness to block alpha radiation) and detection of alpha plus beta radiation.
34 Five 1-minute measurements were made for each combination of material, geometry, and surface
35 material. The results are presented in Table 5.3. Alpha measurements were performed with gas
36 proportional (α -only mode) and ZnS detectors. Results are presented in Table 5.4. Both alpha
37 and beta measurements were taken at contact with the sources. The total efficiency for the point
38 source geometry was determined by simply dividing the average net count rate by the
39 activity dispensed. No correction for the decay of Tc-99 or Th-230 was necessary because of
40 their long half-lives. The total efficiency for the distributed source was determined by the
41 following equation:

Variables Affecting MDCs in the Field

$$\text{Total Efficiency} = \frac{\text{Net Count Rate}}{\left(\frac{\text{Total Activity}}{126 \text{ cm}^2} \right) \text{ Probe Area}} \quad (5-1)$$

1 The total efficiencies determined for the distributed activity on surfaces should use the active or
2 physical probe area, as opposed to the effective probe area, in converting instrument response to
3 surface activity. During instrument calibration, the total efficiency is determined by placing the
4 probe in contact with the calibration source and recording the net counts, and then dividing by the
5 activity of the source. No correction is made for the fact that the probe has a protective screen;
6 the total efficiency and instrument efficiency take into consideration the fact that part of the active
7 area of the probe is covered and may be insensitive to incident radiation. Thus, surface activity
8 measurements in the field should be corrected for the physical area of the probe, with no
9 corrections made for the protective screen, to be consistent with the manner in which the
10 instrument was calibrated. Refer to Section 2 for the comparison of the physical (active) probe
11 area and the effective probe area for each of the detectors studied.

12 The source efficiencies, ϵ_s , were calculated by dividing the total efficiency by the instrument
13 efficiency. The instrument efficiencies were determined for each detector and geometry using
14 appropriate NIST-traceable sources. As discussed in Section 4, following the ISO-7503-1
15 guidance for surface activity measurements requires knowledge of both the instrument and source
16 efficiencies. The instrument efficiency, ϵ_i , is determined during calibration using the stated 2π
17 emission rate of the source. Source efficiencies must be experimentally determined for a given
18 surface type and coating. Tables 5.3 and 5.4 present experimental data on source efficiencies for
19 several common surface types. The data indicate that the source efficiency varies widely
20 depending on the amount of self-absorption and backscatter provided by the surface. The total
21 efficiencies may be determined from Tables 5.3 and 5.4 by simply taking the product of ϵ_i and ϵ_s .

22 The total efficiencies for Tc-99 and Th-230 on various surfaces determined from this experiment
23 may be compared to the average detector efficiencies (historical calibration data from the
24 Environmental Survey and Site Assessment Program (ESSAP) of ORISE) presented in Table 4.2.
25 The average Tc-99 total efficiency for a gas proportional detector operated in an alpha plus beta
26 mode was 0.22 c/dis (on a NIST-traceable source). This study indicates that this is a valid total
27 efficiency to use for untreated wood in a point source geometry (for $\alpha + \beta$ on treated wood, ϵ_i
28 multiplied by ϵ_s equals 0.23), but may be overly conservative for stainless steel surfaces and
29 grossly nonconservative for scabbled concrete. Similarly for the Th-230, the average total
30 efficiencies during calibration were 0.18 and 0.19 c/dis, respectively, for the ZnS and gas
31 proportional (alpha only mode). This study indicates that for a point source geometry on treated
32 wood, the total efficiency is less than 50 percent of the average alpha total efficiency (0.097 and
33 0.061, respectively, for α -only and ZnS detectors), and for scabbled concrete, the alpha total
34 efficiency is approximately 50 to 75 percent of the total efficiency obtained from historic
35 Environmental Survey and Site Assessment Program (ESSAP) calibration data. The effect of
36 reduced total efficiency in the field is an increase in the survey instrumentation MDCs. Table 5.5
37 gives information on the MDCs for these surface types.

1 The minimum detectable concentrations shown in Table 5.5 reflect the differences in the source
2 efficiency for each surface. That is, the background, counting time, and instrument efficiency
3 were constant for each given detector and geometry. The large variations in MDC for the surface
4 types studied should be noted. For example, using an $\alpha + \beta$ gas proportional detector to measure
5 Tc-99 distributed over a 126-cm² area has an MDC range of 260 to 950 dpm/100 cm², depending
6 on the surface type. However, it is the lower bound value that is typically calculated and used as
7 the MDC (because the calibration is performed on a clean, high-backscatter reference source, with
8 no consideration given to the actual surface measured). Furthermore, if the uncertainty in the
9 total efficiency is incorporated into the MDC equation (refer to Equation 3-11), the MDC for
10 finished concrete is 2,300 dpm/100 cm² (compared to 950 dpm/100 cm²).

11 Instrument response can be affected by energy response to the source, backscatter from media,
12 and self-absorption of radiation in the surface. It was likely that the relatively low efficiency
13 obtained for the scabbled concrete was due to the penetration of the reference material into the
14 surface and the resultant self-absorption. This porosity effect was also evident for the untreated
15 wood. The high source efficiencies obtained on the stainless steel surface were due in part to the
16 contribution from backscattered particles entering the detector. The backscatter contribution
17 measured was approximately 50 percent for Tc-99 on stainless steel, somewhat higher than
18 anticipated. The backscatter contribution from Tc-99 on a stainless steel surface has been
19 estimated as 22 percent (NCRP 112).

20 The International Organization for Standardization recommends the use of factors to correct for
21 alpha and beta self-absorption losses when determining the surface activity. Specifically, the
22 recommendation is to use a source efficiency of 0.5 for maximum beta energies exceeding 0.4
23 MeV, and to use a source efficiency of 0.25 for maximum beta energies between 0.15 and 0.4
24 MeV and for alpha-emitters; these values "should be used in the absence of more precisely known
25 values" (ISO 7503-1). Although this guidance provides a starting point for selecting source
26 efficiencies, the data in Tables 5.3 and 5.4 illustrate the need for experimentally determined source
27 efficiencies.

28 In summary, both backscatter and self-absorption effects may produce considerable error in the
29 reported surface activity levels if the field surface is composed of material significantly different in
30 atomic number from the calibration source. Therefore, it is important to consider the effects that
31 result when the calibration source has backscatter and self-absorption characteristics different
32 from the field surface to be measured. The following guidance should prove beneficial when
33 making measurements on concrete surfaces (and source efficiencies are not considered
34 separately): use a calibration source that is mounted on an aluminum disc, since the backscatter
35 characteristics for concrete and aluminum are similar (NCRP 112).

36 **5.3 Attenuation Effects of Overlaying Material**

37 Calibration sources invariably consist of a clean, smooth surface and, as such, do not reproduce
38 the self-absorption characteristics of surfaces in the field. Thus, the surface condition can affect
39 the detection sensitivity of an instrument significantly, depending on the radionuclide of concern.
40 For example, paint has a smaller impact on detection of Co-60 than it does for Am-241. The
41 effects that various surface conditions have on detection sensitivities were evaluated by depositing

Variables Affecting MDCs in the Field

1 varying amounts of the material (i.e., water, dust, oil, paint) between the detector and the
2 radioactive source.

3 **5.3.1 Methodology**

4 The effects of the following surface conditions were evaluated quantitatively: (a) dusty, (b) wet,
5 (c) oily, and (d) painted surfaces. In order to allow intercomparison of the results from this study,
6 it was necessary to simulate known thicknesses of materials such as dust, water, or paint on
7 surfaces, reproducibly. Therefore, known quantities of soil (dust), water, oil, and paint were
8 evenly spread over a surface with standard (known) dimensions to produce the desired thickness
9 of material on the surface.

10 The material to be evaluated (e.g., water, dust, oil, paint) was uniformly deposited between two
11 Mylar sheets, within the area of the Plexiglas jig. The net weight of the material was obtained and
12 the density thickness of the material (in mg/cm²) was calculated by dividing the weight by the area
13 over which the material was deposited (typically 126 cm²). It was necessary to ensure that the
14 material was evenly spread over the active area of the Plexiglas. The following text describes
15 how the surface coatings were prepared (oil is discussed in Section 5.3.2).

16 **Paint**

17 The Mylar was attached tightly to the Plexiglas jig and weighed for initial weight. A 126-cm² hole
18 was cut in a piece of cardboard to match the exact active area of the 43-68 detector. The Mylar
19 was placed beneath the cardboard jig. The paint was sprayed lightly over the surface of the Mylar
20 at a distance that varied from 15 cm to as much as 30 cm. After the paint had dried, a new weight
21 was obtained and subtracted from the initial weight. This yielded the test weight. After
22 measurements were completed and the Mylar was checked for tears, the next quantity of paint
23 was applied.

24 **Water**

25 A piece of Kimwipe was cut exactly to fit the active area of a 43-68 detector (126 cm²) and
26 placed on a new piece of Mylar. In this case, the Mylar was not stretched or attached tightly
27 across the Mylar jig. The initial weights for the Kimwipe and Mylar sheets were then determined.
28 A known quantity of water was then pipetted onto the Kimwipe as evenly as possible. The water
29 was uniformly absorbed over the Kimwipe. After measurements had been performed, the
30 Kimwipe and Mylar were folded and reweighed to measure the amount of evaporation and to
31 determine the next test weight. Evaporation was very rapid in most cases and weight
32 determinations had to be made following each instrument measurement series.

33 **Dust**

34 Dust was obtained by grinding potting soil and sieving it through 250 mesh screen. An empty
35 plastic dish was weighed and dust was added to the dish until the desired weight was obtained.
36 Dust was then poured onto the Mylar that was tightly stretched across the Plexiglas jig. The dish
37 was then reweighed to obtain the exact amount of dust applied to the Mylar. The dust was spread
38 across the Mylar to 126 cm². This was done by using a small (1/4-inch-wide), very fine, bristle

1 brush. The brush was first weighed. The dust was so fine that it could not be brushed or swept,
2 instead it was blotted until it appeared evenly distributed and within the 126-cm² active area of the
3 probe. Another sheet of Mylar was spread over the dust. After the dust was distributed, the
4 brush was again weighed to determine if any dust remained in the brush and to obtain the final test
5 weight. This process was repeated for each test weight.

6 **Uniformity Measurements**

7 The uniformity of the material deposition between the Mylar sheets was evaluated by measuring
8 the attenuation produced by the two Mylar sheets and material at five locations within the active
9 area of the Plexiglas. Specifically, at each location, the GM detector (20-cm² probe area) and
10 radioactive disc source (a low-energy beta or alpha source was used to ensure that the source was
11 being attenuated by the material) were placed on opposite sides of the Mylar sheets. Five 1-
12 minute measurements were obtained at each location. The measurements were averaged and the
13 standard error in the mean was calculated at each location. Uniformity of the material was
14 assumed to be sufficient if the relative standard error in the mean of 25 measurements
15 (5 measurements at each locations) was less than 15 percent. It was recognized that exact
16 uniformity was not practical, or even desirable, since one objective of the study was to reproduce
17 realistic field conditions.

18 If the uniformity test failed, efforts continued to evenly distribute the material until the material
19 was distributed more uniformly. Once the desired level of uniformity had been achieved,
20 measurements were performed using the necessary detectors and calibration sources. The
21 instrument background was determined by a series of five 1-minute counts. For each data point
22 (i.e., combination of material, thickness, detector, and source) evaluated, five 1-minute
23 measurements were collected (in general, the radioactive sources used in this study possessed
24 sufficient activity to ensure that the uncertainty due to counting statistics alone was less than 5%).
25 Each data point was statistically evaluated by calculating the mean of the gross counts and
26 standard error in the mean of the gross counts. The background was subtracted from the mean of
27 the gross counts, and the detector efficiency was calculated by dividing by the activity of the
28 calibration source. The pressure and temperature in the measurement hood were recorded.

29 **5.3.2 Measurement of Various Surface Coatings**

30 Initially, this study was limited to performing MDC measurements with a gas proportional
31 detector (Ludlum Model 43-68) with oil deposited between the Mylar sheets. The radioactive
32 sources used in the pilot study were C-14, Tc-99, and SrY-90. The Tc-99 source used was a
33 100-cm² plate source; the C-14 and Sr-90 sources had 32-mm-diameter, disc-shaped geometries.
34 The detector background for 1 minute was 326 counts. Table 5.6 presents the results of MDC
35 measurements for each source under the following conditions: (a) detector face alone (0.4-
36 mg/cm² window), (b) detector face and two sheets of Mylar (0.8-mg/cm², total density thickness),
37 (c) plus 1.5 mg/cm² of 20W-50 motor oil (2.3-mg/cm², total density thickness), (d) plus 2.9
38 mg/cm² of 20W-50 motor oil (3.7-mg/cm², total density thickness), and (e) plus 4.5 mg/cm² of
39 20W-50 motor oil (5.3-mg/cm², total density thickness).

40 Figure 5.3 shows the effects of oil density thickness on the source efficiency. The first datum
41 point for each source (at 0.4 mg/cm²) in Table 5.6 may be considered to yield the total efficiency

Variables Affecting MDCs in the Field

1 under optimum laboratory conditions (smooth, clean surface). As various density thicknesses of
2 oil were added, the source efficiency was decreased due to absorption. The source efficiency
3 appeared to be reduced more significantly for the lower energy beta emitters as the density
4 thickness of oil on the surface was increased. Figure 5.4 illustrates the effects of oil density
5 thickness on the detector MDC (which is a function of source efficiency). The first data point for
6 each source may be considered as the theoretical detector MDC under optimum laboratory
7 conditions. This figure illustrates how the detector MDC, calibrated to lower energy beta
8 emitters, was significantly affected by the oil density thickness on the surface.

9 This portion of the study continued with the evaluation of various thicknesses of paint, dust, and
10 water deposited between the detector and the source. Measurements were performed with gas
11 proportional, GM, and ZnS detectors. Three variations were used for the gas proportional
12 detectors: (a) detection of alpha radiation only, (b) detection of beta radiation only (using 3.8-
13 mg/cm² window density thickness to block alpha radiation), and (c) detection of alpha and beta
14 radiation. The radioactive sources used in the pilot study were C-14, Tc-99, Tl-204, and SrY-90
15 for beta measurements, and Th-230 for alpha measurements. When measurements were
16 performed over large area sources (i.e., 126 or 150 cm²), the source activity within the physical
17 area of the detector was determined. This corrected activity was used to determine total
18 efficiencies:

$$\text{Corrected Activity} = \frac{(\text{Source Activity}) \cdot (\text{Probe Area})}{(\text{Active Area of Source})} \quad (5-2)$$

19 Tables 5.7 through 5.27 present the results of material density thicknesses for paint, dust, and
20 water versus source efficiency for all of the detector types evaluated. These results are consistent
21 with the results obtained with the oil deposition. As before, the source efficiency appeared to be
22 reduced more significantly for the lower energy beta emitters as the density thickness of the
23 material on the surface was increased. The total efficiency may be calculated for any evaluated
24 surface coating by multiplying the instrument efficiency by the source efficiency. Figures 5.5
25 through 5.28 illustrate the effects of material density thicknesses on source efficiency and MDC.
26 One interesting finding was that the total density thickness produced approximately the same
27 amount of alpha and beta attenuation, regardless of the specific material responsible for the
28 attenuation. Figure 5.29 illustrates that the total efficiencies versus density thickness for SrY-90,
29 Tl-204, Tc-99, and C-14 decrease fairly consistently for each of the materials tested, and may be
30 considered independent of material type (i.e., the total efficiency decreases with increasing density
31 thickness in the same manner for water, dust, and paint). Figure 5.30 shows that there is still
32 considerable variability in the source efficiencies determined for each surface coating studied.

Table 5.1 Background Count Rate for Various Materials

Surface Material	Background Count Rate (cpm) ^a					
	Gas Proportional			GM	ZnS	NaI
	α Only	β Only	$\alpha + \beta$			
Ambient ^b	1.00 ± 0.45^c	349 ± 12	331.6 ± 6.0	47.6 ± 2.6	1.00 ± 0.32	4702 ± 16
Brick	6.00 ± 0.84	567.2 ± 7.0	573.2 ± 6.4	81.8 ± 2.3	1.80 ± 0.73	5167 ± 23
Ceramic Block	15.0 ± 1.1	792 ± 11	770.2 ± 6.4	107.6 ± 3.8	8.0 ± 1.1	5657 ± 38
Ceramic Tile	12.6 ± 0.24	647 ± 14	648 ± 16	100.8 ± 2.7	7.20 ± 0.66	4649 ± 37
Concrete Block	2.60 ± 0.81	344.0 ± 6.2	325.0 ± 6.0	52.0 ± 2.5	1.80 ± 0.49	4733 ± 27
Drywall	2.60 ± 0.75	325.2 ± 8.0	301.8 ± 7.0	40.4 ± 3.0	2.40 ± 0.24	4436 ± 38
Floor Tile	4.00 ± 0.71	308.4 ± 6.2	296.6 ± 6.4	43.2 ± 3.6	2.20 ± 0.58	4710 ± 13
Linoleum	2.60 ± 0.98	346.0 ± 8.3	335.4 ± 7.5	51.2 ± 2.8	1.00 ± 0.45	4751 ± 27
Carbon Steel	2.40 ± 0.68	322.6 ± 8.7	303.4 ± 3.4	47.2 ± 3.3	1.00 ± 0.54	4248 ± 38
Treated Wood	0.80 ± 0.37	319.4 ± 8.7	295.2 ± 7.9	37.6 ± 1.7	1.20 ± 0.20	4714 ± 40
Untreated Wood	1.20 ± 0.37	338.6 ± 9.4	279.0 ± 5.7	44.6 ± 2.9	1.40 ± 0.51	4623 ± 34

^aBackground count rates determined from the mean of five 1-minute counts.

^bAmbient background determined at the same location as for all measurements, but without the surface material present.

^cUncertainties represent the standard error in the mean count rate, based only on counting statistics.

1 **Table 5.2 Minimum Detectable Concentrations for Various Materials**

2	Surface Material	Minimum Detectable Concentration (dpm/100 cm ²) ^a	
		Gas Proportional	
		α Only	β Only
3	Ambient	30	285
4	Brick	57	361
5	Ceramic Block	83	425
6	Ceramic Tile	78	385
7	Concrete Block	41	283
8	Drywall	41	275
9	Floor Tile	49	268
10	Linoleum	41	284
11	Steel	40	275
12	Treated Wood	28	273
13	Untreated Wood	32	281

14 ^aMDCs were calculated based on the background count rates presented in Table 5.1 for the gas proportional
 15 detector. The alpha only and beta only efficiencies were assumed to be 0.20 and 0.25 count per disintegration,
 16 respectively. Probe area corrections of 126 cm² were made for the gas proportional detectors. The following
 17 MDC equation was used for 1-minute counts:

$$MDC = \frac{3 + 4.65\sqrt{C_B}}{KT}$$

1 **Table 5.3 Surface Material Effects on Source Efficiency for Tc-99 Distributed on**
 2 **Various Surfaces**

Surface Material	Source Efficiency ^{a,b}		
	Gas Proportional		GM
	β Only	$\alpha + \beta$	
Point Source^c			
Scabbled Concrete	0.106 ± 0.097^d	0.089 ± 0.033	0.088 ± 0.022
Stainless Steel	0.755 ± 0.096	0.761 ± 0.076	0.773 ± 0.091
Untreated Wood	0.53 ± 0.11	0.504 ± 0.053	0.512 ± 0.061
Distributed Source^e			
Sealed Concrete	0.299 ± 0.096	0.20 ± 0.12	0.19 ± 0.18
Stainless Steel	0.81 ± 0.13	0.73 ± 0.11	--- ^f
Treated Wood	0.66 ± 0.11	0.551 ± 0.088	0.61 ± 0.52

12 ^aSource efficiency determined by dividing the total efficiency by the instrument efficiency.

13 ^bThe instrument efficiencies for the point source geometry were 0.25, 0.45, and 0.28, respectively, for the β
 14 only, $\alpha + \beta$, and GM detectors. Instrument efficiencies for the distributed source geometry were 0.20, 0.38,
 15 and 0.20, respectively, for the β only, $\alpha + \beta$, and GM detectors.

16 ^cThe Tc-99 activity (2828 ± 91 dpm) was dispensed in an area less than 5 cm^2 .

17 ^dUncertainties represent the 95% confidence interval, based on propagating the errors in pipetting, volumetric
 18 measurements, calibration source activity, and in counting statistics.

19 ^eThe Tc-99 activity (2830 ± 100 dpm) was evenly distributed over an area of 126 cm^2 .

20 ^fMeasurement not performed.

1 **Table 5.4 Surface Material Effects on Source Efficiency for Th-230 Distributed on**
 2 **Various Surfaces**

Surface Material	Source Efficiency ^{a,b}	
	Gas Proportional (α only)	ZnS
Point Source^c		
Scabbled Concrete	0.276 ± 0.013^d	0.288 ± 0.026
Stainless Steel	0.499 ± 0.028	0.555 ± 0.043
Untreated Wood	0.194 ± 0.023	0.185 ± 0.025
Distributed Source^e		
Sealed Concrete	0.473 ± 0.053	0.428 ± 0.054
Carbon Steel	0.250 ± 0.042	0.216 ± 0.031
Treated Wood	0.527 ± 0.057	0.539 ± 0.065

12 ^aSource efficiency determined by dividing the total efficiency by the instrument efficiency.

13 ^bThe instrument efficiencies for the point source geometry were 0.50 and 0.33, respectively, for the α -only and
 14 ZnS detectors. Instrument efficiencies for the distributed source geometry were 0.40 and 0.31, respectively, for
 15 the α -only and ZnS detectors.

16 ^cThe Th-230 activity (4595 ± 79 dpm) was dispensed in an area less than 10 cm^2 .

17 ^dUncertainties represent the 95% confidence interval, based on propagating the errors in pipetting, volumetric
 18 measurements, calibration source activity, and in counting statistics.

19 ^eThe Th-230 activity (4600 ± 170 dpm) was evenly distributed over an area of 126 cm^2 .

1 **Table 5.5 Surface Material Effects on MDC for Tc-99 and Th-230 Distributed on**
 2 **Various Surfaces**

Surface Material	Minimum Detectable Concentration ^a (dpm/100cm ²)				
	Tc-99			Th-230	
	$\alpha + \beta$	β only	GM	α only	ZnS
Point Source^b					
Scabbled Concrete	1660 ± 620 ^c	2700 ± 2500	7300 ± 2100	88 ± 16	131 ± 89
Stainless Steel	192 ± 19	359 ± 47	850 ± 130	32 ± 13	68 ± 28
Untreated Wood	285 ± 31	520 ± 110	1200 ± 150	67 ± 30	190 ± 100
Distributed Source^d					
Sealed Concrete	950 ± 560	1220 ± 380	5100 ± 4800	37 ± 23	84 ± 40
Stainless Steel	260 ± 34	446 ± 64	---	---	---
Treated Wood	312 ± 44	523 ± 79	1500 ± 1300	27.1 ± 7.7	64.8 ± 9.8
Carbon Steel	---	---	---	81 ± 21	153 ± 54

13 ^aThe minimum detectable concentration was calculated using 1-minute counts and total efficiencies determined on the basis of the known
 14 amount of activity deposited.

15 ^bThe point (disc) source area for Tc-99 and Th-230 were 5 and 10 cm², respectively.

16 ^cUncertainties represent the 95% confidence interval, based on propagating the errors in pipetting, volumetric measurements,
 17 calibration source activity, and in counting statistics.

18 ^dThe distributed source area for both Tc-99 and Th-230 was 126 cm².

Table 5.6 Effects of Oil Density Thickness on Source Efficiency and MDC (Gas Proportional— $\alpha + \beta$)

Surface Material	Density Thickness (mg/cm ²)	C-14 (0.254) ^d		Tc-99 (0.364)		SrY-90 (0.536)	
		Source Efficiency ^e	MDC ^f (dpm/100 cm ²)	Source Efficiency	MDC (dpm/100 cm ²)	Source Efficiency	MDC (dpm/100 cm ²)
Detector Face ^a	0.4	NA	605	NA	304	NA	164
Detector Face ^b Plus 2 sheets Mylar	0.8	0.386	703	0.596	317	0.772	167
Plus 1.5 mg/cm ² Oil ^c	2.3	0.236	1,148	0.467	406	0.744	173
Plus 2.9 mg/cm ² Oil	3.7	0.193	1,406	0.401	472	0.700	184
Plus 4.5 mg/cm ² Oil	5.3	0.102	2,651	0.349	543	0.677	190

^aMeasurements performed with a Ludlum 43-68 gas proportional detector with a standard 0.4 mg/cm² window.

^bEach sheet of Mylar has a density thickness of 0.2 mg/cm².

^c20W-50 motor oil used for study.

^dInstrument efficiency provided in parentheses.

^eSource efficiency was determined by dividing the total efficiency by the instrument efficiency.

^fProbe area corrections of 126 cm² were made for the gas proportional detectors. The following MDC equation was used for 1-minute counts and a background of 326 cpm:

$$MDC = \frac{3 + 4.65 \sqrt{C_B}}{KT}$$

Table 5.7 Effects of Paint Density Thickness on Source Efficiency and MDC (Gas Proportional— $\alpha + \beta$)

Surface Material	Density Thickness (mg/cm ²)	C-14 (0.254) ^d		Tc-99 (0.364)		Tl-204 (0.450)		SrY-90 (0.536)	
		Source Efficiency ^a	MDC ^f (dpm/100 cm ²)	Source Efficiency	MDC (dpm/100 cm ²)	Source Efficiency	MDC (dpm/100 cm ²)	Source Efficiency	MDC (dpm/100 cm ²)
Detector Face ^a	0.4	NA	515	NA	278	NA	202	NA	177
Detector Face ^b Plus 2 sheets Mylar	0.84	0.436	604	0.626	291	0.715	206	0.697	178
Plus 1.9 mg/cm ² Paint ^c	2.7	0.252	1,046	0.427	427	0.596	247	0.585	212
Plus 2.4 mg/cm ² Paint	3.3	0.215	1,226	— ^g	NA	NA	NA	NA	NA
Plus 5.5 mg/cm ² Paint	6.3	0.074	3,575	0.300	608	0.515	286	0.530	233
Plus 9.5 mg/cm ² Paint	10.3	0.026	10,045	0.201	907	0.448	329	0.513	241
Plus 12.6 mg/cm ² Paint	13.5	0.012	22,799	0.147	1,238	0.410	360	0.498	249

^aMeasurements performed with a Ludlum 43-68 gas proportional detector with a standard 0.4 mg/cm² window.

^bEach sheet of Mylar has a density thickness of 0.22 mg/cm².

^cOrange fluorescent waterbase paint.

^dInstrument efficiency provided in parentheses.

^eSource efficiency was determined by dividing the total efficiency by the instrument efficiency.

^fProbe area corrections of 126 cm² were made for the gas proportional detectors. The following MDC equation was used for 1 minute counts and a background of 301 cpm:

$$MDC = \frac{3 + 4.65\sqrt{C_B}}{KT}$$

^gMeasurement not performed.

Table 5.8 Effects of Paint Density Thickness on Source Efficiency and MDC (Gas Proportional— α -Only)

Surface Material	Density Thickness (mg/cm ²)	Th-230 (0.349) ^d	
		Source Efficiency ^e	MDC ^f (dpm/100 cm ²)
Detector Face ^a	0.4	NA	30
Detector Face ^b plus 2 Sheets of Mylar	0.84	0.508	34
Plus 1.9 mg/cm ² Paint ^c	2.7	0.129	135
Plus 2.4 mg/cm ² Paint	3.3	0.078	223
Plus 5.5 mg/cm ² Paint	6.3	0.008	2,060
Plus 9.5 mg/cm ² Paint	10.3	0.001	17,369

^aMeasurements performed with a Ludlum 43-68 gas proportional detector with a standard 0.4-mg/cm² window.

^bEach sheet of Mylar has a density thickness of 0.22 mg/cm².

^cOrange fluorescent waterbase paint.

^dInstrument efficiency provided in parentheses.

^eSource efficiency was determined by dividing the total efficiency by the instrument efficiency.

^fProbe area corrections of 126 cm² were made for the gas proportional detectors. The following MDC equation was used for 1-minute counts and a background of 1 cpm:

$$MDC = \frac{3 + 4.65\sqrt{C_B}}{KT}$$

Table 5.9 Effects of Paint Density Thickness on Source Efficiency and MDC (Gas Proportional— β -Only)

Surface Material	Density Thickness (mg/cm ²)	C-14 (0.081) ^d		Tc-99 (0.191)		Tl-204 (0.355)		SrY-90 (0.465)	
		Source Efficiency ^e	MDC ^f (dpm/100 cm ²)	Source Efficiency	MDC (dpm/100 cm ²)	Source Efficiency	MDC (dpm/100 cm ²)	Source Efficiency	MDC (dpm/100 cm ²)
Detector Face ^a	3.8	NA	1,823	NA	577	NA	280	NA	222
Detector Face ^b Plus 2 Sheets Mylar	4.2	0.436	2,039	0.626	599	0.715	283	0.697	222
Plus 1.9 mg/cm ² Paint ^c	6.1	0.270	3,296	0.520	722	0.657	308	0.670	231
Plus 2.4 mg/cm ² Paint	6.6	0.229	3,882	NA ^g	NA	NA	NA	NA	NA
Plus 5.5 mg/cm ² Paint	9.7	0.082	10,893	0.370	1,105	0.593	342	0.627	246
Plus 9.5 mg/cm ² Paint	13.7	0.028	31,920	0.259	1,450	0.500	405	0.583	265
Plus 12.6 mg/cm ² Paint	16.7	0.012	72,542	0.192	1,958	0.475	426	0.570	271

^aMeasurements performed with a Ludlum 43-58 gas proportional detector with a standard alpha-blocking 3.8-mg/cm² window.

^bEach sheet of Mylar has a density thickness of 0.22 mg/cm².

^cOrange fluorescent water base paint.

^dInstrument efficiency provided in parentheses.

^eSource efficiency was determined by dividing the total efficiency by the instrument efficiency.

^fProbe area corrections of 126 cm² were made for the gas proportional detectors. The following MDC equation was used for 1-minute counts and a background of 354 cpm:

$$MDC = \frac{3 + 4.65\sqrt{C_B}}{KT}$$

^gMeasurement not performed.

Table 5.10 Effects of Paint Density Thickness on Source Efficiency and MDC (GM Detector)

Surface Material	Density Thickness (mg/cm ²)	C-14 (0.099) ^d		Tc-99 (0.193)		Tl-204 (0.278)		SrY-90 (0.388)	
		Source Efficiency ^e	MDC ^f (dpm/100 cm ²)	Source Efficiency	MDC (dpm/100 cm ²)	Source Efficiency	MDC (dpm/100 cm ²)	Source Efficiency	MDC (dpm/100 cm ²)
Detector Face ^a	— ^b	NA	3,757	NA	1,454	NA	888	NA	648
Detector Face ^b Plus 2 Sheets of Mylar	0.4	0.436	4,098	0.626	1,468	0.715	894	0.697	657
Plus 1.9 mg/cm ² Paint ^c	2.3	0.284	6,294	0.526	1,748	0.671	952	0.665	688
Plus 2.4 mg/cm ² Paint	2.8	0.239	7,485	NA ^h	NA	NA	NA	NA	NA
Plus 5.5 mg/cm ² Paint	5.9	0.099	20,012	0.388	2,373	0.598	1,068	0.594	771
Plus 9.5 mg/cm ² Paint	9.8	0.029	61,664	0.244	3,767	0.516	1,238	0.575	797
Plus 12.6 mg/cm ² Paint	13.0	0.012	145,037	0.171	5,362	0.487	1,312	0.571	802

^aMeasurements performed with an Eberline HP-260 GM detector with a standard mica window, typical thickness 1.4 to 2.0 mg/cm².

^bEach sheet of Mylar has a density thickness of 0.22 mg/cm².

^cOrange fluorescent water base paint.

^dInstrument efficiency provided in parentheses.

^eSource efficiency was determined by dividing the total efficiency by the instrument efficiency.

^fThe following MDC equation was used for 1-minute counts, with a background of 49 cpm and a probe area of 20 cm²:

$$MDC = \frac{3 + 4.65\sqrt{C_B}}{KT}$$

^gDetector face is fixed part of detector and is not removable.

^hMeasurement not performed.

1 **Table 5.11 Effects of Paint Density Thickness on Source Efficiency and MDC (ZnS**
 2 **Scintillation Detector)**

3 Surface Material	4 Density Thickness (mg/cm ²)	5 Th-230 (0.069) ^d	
		6 Source Efficiency ^e	7 MDC ^f (dpm/100 cm ²)
8 Detector Face ^a	--- ^b	NA	65
9 Detector Face ^b Plus 2 10 Sheets of Mylar	0.4	0.508	294
11 Plus 1.9 mg/cm ² Paint ^c	2.3	0.369	404
12 Plus 2.4 mg/cm ² Paint	2.8	0.198	756
13 Plus 5.5 mg/cm ² Paint	5.9	0.013	11,619
14 Plus 9.5 mg/cm ² Paint	9.9	0.002	64,800

11 ^aMeasurements performed with an Eberline AC3-7 ZnS scintillation detector with a standard 1.5-mg/cm² window.

12 ^bEach sheet of Mylar has a density thickness of 0.22 mg/cm².

13 ^cOrange fluorescent waterbase paint.

14 ^dInstrument efficiency provided in parentheses.

15 ^eSource efficiency was determined by dividing the total efficiency by the instrument efficiency.

16 ^fThe following MDC equation was used for 1-minute counts, with a background of 1 cpm and a probe area of 74 cm²:

$$MDC = \frac{3 + 4.65\sqrt{C_B}}{KT}$$

17 ^gDetector face is fixed part of detector and is not removable.

Table 5.12 Effects of Dust Density Thickness on Source Efficiency and MDC (Gas Proportional— $\alpha + \beta$)

Surface Material	Density Thickness (mg/cm ²)	C-14 (0.254) ^d		Tc-99 (0.363)		Tl-204 (0.450)		Sr-Y-90 (0.536)	
		Source Efficiency ^a	MDC ^f (dpm/100 cm ²)	Source Efficiency	MDC (dpm/100 cm ²)	Source Efficiency	MDC (dpm/100 cm ²)	Source Efficiency	MDC (dpm/100 cm ²)
Detector Face ^a	0.4	NA	510	NA	278	NA	202	NA	177
Detector Face ^b plus 2 Sheets of Mylar	0.84	0.436	599	0.626	292	0.715	206	0.696	178
Plus 2.3 mg/cm ² Dust ^c	3.1	0.217	1,201	0.425	430	0.619	238	0.642	193
Plus 4.1 mg/cm ² Dust	4.9	0.205	1,276	0.407	449	0.594	248	0.616	201
Plus 6.1 mg/cm ² Dust	6.9	0.141	1,847	0.298	614	0.535	275	0.594	208
Plus 8.0 mg/cm ² Dust	8.8	0.071	3,675	0.245	745	0.474	311	0.536	231
Plus 10.0 mg/cm ² Dust	10.8	0.047	5,534	0.215	848	0.456	323	0.532	233

^aMeasurements performed with a Ludlum 43-68 gas proportional detector with a standard 0.4-mg/cm² window.

^bEach sheet of Mylar has a density thickness of 0.22 mg/cm².

^cDust obtained by grinding potting soil and sieving through 250 mesh screen.

^dInstrument efficiency provided in parentheses.

^eSource efficiency was determined by dividing the total efficiency by the instrument efficiency.

^fProbe area corrections of 126 cm² were made for the gas proportional detectors. The following MDC equation was used for 1-minute counts and a background of 301 cpm:

$$MDC = \frac{3 + 4.65\sqrt{C_B}}{KT}$$

1 **Table 5.13 Effects of Dust Density Thickness on Source Efficiency and MDC (Gas**
 2 **Proportional— α Only)**

3	Surface Material	Density Thickness (mg/cm ²)	Th-230 (0.349) ^d	
			Source Efficiency ^e	MDC ^f (dpm/100 cm ²)
4	Detector Face ^a	0.4	NA	34
5	Detector Face ^b Plus 2 Sheets of Mylar	0.84	0.508	34
6	Plus 2.3 mg/cm ² Dust ^c	3.1	0.144	120
7	Plus 4.1 mg/cm ² Dust	4.9	0.134	130
8	Plus 6.1 mg/cm ² Dust	6.9	0.056	310
9	Plus 8.0 mg/cm ² Dust	8.8	0.026	674
10	Plus 10.0 mg/cm ² Dust	10.8	0.018	974

11 ^aMeasurements performed with a Ludlum 43-68 gas proportional detector with a standard 0.4-mg/cm² window.

12 ^bEach sheet of Mylar has a density thickness of 0.22 mg/cm².

13 ^cDust obtained by grinding potting soil and sieving through 250 mesh screen.

14 ^dInstrument efficiency provided in parentheses.

15 ^eSource efficiency was determined by dividing the total efficiency by the instrument efficiency.

16 ^fProbe area corrections of 126 cm² were made for the gas proportional detectors. The following MDC equation was used for
 17 1-minute counts and a background of 301 cpm:

$$MDC = \frac{3 + 4.65\sqrt{C_B}}{KT}$$

Table 5.14 Effects of Dust Density Thickness on Source Efficiency and MDC (Gas Proportional— β Only)

Surface Material	Density Thickness (mg/cm ²)	C-14 (0.808) ^a		Tc-99 (0.191)		Tl-204 (0.355)		SrY-90 (0.465)	
		Source Efficiency ^a	MDC ^d (dpm/100 cm ²)	Source Efficiency	MDC (dpm/100 cm ²)	Source Efficiency	MDC (dpm/100 cm ²)	Source Efficiency	MDC (dpm/100 cm ²)
Detector Face ^a	3.8	NA	1,823	NA	577	NA	280	NA	222
Detector Face ^b Plus 2 Sheets of Mylar	4.2	0.436	2,039	0.626	599	0.715	283	0.697	222
Plus 2.3 mg/cm ² Dust ^c	6.5	0.243	3,659	0.500	751	0.649	312	0.649	238
Plus 4.1 mg/cm ² Dust	8.3	0.218	4,074	0.478	785	0.627	323	0.656	236
Plus 6.1 mg/cm ² Dust	10.3	0.149	5,957	0.370	1,013	0.595	340	0.628	246
Plus 8.0 mg/cm ² Dust	12.2	0.076	11,680	0.304	1,233	0.530	382	0.593	260
Plus 10.0 mg/cm ² Dust	14.2	0.052	17,243	0.269	1,395	0.503	403	0.565	274

^aMeasurements performed with a Ludlum 43-68 gas proportional with a standard alpha-blocking 3.8-mg/cm² window.

^bEach sheet of Mylar has a density thickness of 0.22 mg/cm².

^cDust obtained by grinding potting soil and sieving through 250 mesh screen.

^dInstrument efficiency provided in parentheses.

^eSource efficiency was determined by dividing the total efficiency by the instrument efficiency.

^fProbe area corrections of 126 cm² were made for the gas proportional detectors. The following MDC equation was used for 1-minute counts and a background of 1 cpm:

$$MDC = \frac{3 + 4.65\sqrt{C_B}}{KT}$$

Table 5.15 Effects of Dust Density Thickness on Source Efficiency and MDC (GM Detector)

Surface Material	Density Thickness (mg/cm ²)	C-14 (0.995) ^d		Tc-99 (0.193)		Tl-204 (0.278)		SrY-9 (0.388)	
		Source Efficiency ^e	MDC ^f (dpm/100 cm ²)	Source Efficiency	MDC (dpm/100 cm ²)	Source Efficiency	MDC (dpm/100 cm ²)	Source Efficiency	MDC (dpm/100 cm ²)
Detector Face ^a	— ^a	NA	3,758	NA	1,454	NA	888	NA	648
Detector Face ^b Plus 2 Sheets of Mylar	0.4	0.436	4,098	0.626	1,469	0.715	894	0.697	657
Plus 2.3 mg/cm ² Dust ^c	2.7	0.257	6,941	0.490	1,877	0.657	973	0.667	686
Plus 4.1 mg/cm ² Dust	4.5	0.234	7,644	0.472	2,949	0.617	1,036	0.645	710
Plus 6.1 mg/cm ² Dust	6.5	0.160	11,133	0.392	2,345	0.590	1,084	0.632	725
Plus 8.0 mg/cm ² Dust	8.4	0.080	22,344	0.300	3,067	0.543	1,178	0.590	776
Plus 10.0 mg/cm ² Dust	10.4	0.049	36,720	0.243	3,789	0.503	1,270	0.546	838

^aMeasurements performed with an Eberline HP-260 GM detector with a standard mica window with typical thickness 1.4 to 2.0 mg/cm².

^bEach sheet of Mylar has a density thickness of 0.22 mg/cm².

^cDust obtained by grinding potting soil and sieving through 250 mesh screen.

^dInstrument efficiency provided in parentheses.

^eSource efficiency was determined by dividing the total efficiency by the instrument efficiency.

^fThe following equation was used for 1 minute counts, with a background of 49 cpm and a probe area of 20 cm²:

$$MDC = \frac{3 + 4.65\sqrt{C_B}}{KT}$$

^aDetector face is fixed part of detector and is not removable.

Variables Affecting MDCs in the Field

1 **Table 5.16 Effects of Dust Density Thickness on Source Efficiency and MDC (ZnS**
 2 **Scintillation Detector)**

3	Surface Material	Density Thickness (mg/cm ²)	Th-230 (0.069) ^d	
			Source Efficiency ^e	MDC ^f (dpm/100 cm ²)
4	Detector Face ^a	--- ^b	NA	65
5	Detector Face ^b Plus 2 Sheets of Mylar	0.4	0.508	294
6	Plus 2.2 mg/cm ² Dust ^c	2.6	0.439	340
7	Plus 4.1 mg/cm ² Dust	4.5	0.407	367
8	Plus 6.1 mg/cm ² Dust	6.5	0.169	885
9	Plus 8.0 mg/cm ² Dust	8.4	0.086	1,735
10	Plus 10.0 mg/cm ² Dust	10.4	0.062	2,390

12 ^aMeasurements performed with an Eberline AC3-7 ZnS scintillation detector with a standard 1.5-mg/cm² window.

13 ^bEach sheet of Mylar has a density thickness of 0.22 mg/cm².

14 ^cDust obtained by grinding potting soil and sieving through 250 mesh screen.

15 ^dInstrument efficiency provided in parentheses.

16 ^eSource efficiency was determined by dividing the total efficiency by the instrument efficiency.

17 ^fThe following MDC equation was used for 1-minute counts, with a background of 1 cpm and a probe area of 74 cm²:

$$MDC = \frac{3 + 4.65\sqrt{C_B}}{KT}$$

19 ^aDetector face is fixed part of detector and is not removable.

1 **Table 5.17 Effects of Water Density Thickness on Source Efficiency and MDC (Gas**
 2 **Proportional— $\alpha+\beta/C-14$)**

3	Surface Material	Density Thickness (mg/cm ²)	C-14 (0.139) ^d	
			Source Efficiency ^e	MDC ^f (dpm/100 cm ²)
4	Detector Face ^a	0.4	NA	629
5	Detector Face Plus 2 Mylar Sheets With	2.7	0.436	1,249
6	1 Kimwipe ^b			
7	Plus 0.44 mg/cm ² Water ^c	3.1	0.362	1,502
8	Plus 0.62 mg/cm ² Water	3.3	0.360	1,513
9	Plus 0.78 mg/cm ² Water	3.5	0.350	1,558
10	Plus 1.2 mg/cm ² Water	3.9	0.332	1,637
11	Plus 2.3 mg/cm ² Water	5.0	0.284	1,920
12	Plus 3.0 mg/cm ² Water	5.7	0.237	2,297
13	Plus 5.1 mg/cm ² Water	7.8	0.138	3,940
14	Plus 6.5 mg/cm ² Water	9.2	0.083	6,533
15	Plus 7.6 mg/cm ² Water	10.3	0.063	8,599

16 ^aMeasurements performed with a Ludlum 43-68 gas proportional detector with a standard 0.4 mg/cm² window.

17 ^bEach sheet of Mylar has a density thickness of 0.22 mg/cm² and one Kimwipe has a density thickness of 1.86
 18 mg/cm².

19 ^cReagent water used in analytical procedures from radiochemistry laboratory.

20 ^dInstrument efficiency provided in parentheses.

21 ^eSource efficiency was determined by dividing the total efficiency by the instrument efficiency.

22 ^fProbe area corrections of 126 cm² were made for the gas proportional detectors. The following MDC equation
 23 was used for 1-minute counts and a background of 396 cpm:

$$MDC = \frac{3 + 4.65\sqrt{C_B}}{KT}$$

Variables Affecting MDCs in the Field

1 **Table 5.18 Effects of Water Density Thickness on Source Efficiency and MDC (Gas**
 2 **Proportional— $\alpha+\beta$ /Tc-99)**

3	Surface Material	Density Thickness (mg/cm ²)	Tc-99 (0.239) ^d	
			Source Efficiency ^e	MDC ^f (dpm/100 cm ²)
4	Detector Face ^a	0.4	NA	368
5	Detector Face Plus 2 Mylar Sheets With 1	2.7	0.626	506
6	Kimwipe ^b			
7	Plus 0.19 mg/cm ² Water ^c	2.9	0.628	505
8	Plus 0.76 mg/cm ² Water	3.5	0.595	533
9	Plus 2.8 mg/cm ² Water	5.5	0.501	633
10	Plus 4.0 mg/cm ² Water	6.7	0.443	716
11	Plus 5.5 mg/cm ² Water	8.2	0.386	822
12	Plus 6.7 mg/cm ² Water	9.4	0.327	969
13	Plus 8.2 mg/cm ² Water	10.9	0.287	1,104

14 ^aMeasurements performed with a Ludlum 43-68 gas proportional detector with a standard 0.4-mg/cm²
 15 window.

16 ^bEach sheet of Mylar has a density thickness of 0.22 mg/cm² and one Kimwipe has a density thickness
 17 of 1.86 mg/cm².

18 ^cReagent water used in analytical procedures from radiochemistry laboratory.

19 ^dInstrument efficiency provided in parentheses.

20 ^eSource efficiency was determined by dividing the total efficiency by the instrument efficiency.

21 ^fProbe area corrections of 126 cm² were made for the gas proportional detectors. The following MDC equation
 22 was used for 1-minute counts and a background of 396 cpm:
 23

$$MDC = \frac{3 + 4.65\sqrt{C_B}}{KT}$$

1 **Table 5.19 Effects of Water Density Thickness on Source Efficiency and MDC (Gas**
 2 **Proportional— $\alpha+\beta$ /SrY-90)**

3	Surface Material	Density Thickness (mg/cm ²)	SrY-90 (0.484) ^d	
			Source Efficiency ^e	MDC ^f (dpm/100 cm ²)
4	Detector Face ^a	0.4	NA	207
5	Detector Face Plus 2 Mylar Sheets With	2.7	0.697	225
6	1 Kimwipe ^b			
7	Plus 2.6 mg/cm ² Water ^c	5.3	0.666	235
8	Plus 3.3 mg/cm ² Water	6.0	0.666	235
9	Plus 4.8 mg/cm ² Water	7.5	0.627	250
10	Plus 6.3 mg/cm ² Water	9.0	0.608	258
11	Plus 7.9 mg/cm ² Water	10.6	0.582	269

12 ^aMeasurements performed with a Ludlum 43-68 gas proportional detector with a standard 0.4-mg/cm² window.

13 ^bEach sheet of Mylar has a density thickness of 0.22 mg/cm² and one Kimwipe has a density thickness of 1.86 mg/cm².

14 ^cReagent water used in analytical procedures from radiochemistry laboratory.

15 ^dInstrument efficiency provided in parentheses.

16 ^eSource efficiency was determined by dividing the total efficiency by the instrument efficiency.

17 ^fProbe area corrections of 126 cm² were made for the gas proportional detectors. The following MDC equation was
 18 used for 1-minute counts and a background of 396 cpm:
 19

$$MDC = \frac{3 + 4.65\sqrt{C_B}}{KT}$$

20

1 **Table 5.20 Effects of Water Density Thickness on Source Efficiency and MDC (Gas**
 2 **Proportional— α -Only)**

3	Surface Material	Density Thickness (mg/cm ²)	Th-230 (0.085) ^d	
			Source Efficiency ^e	MDC ^f (dpm/100 cm ²)
4	Detector Face ^a	0.4	NA	30
5	Detector Face Plus 2 Mylar Sheets With 1	2.7	0.508	140
6	Kimwipe ^b			
7	Plus 0.11 mg/cm ² Water ^c	2.8	0.469	151
8	Plus 0.25 mg/cm ² Water	2.9	0.441	161
9	Plus 0.48 mg/cm ² Water	3.2	0.372	191
10	Plus 1.2 mg/cm ² Water	3.9	0.274	259
11	Plus 2.0 mg/cm ² Water	4.7	0.168	423
12	Plus 3.5 mg/cm ² Water	6.2	0.090	787
13	Plus 4.2 mg/cm ² Water	6.9	0.039	1,827
14	Plus 5.9 mg/cm ² Water	8.6	0.018	3,983

15 ^aMeasurements performed with a Ludlum 43-68 gas proportional detector with a standard 0.4-mg/cm²
 16 window.

17 ^bEach sheet of Mylar has a density thickness of 0.22 mg/cm² and one Kimwipe has a density thickness
 18 of 1.86 mg/cm².

19 ^cReagent water used in analytical procedures from radiochemistry laboratory.

20 ^dInstrument efficiency provided in parentheses.

21 ^eSource efficiency was determined by dividing the total efficiency by the instrument efficiency.

22 ^fProbe area corrections of 126 cm² were made for the gas proportional detectors. The following MDC equation
 23 was used for 1-minute counts and a background of 396 cpm:

$$MDC = \frac{3 + 4.65\sqrt{C_B}}{KT}$$

24

1 **Table 5.21 Effects of Water Density Thickness on Source Efficiency and MDC (Gas**
 2 **Proportional— β -Only/C-14)**

3	Surface Material	Density Thickness (mg/cm ²)	C-14 (0.046) ^d	
			Source Efficiency ^e	MDC ^f (dpm/100 cm ²)
4	Detector Face ^a	3.8	NA	1,869
5	Detector Face Plus 2 Mylar Sheets With 1 6 Kimwipe ^b	6.1	0.436	3,544
7	Plus 0.44 mg/cm ² Water ^c	6.5	0.367	4,209
8	Plus 0.62 mg/cm ² Water	6.7	0.358	4,317
9	Plus 0.78 mg/cm ² Water	6.9	0.354	4,363
10	Plus 1.2 mg/cm ² Water	7.3	0.338	4,576
11	Plus 2.3 mg/cm ² Water	8.4	0.282	5,480
12	Plus 3.0 mg/cm ² Water	9.1	0.239	6,457
13	Plus 5.1 mg/cm ² Water	11.2	0.136	11,359
14	Plus 6.5 mg/cm ² Water	12.6	0.084	18,320
15	Plus 7.6 mg/cm ² Water	13.7	0.063	24,606

16 ^aMeasurements performed with a Ludlum 43-68 gas proportional detector with a standard alpha-blocking
 17 3.8-mg/cm² window.

18 ^bEach sheet of Mylar has a density thickness of 0.22 mg/cm² and one Kimwipe has a density thickness of
 19 1.86 mg/cm².

20 ^cReagent water used in analytical procedures from radiochemistry laboratory.

21 ^dInstrument efficiency provided in parentheses.

22 ^eSource efficiency was determined by dividing the total efficiency by the instrument efficiency.

23 ^fProbe area corrections of 126 cm² were made for the gas proportional detectors. The following MDC equation
 24 was used for 1-minute counts and a background of 396 cpm:

$$MDC = \frac{3 + 4.65\sqrt{C_B}}{KT}$$

25

Variables Affecting MDCs in the Field

1 **Table 5.22 Effects of Water Density Thickness on Source Efficiency and MDC (Gas**
 2 **Proportional—β-Only/Tc-99)**

3	Surface Material	Density Thickness (mg/cm ²)	Tc-99 (0.148)	
			Source Efficiency ^e	MDC ^f (dpm/100 cm ²)
4	Detector Face ^a	3.8	NA	620
5	Detector Face Plus 2 Mylar Sheets With	6.1	0.626	773
6	1 Kimwipe ^b			
7	Plus 0.19 mg/cm ² Water ^c	6.3	0.630	769
8	Plus 0.73 mg/cm ² Water	6.8	0.590	821
9	Plus 2.8 mg/cm ² Water	8.9	0.518	934
10	Plus 3.9 mg/cm ² Water	10.1	0.469	1,033
11	Plus 5.4 mg/cm ² Water	11.6	0.402	1,206
12	Plus 6.6 mg/cm ² Water	12.8	0.357	1,356
13	Plus 8.1 mg/cm ² Water	14.3	0.300	1,614

14 ^aMeasurements performed with a Ludlum 43-68 gas proportional detector with a standard alpha- blocking 3.8-
 15 mg/cm²
 16 window.

17 ^bEach sheet of Mylar has a density thickness of 0.22 mg/cm² and one Kimwipe has a density thickness of 1.86
 18 mg/cm².

19 ^cReagent water used in analytical procedures from radiochemistry laboratory.

20 ^dInstrument efficiency provided in parentheses.

21 ^eSource efficiency was determined by dividing the total efficiency by the instrument efficiency.

22 ^fProbe area corrections of 126 cm² were made for the gas proportional detectors. The following MDC equation was
 23 used for 1-minute counts and a background of 396 cpm:

$$MDC = \frac{3 + 4.65\sqrt{C_B}}{KT}$$

24

1 **Table 5.23 Effects of Water Density Thickness on Source Efficiency and MDC (Gas**
 2 **Proportional— β -Only/SrY-90)**

3	Surface Material	Density Thickness (mg/cm ²)	SrY-90 (0.429) ^d	
			Source Efficiency ^e	MDC ^f (dpm/100 cm ²)
4	Detector Face ^a	3.8	NA	222
5	Detector Face Plus 2 Mylar Sheets With	6.1	0.696	241
6	1 Kimwipe ^b			
7	Plus 2.6 mg/cm ² Water ^c	8.7	0.665	252
8	Plus 3.3 mg/cm ² Water	9.4	0.661	253
9	Plus 4.8 mg/cm ² Water	10.9	0.635	264
10	Plus 6.3 mg/cm ² Water	12.4	0.632	265
11	Plus 7.9 mg/cm ² Water	14.0	0.590	284

12 ^aMeasurements performed with a Ludlum 43-68 gas proportional detector with a standard alpha-blocking
 13 3.8-mg/cm² window.

14 ^bEach sheet of Mylar has a density thickness of 0.22 mg/cm² and one Kimwipe has a density thickness of
 15 1.86 mg/cm².

16 ^cReagent water used in analytical procedures from radiochemistry laboratory.

17 ^dInstrument efficiency provided in parentheses.

18 ^eSource efficiency was determined by dividing the total efficiency by the instrument efficiency.

19 ^fProbe area corrections of 126 cm² were made for the gas proportional detectors. The following MDC equation
 20 was used for 1-minute counts and a background of 396 cpm:

$$MDC = \frac{3 + 4.65\sqrt{C_B}}{KT}$$

21

Variables Affecting MDCs in the Field

1 **Table 5.24 Effects of Water Density Thickness on Source Efficiency and MDC (GM**
 2 **Detector/C-14)**

3	Surface Material	Density Thickness (mg/cm ²)	C-14 (0.056) ^d	
			Source Efficiency ^e	MDC ^f (dpm/100 cm ²)
4	Detector Face ^a	--- ^b	NA	3,758
5	Detector Face Plus 2 Mylar Sheets	2.3	0.436	7,294
6	With 1 Kimwipe ^b			
7	Plus 0.44 mg/cm ² Water ^c	2.7	0.422	7,526
8	Plus 0.62 mg/cm ² Water	2.9	0.412	7,716
9	Plus 0.78 mg/cm ² Water	3.1	0.405	7,847
10	Plus 1.2 mg/cm ² Water	3.5	0.382	8,320
11	Plus 2.3 mg/cm ² Water	4.6	0.320	9,925
12	Plus 3.0 mg/cm ² Water	5.3	0.277	11,481
13	Plus 5.1 mg/cm ² Water	7.4	0.162	19,622
14	Plus 6.5 mg/cm ² Water	8.8	0.104	30,496
15	Plus 7.6 mg/cm ² Water	9.9	0.071	44,680

16 ^aMeasurements performed with an Eberline HP-260 GM detector with a standard mica window, typical thickness
 17 1.4 to 2.0 mg/cm².

18 ^bEach sheet of Mylar has a density thickness of 0.22 mg/cm² and one Kimwipe has a density thickness of
 19 1.86 mg/cm².

20 ^cReagent water used in analytical procedures from radiochemistry laboratory.

21 ^dInstrument efficiency provided in parentheses.

22 ^eSource efficiency was determined by dividing the total efficiency by the instrument efficiency.

23 ^fThe following MDC equation was used for 1-minute counts, with a background of 49 cpm and probe area of
 24 20 cm²:

$$MDC = \frac{3 + 4.65\sqrt{C_B}}{KT}$$

25 ^aDetector face is fixed part of detector and is not removable.
 26

1 **Table 5.25 Effects of Water Density Thickness on Source Efficiency and MDC (GM**
 2 **Detector/Tc-99)**

3	Surface Material	Density Thickness (mg/cm ²)	Tc-99 (0.161) ^d	
			Source Efficiency ^e	MDC ^f (dpm/100 cm ²)
4	Detector Face ^a	---	NA	1,454
5	Detector Face Plus 2 Mylar Sheets With	2.3	0.626	1,762
6	1 Kimwipe ^b			
7	Plus 0.19 mg/cm ² Water ^c	2.5	0.611	1,805
8	Plus 0.76 mg/cm ² Water	3.1	0.580	1,902
9	Plus 2.8 mg/cm ² Water	5.1	0.501	2,204
10	Plus 4.0 mg/cm ² Water	6.3	0.463	2,383
11	Plus 5.5 mg/cm ² Water	7.8	0.392	2,814
12	Plus 6.7 mg/cm ² Water	8.9	0.347	3,179
13	Plus 8.2 mg/cm ² Water	10.4	0.296	3,731

14 ^aMeasurements performed with an Eberline HP-260 GM detector with a standard mica window, typical thickness
 15 1.4 to 2.0 mg/cm².

16 ^bEach sheet of Mylar has a density thickness of 0.22 mg/cm² and one Kimwipe has a density thickness of
 17 1.86 mg/cm².

18 ^cReagent water used in analytical procedures from radiochemistry laboratory.

19 ^dInstrument efficiency provided in parentheses.

20 ^eSource efficiency was determined by dividing the total efficiency by the instrument efficiency.

21 ^fThe following MDC equation was used for 1-minute counts, with a background of 49 cpm and probe area of
 22 20 cm²:

$$MDC = \frac{3 + 4.65\sqrt{C_B}}{KT}$$

23
 24 ^aDetector face is fixed part of detector and is not removable.

Variables Affecting MDCs in the Field

1 **Table 5.26 Effects of Water Density Thickness on Source Efficiency and MDC (GM**
 2 **Detector/SrY-90)**

3	Surface Material	Density Thickness (mg/cm ²)	SrY-90 (0.373) ^d	
			Source Efficiency ^e	MDC ^f (dpm/100 cm ²)
4	Detector Face ^a	--- ^g	NA	648
5	Detector Face Plus 2 Mylar Sheets With	2.3	0.697	684
6	1 Kimwipe ^b			
7	Plus 2.6 mg/cm ² Water ^c	4.9	0.678	703
8	Plus 3.3 mg/cm ² Water	5.5	0.678	703
9	Plus 4.8 mg/cm ² Water	7.1	0.665	717
10	Plus 6.3 mg/cm ² Water	8.6	0.621	768
11	Plus 7.9 mg/cm ² Water	10.2	0.609	783

12 ^aMeasurements performed with an Eberline HP-260 GM detector with a standard mica window, typical thickness
 13 1.4 to 2.0 mg/cm².

14 ^bEach sheet of Mylar has a density thickness of 0.22 mg/cm² and one Kimwipe has a density thickness of
 15 1.86 mg/cm².

16 ^cReagent water used in analytical procedures from radiochemistry laboratory.

17 ^dInstrument efficiency provided in parentheses.

18 ^eSource efficiency was determined by dividing the total efficiency by the instrument efficiency.

19 ^fThe following MDC equation was used for 1-minute counts, with a background of 49 cpm and probe area of
 20 20 cm²:

$$MDC = \frac{3 + 4.65\sqrt{C_B}}{KT}$$

21 ^gDetector face is fixed part of detector and is not removable.
 22

1 **Table 5.27 Effects of Water Density Thickness on Source Efficiency and MDC (ZnS**
 2 **Scintillation Detector)**

3	Surface Material	Density Thickness (mg/cm ²)	Th-230 (0.069) ^d	
			Source Efficiency ^e	MDC ^f (dpm/100 cm ²)
4	Detector Face ^a	--- ^g	NA	65
5	Detector Face Plus 2 Mylar Sheets With	2.3	0.508	294
6	1 Kimwipe ^b			
7	Plus 0.11 mg/cm ² Water	2.4	0.433	345
8	Plus 0.25 mg/cm ² Water	2.6	0.367	407
9	Plus 0.48 mg/cm ² Water	3.1	0.296	504
10	Plus 1.2 mg/cm ² Water	3.5	0.232	645
11	Plus 2.0 mg/cm ² Water	4.3	0.145	1,030
12	Plus 3.5 mg/cm ² Water	5.8	0.046	3,265
13	Plus 4.2 mg/cm ² Water	6.5	0.031	4,814
14	Plus 5.9 mg/cm ² Water	8.2	0.014	10,465

15 ^aMeasurements performed with an Eberline AC3-7 ZnS scintillation detector with a standard 1.5-mg/cm²
 16 window.

17 ^bEach sheet of Mylar has a density thickness of 0.22 mg/cm² and one Kimwipe has a density thickness of
 18 1.86 mg/cm².

19 ^cReagent water used in analytical procedures from radiochemistry laboratory.

20 ^dInstrument efficiency provided in parentheses.

21 ^eSource efficiency was determined by dividing the total efficiency by the instrument efficiency.

22 ^fThe following MDC equation was used for 1-minute counts, with a background of 1 cpm and probe area of
 23 74 cm²:-

$$MDC = \frac{3 + 4.65\sqrt{C_B}}{KT}$$

24 ^gDetector face is fixed part of detector and is not removable.
 25

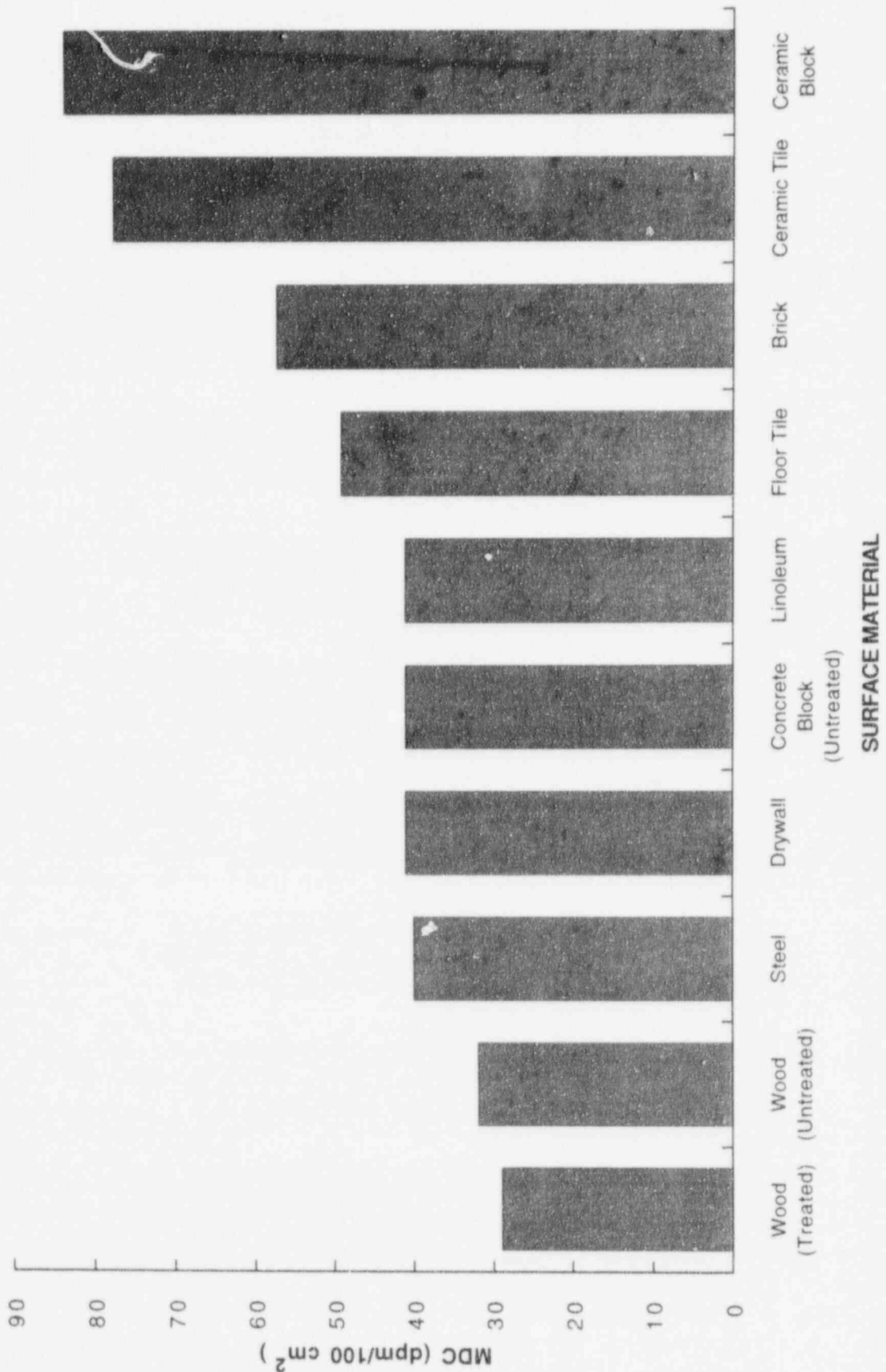
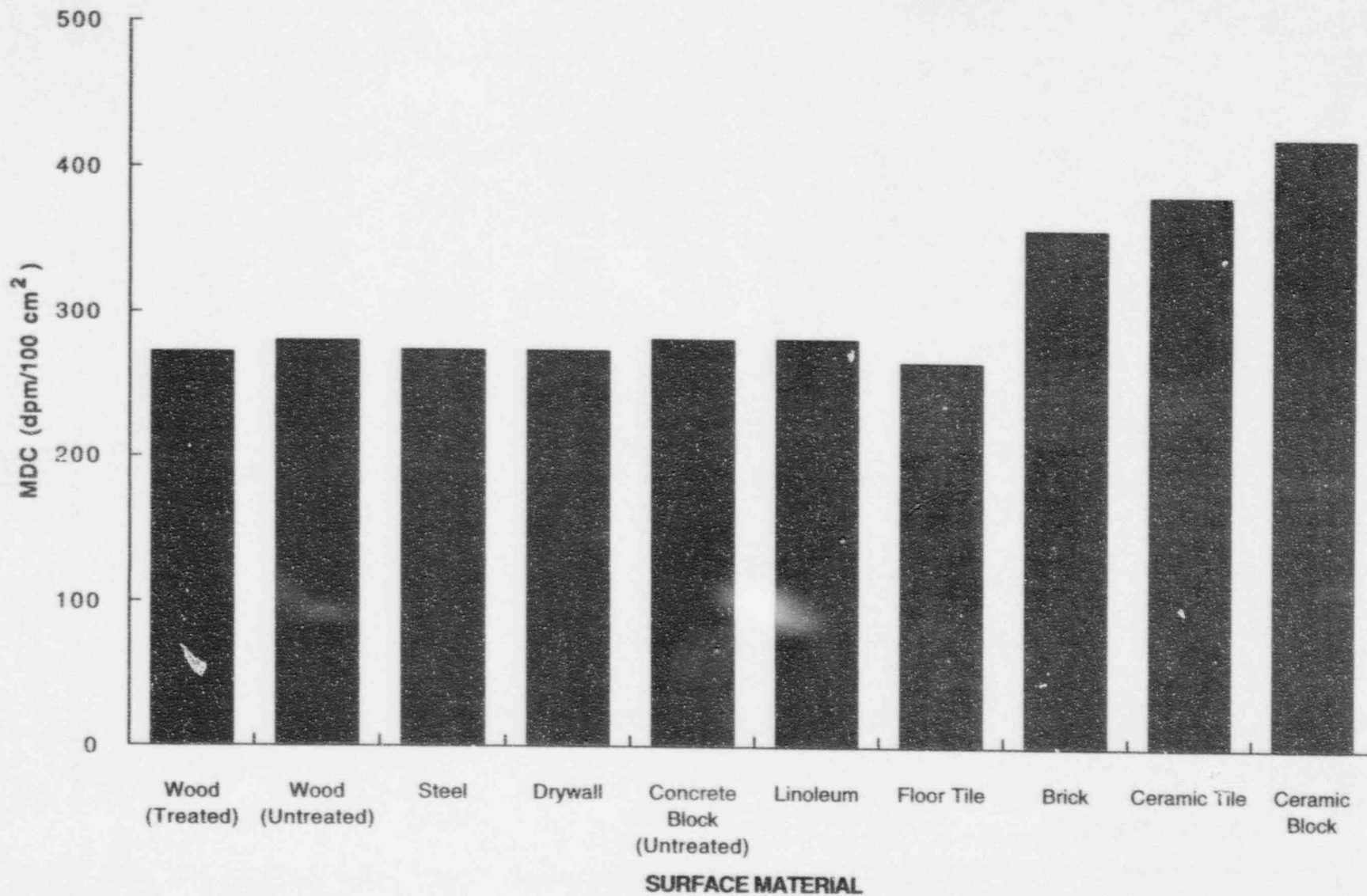


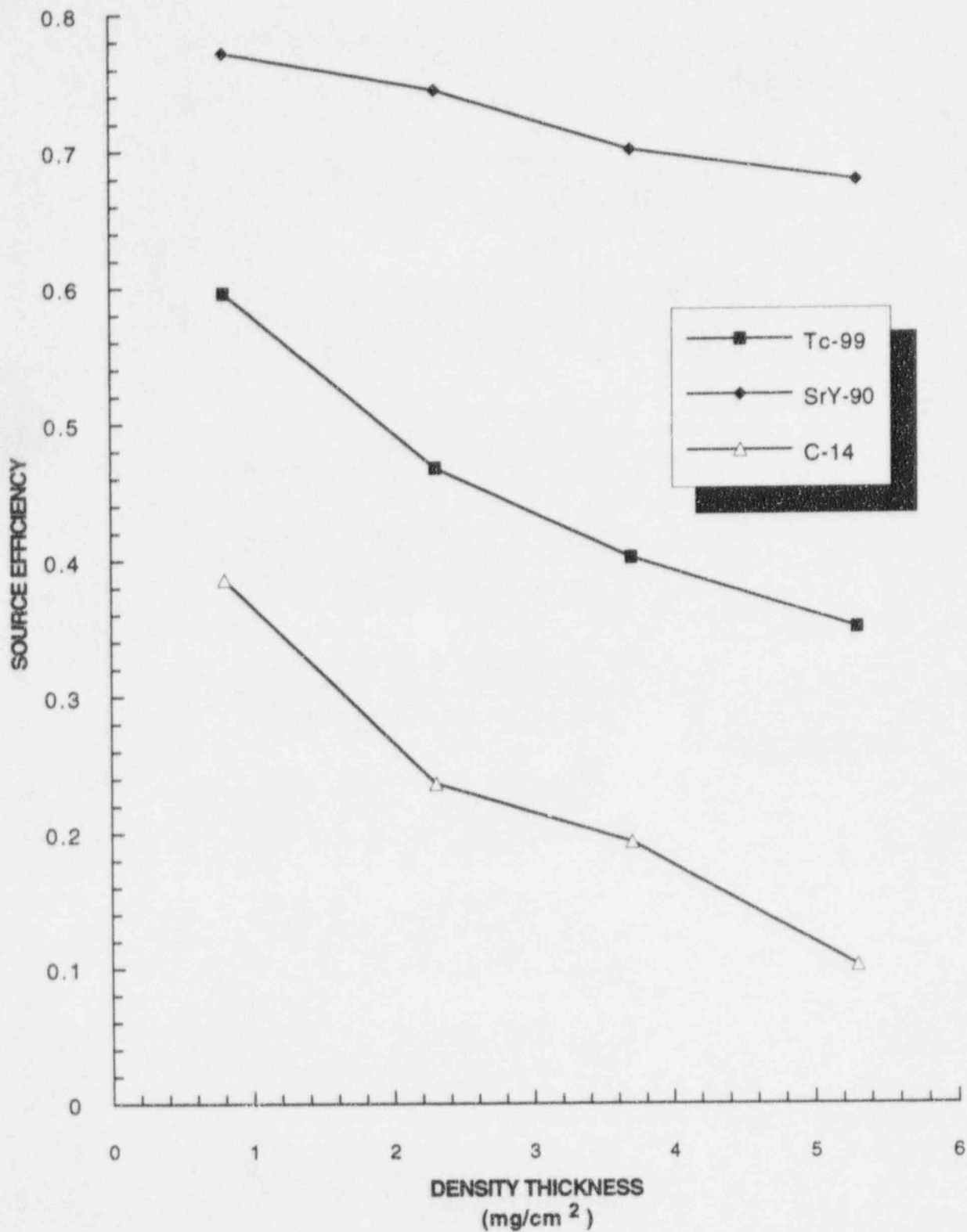
Figure 5.1 Effect of Surface Material on Gas Proportional Detector (α Only) MDC



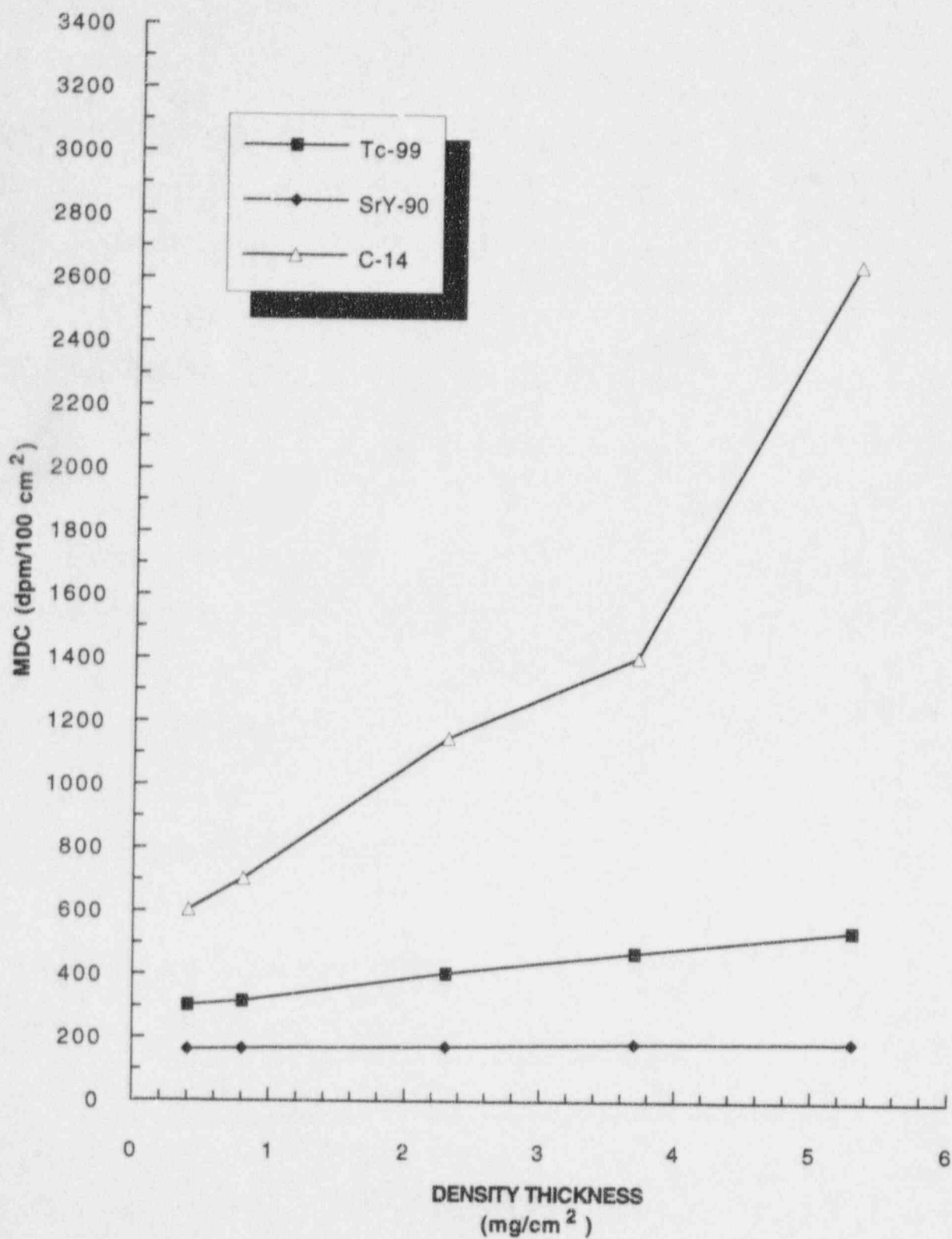
Variables Affecting MDCs in the Field

1 Figure 5.2 Effect of Surface Material on Gas Proportional Detector (β Only) MDC

Variables Affecting MDCs in the Field



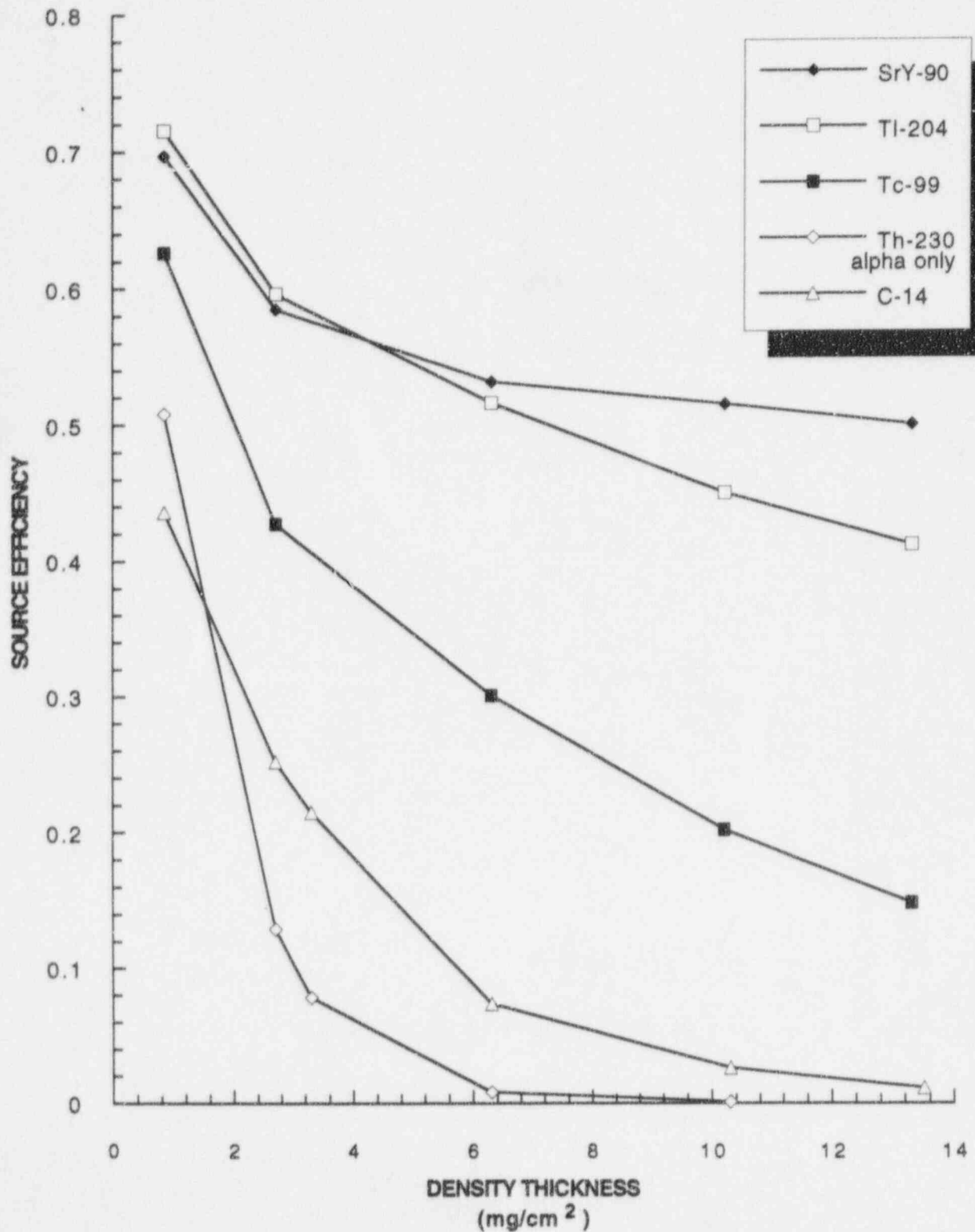
1 Figure 5.3 Effects of Oil Density Thickness on Source Efficiency for Various Sources



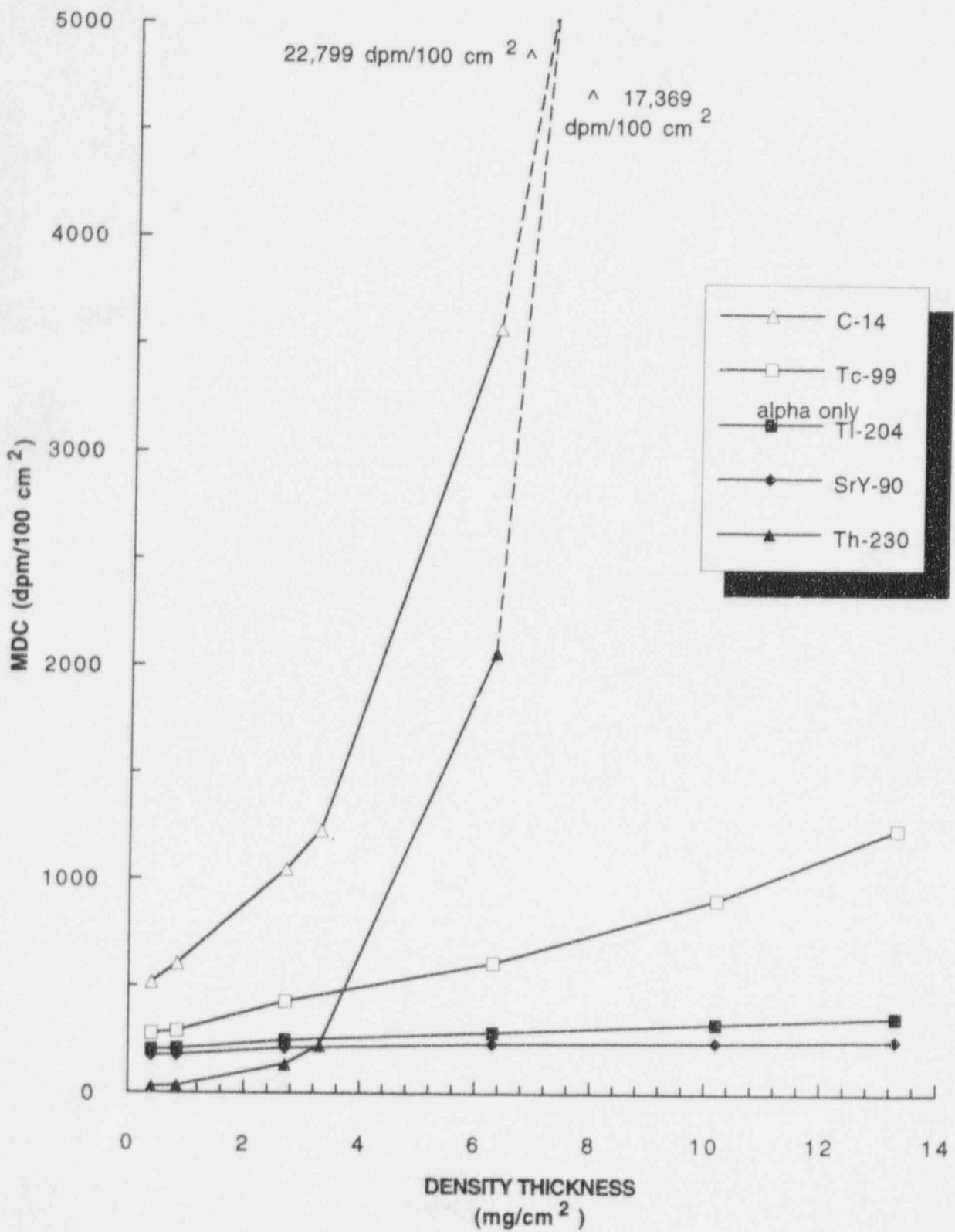
1

Figure 5.4 Effects of Oil Density Thickness on MDC for Various Sources

Variables Affecting MDCs in the Field

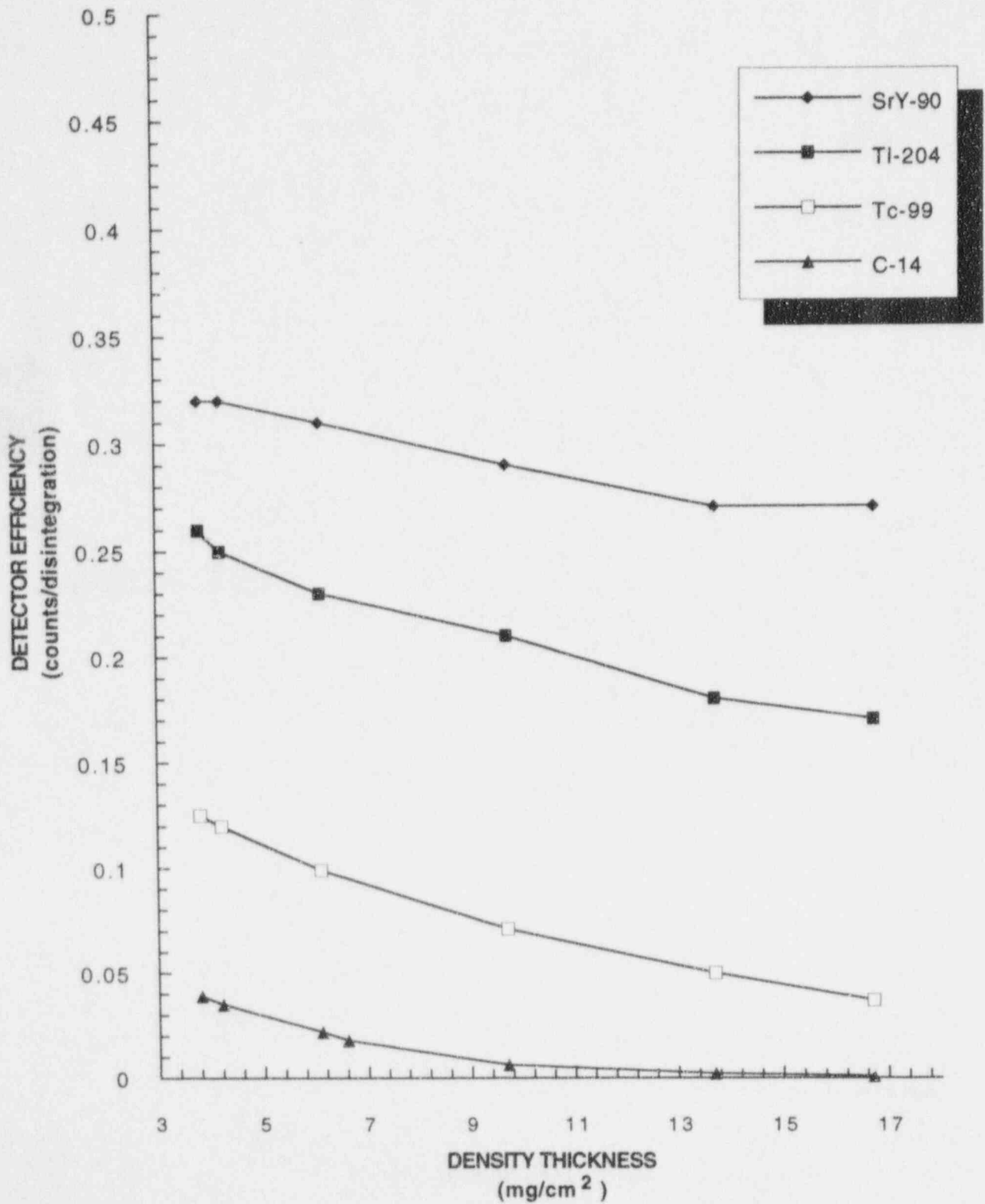


1 Figure 5.5 Effects of Paint Density Thickness on Source Efficiency for Various Sources
2 Using the Gas Proportional Detector in $\alpha+\beta$ and α -Only Modes

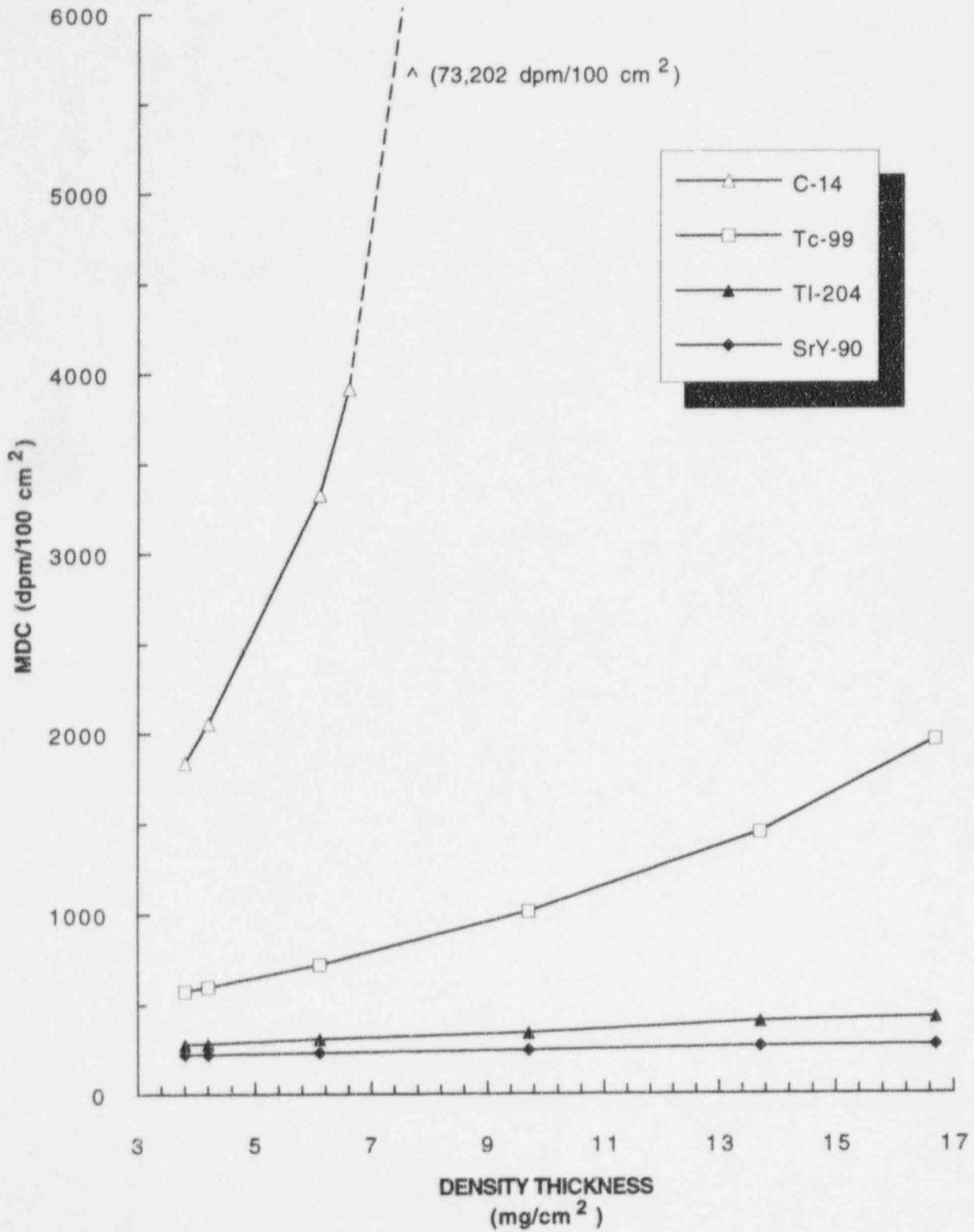


1 Figure 5.6 Effects of Paint Density Thickness on MDC for Various Sources Using the
 2 Gas Proportional Detector in $\alpha+\beta$ and α -Only Modes

Variables Affecting MDCs in the Field

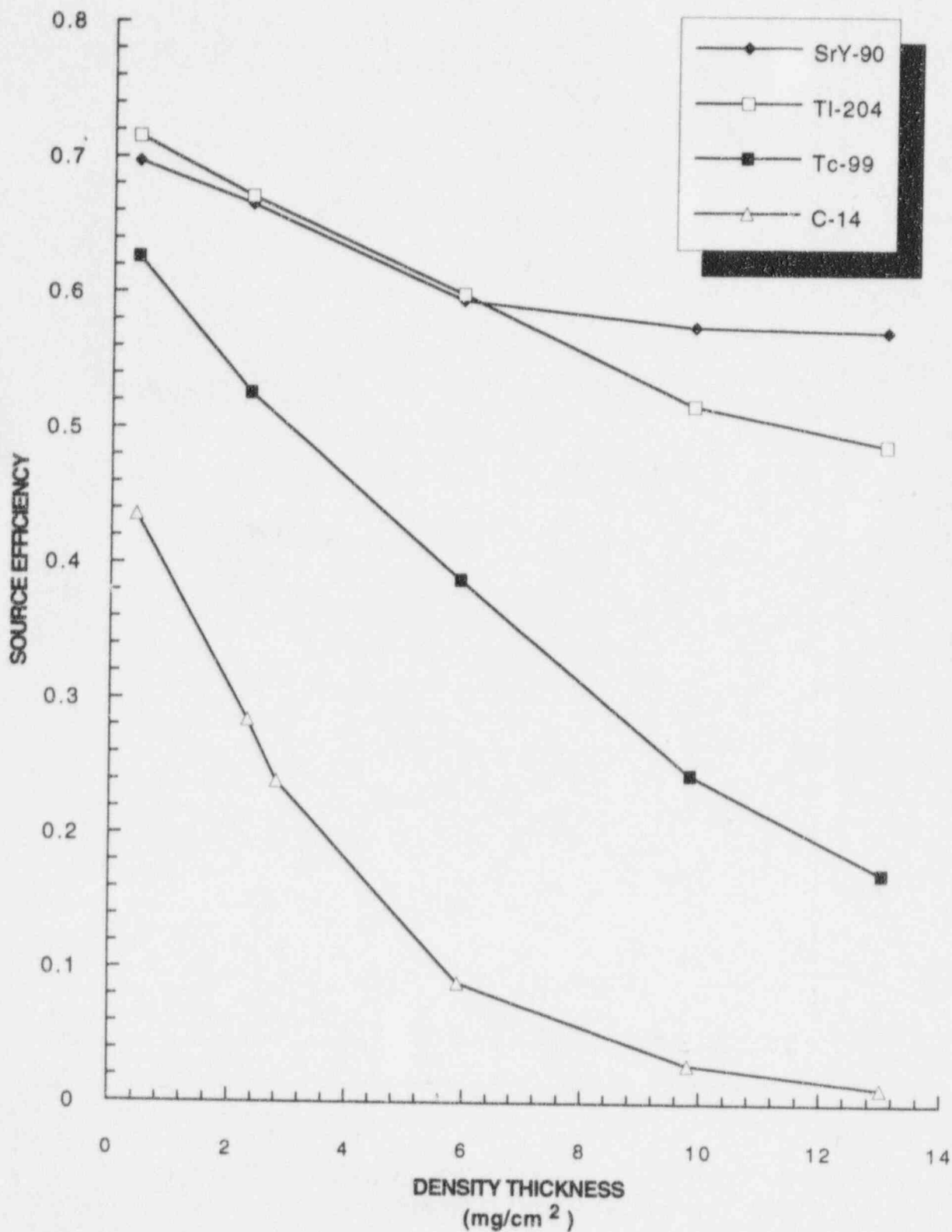


1 Figure 5.7 Effects of Paint Density Thickness on Source Efficiency for Various Sources
2 Using the Gas Proportional Detector in β -Only Mode

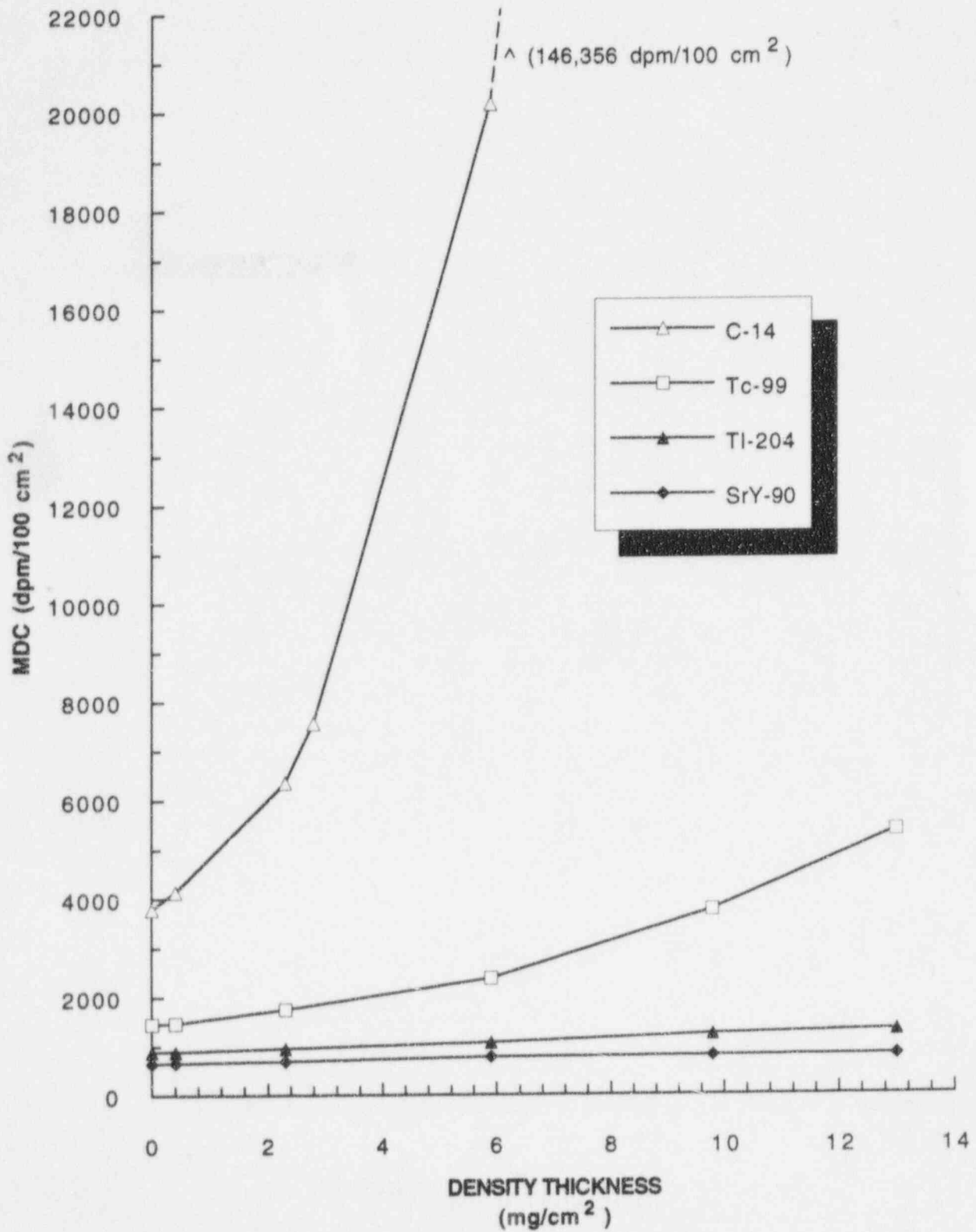


1 Figure 5.8 Effects of Paint Density Thickness on MDC for Various Sources Using the
 2 Gas Proportional Detector in β -Only Mode

Variables Affecting MDCs in the Field



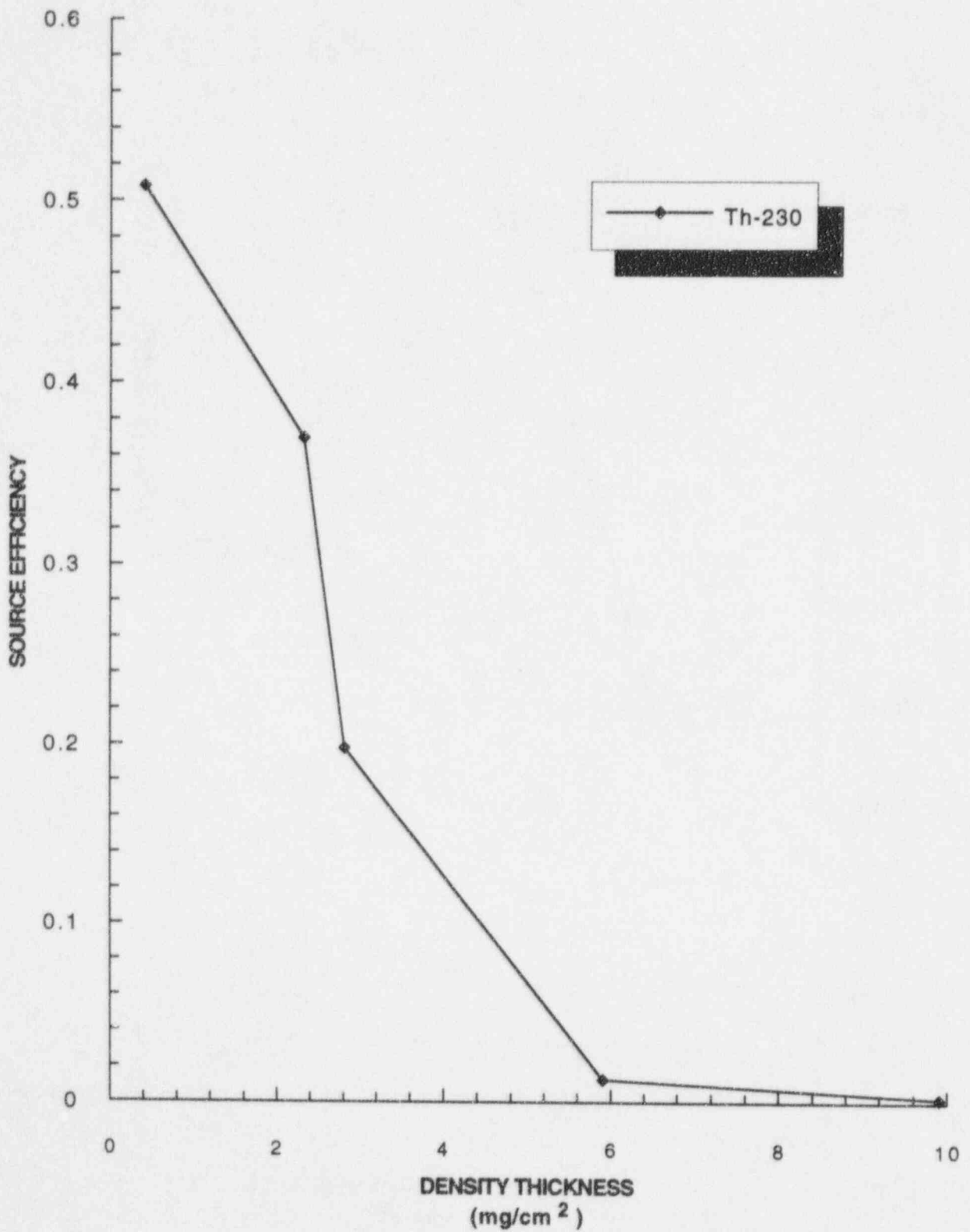
1 Figure 5.9 Effects of Paint Density Thickness on Source Efficiency for Various Sources
2 Using the GM Detector



1
2

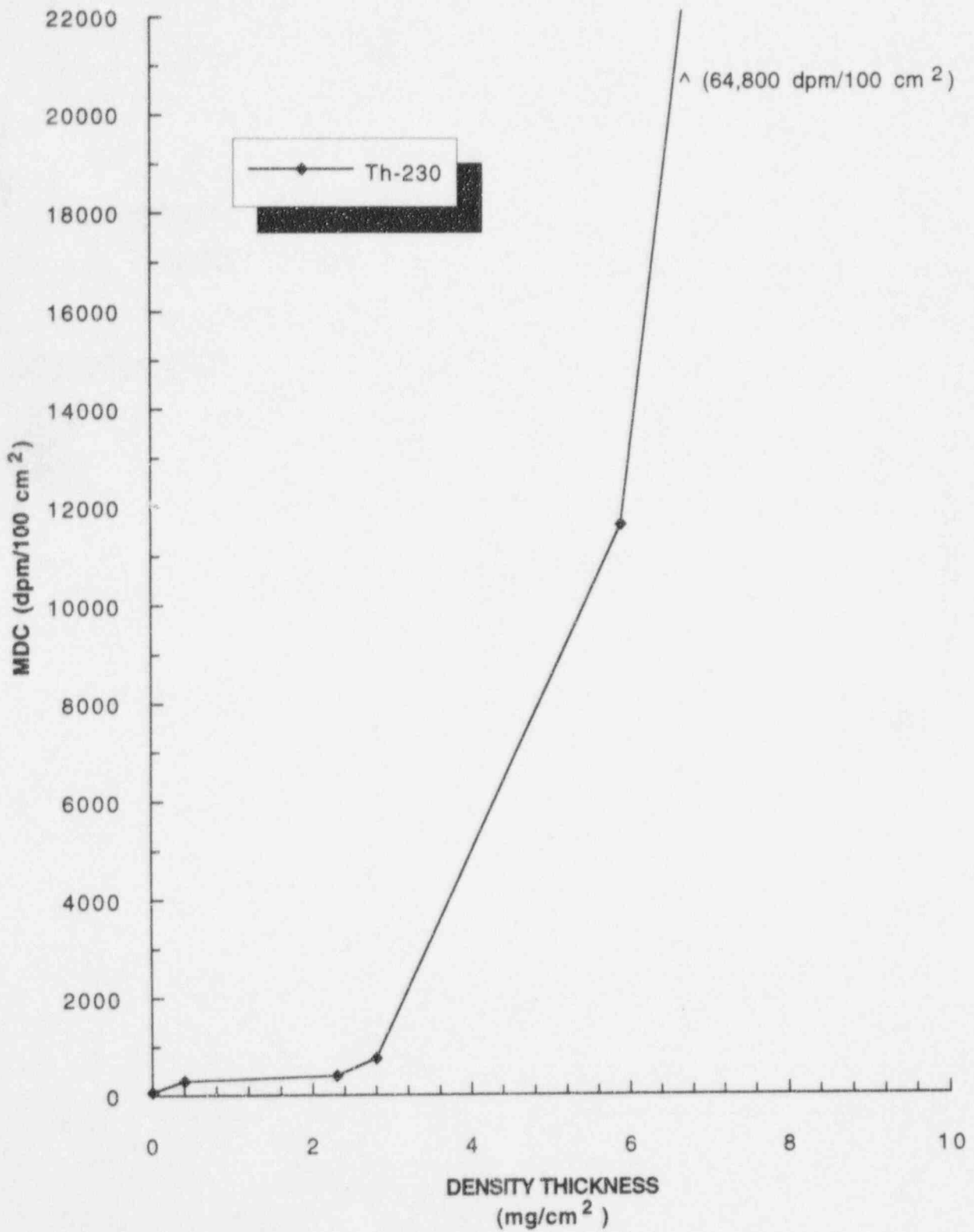
Figure 5.10 Effects of Paint Density Thickness on MDC for Various Sources Using the GM Detector

Variables Affecting MDCs in the Field



1
2

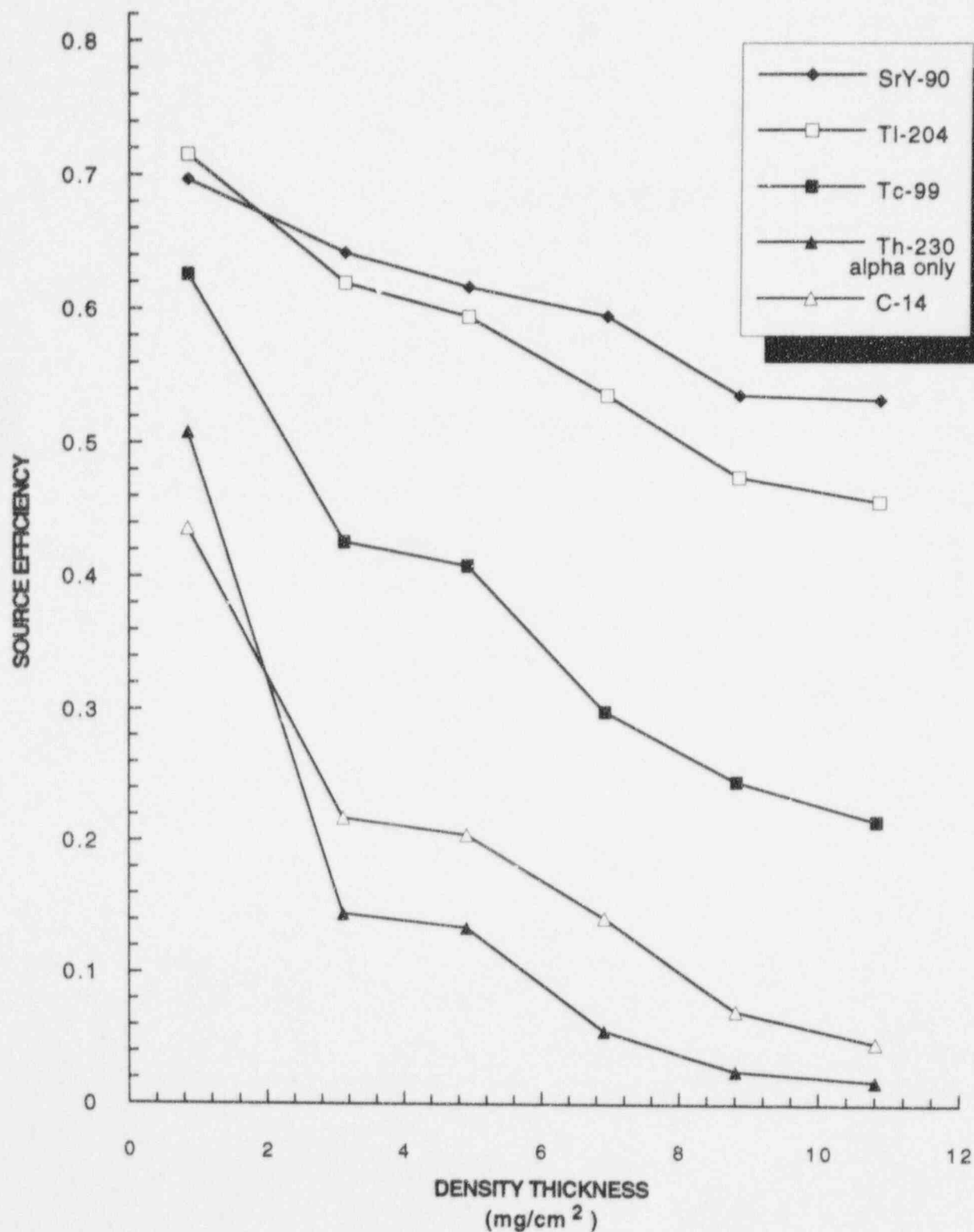
Figure 5.11 Effects of Paint Density Thickness on Source Efficiency for an Alpha Source Using the ZnS Scintillation Detector



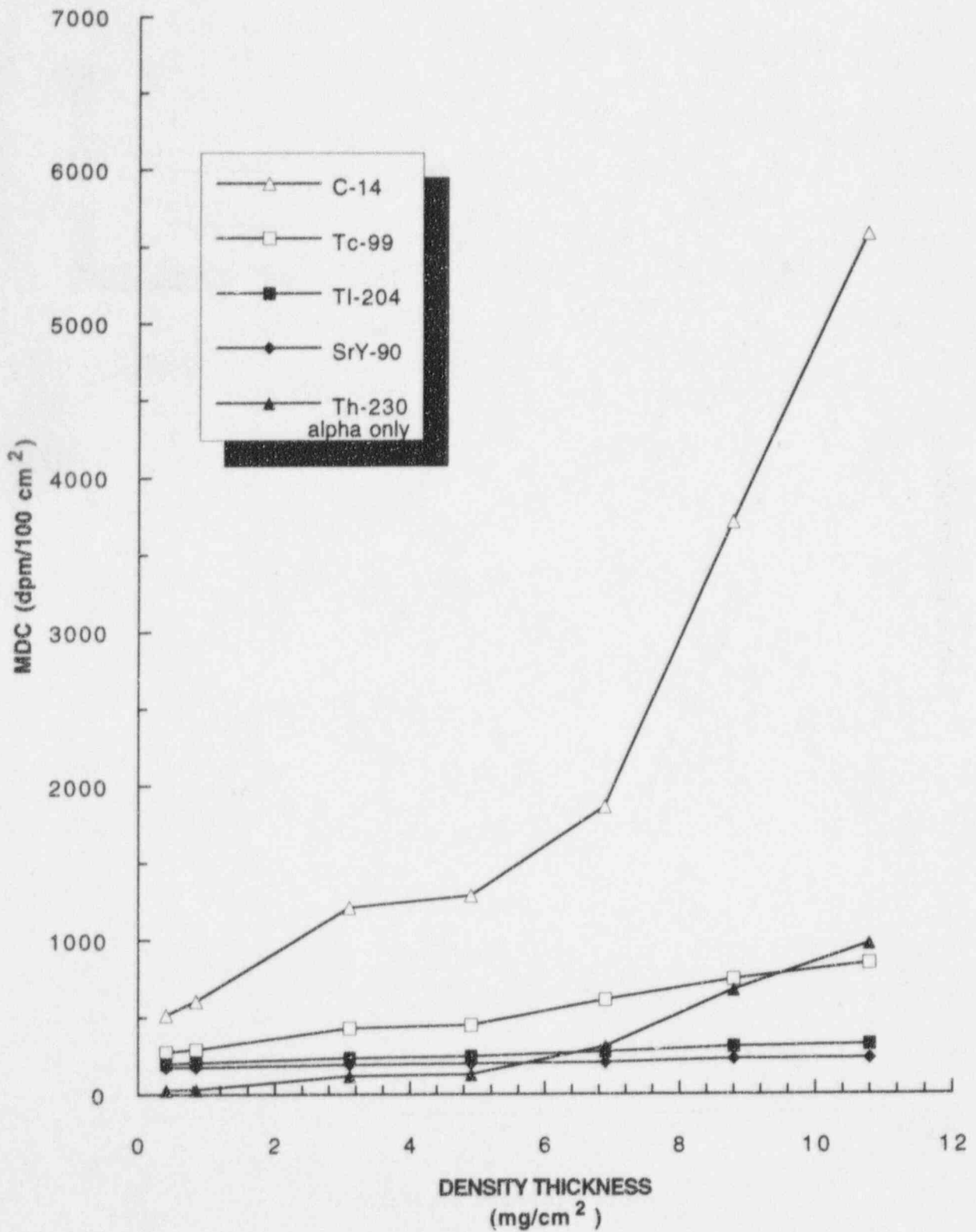
1
2

Figure 5.12 Effects of Paint Density Thickness on MDC for an Alpha Source Using the ZnS Scintillation Detector

Variables Affecting MDCs in the Field

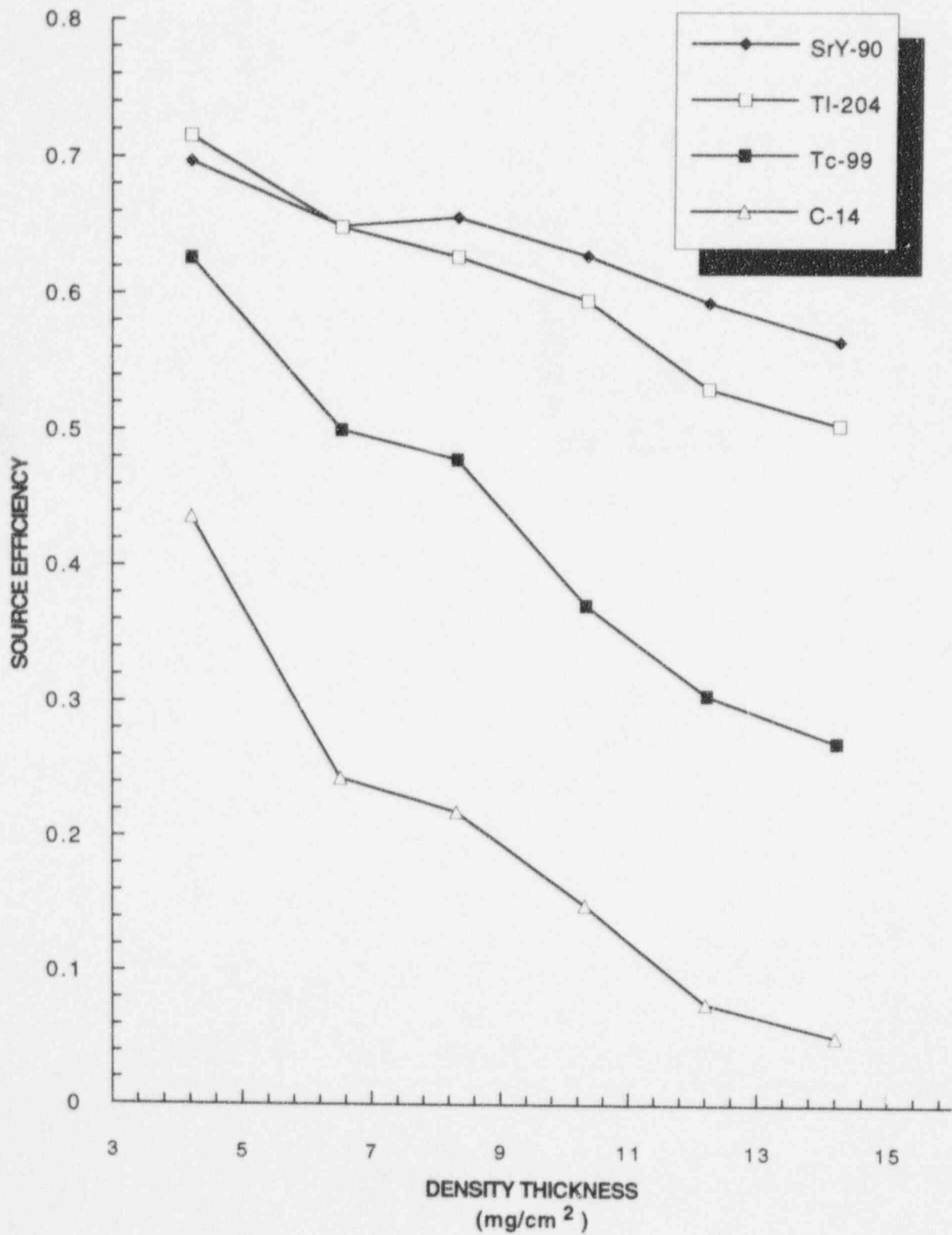


1 Figure 5.13 Effects of Dust Density Thickness on Source Efficiency for Various Sources
 2 Using the Gas Proportional Detector in $\alpha+\beta$ and α -Only Modes

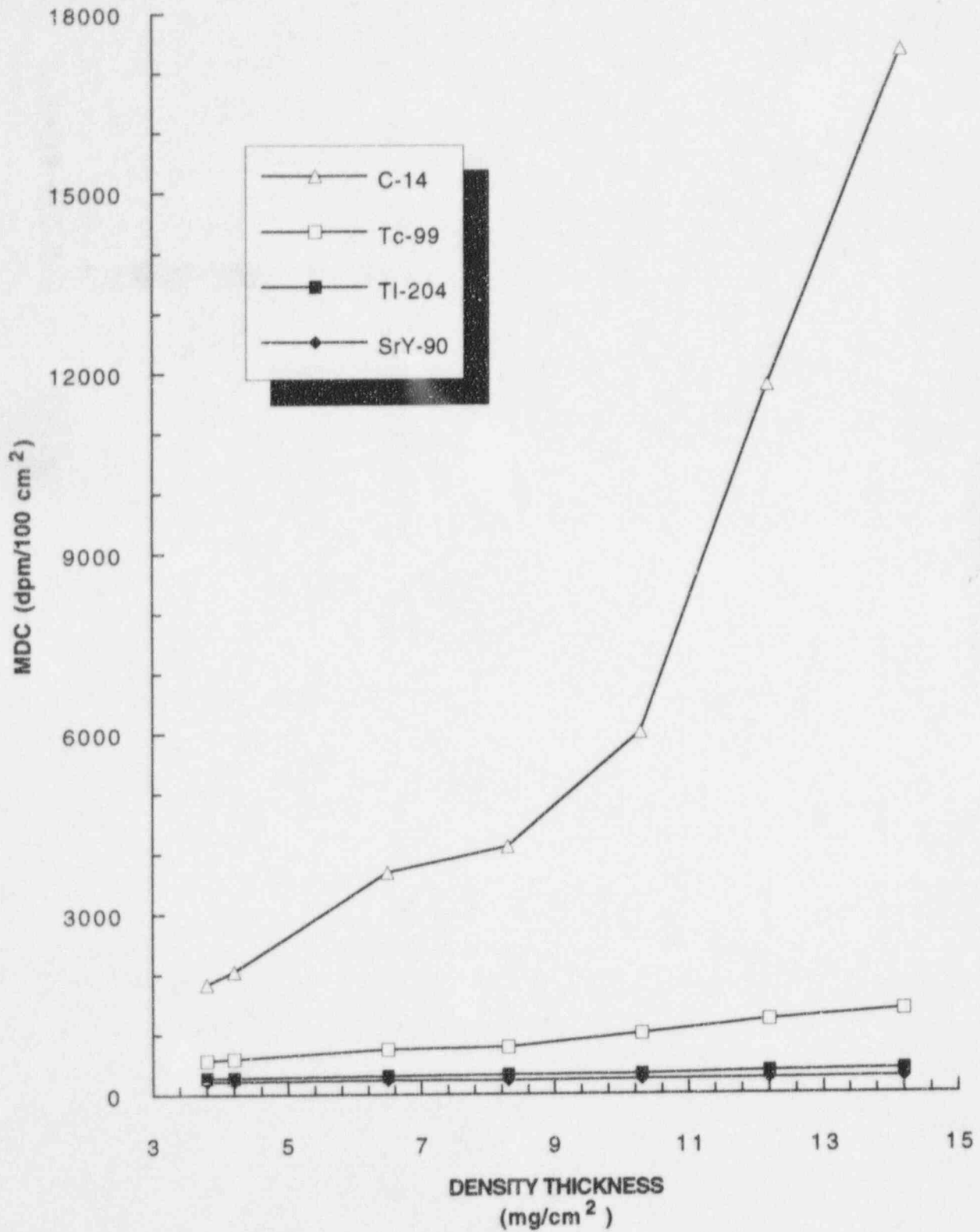


1 **Figure 5.14 Effects of Dust Density Thickness on MDC for Various Sources Using the**
 2 **Gas Proportional Detector in $\alpha+\beta$ and α -Only Modes**

Variables Affecting MDCs in the Field



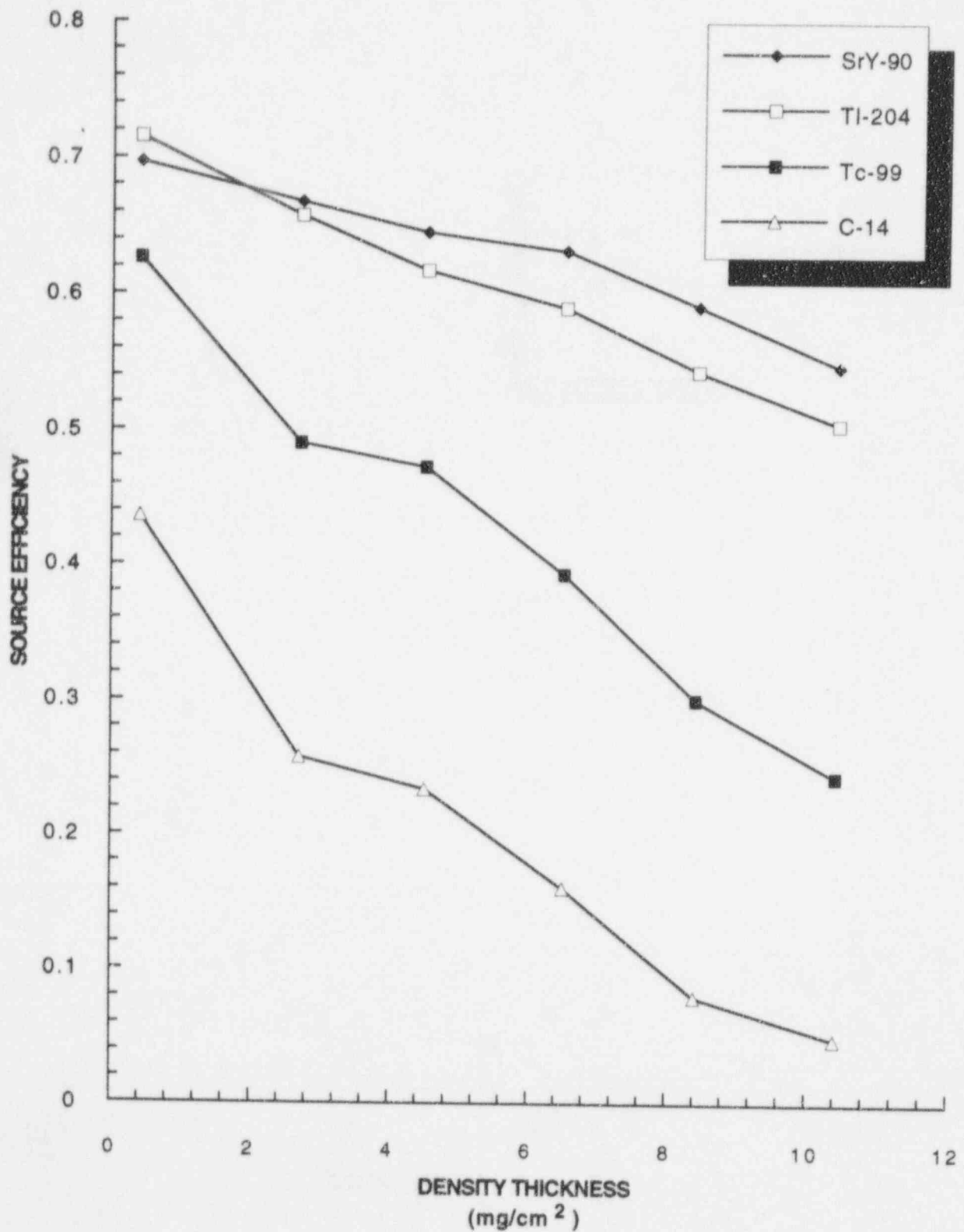
1 Figure 5.15 Effects of Dust Density Thickness on Source Efficiency for Various Sources
2 Using the Gas Proportional Detector in β -Only Mode



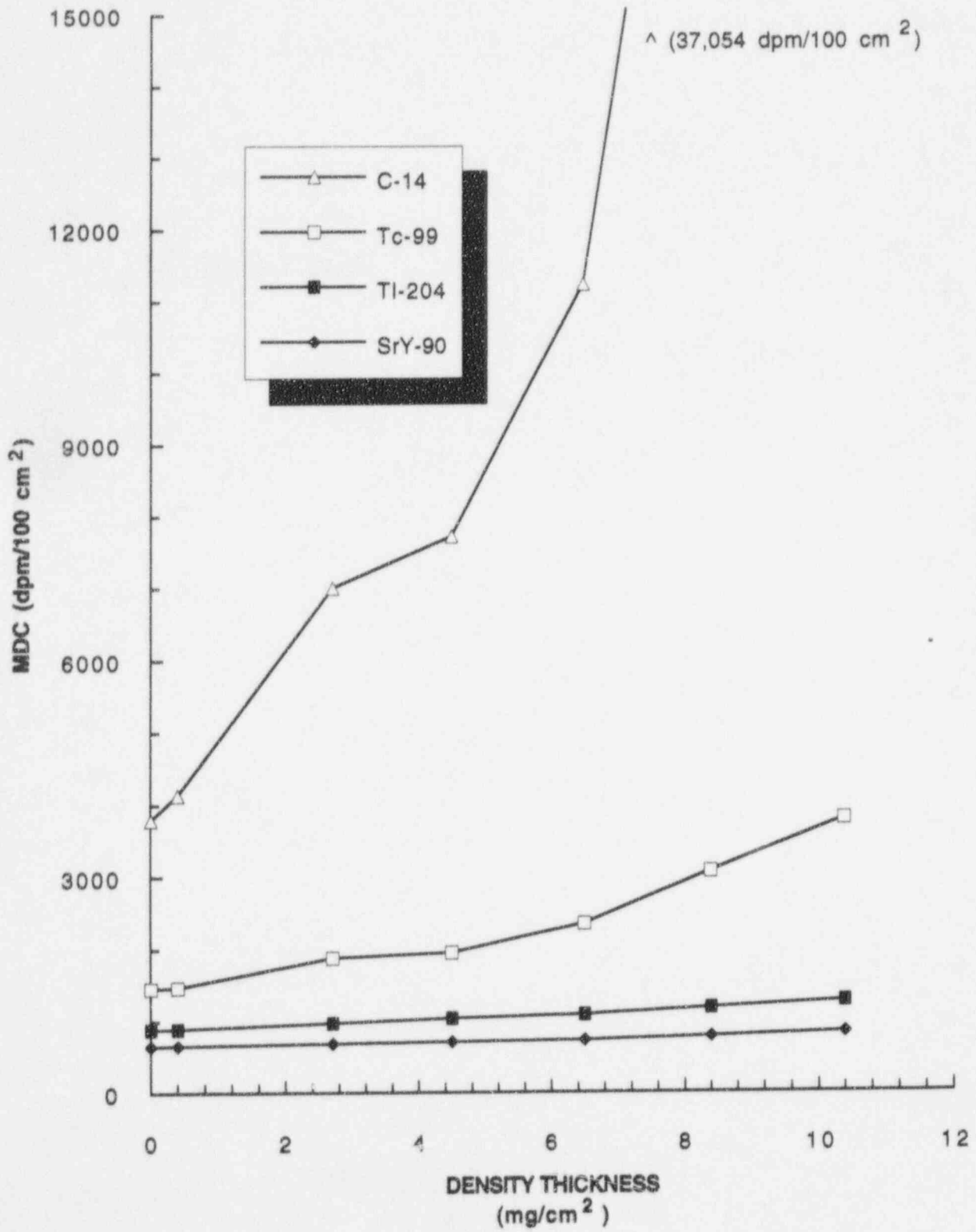
1
2

Figure 5.16 Effects of Dust Density Thickness on MDC for Various Sources Using the Gas Proportional Detector in β -Only Mode

Variables Affecting MDCs in the Field



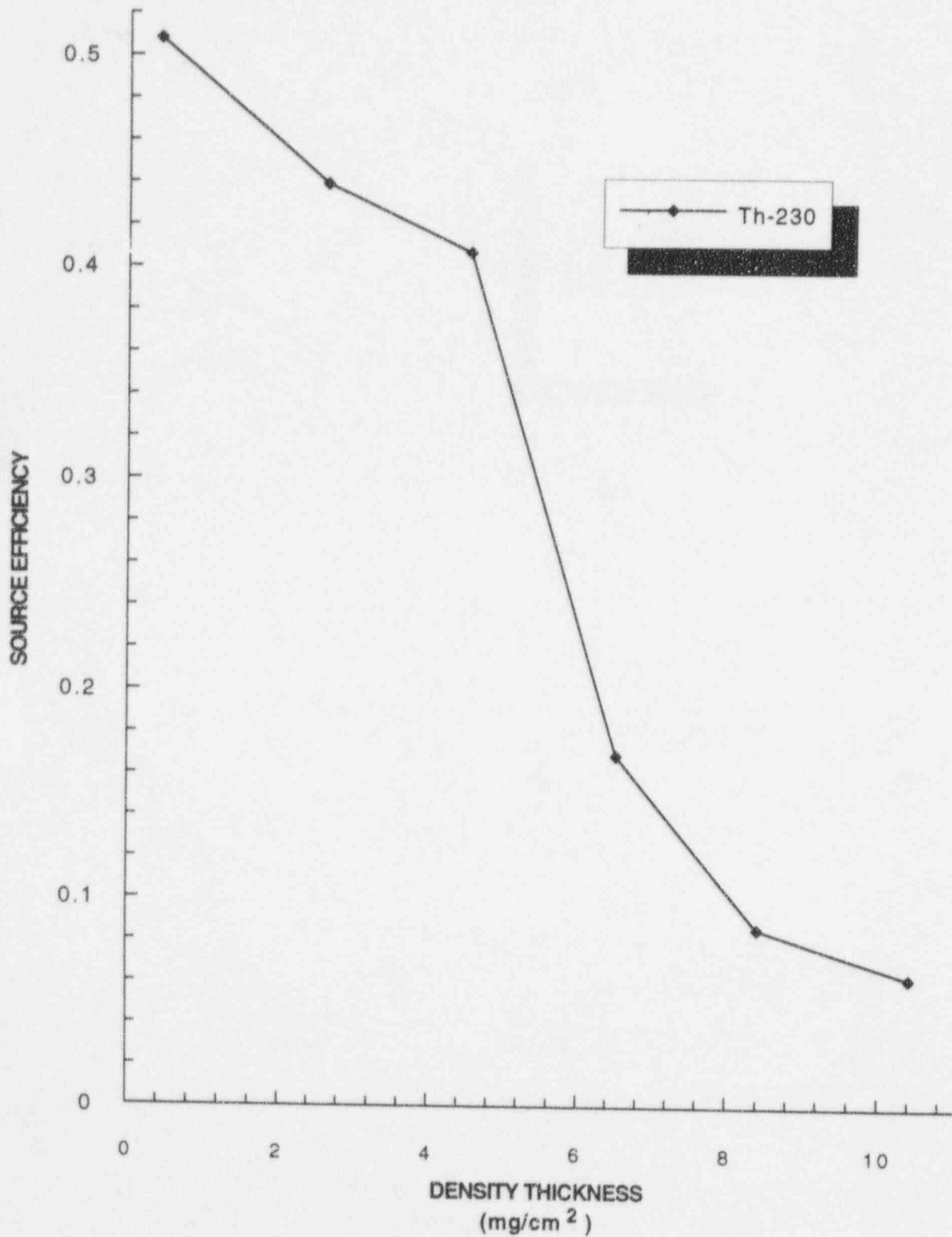
1 **Figure 5.17 Effects of Dust Density Thickness on Source Efficiency for Various Sources**
2 **Using the GM Detector**



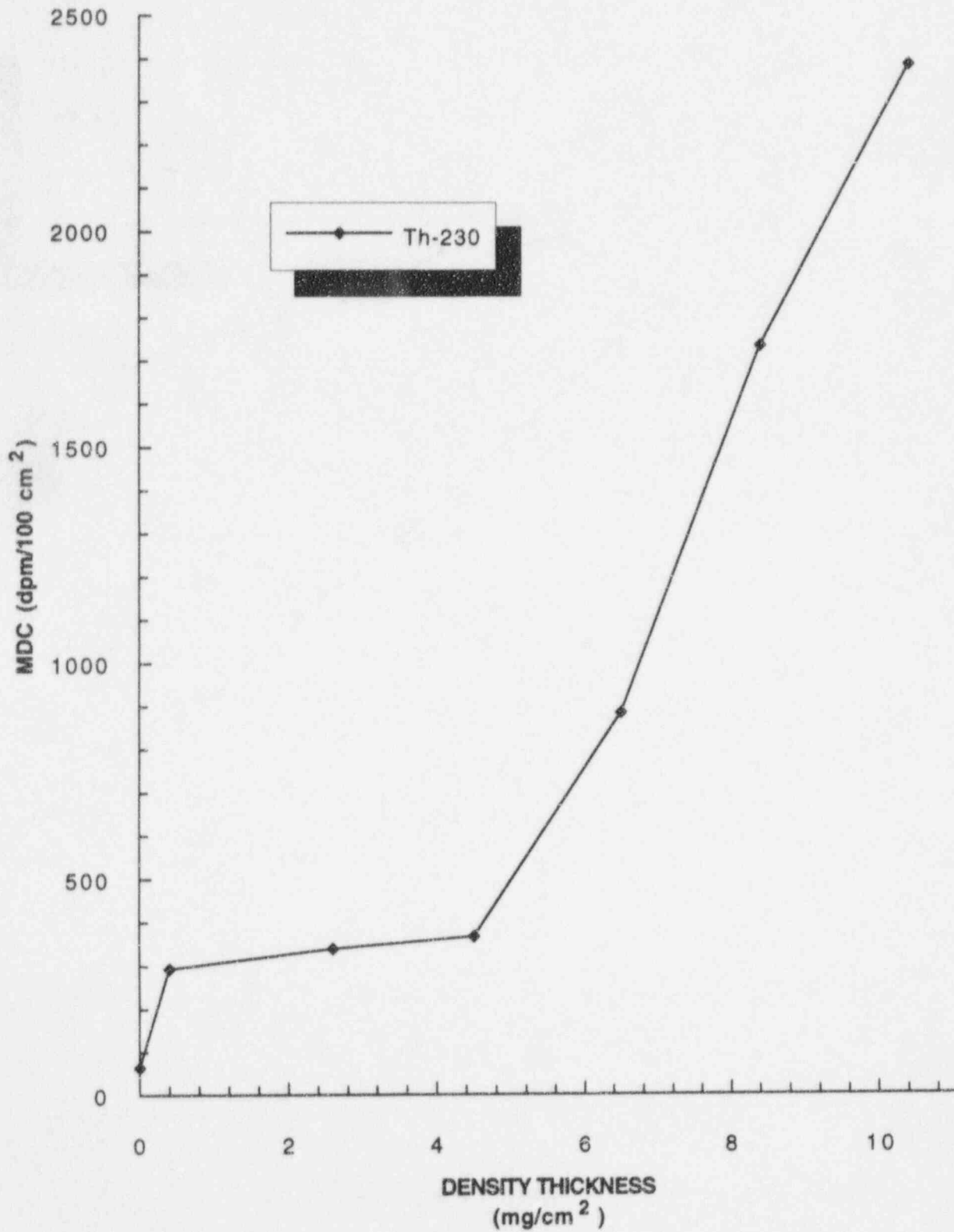
1
2

Figure 5.18 Effects of Dust Density Thickness on MDC for Various Sources Using the GM Detector

Variables Affecting MDCs in the Field

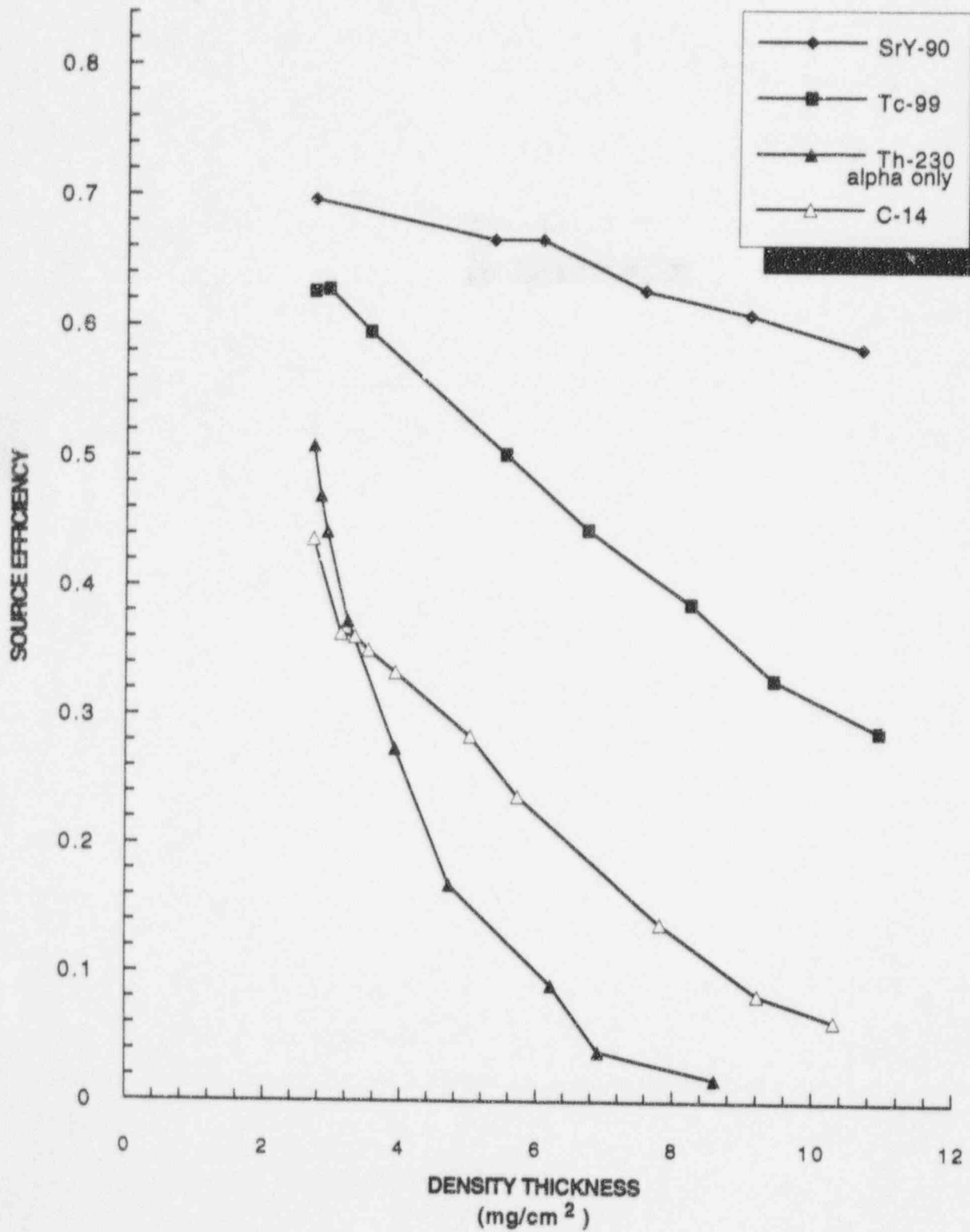


1 Figure 5.19 Effects of Dust Density Thickness on Source Efficiency for an Alpha Source
2 Using the ZnS Scintillation Detector



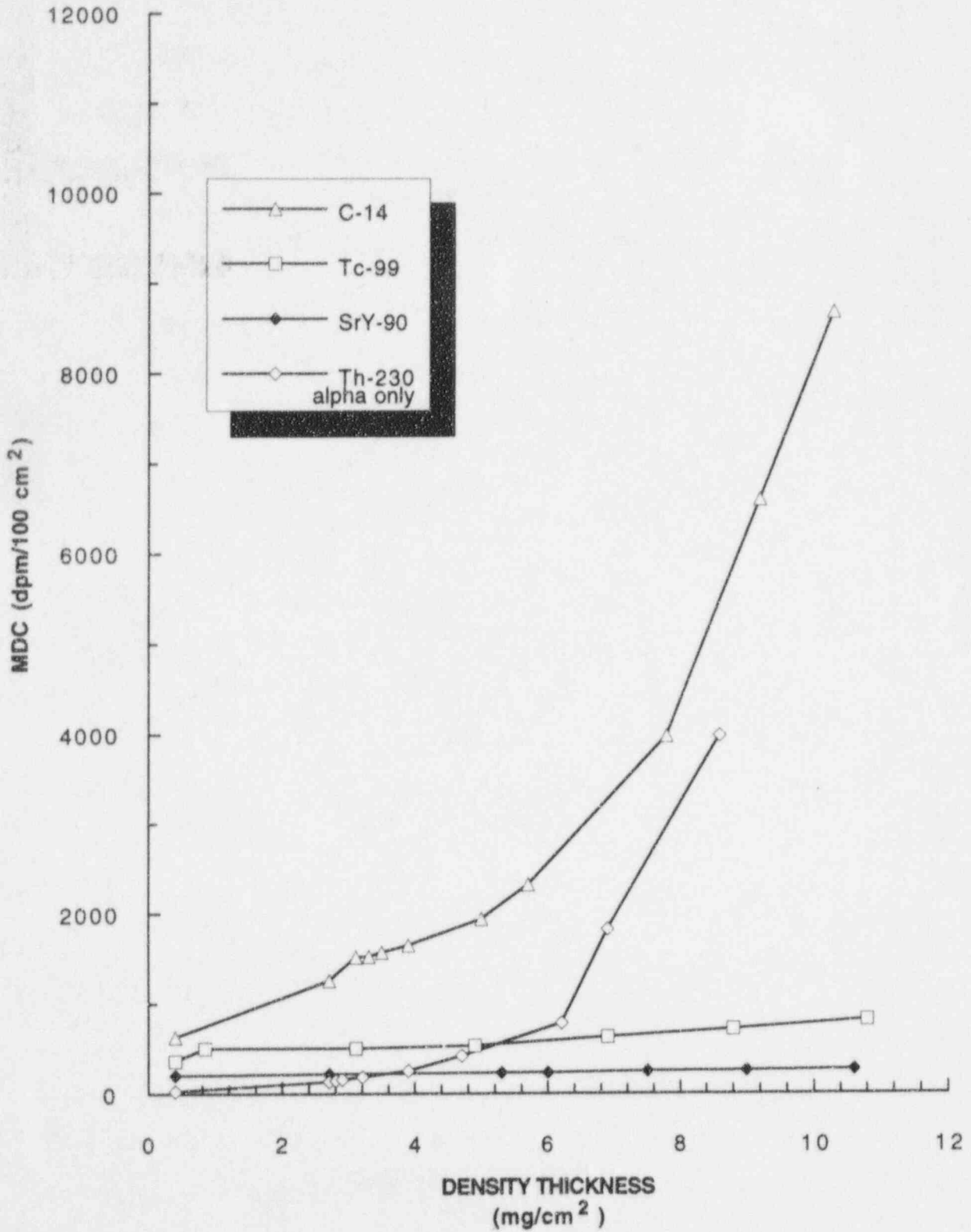
1 **Figure 5.20 Effects of Dust Density Thickness on MDC for an Alpha Source Using the**
2 **ZnS Scintillation Detector**

Variables Affecting MDCs in the Field



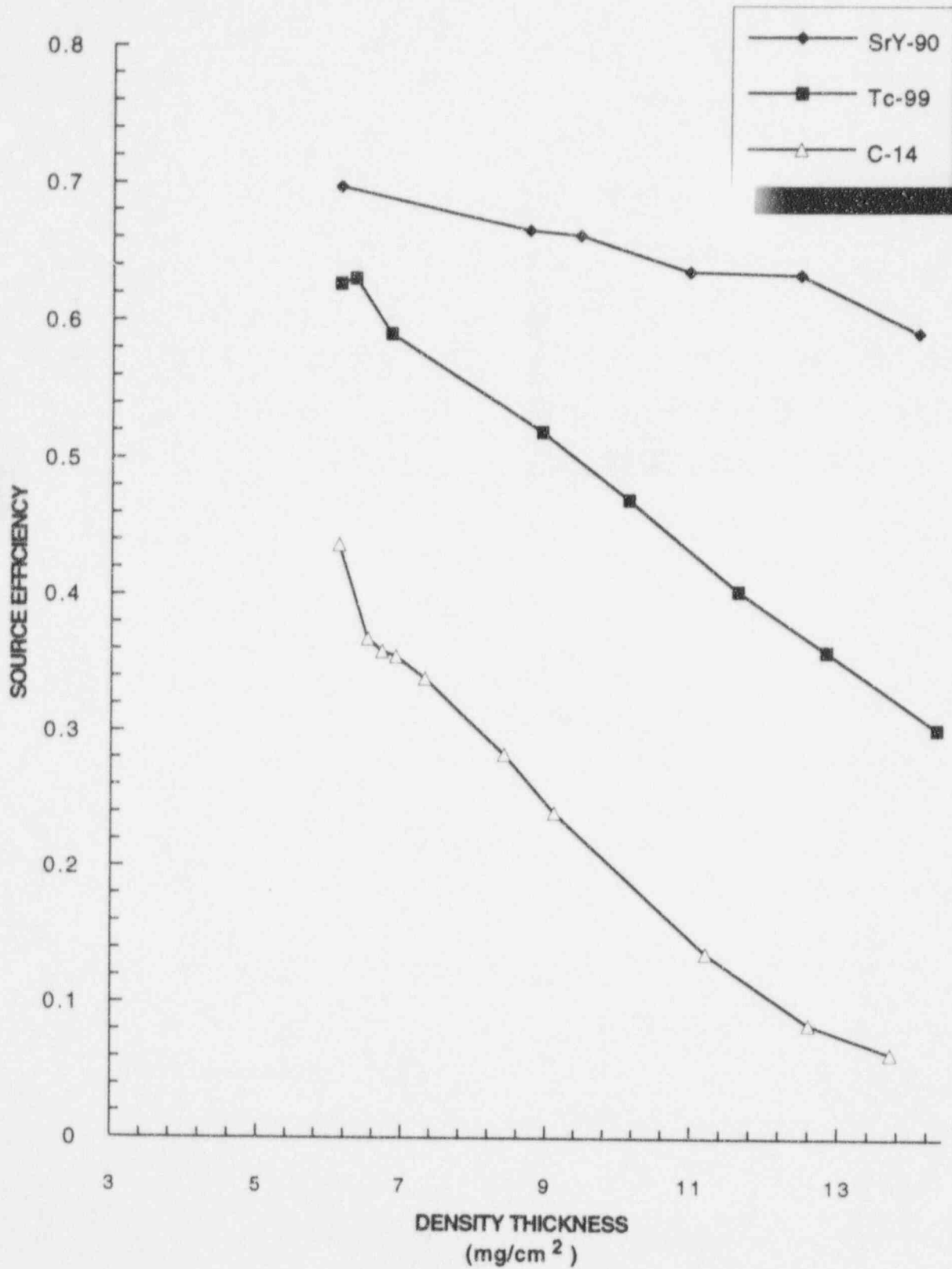
1
2

Figure 5.21 Effects of Water Density Thickness on Source Efficiency for Various Sources Using the Gas Proportional Detector in $\alpha+\beta$ and α -Only Modes

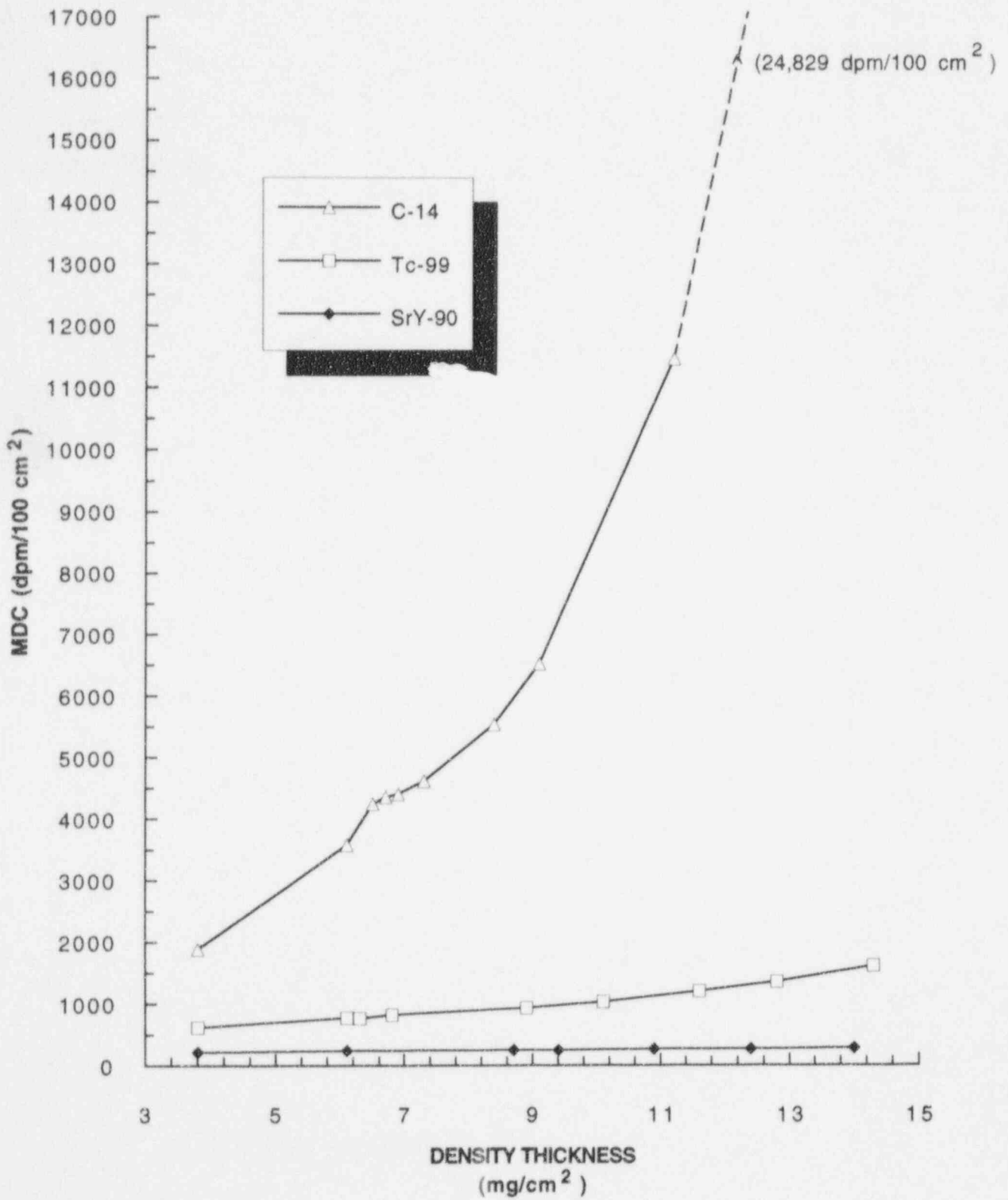


1 **Figure 5.22 Effects of Water Density Thickness on MDC for Various Sources Using the**
 2 **Gas Proportional Detector in $\alpha+\beta$ and α -Only Modes**

Variables Affecting MDCs in the Field

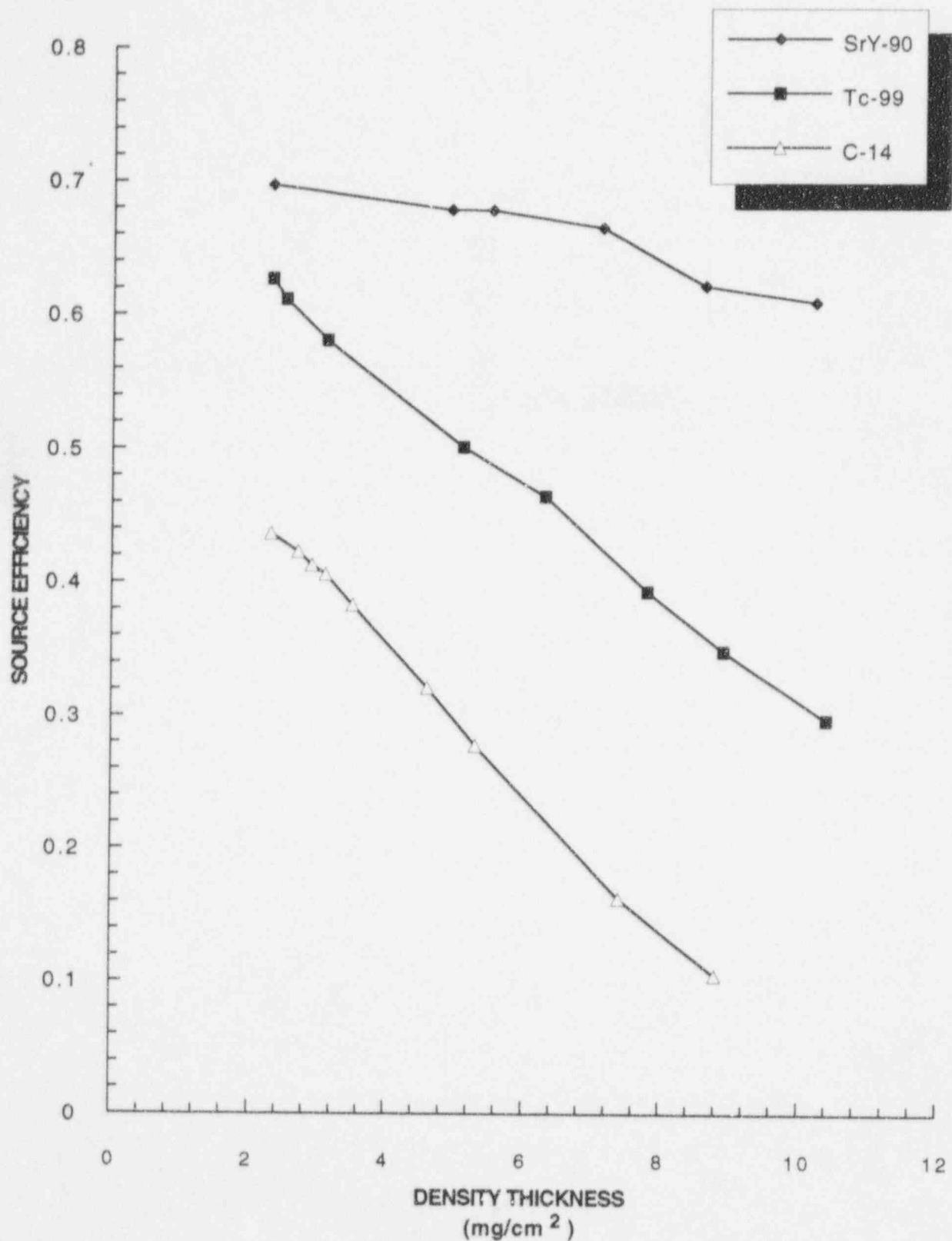


1 Figure 5.23 Effects of Water Density Thickness on Source Efficiency for Various
2 Sources Using the Gas Proportional Detector in β -Only Mode

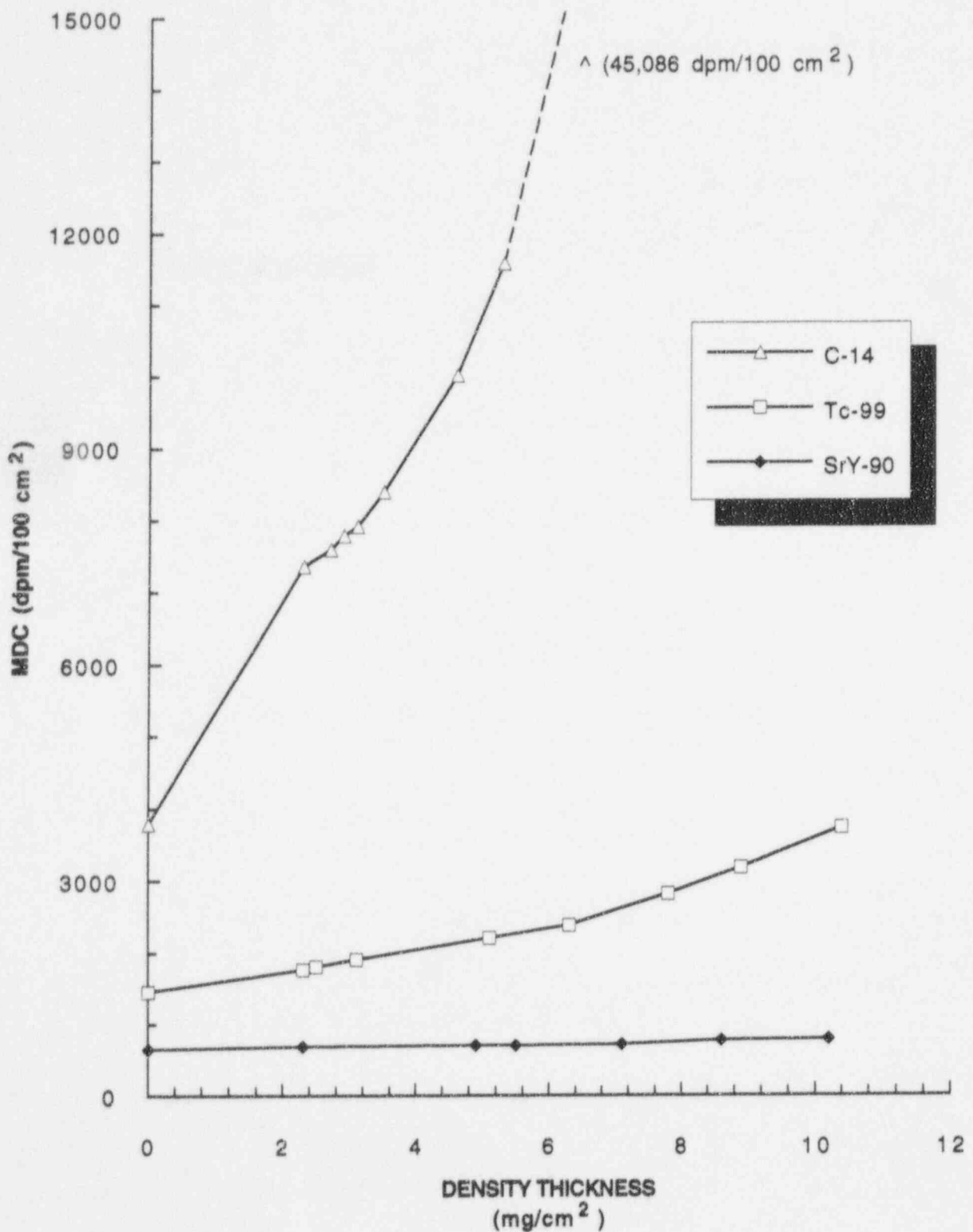


1 **Figure 5.24 Effects of Water Density Thickness on MDC for Various Sources Using the**
 2 **Gas Proportional Detector in β -Only Mode**

Variables Affecting MDCs in the Field

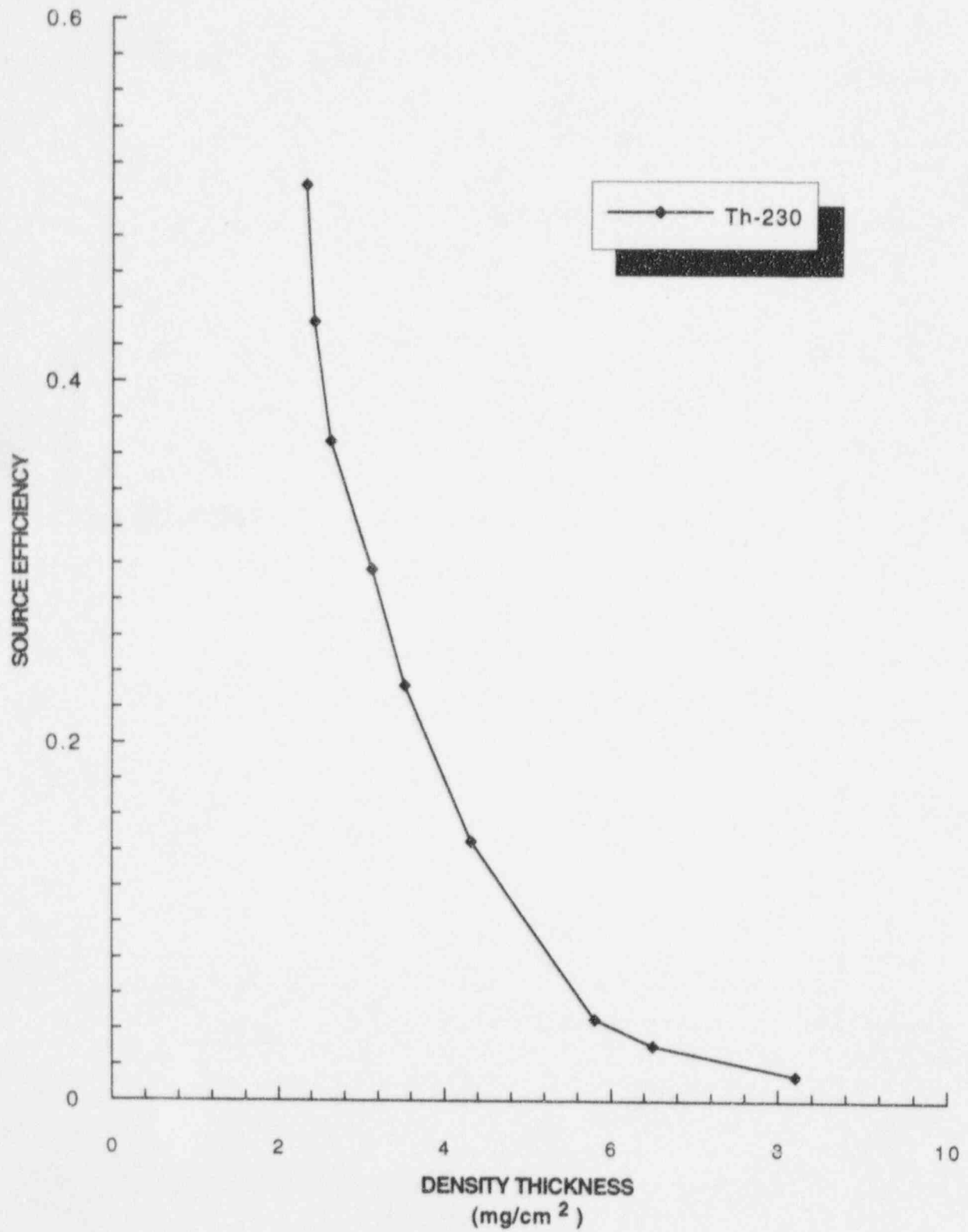


1 **Figure 5.25 Effects of Water Density Thickness on Source Efficiency for Various**
2 **Sources Using the GM Detector**

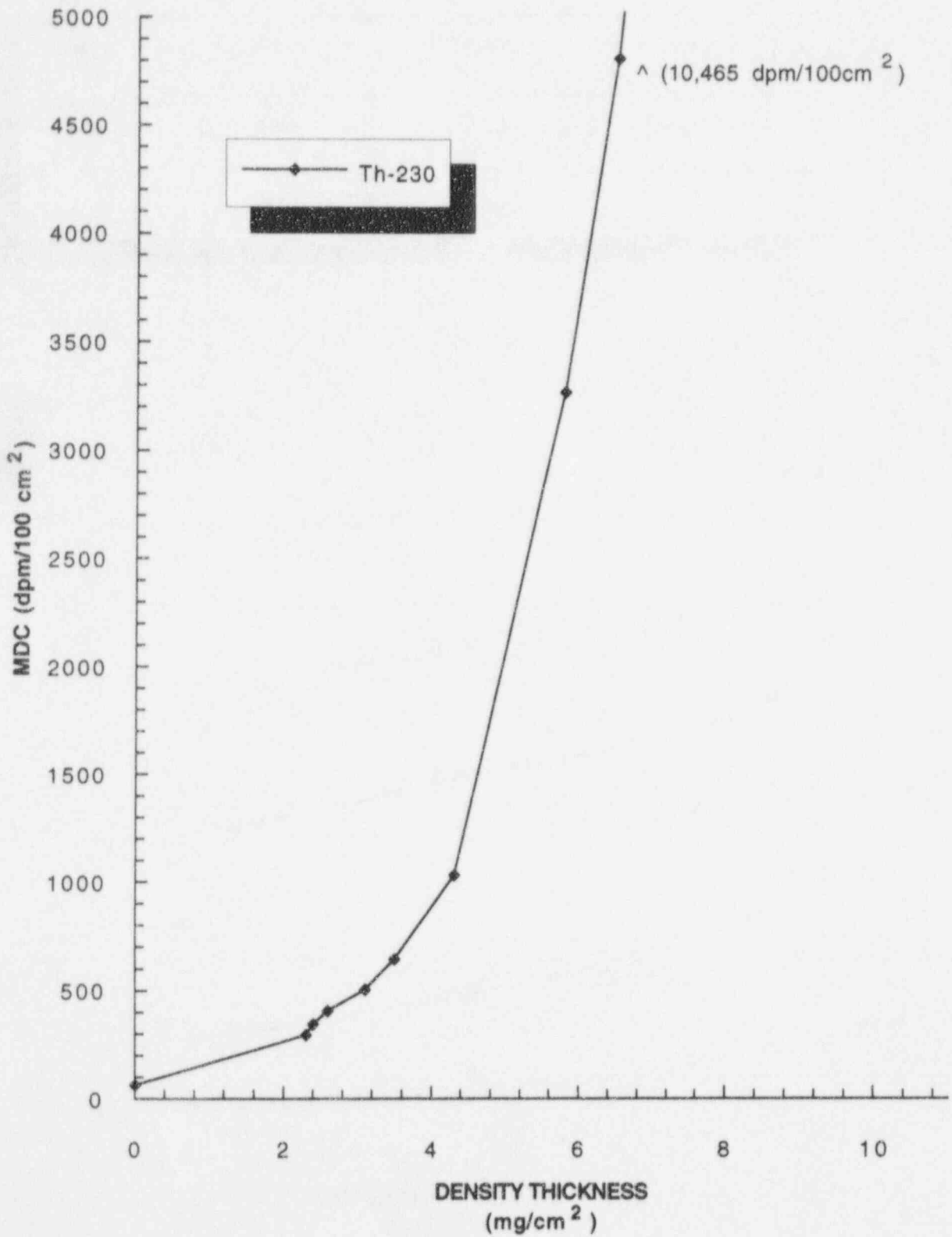


1 Figure 5.26 Effects of Water Density Thickness on MDC for Various Sources Using the
 2 GM Detector

Variables Affecting MDCs in the Field

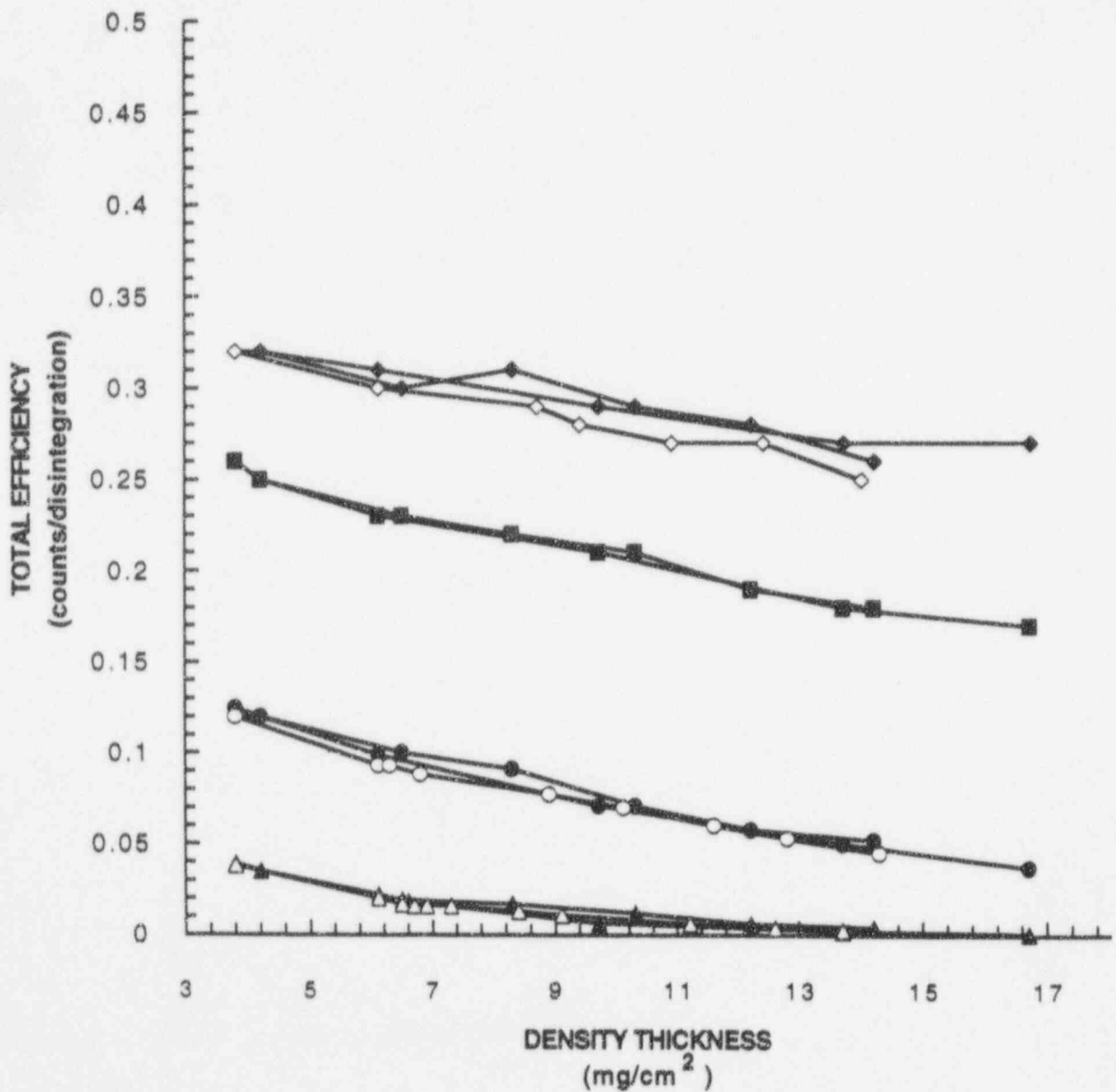
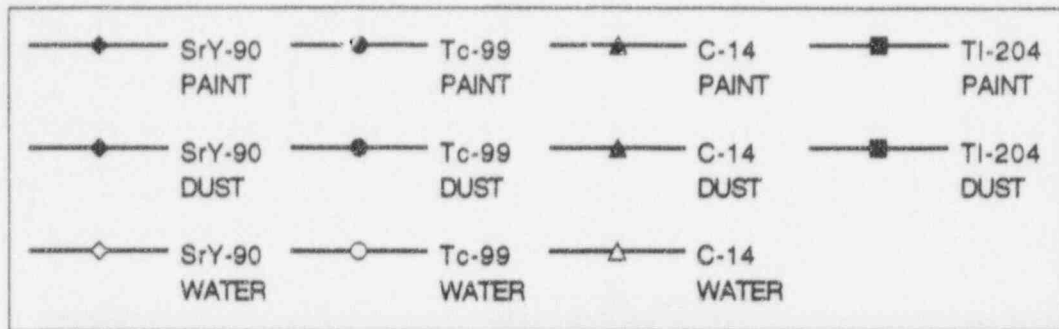


1 Figure 5.27 Effects of Water Density Thickness on Source Efficiency for an Alpha
2 Source Using the ZnS Scintillation Detector

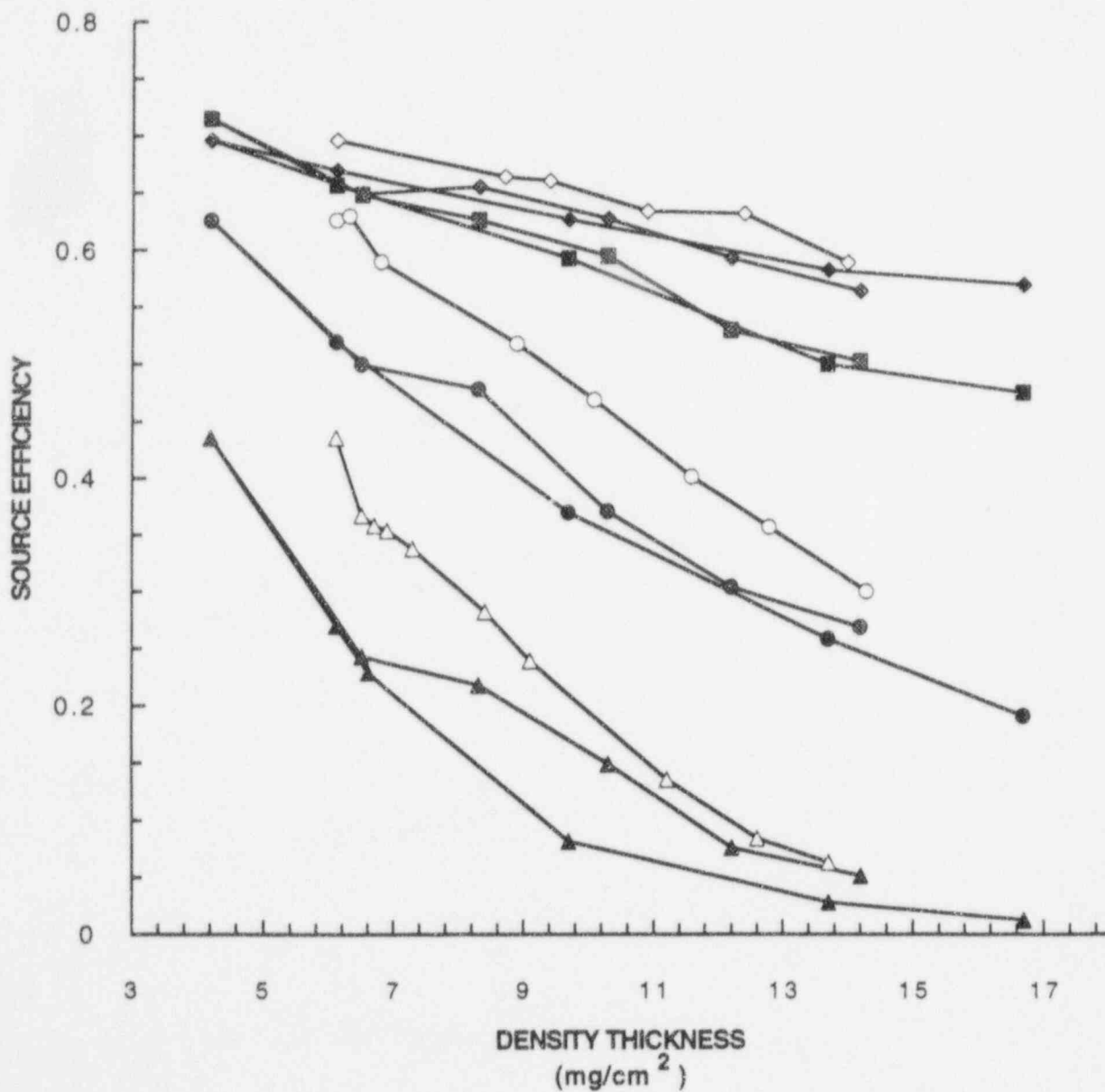
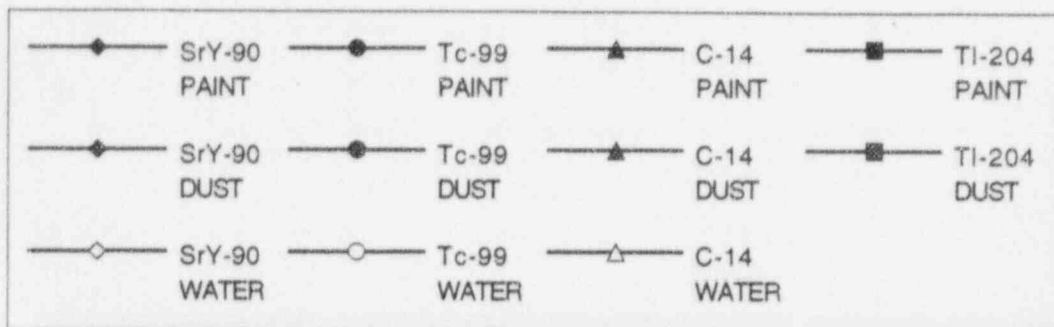


1 Figure 5.28 Effects of Water Density Thickness on MDC for an Alpha Source Using the
2 ZnS Scintillation Detector

Variables Affecting MDCs in the Field



1 Figure 5.29 Overall Effects of Paint, Dust, and Water Density Thickness on Total
 2 Efficiency for Various Sources Using the Gas Proportional Detector in
 3 β -Only Mode



1 Figure 5.30 Overall Effects of Paint, Dust, and Water Density Thickness on Source
 2 Efficiency for Various Sources Using the Gas Proportional Detector in
 3 β -Only Mode

1 **6 HUMAN PERFORMANCE AND SCANNING SENSITIVITY**

2 Scanning is often performed during radiological surveys in support of decommissioning to identify
3 the presence of any locations of elevated direct radiation (hot spots). The probability of detecting
4 residual contamination in the field is not only affected by the sensitivity of the survey
5 instrumentation when used in the scanning mode of operation, but also by the surveyor's ability.
6 The surveyor must decide whether the signals represent only the background activity, or whether
7 they represent residual contamination in excess of background.

8 **6.1 Review of Scanning Sensitivity Expressions and Results**

9 At present, scanning sensitivities are often empirically determined, depending on the experience of
10 the surveyor. One common expression for scanning sensitivity is based on the surveyor being able
11 to detect three times the background level for low count rates (NUREG/CR-5849). Limited
12 guidance on scanning capabilities is given in draft ANSI Standard 13.12, "Control of Radioactive
13 Surface Contamination on Materials, Equipment, and Facilities To Be Released for Uncontrolled
14 Use." This document states that the scanning speed shall be slow enough to ensure that a small-
15 diameter source is detected with a 67-percent probability.

16 A few attempts to quantify scanning sensitivity experimentally have been reported. Scanning
17 minimum detectable concentrations (MDCs) have been evaluated for both alpha and beta
18 instrumentation under varying background conditions using a semi-empirical approach (Goles et
19 al.). MDCs were defined as that activity that could be detected 67 percent of the time under
20 standard survey conditions. The instruments evaluated were, for alpha detection, a 50- cm²
21 portable alpha monitor, a 100-cm² large-area scintillation monitor, and a 100-cm² gas proportional
22 counter; for beta/gamma detection, a pancake GM probe, a 100-cm² large-area scintillation
23 monitor, and a 100-cm² gas proportional counter. The test procedure involved maintaining a scan
24 rate of 5 cm/s, with a scan height held at 0.64 cm. Alpha sources were 2.54-cm-diameter,
25 electroplated sources; beta/gamma sources consisted of point source geometries and uniformly
26 dispersed geometries. The MDC for alpha activity was defined as the amount of activity that
27 produces one count as the detector passes over the surface (alpha background was considered to
28 be zero) and the MDC for beta/gamma activity was determined for different background activities
29 (e.g., 50, 250, and 500 cpm), based on whether it could be detected 67 percent of the time. For
30 the most part, the researchers concluded that detectors were more sensitive to point sources than
31 to areal sources. The reported scanning sensitivities for the GM detectors demonstrated that
32 activities producing net instrument responses of 305, 310, and 450 cpm could be statistically
33 recognized 67 percent of the time in 50-, 250-, and 500-cpm background fields, respectively.
34 Goles et al. (p. 4d) cautioned that the "data are highly idealized, and that the performance of these
35 instruments may differ considerably under field conditions."

36 Sommers obtained experimental data to check the validity of the theoretical calculations of source
37 detection frequency. Calibrated sources were moved past the detector windows to determine
38 source detection frequencies for various velocities (ranging from 2.4 to 15 cm/s), and source-
39 detector distances in a background of 120 cpm. The experimental results are averages over 100

1 observations per datum point from two or more experienced surveyors. The effects of varying
2 instrument time constants, probe velocity, and background activities on source detection
3 frequencies (in %) were plotted. The researcher concluded that source detection frequencies
4 were strongly dependent on source strength, survey velocity, background activity, detector
5 sensitivity, and the time constant of the survey meter. At scanning speeds of 10 to 15 cm/s, a
6 source strength of 10,000 to 15,000 betas/min was required to provide a detection frequency of
7 90 percent. It was also determined that "with small diameter sources emitting 5,000 betas/min,
8 source detection frequency at 120 counts/min background is about 80 percent using the speaker
9 outputs, regardless of the survey velocities between 3.5 and 15 cm/s" (Sommers, p. 760).

10 Lastly, in LA-10729, Olsher et al. report a study intended to determine the scanning sensitivity of
11 alpha detection instrumentation by measuring the hot spot detection frequency under realistic
12 survey conditions. The procedure involved more than 40 surveyors with varying levels of
13 experience, who were asked to survey five stations, each consisting of a 4-foot by 4-foot section
14 of masonite that was painted with a Th-232-based paint. The thorium-based paint, which was the
15 same color as the original paint and thus hid the hot spots, was applied to nine locations at each
16 station. The alpha activity levels ranged from 64 to 672 dpm. The surveyors were instructed to
17 survey each of the five stations and to record their results on a survey grid map. The detection
18 frequency and false positive frequency were determined for each survey group. The alpha source
19 activity for a 50 percent detection frequency was determined to range from 392 to 913 dpm for
20 the ZnS scintillation detectors evaluated. One interesting result of this evaluation was that less-
21 experienced surveyors had a higher detection probability than did experienced surveyors. The
22 authors attributed this to the fact that the inexperienced surveyors took approximately twice as
23 long to complete the scan survey.

24 6.2 Scanning as a Signal Detection Problem

25 The probability of detecting residual contamination in the field depends not only on the sensitivity
26 of the survey instrumentation when used in the scanning mode of operation, but also on the
27 surveyor's ability. Personnel conducting radiological surveys for residual contamination at
28 decommissioning sites must interpret the audible output or visual reading of a portable survey
29 instrument to determine when the signal (clicks or visual readings) exceeds the background level
30 by a margin sufficient to conclude that contamination is present. It is hard to detect low levels of
31 contamination because both the signal and the background vary widely.

32 In abstract terms, the task of personnel conducting radiological surveys can be briefly
33 characterized as follows. The condition of the object being surveyed is represented to the
34 surveyors by samples from random processes. Furthermore, the samples are limited in size (i.e.,
35 time) for practical reasons. On the basis of the samples, the surveyors must decide whether they
36 have sampled the distribution of activity associated with a contaminated object or an
37 uncontaminated object. Under these circumstances, the number of signals correctly detected by
38 observers will depend to a significant extent on their willingness to report the presence of a signal,
39 i.e., their criterion for responding positively. The concepts and methods of signal detection theory
40 are well suited to the analysis of performance on such tasks.

41 Signal detection theory, as originally conceived, applied the principles of statistical decision theory
42 to the detection of radar signals in the presence of electromagnetic noise. It was soon recognized,

1 however, that the theory could also be used to characterize the detection of sensory signals by
 2 human observers (Green & Swets). The theory postulates that the sensory input that constitutes
 3 an observation can be represented at some point in the sensory/perceptual system on a single,
 4 continuous dimension. It is assumed that any particular observation (or value on the continuum)
 5 can arise from either noise alone or from signal-plus-noise. Thus the information available to the
 6 observer can be represented by two (typically overlapping) probability density distributions (see
 7 Figure 6.1). The task of the observer is to indicate whether a stimulus arose from a "noise alone"
 8 or a "noise plus signal" event. This decision is based on the likelihood ratio, i.e., the odds in favor
 9 of an observation x having resulted from a signal-plus-noise event. Other things being equal, an
 10 ideal observer will locate the yes/no criterion at a point corresponding to a likelihood ratio of one
 11 (criterion B in Figure 6.1). The area of the signal-plus-noise and noise distributions lying beyond
 12 the criterion is estimated by the proportion of positive responses given when signal-plus-noise and
 13 noise alone, respectively, were in fact present. If the underlying distributions can be assumed to
 14 be normal and of equal variance, an index of sensitivity (d') can be calculated which represents the
 15 distance between the means of the distributions in units of their common standard deviation. The
 16 index is calculated by transforming the true positive rates to standard deviation units, i.e., z-scores
 17 (Macmillan & Creelman) and taking the difference:

$$d' = z(\text{true positive}) - z(\text{false positive}) \quad (6-1)$$

18 The d' measure is independent of the criterion adopted by the observer, thus allowing meaningful
 19 comparisons of sensitivity under conditions in which observers' criteria may be different. The
 20 relative operating characteristic (ROC) relates the probability of a correct detection to that of a
 21 false report as the response criterion is varied.

22 It is conventional in signal detection theory analysis to describe performance in terms of the true
 23 positive (or correct detection) rate and the false positive rate. The remaining two response
 24 conjunctions, true negatives (or correct rejections) and false negatives ("misses") are simply the
 25 complements of the preceding quantities.

26 According to statistical decision theory, the *a priori* probabilities of the events and the values and
 27 costs associated with the outcomes will influence the placement of the criterion. Thus the
 28 detection of a signal in a noise background is determined not only by the magnitude of the signal
 29 relative to the background, but also by the willingness of the observer to report that a signal is
 30 present, i.e., the criterion for responding "yes." The criterion depends on two factors: response
 31 value/cost and signal probability. If, for example, a false positive entails a significant cost, the
 32 observer will position the criterion more conservatively (e.g., criterion C in Figure 6.1); if it is
 33 expected that signals will greatly outnumber non-signals, a more liberal placement of the criterion
 34 will yield optimal results (e.g., criterion A in Figure 6.1).

35 6.3 Influences on Surveyor Performance

36 Figure 6.2 depicts the survey process as a series of stages. At each stage, beginning at the source,
 37 evidence of contamination is transformed (e.g., attenuated by surface conditions and/or probe
 38 characteristics, scaled by instrument circuitry). In static surveys, the "operator" (i.e., surveyor)
 39 stage is bypassed. At the final stage, the transformed evidence is compared to a criterion, and a
 40 decision is made as to the presence of contamination.

Human Performance and Scanning Sensitivity

1 As shown in Figure 6.2, factors related to the surveyor can influence the performance of the
2 surveyor/instrument system at each stage. The amount of radiation reaching the probe is affected
3 by the source-to-detector geometry, which is a function of the source and detector dimensions
4 and the distance of the probe from the surface, as well as the speed at which the surveyor moves
5 the probe over the surface. In terms of signal detection, these aspects of the surveyor's technique
6 determine the degree of overlap of the background and source distributions. The difficulty of the
7 detection decision also depends on the audibility or visibility or both, of the instrument's display(s)
8 and the surveyor's attention to these. Finally, the surveyor's decision itself is influenced by a
9 variety of factors, including the relative costs of "misses" and "false positives," and the surveyor's
10 assumptions regarding the likelihood of contamination being present. The nature of this final
11 decision stage is considered in more detail below.

12 In practice, surveyors do not make decisions on the basis of a single indication. Rather, upon
13 noting an increased number of counts, they pause briefly and then decide whether to move on or
14 take further measurements. Thus, surveying consists of two components: continuous monitoring
15 and stationary sampling. In the first component, characterized by continuous movement of the
16 probe, the surveyor has only a brief "look" at potential sources. The surveyor's criterion (i.e.,
17 willingness to decide that a signal is present) at this stage is likely to be liberal, in that the
18 surveyor should respond positively on scant evidence, since the only "cost" of a false positive is a
19 little time. The second component occurs only after a positive response was made at the first
20 stage. It is marked by the surveyor interrupting his scanning and holding the probe stationary for
21 a period of time, while comparing the instrument output signal during that time to the background
22 counting rate. For this decision, the criterion should be more strict, since the cost of a "yes"
23 decision is to spend considerably more time taking a static measurement. If the sample is
24 sufficiently long, an acceptable rate of source detection can be maintained despite application of
25 the more stringent criterion. For example, the solid line in Figure 6.3 represents performance for
26 a 4-second observation. Under these conditions, roughly 95-percent correct detections can be
27 achieved with only 10-percent false positives.

28 Observers' estimates of the likelihood/frequency of signals will also influence their willingness to
29 decide that a signal is present. Other things being equal, a surveyor will adopt a less-strict
30 criterion when examining areas in which contamination may be expected. Similarly, surveyors'
31 criteria may be more strict when examining areas in which they do not expect contamination to be
32 present. During an extended period of scanning, the surveyor's subjective estimate of the
33 likelihood of contamination may decrease if no contaminated areas are found. The criterion will,
34 therefore, become stricter as the task progresses and the surveyor will become less likely to find
35 contamination if it does exist. This decrease in hit rate with time on task, referred to as the
36 "vigilance decrement," is typically a criterion effect—that is, sensitivity is not affected. However,
37 in radiological surveying, the expectation of a low probability of contamination may affect
38 sensitivity of the surveyor/instrument system as well, since the surveyor may move the probe more
39 quickly, thereby degrading the input to the system.

40 **6.4 Ideal Observer and Real Performance**

41 In addition to allowing observers' sensitivity to be evaluated independently from their decision
42 criteria, signal detection theory also allows their performance to be compared to that of an ideal

1 observer. In this section, an ideal observer approach to detection in the context of radiological
2 surveys is outlined, and the results of relevant laboratory findings are summarized.

3 **6.4.1 The Ideal Poisson Observer**

4 If the nature of the distributions underlying a detection decision can be specified, it is possible to
5 examine the performance expected of an ideal observer, i.e., one that makes optimal use of the
6 available information. This is of interest in the present context because it allows the basic
7 relationships among important parameters (e.g., background rate and length of observation) to be
8 anticipated, and it provides a standard of performance (actually an upper bound) against which to
9 compare performance of actual surveyors.

10 The audio output of a survey instrument represents randomly occurring events. It will be
11 assumed that the surveyor is a "counting" observer, i.e., one who makes a decision about the
12 presence or absence of contamination based on the number of counts occurring in a given period
13 of time. This number will have a Poisson distribution, and the mean of the distribution will be
14 greater in the presence of contamination than when only background activity is present. When the
15 intensity of radiation associated with contamination is low, as it often is during final status
16 surveys, these distributions will overlap. The ideal observer decides that contamination is present
17 if the number of counts is greater than x , where the criterion value x is chosen according to some
18 rule (e.g., maximize percent correct or maintain a false positive rate of no more than 0.10).

19 If the number of counts per minute representing background activity and contamination is
20 specified, and an observation interval is postulated, the performance expected for an ideal
21 observer (in terms of correct detection and false positive rates) can be determined from tabled
22 values of the cumulative Poisson distribution. The following example will illustrate this approach.
23 Consider an observer attempting to detect 180 cpm in a background of 60 cpm based on
24 observations that last 1 second. The observer's decision will be based on two overlapping
25 (Poisson) distributions of counts, one having a mean of one (corresponding to the background
26 activity) and the other having a mean of three (corresponding to the source plus background
27 activity).

28 If the background and source are equally likely events, and positive and negative responses are
29 equally valued, the ideal observer attempting to maximize the percent correct will choose
30 two counts as a criterion for a positive response (see the point labeled 2 in Figure 6.3). From the
31 values of the cumulative Poisson probabilities given in Table 6.1, the observer would be expected
32 to correctly detect 80 percent of the 180-cpm sources, and would also identify background
33 activity as a source roughly 26 percent of the time. If the situation were such that missed signals
34 should be strongly avoided, the observer might adopt a criterion of one count (see the point
35 labeled 1 in Figure 6.3). In this case 95 percent of the sources would be detected, but the rate of
36 false positives would increase to roughly 63 percent. If for all of the possible criteria, the
37 corresponding true positive rates are plotted against the corresponding false positive rates, the
38 result is the relative operating characteristic (ROC) for a given condition (Figure 6.3).

39 The scanning sensitivity of the ideal Poisson observer may be estimated for various background
40 levels and observation intervals. It can be shown that detectability varies with the square root of
41 the background rate (Egan, pp. 192-187). Table 6.2 lists minimum scanning sensitivities for

Human Performance and Scanning Sensitivity

1 **Table 6.1 Cumulative Poisson Probabilities of Observed Values for Selected Average**
 2 **Numbers of Counts per Interval^a**

3	4	5	6	7	8	9	10	11	12	13	14	15	16	17	18	19	20	21
Criterion Value	60 cpm (1 sec = 1 count)	180 cpm (1 sec = 3 counts)	Criterion Value	60 cpm (4 sec = 4 counts)	180 cpm (4 sec = 12 counts)													
0	1.000	1.000	0	1.000	1.0000													
1	.6321	.9502	1	.9817	1.0000													
2	.2642	.8009	2	.9084	.9999													
3	.0803	.5768	3	.7619	.9995													
4	.0190	.3528	4	.5665	.9977													
5	.0037	.1847	5	.3712	.9924													
6	.0006	.0839	6	.2149	.9797													
7	.0001	.0335	7	.1107	.9542													
8		.0119	8	.0511	.9105													
9		.0038	9	.0214	.8450													
10		.0011	10	.0081	.7576													
11		.0003	11	.0028	.6528													
12		.0001	12	.0009	.5384													
			13	.0003	.4240													
			14	.0001	.3185													
			15		.2280													
			16		.1556													

22 ^aBased on tabled values of the cumulative Poisson distribution given in R.H. Beyer (ed.), *Handbook of Tables for Probability and*
 23 *Statistics*, Cleveland: Chemical Rubber Co.

24 **Table 6.2 Scanning Sensitivity of the Ideal Poisson Observer for Various Background Levels^a**

25	26	27	28	29	30	31	32	33	34
Background (cpm)	Scan Sensitivity (gross cpm)	Ratio of Scan Sensitivity to Background							
45	150	3.3							
60	180	3							
75	210	2.8							
300	570	1.9							
400	710	1.8							
500	845	1.7							
1,800	2,460	1.4							
2,400	3,160	1.3							
3,000	3,850	1.3							

35 ^aThe scanning sensitivity of the ideal Poisson observer is based on an index of sensitivity (d') of 2 and a 1-second observation interval.

1 background levels typical of GM detectors (45 to 75 cpm), gas proportional detectors in β or $\alpha+\beta$
2 modes (300 to 500 cpm), and NaI scintillation detectors (1,800 to 3,000 cpm). These scanning
3 sensitivities are based on an observation interval of 1 second and a d' of 2. The results indicate
4 that the minimum detectable net signal is a multiple of the background level at count rates typical
5 for GM detectors, and a fraction (about 30%) of the background level at count rates typical for
6 gas proportional and NaI scintillation detectors.

7 It can similarly be shown (Egan, p. 187) that, for the Poisson observer, detectability increases
8 with the square root of the observation interval; this interval is of course determined by probe
9 speed. The relationship of the performance of actual observers to the prediction based on the
10 ideal observer is considered in the next section.

11 It should be recognized that because the scan MDCs are presented in the context of signal
12 detection theory (distinguishing between "noise alone" and "noise plus signal"), the detector
13 response (in cpm) alone is necessary to make a decision on the presence (or absence) of radiation
14 levels above background. Scan parameters, such as detector dimensions, source-to-detector
15 geometry, scan speed, and the time constant of the meter, are all folded into the detector
16 response. For example, an observation interval of 1 second translates into different scan rates,
17 depending on the scan distance covered in that time for each detector type.

18 6.4.2 Actual Observer Performance

19 Brown and Emmerich compared the performance of the ideal observer to that of real observers
20 detecting signals similar to the audio output of a survey meter. The intensities of two random
21 processes (background and source) were indicated by brief audio pulses. In one experiment,
22 detection performance of actual observers was examined for background and source levels and
23 observation intervals chosen to yield equal ideal detectabilities. In a second experiment,
24 background and source levels were held constant and observation interval was increased. In both
25 experiments, performance was inferior to that predicted for the ideal observer. Interestingly, the
26 difference between actual and ideal performance was not constant for all conditions. That is,
27 actual performance as a function of background rate and observation interval did not necessarily
28 parallel the functions expected for the ideal observer. The patterns of results for the two
29 observers in the experiments were quite similar however, leading the authors to suggest that it
30 may be possible specify a generally applicable "efficiency factor" (see the discussion in Egan,
31 p. 188) that relates actual to ideal performance.

32 The results described above took place under controlled conditions designed to support optimal
33 performance. In the next section, the performance of surveyors under field conditions is
34 examined.

35 6.5 Actual Surveyor Performance—Field Tests

36 Three scan survey experiments (two conducted indoors and one outdoors) were designed and
37 conducted to determine scanning MDCs under field conditions. The experiments employed actual
38 radioactive sources and scanning instrumentation. The following section describes the general
39 procedures and analysis approach common to all three studies. Details of the procedures and

Human Performance and Scanning Sensitivity

1 results for the indoor surveys using GM and gas proportional detectors detector are given in
2 Sections 6.5.2 and 6.5.3, respectively. The outdoor survey (using a NaI scintillation detector) is
3 described in Section 6.5.4. Section 6.5.5 contains a general discussion of the results of the field
4 experiments.

5 6.5.1 General Method

6 Procedure

7 Radioactive sources were positioned so that the surveyors could not see them. The surveyors
8 were given written instructions (Figures 6.4 and 6.5) and scale maps of the test areas to be
9 scanned (Figures 6.6, 6.7, and 6.8), and were then instructed to perform a 100-percent scan of the
10 test area at a specified scan rate. Surveyors marked on the map the areas they judged as
11 containing residual activity in excess of background along with the actual meter reading (in cpm)
12 for those areas. While the surveys were being conducted, observers recorded on a similar map
13 any locations at which the surveyor briefly held the probe stationary.

14 The indoor experiments consisted of performing scans for beta activity on an interior wall at a
15 height of 0.5 to 2 meters with a GM detector (20-cm² probe area) and a gas proportional detector
16 (126-cm² probe area). The length of the wall section surveyed was 5 meters, resulting in a test
17 area of 7.5 m². In the outdoor experiment, an area measuring 20 meters by 30 meters was
18 surveyed.

19 Analysis Approach

20 The true positive rates for the continuous and the stationary components of the scanning task
21 were determined by dividing the number of sources to which one or more positive responses were
22 made by the number of radioactive source configurations. For the continuous scanning
23 component, a pause in the movement of the probe was considered a positive response. A
24 response was considered to have been associated with a source if it fell within any of the areas of
25 elevated activity as mapped prior to the start of the field trials. (It should be emphasized that
26 positive responses occurred simply by the surveyor pausing at these source locations, even if the
27 surveyor subsequently concluded that the response did not represent a signal above background.)
28 For the stationary component, a positive response was a surveyor's identification of a location as
29 exceeding background.

30 The number of false positives for the continuous task was computed as the total number of times
31 the surveyor paused minus the number of pauses associated with sources. A difficulty arises in
32 analyzing a continuous detection task since the rate at which false alarms occur cannot be
33 specified simply, as it can for performance on discretely presented trials (see, e.g., Egan et al.;
34 Watson & Nichols). An estimate of the number of opportunities for a false positive must be
35 arrived at in order to compute a rate. The number of false positive opportunities was determined
36 by estimating the average area covered by the source configurations, and then dividing this area
37 into the entire area represented by the false positives (which is equal to the entire area minus the
38 total source configuration area). For the interior example, the entire area tested was 7.5 m², with
39 the total source configuration area occupying roughly 0.5 m². The area of a typical source was
40 estimated to be roughly 500 cm². Thus, the number of false positive opportunities was estimated

1 as 140. If it is assumed that false positive responses are distributed randomly over the "non-
2 contaminated" area (and there is no reason to assume otherwise), the false positive rate is then
3 roughly the number of responses divided by number of opportunities. This estimate is not exactly
4 correct, however, since it is possible for two (or more) responses to fall in the same area. If the
5 false positive rate is to be considered the proportion of opportunities having at least one response
6 associated with them, the calculation must take into account the expectation of two (or more)
7 responses occurring in the same area. This proportion is formally the complement of an estimate
8 of the probability of an unobserved outcome (e.g., Robbins) and can be calculated by an
9 analogous method.¹

10 The results of the each field experiment are presented by plotting (individually for each surveyor)
11 the true positive rate as a function of false positive rate for both the pauses and final decisions. A
12 line is drawn connecting the two points representing each subject. It should be noted that these
13 plots are not typical ROCs. The connected points do not represent different criteria applied to the
14 same presentation. Rather, they represent performance by the same individual for two situations
15 in which detectability was expected to differ.

16 6.5.2 Indoor Scan Using GM Detector

17 Procedure

18 Sheets of cardboard were cut to fit over the entire 1.5 meter by 5 meter test area surface.
19 Sections of the cardboard were removed from the wall and radioactive sources were fastened to
20 the side of the cardboard in contact with the wall. The radioactive sources were C-14, Co-60, Sr-
21 90, Tc-99, Cs-137, and processed natural uranium. Sixteen sources were randomly positioned on
22 the cardboard, either singly or in groups (resulted in nine discrete source configurations), so as to
23 provide varying radiation levels and geometries (Figure 6.6). The radiation source levels were
24 selected to be near the expected scanning sensitivity based on ESSAP field experience. The
25 cardboard sections were then repositioned on the wall and the entire surface was characterized to
26 provide information on the location and beta radiation level of each source configuration. The
27 gross radiation levels ranged from 60 to 950 cpm, and the source geometries ranged from
28 approximately 10 to 2,000 cm². The sources were characterized in counts per minute to allow
29 comparison to the background level in counts per minute. The background radiation was
30 determined for the GM detector in this geometry by scanning a nearby section of cardboard that
31 contained no hidden sources.

32 Six surveyors performed scans; their scanning experience ranged from no experience to several
33 years of performing scanning surveys. Each was given a brief description of the GM detector and
34 procedure for scanning and documenting results on the scale drawing. They were instructed to
35 scan the surface at a slow rate (one detector width per second). Surveyors were oriented to the
36 audible response to background radiation by performing a scan survey on an adjacent section of
37 cardboard that contained no hidden sources. Once the surveyors indicated that they were ready

¹ This approach for calculating the number of opportunities for which one or more responses would be expected to occur was suggested by Dr. David Stock.

Human Performance and Scanning Sensitivity

1 to initiate the scan, headsets were donned and the survey commenced. The surface scan was
2 typically completed in 45 to 60 minutes.

3 **Results**

4 Correct detection rate is plotted as a function of false positive rate (calculated on the basis of the
5 assumptions described above) for each surveyor in Figure 6.9. Results for pauses (data points
6 near the top center of the plot) are considered first. As expected, surveyors adopted a liberal
7 criterion during continuous scanning; i.e., they paused often. Most surveyors paused over eight
8 of the nine sources. The rate of pausing over non-source areas varied considerably among
9 surveyors, ranging from roughly 0.30 to 0.60. Results for the final decision are represented by the
10 points near the y-axis. A more stringent criterion was employed when the probe was held
11 stationary; most false positive rates were less than 0.10. Surveyors typically did not mark as hot
12 spots (locations identified as exceeding background) all of the sources they paused over; i.e., the
13 points representing the final decision tended to be lower on the true positive axis. Most surveyors
14 identified five or six of the nine source configurations. In other words, performance for the
15 stationary sample was less than perfect.

16 The sources that were correctly detected most often (five of six surveyors) were the two sources
17 with the largest areas, and a small source located at the upper left of the surface to be scanned. It
18 is not surprising that sources covering larger areas were more readily detected, since the extended
19 geometry (increased detection efficiency) provides the equivalent of a longer observation interval.
20 As for the smaller source, it might be that the surveyors were more vigilant at the start of the scan
21 (at the upper left) than they were later in the exercise. Repeated scans using sources of uniform
22 intensity (perhaps in simulation) would be required to formally test for the presence of a vigilance
23 decrement.

24 **6.5.3 Indoor Scan Using Gas Proportional Detector**

25 **Procedure**

26 As in the experiment using the GM detector, the section of wall to be surveyed measured 1.5
27 meters high and 5 meters wide, resulting in a test area of 7.5 m². The same analysis described
28 above for the GM scan was applied to the results obtained using the gas proportional detector.
29 Although additional radionuclide sources (in a different arrangement) were used for the gas
30 proportional scan experiment, the total source configuration area and the area of a typical source
31 did not change significantly. Thus, the same number of opportunities for a false positive response
32 was assumed.

33 **Results**

34 Correct detection rate is plotted as a function of false positive rate for each surveyor in
35 Figure 6.10. Results for pauses (data points near the top center of the plot) are considered first.
36 Most surveyors paused over all (or nearly all) of the sources. The rate of pausing over non-
37 source areas ranged from roughly 0.20 to 0.50. Results for the final decision are represented by
38 the points near the y-axis. Again, surveyors typically did not mark all of the sources they paused
39 over as locations exceeding background; i.e., the points representing the final decision tended to

1 be lower on the true positive axis. Surveyors identified from 9 to 13 of the 14 source
2 configurations.

3 **6.5.4 Outdoor Scan Using NaI Scintillation Detector**

4 **Procedure**

5 An outdoor test grid, a 20-meter by 30-meter plot of land, was gridded and various gamma-
6 emitting sources were hidden (buried) within this area. Twenty-five radioactive sources were
7 randomly located throughout the gridded area in 13 discrete configurations. The radioactive
8 sources were Co-60, Cs-137, Ra-226, and depleted uranium. The radioactive source
9 configurations were prepared to provide varying radiation levels and geometries (Figure 6.8).
10 The gross radiation levels ranged from 6 to 24 kcpm using a 3.2 cm by 3.8 cm NaI scintillation
11 detector. The background radiation level of the NaI scintillation detector was determined on a
12 parcel of land adjacent to the test grid.

13 Twelve surveyors performed scans; their scanning experience ranged from no experience to
14 several years of performing scanning surveys. They were instructed to scan the surface at a slow
15 rate (approximately 0.5 m/s). The scanning procedure consisted of swinging the detector from
16 side to side, keeping the detector just above the ground surface at its lowest point. Surveyors
17 covered 100 percent of the test area using 1-meter-wide lanes.

18 Because of the differences between the indoor and outdoor scan with respect to the area to be
19 surveyed, and the detector type and survey techniques used, a somewhat different procedure was
20 used to estimate the number of opportunities for false positives in the outdoor scan.

21 **Results**

22 Correct detection rate is plotted as a function of false positive rate for each surveyor in
23 Figure 6.11. Results for pauses (the leftmost points in the figure) show considerable variation
24 among surveyors as to the number of sources paused over. The number of the 13 sources paused
25 over ranged from 7 to 12. As might be expected, large or intense sources were
26 identified more readily than less-intense or smaller sources. The proportion of pauses over non-
27 source areas ranged from roughly 0.15 to 0.45. The variation in the final true positive rate is
28 similar to that for the pauses. With just two exceptions, surveyors correctly identified every
29 source that they had paused over. Furthermore, the final decision typically resulted in no false
30 positives. Thus, performance for the final detection stage was essentially perfect. This indicates
31 that sources were well above the just-detectable level for most if not all of the surveyors and that
32 success depended on the criterion adopted for the first (scanning) component (i.e., the likelihood
33 of pausing) and the quality of the input to that process.

34 **6.5.5 General Discussion**

35 The surveyor-related factors identified earlier as potential influences on the minimum detectable
36 concentration will now be briefly reconsidered in light of the results of the ideal observer analysis
37 and the field experiments. The analysis of the ideal observer demonstrated that the time for which
38 the activity is sampled determines the information that is available to the surveyor. Thus, if the

Human Performance and Scanning Sensitivity

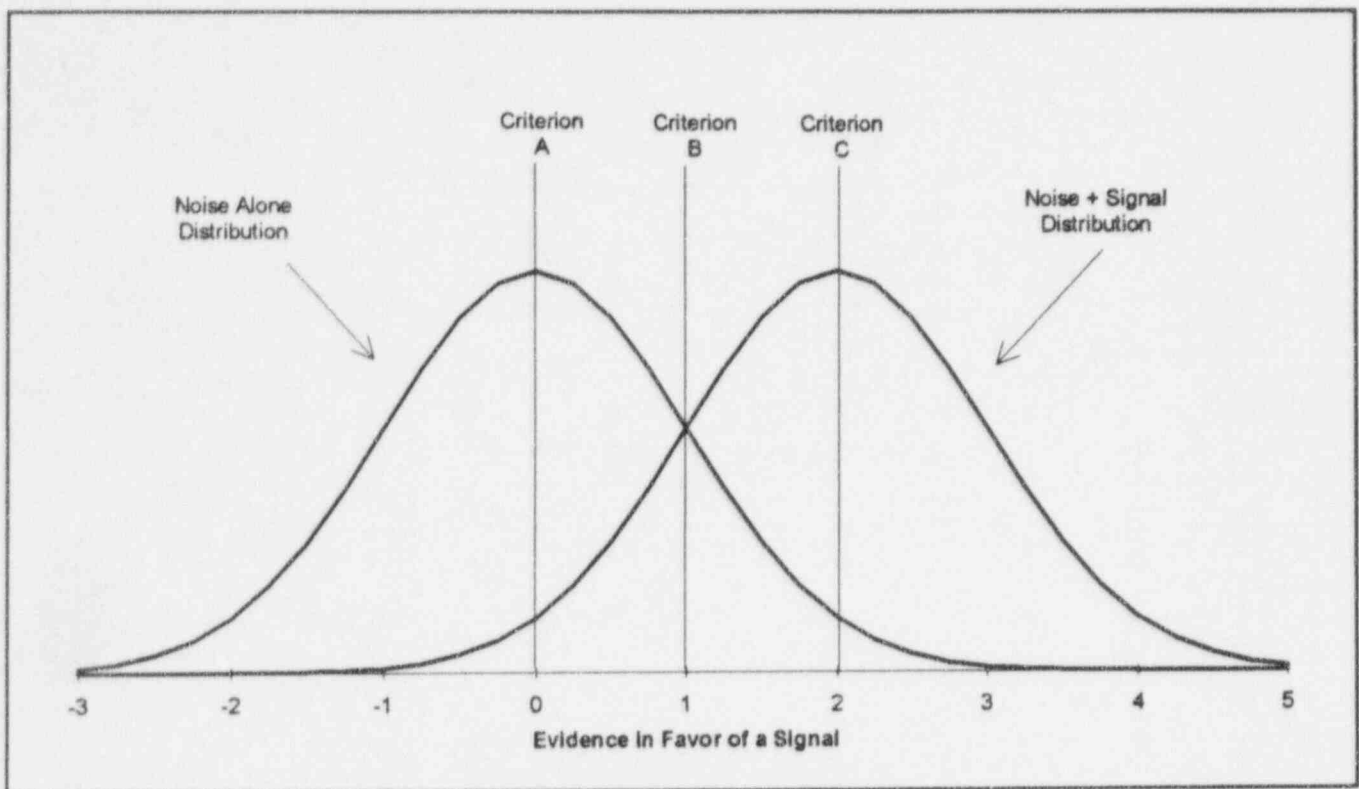
1 probe is moved too quickly, the distributions of radiation on which the surveyor's decision is
2 based will not be sufficiently distinct to support acceptable performance. This effect may have
3 been the reason for some relatively intense sources going undetected in the outdoor survey. The
4 detector response is directly related to the time that the detector "sees" the source, and is a
5 function of the source-to-detector geometry and the scan rate. The longer that the detector
6 "sees" the source, the greater the chances that the surveyor will pause to investigate the response.
7 Although the movement of the probes was not directly measured in any of the field tests,
8 differences in technique among surveyors were noted by the observers and probably account for
9 apparent differences in sensitivity.

10 Similarly, the failure of surveyors to correctly identify sources at locations they had paused over
11 (especially the results of the GM scan survey) may have been due to the probe being held
12 stationary for too short a time to support a sufficiently high correct detection rate given the strict
13 criterion for a final positive response.

14 The importance of the surveyor's criterion for pausing the probe is evident from the analysis of the
15 ideal observer. The operating point for the first (continuous) component establishes the upper
16 bound for correct detection rate and the criterion should, therefore, be quite liberal. The field
17 tests confirmed that surveyors do in fact adopt liberal criteria (i.e., they pause often), but the data
18 indicated that there is much variation among surveyors in this regard. This is important since
19 correct detections vary greatly with changes in this criterion, especially for difficult-to-detect
20 sources (e.g., the indoor GM survey). It would be of interest to determine the degree to which
21 surveyor's criteria in continuous scanning are affected by the assumed likelihood of a source being
22 present, or the frequency of sources being found as a survey progresses. If the criterion becomes
23 more stringent when sources are assumed or found to be unlikely (as signal detection theory
24 predicts it should), the number of weak sources missed may become unacceptably large.

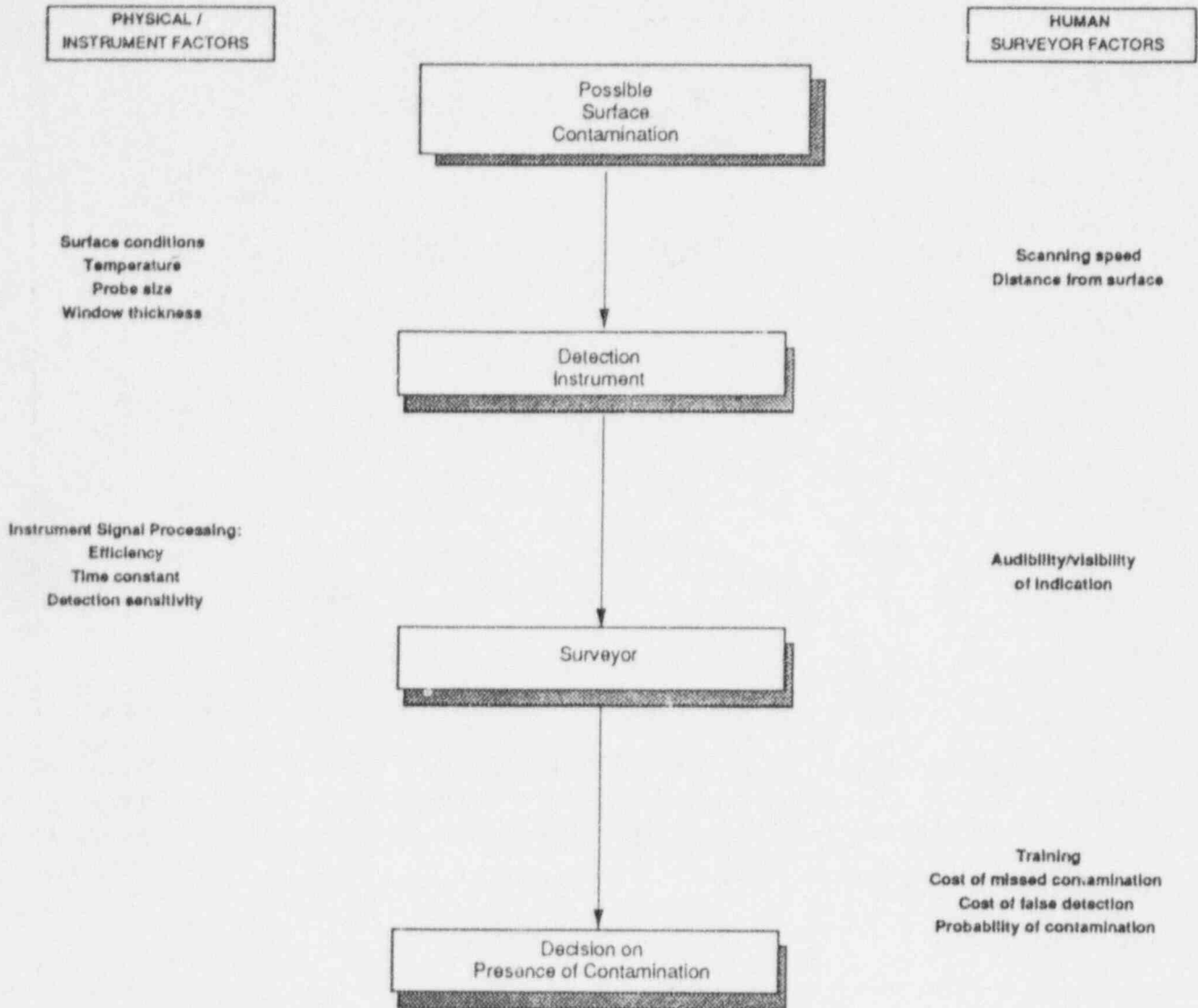
25 Equally important in determining the minimum detectable concentration is the surveyor's criterion
26 for identifying areas as contaminated. Here, too, there was considerable variation among
27 surveyors in the field tests—even between surveyors with roughly equal sensitivity. The extent to
28 which surveyor's performance in this case is subject to the influences described above is also
29 unknown.

30 As a whole, the results of the experiments show that sensitivity can vary considerably among
31 surveyors. The results also demonstrate that the surveyor's choice for a positive response is
32 equally important in determining success in identifying sources. This applies both to the decision
33 to momentarily stop moving the probe and to the final decision regarding the presence of
34 contamination. Although a surveyor's training, experience, and scanning technique may afford
35 adequate sensitivity to detect a given source level, detection performance may not be optimal
36 unless *both* of these decisions are based on appropriate criteria that do not vary significantly over
37 the course of the survey.



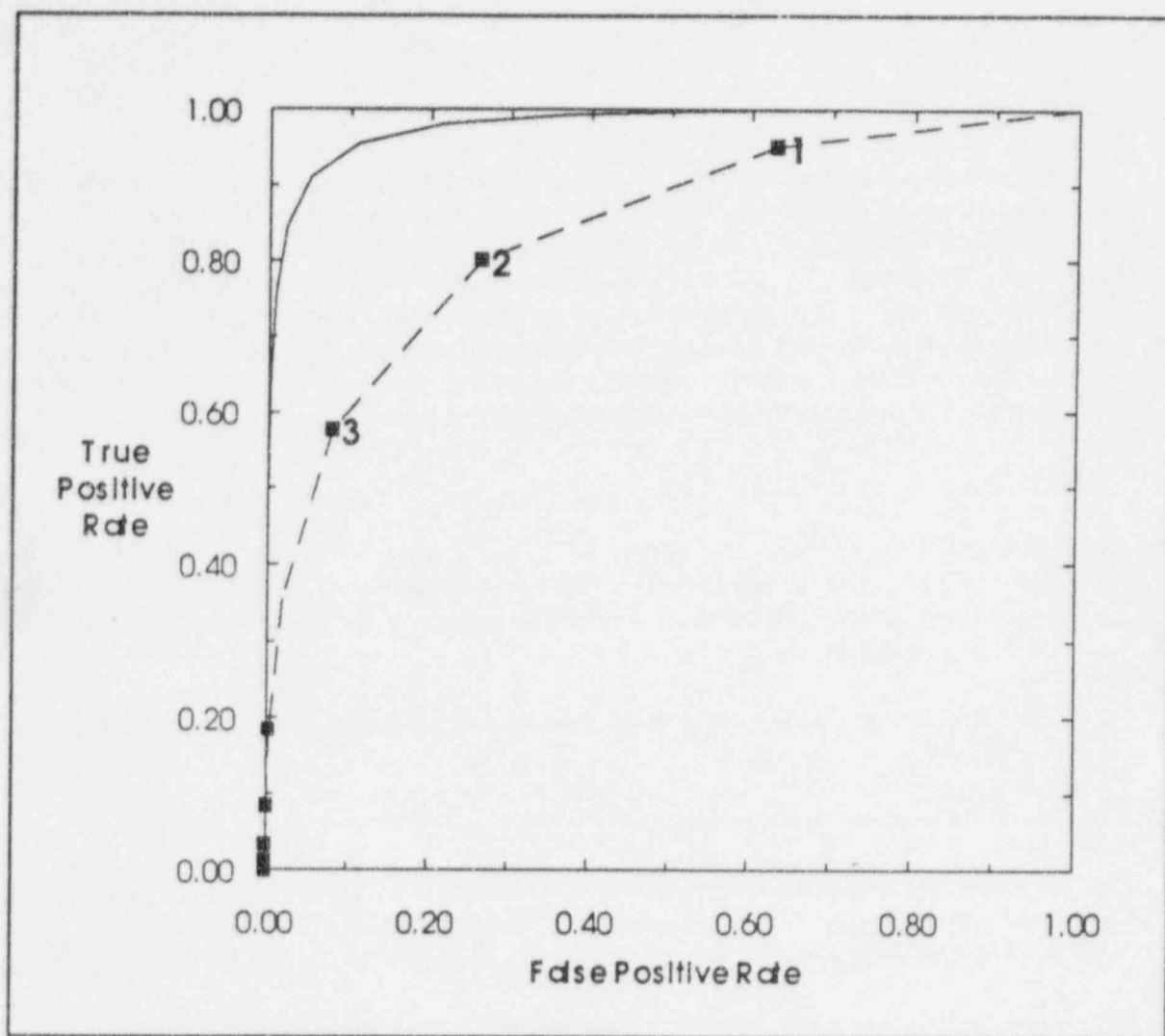
1 **Figure 6.1 A Signal Detection Theory View of the Detection of Signals in Noise.** The false positive
 2 rate and true positive rate are assumed to be estimates of the proportions of the noise alone
 3 and noise-plus-signal functions, respectively, lying to the right of the criterion employed by
 4 the observer.

Human Performance and Scanning Sensitivity



1

Figure 6.2 Scan Survey as a Series of Stages



1 Figure 6.3 Relative Operating Characteristic (ROC) for Poisson Observer Detecting
2 180 cpm in a 60-cpm Background

Human Performance and Scanning Sensitivity

Field Determination of Scanning Sensitivity Survey Instructions

Introduction

Sections of the cardboard are covering radioactive sources that were fastened to the back-side of the cardboard in contact with the wall. Sixteen radioactive sources were randomly positioned on the cardboard in nine discrete configurations. The radioactive sources included C-14, Co-60, Sr-90, Tc-99, Cs-137, and uranium. The radioactive source configurations were prepared to provide varying radiation levels and geometries. The radioactive sources were purposely chosen to emit levels of radiation that are barely discernible above background. Your task is to identify the locations of the areas of direct radiation and record count rate (in cpm) on the provided survey map. You will need a pen and a clipboard to record the results of your survey. Expect to spend 45 to 60 minutes on this exercise.

Specific Tasks

1. Prior to initiating the scan survey, determine the background radiation level of the GM detector the section of cardboard on the wall denoted "Background Check". At this time it is also necessary to compare the cardboard wall with the provided survey map, to ensure that you will record the results on the proper locations on the map.
2. Record the background value of your survey map. Observers will also be recording the results of your scan survey.
3. Put on the headphones and get adjusted to the background counting rate again.
4. Scan the cardboard at a rate of approximately 1 detector width per second (about 5 cm per second with the GM detector), 1 grid section at a time. Instructors will be available to ensure you are scanning at the desired rate. You should keep the detector in contact with the surface during the scan.
5. Listen carefully for an increased click rate above the background count rate.
6. When you think that you have identified an area of elevated direct radiation or "hit", stop and immediately mark that point on your map. Once you have stopped for a few seconds you must make a further determination whether (1) the location was not above background and you continue scanning, or (2) if the count rate is determined to be above background, you record count rate on map and proceed with scan. It is very important that you record these "stops", even if you can immediately determine that the location was really just a variation of background clicks.
7. Use the following notation when recording the results:

Record actual cpm on map for hits.

Figure 6.4 Instructions Provided to Field Survey Test Participants for Indoor GM Scans

**Field Determination of NaI Scanning Sensitivity
Survey Instructions**

Introduction

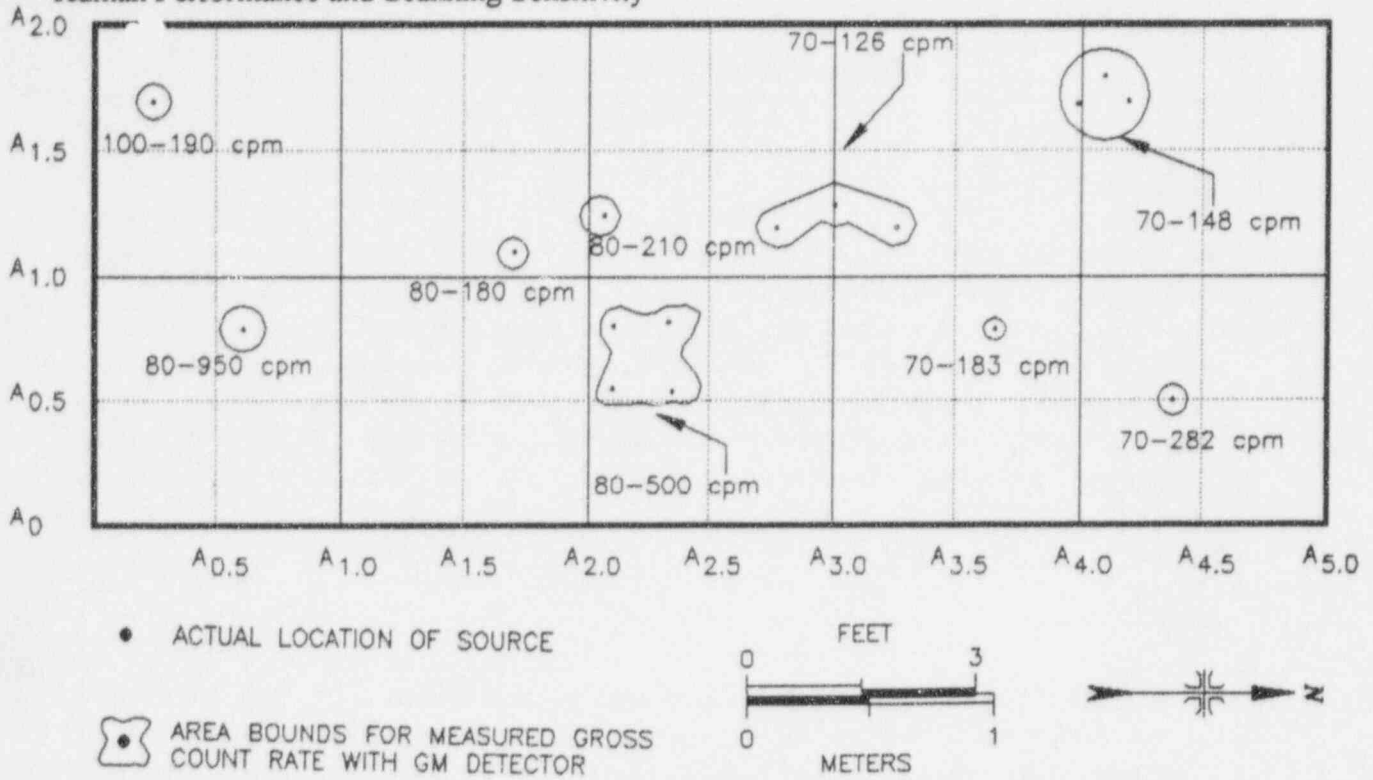
An outdoor test grid, 20 m x 30 m plot of land, was gridded and various gamma-emitting sources were hidden (buried) within this area. Twenty-five radioactive sources were randomly located throughout the gridded area in 13 discrete configurations. The radioactive sources included Co-60, Cs-137, Ra-226, and depleted uranium. The radioactive source configurations were prepared to provide varying radiation levels and geometries. The radioactive sources were purposely chosen to emit levels of gamma radiation that are barely discernible above background. Your task is to identify the locations of the areas of direct radiation and record count rate (in cpm) on the provided survey map. You will need a pen and a clipboard to record the results of your survey. Expect to spend 60 minutes on this exercise.

Specific Tasks

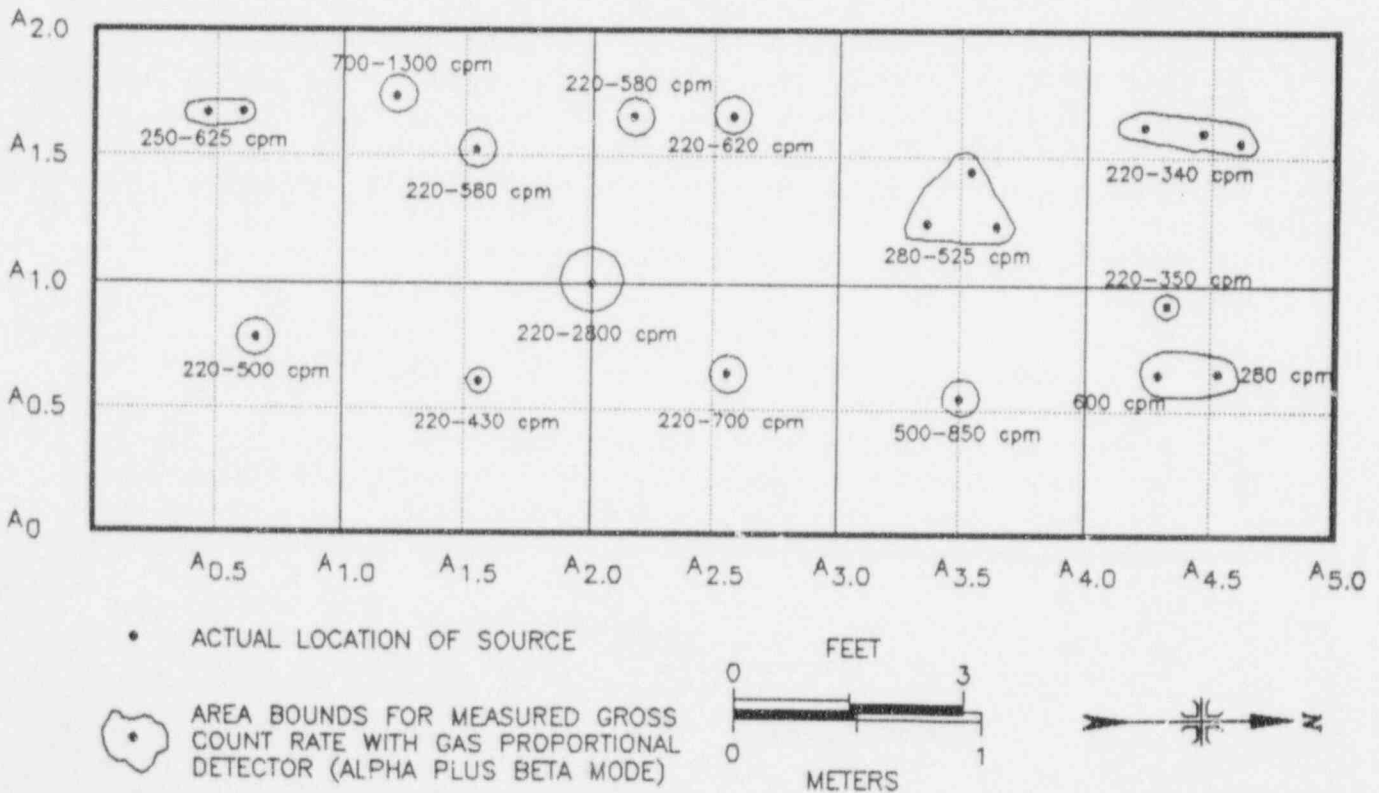
1. Prior to initiating the scan survey, determine the background radiation level of the NaI scintillation on a parcel of land adjacent to the test grid. At this time it is also necessary to compare the outdoor test grid with the provided survey map, to ensure that you will record the results on the proper locations on the map.
2. Record the background range of the NaI scintillation detector on your survey map.
3. Put on the headphones and get adjusted to the background counting rate again.
4. Scan the test grid at a rate of approximately 0.5 meters per second, 1 grid block section (100 m²) at a time. An acceptable scanning procedure consists of swinging the detector from side-to-side, keeping the detector just above the ground surface at its lowest point. Instructors will be available to ensure you are scanning at the desired rate.
5. Listen carefully for an increased click rate above the background count rate.
6. When you think that you have identified an area of elevated direct radiation or "hit", stop and immediately mark that point on your map. Once you have stopped for a few seconds you must make a further determination whether (1) the location was not above background and you continue scanning, or (2) if the count rate is determined to be above background, you record count rate on map and proceed with scan. The observer (instructor) will record these "stops", even if you can immediately determine that the location was really just a variation of background clicks.
7. Use the following notation when recording the results:
Record actual cpm on map for hits.

Figure 6.5 Instructions Provided to Field Survey Test Participants for Outdoor NaI Scans

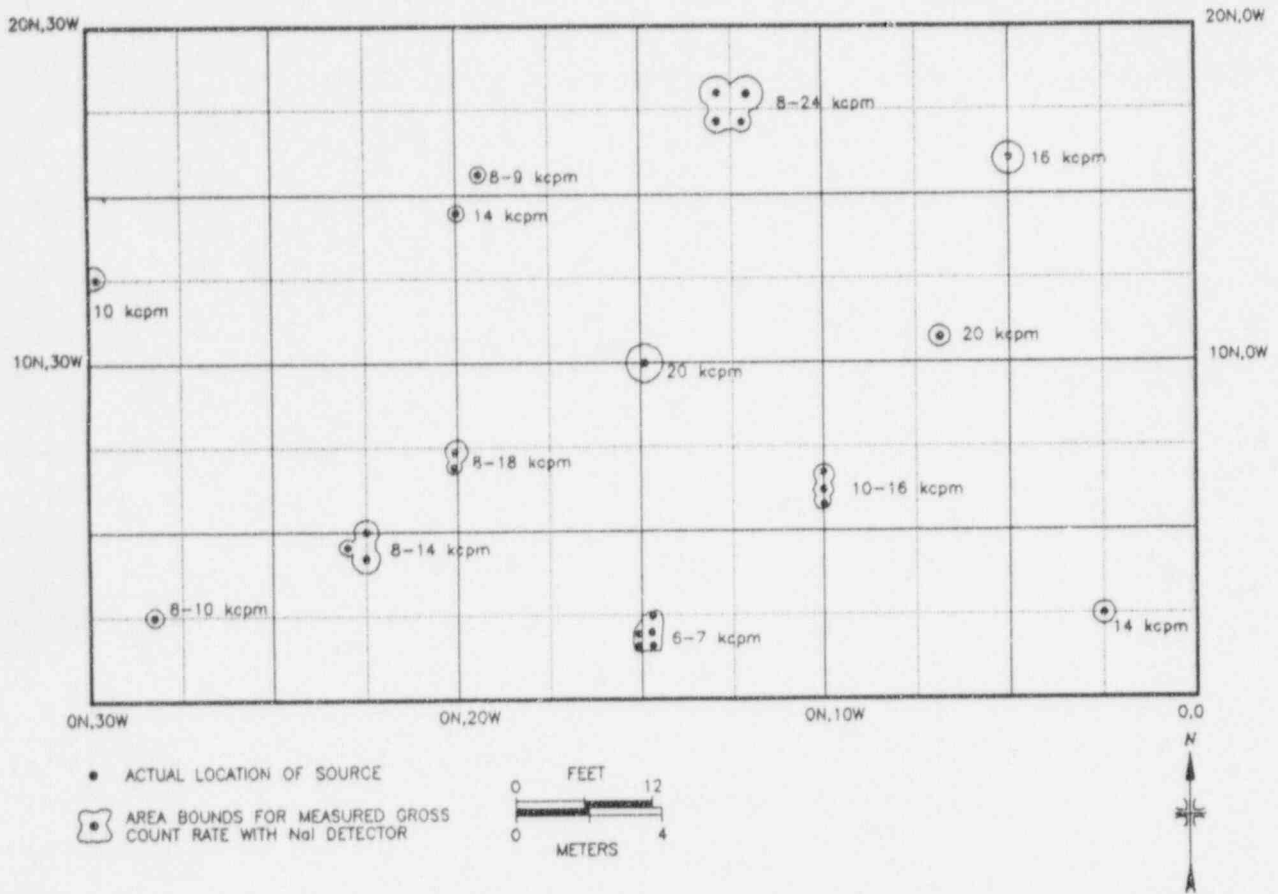
Human Performance and Scanning Sensitivity



1 **Figure 6.6 Scale Map of the Wall Showing Location, Extent, and Radiation Levels of**
2 **Hidden Sources for GM Scans**



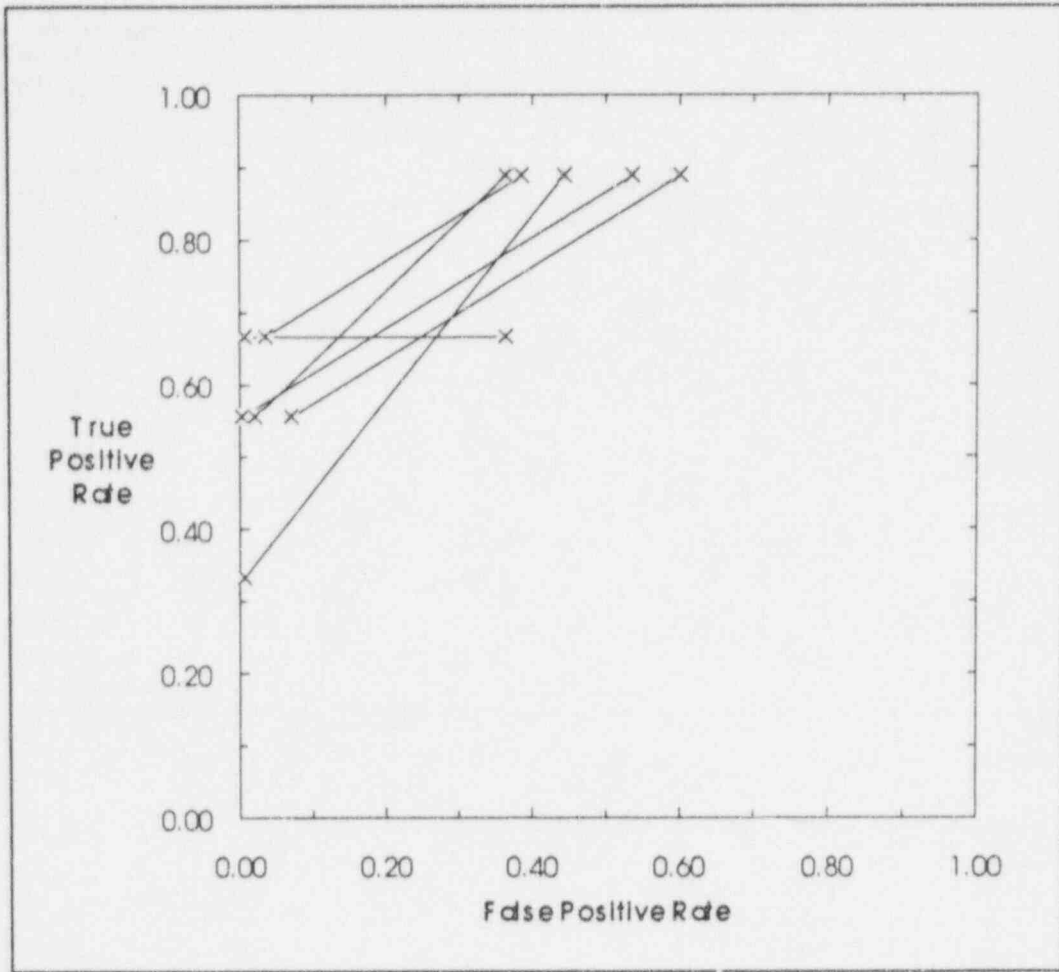
3 **Figure 6.7 Scale Map of the Wall Showing Location, Extent, and Radiation Levels of**
4 **Hidden Sources for Gas Proportional Scans**



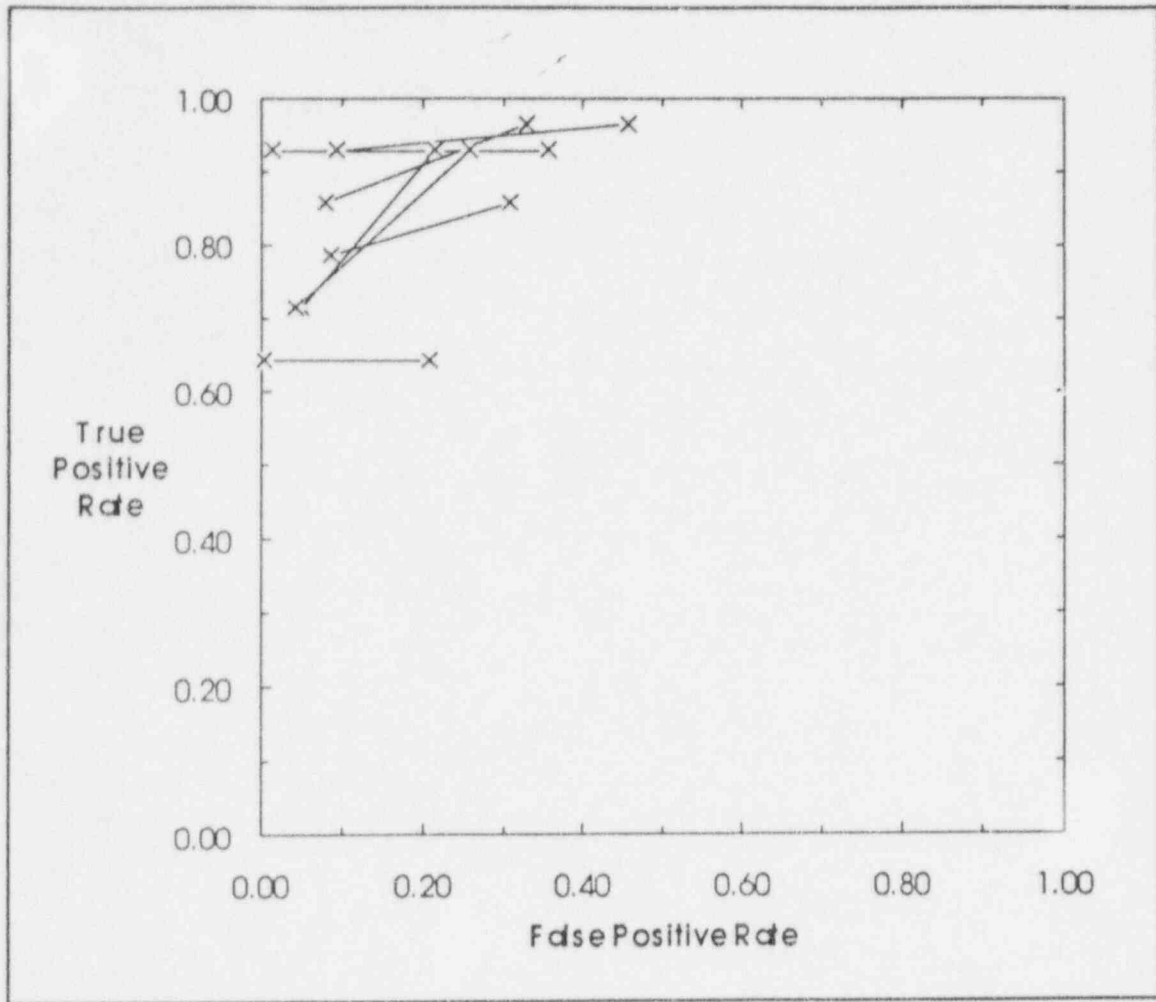
1
2

Figure 6.8 Scale Map of the Outdoor Scan Test Area Showing Location, Extent, and Radiation Levels of Hidden Sources for NaI Scans

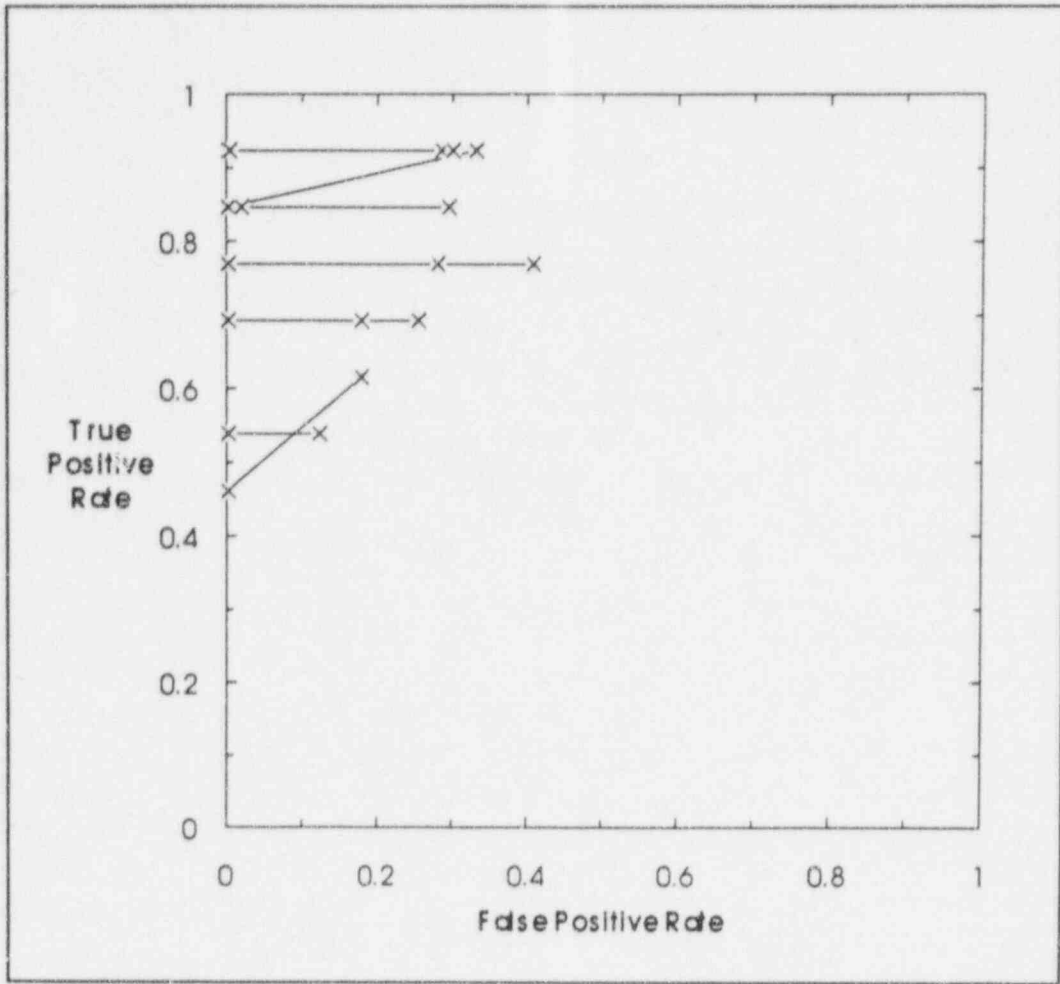
Human Performance and Scanning Sensitivity



1 **Figure 6.9 Surveyor Performance in Indoor Scan Survey Using GM Detector** (Lines connect
2 points representing the same surveyor. See text for details.)



1 **Figure 6.10 Surveyor Performance in Indoor Scan Survey Using Gas Proportional**
 2 **Detector** (Lines connect points representing the same surveyor. See text for
 3 details.)



1 **Figure 6.11** Surveyor Performance in Outdoor Scan Survey Using NaI Scintillation
2 **Detector** (Lines connect points representing the same surveyor. See text for
3 details.)

7 *IN SITU* GAMMA SPECTROMETRY AND EXPOSURE RATE MEASUREMENTS

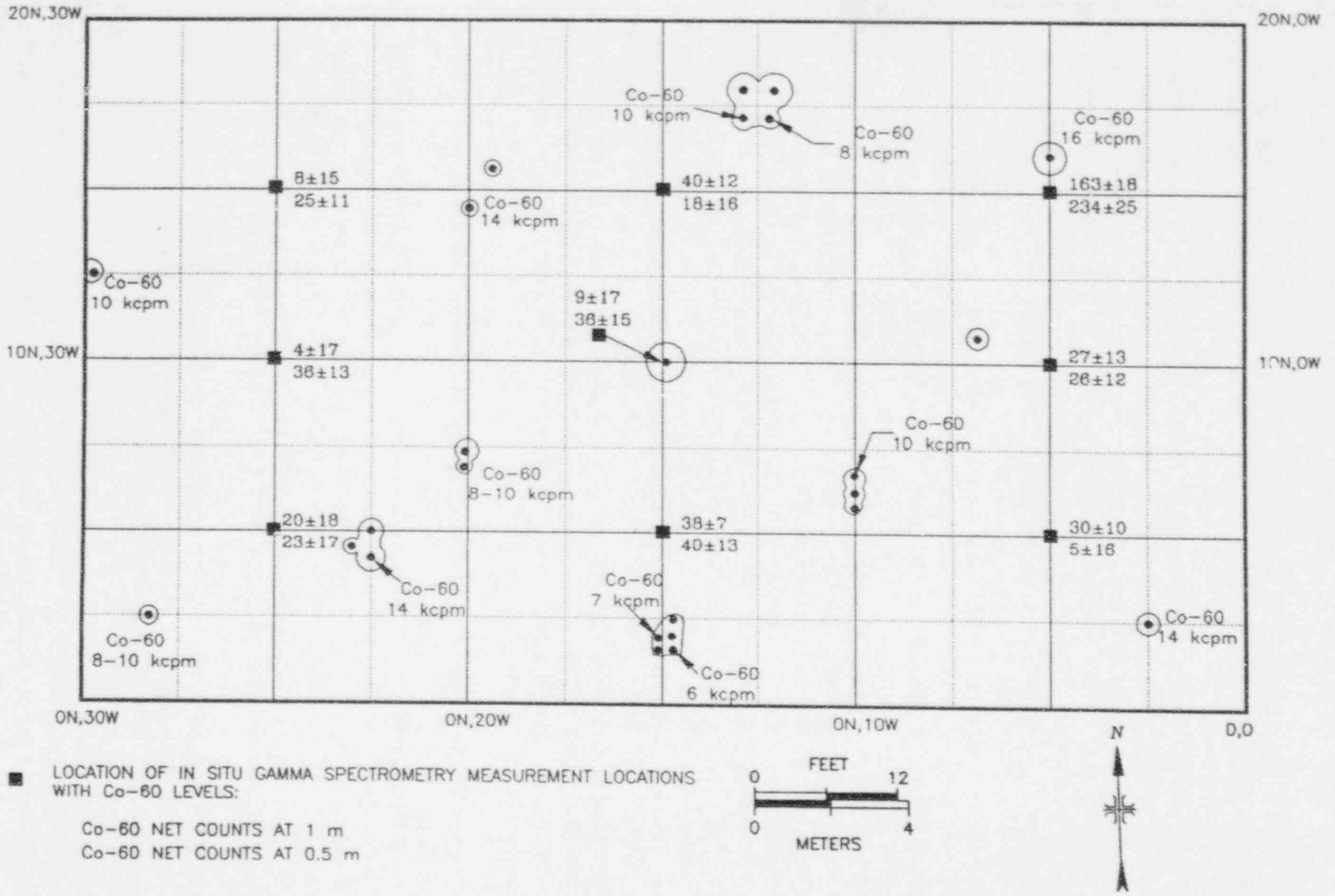
The use of spectrometric techniques to assess radioactivity may produce a significant increase in sensitivity as compared to radiation measurements that rely on gross instrument counts. Spectrometry allows a specific radionuclide to be measured, relying on characteristic energies of the radionuclide of concern to discriminate from all sources present. *In situ* gamma spectrometry refers to the assessment of the ambient gamma ray flux that is collected in the field (i.e., *in situ*), and analyzed to identify and quantify the radionuclides present.

The Environmental Measurement Laboratory (EML) at the U.S. Department of Energy has performed detailed and quantitative evaluations of portable gamma spectrometry systems. The reader is referred to "Measurement Methods for Radiological Surveys in Support of New Decommissioning Criteria (Draft Report for Comment)" (NUREG-1506) for detailed guidance on how to employ *in situ* gamma spectrometry during survey activities. That report gives examples of minimum detectable concentrations using a typical 25-percent relative efficiency p-type germanium detector and a 10-minute count time at typical background radiation levels. Using these assumptions, the minimum detectable concentrations (MDCs) for Co-60, Cs-137, Eu-152, Ra-226 (based on measurement of progeny) and Ac-228 (to infer Th-232) are all approximately 0.05 pCi/g. It is necessary to use a more efficient detector, such as a 75-percent relative efficiency n-type germanium detector, to measure the radionuclides that are more difficult to detect. For example, using the 75-percent relative efficiency n-type germanium detector for a 10-minute count time, results in an MDC of 0.5 pCi/g for Am-241, and 2 pCi/g for U-238 (based on measurement of short-lived Th-234 progeny) and Ra-226 (based on measurement of the 186-keV gamma energy line). These typical MDCs scale as the square root of the count time; that is, quadrupling the count time results in a factor of two increase in the sensitivity of the *in situ* measurement.

7.1 *In Situ* Gamma Spectrometry Measurements in Outdoor Test Area

In situ gamma spectrometry measurements were performed within the outdoor test area (this same area was also used to evaluate the scan sensitivity of surveyors) to determine the spectrometer's ability to identify and locate the sources. It should be understood that this particular exercise was intended to evaluate the scanning capabilities of the *in situ* gamma spectrometer, not its ability to determine radionuclide concentrations in soil, which requires detailed detector calibration and modeling of the contaminant distribution in the soil.

As stated in Section 6, 25 gamma-emitting sources were buried in the test area, including 12 Co-60 sources and 5 Cs-137 sources. Measurements were made at nine grid locations in the test area, at both 0.5 meter and 1 meter above the ground (Figure 7.1). A background measurement at 1 meter above the ground was performed in an adjacent area unaffected by the test area sources. ESSAP used a 13-percent relative efficiency p-type germanium detector and a 30-minute count time at each measurement location. The net counts collected in both the Co-60 and Cs-137 peak regions were determined and are given in Table 7.1. The Co-60 data were



In Situ Gamma Spectrometry Measurements in Outdoor Test Area

Figure 7.1 Co-60 In Situ Gamma Spectrometry Results in Outdoor Test Area

1 **Table 7.1 In Situ Gamma Spectrometry Data From Outdoor Test Area**

Measurement Location ^a		Net Count in Peak Region	
		Cs-137 (662 keV)	Co-60 (1332 keV)
Background	1 m ^b	-4 ± 8	6 ± 14
5N, 5W	1 m	-18 ± 10	30 ± 10
5N, 5W	0.5 m	-4 ± 8	5 ± 16
10N, 5W	1 m	5 ± 7	27 ± 13
10N, 5W	0.5 m	15 ± 7	26 ± 12
15N, 5W	1 m	11 ± 8	163 ± 18
15N, 5W	0.5 m	-2 ± 7	234 ± 25
5N, 15W	1 m	-1 ± 8	38 ± 7
5N, 15W	0.5 m	4 ± 8	40 ± 13
10N, 15W	1 m	7 ± 9	9 ± 17
10N, 15W	0.5 m	8 ± 9	36 ± 15
15N, 15W	1 m	7 ± 8	40 ± 12
15N, 15W	0.5 m	-11 ± 9	18 ± 16
5N, 25W	1 m	7 ± 8	20 ± 18
5N, 25W	0.5 m	19 ± 9	23 ± 17
10N, 25W	1 m	3 ± 8	4 ± 17
10N, 25W	0.5 m	17 ± 8	36 ± 13
15N, 25W	1 m	-6 ± 8	8 ± 15
15N, 25W	0.5 m	10 ± 8	25 ± 11

23 ^aRefer to Figure 7.1.
 24 ^bDistance refers to detector height above the surface.

In Situ Gamma Spectrometry Measurements in Outdoor Test Area

1 presented in Figure 7.1 to allow a visual correlation between the detector response and the Co-60
2 source location. Cs-137 data were not evaluated in this manner because in only a few locations
3 did levels of Cs-137 exceed background.

4 The results indicated that the portable gamma spectrometry system was able to identify the
5 presence of Cs-137 and Co-60 contamination in the test area. This elementary finding warrants
6 additional thought and should not be dismissed without consideration as to its implications on the
7 use of *in situ* gamma spectrometry as a scanning tool. Recognizing that *in situ* gamma
8 spectrometry is able to detect relatively low levels of gamma-emitting radionuclides is of
9 particular value when the detector is used to verify the absence of contamination in an area. That
10 is, if the detector's MDC can be demonstrated to be sufficiently below the contamination
11 guidelines, then *in situ* gamma spectrometry measurements may be used to demonstrate that
12 further survey efforts in an area are not warranted. Furthermore, using *in situ* gamma
13 spectrometry to determine that residual radioactivity is below a specified concentration has an
14 additional benefit in the improved documentation of the scan survey. Records of *in situ* gamma
15 spectrometry measurements are generally more objective and less likely to be influenced by human
16 factors than the conventional scan survey records obtained with NaI scintillation detectors or
17 other portable field instrumentation, which require subjective interpretation of the detector
18 response by the surveyor.

19 For the present experimentation, the *in situ* gamma spectrometer did identify the presence of
20 Co-60 and Cs-137 contamination and, therefore, the data should be analyzed in an effort to locate
21 the contamination. Figure 7.1 shows the net counts in the Co-60 peak region at both 1 meter and
22 0.5 meter above the surface at each grid coordinate (top number is 1-meter value, bottom number
23 is 0.5 m value). In the case of uniform contamination and a detector height of 1 meter,
24 approximately 80 percent of the detector's response would be from a 5-meter radius (NUREG-
25 1506). Because detector height above the surface affects the amount of ground being viewed,
26 moving the detector closer to the ground results in a smaller section of the ground being viewed.

27 The greatest quantity of Co-60 activity was identified at grid location 15N,5W. The fact that the
28 net counts for Co-60 increased as the detector was moved closer to the ground indicates that the
29 source is relatively close to the sampled grid coordinate. Also, because the Co-60 result at
30 coordinate 10N,5W has significantly less Co-60 activity than at 15N,5W, it is likely that the
31 source is not south of grid coordinate 15N,5W.

32 The Co-60 results for grid coordinates 5N,5W and 15N,10W (both have 1-meter readings greater
33 than 0.5-meter readings) indicate that Co-60 contamination is nearby, but not necessarily in the
34 immediate vicinity of the sampled grid coordinate. Although this analysis does not direct the
35 surveyor to the exact location of the contamination, it does provide for a focused plan for
36 subsequent NaI scintillation scan surveys.

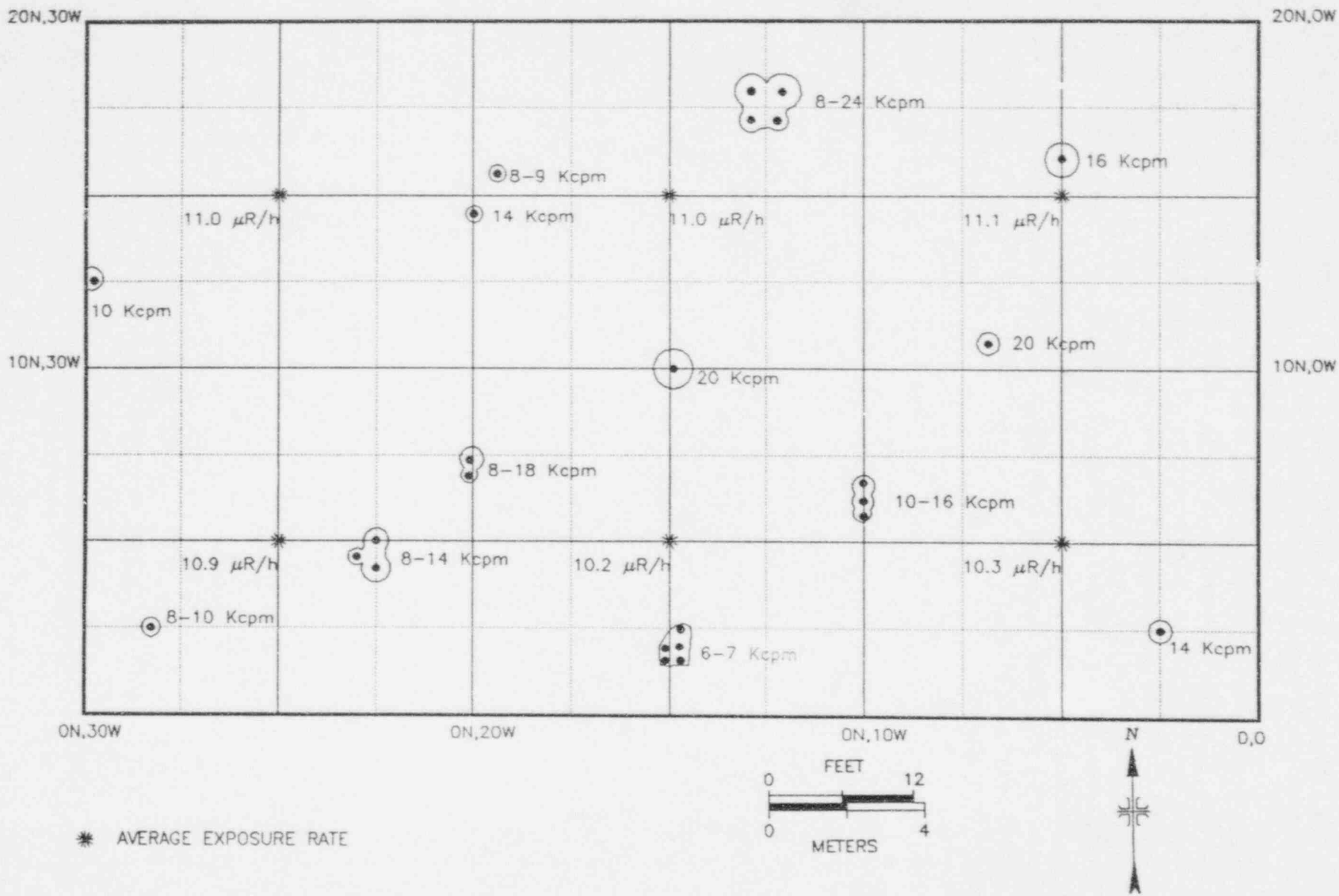
7.2 Exposure Rate Measurements in Outdoor Test Area

38 Exposure rate measurements using a pressurized ionization chamber (PIC) were performed within
39 the outdoor test area to evaluate the PIC's sensitivity in measuring exposure rate. Measurements
40 were performed at six grid coordinate locations, each reading at 1 meter above the surface

In Situ Gamma Spectrometry Measurements in Outdoor Test Area

1 (Figure 7.2). The background exposure rate ($10.3 \mu\text{R/h}$) was determined in an area adjacent to
2 the test area, but unaffected by the test area sources.

3 The sensitivity of the PIC is directly proportional to the standard deviation of the background
4 exposure rate. Therefore, areas exhibiting only minor background exposure rate variations will
5 have the lowest minimum detectable exposure rates. The exposure rate measurements in the test
6 area ranged from 10.2 to $11.1 \mu\text{R/h}$ (Table 7.2). Figure 7.2 illustrates the correlation between the
7 exposure rate measurements and the source locations. The larger exposure rates correspond to
8 the larger gamma radiation levels that were obtained during characterization of the test area (refer
9 to grid locations 15N,15W and 15N,5W). These results indicate that the PIC response was
10 affected by the gamma-emitting sources. The minimum detectable exposure rate obtained with
11 the PIC can be expected to be approximately $1 \mu\text{R/h}$ above background levels, depending on the
12 background variability.



* AVERAGE EXPOSURE RATE

Figure 7.2 Exposure Rate Measurements in the Outdoor Test Area

1 **Table 7.2 Exposure Rate Measurements From Outdoor Test Area**

2	Measurement Location ^a	Exposure Rate ^b (μR/h)
3	Background	10.3
4	5N, 5W	10.8
5	5N, 15W	10.2
6	5N, 25W	10.9
7	15N, 5W	11.1
8	15N, 15W	11.0
9	15N, 25W	11.0

10 ^aRefer to Figure 7.2.

11 ^bMeasurements made at 1 meter above the surface.

8 LABORATORY INSTRUMENTATION DETECTION LIMITS

Frequently, during surveys in support of decommissioning, it is not feasible, or even possible, to detect the contaminants with portable field instrumentation; thus arises the need for laboratory analysis of media samples. This is especially the case for such media samples as soil, that result in significant self-absorption of the radiation from the contamination. Another common situation that necessitates the use of laboratory analyses occurs when the contaminants are difficult to detect even under ideal conditions. This includes contamination that emits only low-energy beta radiation (e.g., H-3 and Ni-63) or x-ray radiation (e.g., Fe-55).

Laboratory analyses for radionuclide identification, using spectrometric techniques, are often performed during scoping or characterization surveys. Here the principal objective is to simply determine the specific radionuclides in the contamination, without necessarily having to assess the quantity of contamination. Once the radioactive contaminants have been identified, sufficiently sensitive field survey instrumentation and techniques are selected to demonstrate compliance with the residual radioactivity guidelines.

8.1 Review of Analytical Minimum Detectable Concentrations

In 1993, M. H. Chew and Associates prepared a database which contains a listing of minimum detectable concentrations (MDCs) for various radionuclides, sample sizes, count times, instrument efficiencies, and background count rates. This information was compiled by surveying several government and commercial laboratories which provided their "best estimates" in response to the survey. The instrumentation used, instrument efficiencies, and sample geometries varied among laboratories, and, for the same laboratory, varied from one radionuclide to the other. These variations are given as ranges. In short, the report constitutes a survey, not a controlled study.

The listing prepared by Chew and Associates is helpful in identifying approximate MDCs to be expected for detection of specific radionuclides. However, on the basis of that information, it is not possible to make accurate predictions as to how the MDC will be affected quantitatively if sample density, sample background activity, the mixture of radionuclides, or chemical composition of soil samples are altered. These can be very significant factors in determining the MDC. For example, in some geographic locations, there may be increased concentrations of aluminum in the soil. These interfere with the nitric acid leaching procedure in radiochemical analysis for thorium or uranium; increased levels of calcium or potassium interfere with radiochemical analysis for Sr-90; increased levels of iron interferes with several radiochemical analysis procedures. Other field conditions may affect the detectability of contaminants. The effects of these conditions were quantitatively evaluated for various types of radionuclides.

8.2 Background Activities for Various Soil Types

Radionuclide concentrations in background soil samples vary for numerous reasons, such as the soil type and density, geology, geographic location, radioactive fallout patterns, and many other

Laboratory Instrumentation Detection Limits

1 reasons. NUREG-1501 provides an in-depth study of the factors that are responsible for
2 variations in the background radioactivity in soil.

3 During the course of performing environmental assessments of background radioactivity
4 throughout the United States, Environmental Survey and Site Assessment Program (ESSAP)
5 investigators at the Oak Ridge Institute for Science and Education (ORISE) stated that
6 background radionuclide concentrations vary both on a regional basis (e.g., western U.S.,
7 southeastern U.S., coastal areas) and within a particular region. Table 8.1 gives typical U-238,
8 Th-232, and Cs-137 concentrations found in background soil samples in the United States. These
9 data were compiled from historical databases on background soil concentrations and are intended
10 to give information on the variations that exist both among and within various regions. For many
11 locations, the soil samples represent different soil types, such as silty loam, sandy loam, and clay.
12 The radionuclide analyses performed on these samples used both alpha and gamma spectrometry.

13 **Table 8.1 Typical Radionuclide Concentrations Found in Background Soil Samples in**
14 **the United States**

Location	Radionuclide Concentration (pCi/g)		
	U-238	Th-232	Cs-137
Boston, Massachusetts	0.7 to 1.3	<0.2 to 1.5	--*
Cambridge, Massachusetts	0.4 to 1.2	NA	0.1 to 0.7
Cincinnati, Ohio	<0.4 to 2.5	0.3 to 1.5	0.2 to 1.5
Jacksonville, Florida	0.4 to 1.0	0.5 to 1.0	<0.1 to 0.5
Kingsport, Tennessee	<0.5 to 2.2	0.8 to 1.8	NA
Platteville, Colorado	0.9 to 2.1	1.5 to 2.2	<0.1 to 0.2
San Diego, California	1.0 to 1.6	0.7 to 1.6	<0.1 to 0.4

23 *Radionuclide measurement not performed.

24 The fallout radioactivity, Cs-137, was determined to have the greatest variability within a
25 particular region, as compared to the terrestrial radionuclides from the uranium and thorium decay
26 series. The large variation in fallout radioactivity may be due to the specific soil sample locations.
27 Wooded areas tend to exhibit higher concentrations of fallout radioactivity than open field areas,
28 possibly due to the increased foliar interception in forested areas.

29 **8.3 Effects of Soil Condition on MDC**

30 The density and chemical composition of the soil can affect the detection sensitivity of survey
31 instruments. Soil density and composition can also affect the MDC of laboratory instrumentation
32 and procedures. For example, higher densities may result in an underestimation of gamma
33 activity, particularly for low-energy gamma emitters.

1 Within each category of soil, detection sensitivity of the instruments may be affected by variations
2 in (a) moisture content, (b) soil density, and (c) presence of high-Z (atomic number) materials in
3 the sample. As part of this study, the effects of soil density and composition, moisture content,
4 and presence of high-Z material on the gamma spectrometry analysis was evaluated. It was
5 necessary to prepare soil standards for this evaluation.

6 Each germanium detector was calibrated for each counting geometry using a NIST-traceable
7 standard (typically mixed gamma-emitting activity in liquid form). Vendors that supplied the
8 standards can demonstrate traceability to the National Institute of Standards and Technology
9 (NIST).

10 The ESSAP counting room presently prepares two standards for the 0.5-liter Marinelli soil
11 geometry. One standard is prepared from top soil and weighs between 700 and 800 g. This
12 standard was used to quantify soil samples that weigh in the range of 450 to 850 g. The second
13 Marinelli standard was prepared using sand; it weighs approximately 1000 g. This standard was
14 used to quantify soil samples that weigh between 850 and 1,150 g.

15 For the smaller aluminum-can geometries (approximately 120-g capacity), a comparison of the
16 counting efficiencies obtained from both the top soil and sand standards resulted in the counting
17 efficiencies being equal within the statistical limits. For this reason, only one counting efficiency
18 curve was used for the aluminum-can geometry.

19 The soil calibration standard, consisting of Am-241, Ce-139, Cs-137, and Co-60, was prepared by
20 weighing a known quantity of the liquid standard and adding this quantity to either the top soil or
21 sand matrix. To ensure that the soil standard has been adequately mixed, equal aliquots (soil
22 fractions) were placed in the aluminum-can geometry and analyzed with the germanium detector.
23 The radionuclide concentration of each soil fraction was determined. The radionuclide
24 concentrations of the soil fractions were evaluated to determine if they were statistically equal
25 and, thus, to conclude that the soil standard was homogeneous. Once homogeneity was
26 demonstrated, the standard was used to calibrate the germanium detectors for the various soil
27 counting geometries.

28 **8.3.1 Effects of Soil Moisture on MDC**

29 The moisture content of the soil can vary significantly, depending on geographic location, time
30 after rainfall, etc., and can have significant impact on detection of radionuclides with beta and
31 low-energy gamma emissions. Therefore, a relatively wide range of moisture content was
32 examined in this study.

33 Water content can be measured accurately in the laboratory and can be changed by homogenizing
34 known quantities of water in the soil. A calibrated counting geometry with a known weight was
35 obtained. The initial weight was 112.9 g. At first, 5.9-percent moisture was added to the initial
36 weight. This amount of water was not great enough to evenly disburse throughout the soil. To
37 evenly disburse the water, 95-percent ETOH was used. A visual check was used to determine if
38 the soil was saturated. The soil was allowed to air dry to the desired weight of 119 g. Among the

1 problems discovered while working with smaller moisture contents were soil loss by airflow
2 because of the small particle size and not being able to return all of the soil into the container after
3 the water was added. These soil loss problems were controlled by increasing the amount of water
4 added and then allowing the soil to dry to the next desired weight. At this point, 20-percent
5 moisture was added for a test weight of 125.6 g. Due to the increased volume of water added,
6 8.7 g of dry soil could not be returned to the container. The moisture added was sufficient to
7 saturate the soil thoroughly. After the addition of water, the soil was allowed to absorb the
8 moisture for approximately 1 hour. The next percent moisture was obtained by simply allowing
9 the soil to air dry. The next moisture percentage to be tested was 15 percent at a weight of
10 118.3 g. The 10.5-percent moisture was obtained in the same manner as above for a test weight
11 of 112.25 g. At this point, it was necessary to increase the moisture content. A moisture content
12 of 35.5 percent was obtained for a total weight of 152.70 g. This amount was then allowed to air
13 dry to 31-percent moisture for a total weight of 145.03 g. At this moisture content, the soil
14 started to exhibit inabilities to absorb all the water added. Finally, water was added to the point
15 of total saturation. The maximum amount of water that could be added to the container geometry
16 was 38.5 percent, for a final weight of 162.7 g.

17 Because the addition of water to the soil standard diluted the radionuclide concentration, it was
18 necessary to account for the dilution factor. This was done by increasing the measured
19 concentration by a degree equal to the weight percent of the water added to the standard. This
20 concentration corrected for dilution was compared to the measured concentration (Table 8.2).
21 The results indicate that lower concentrations obtained from the increasing moisture content are
22 largely due to the dilution effect. That is, the radionuclide concentration in soil is lower as a result
23 of the contaminated soil being replaced by water.

24 **8.3.2 Effects of Soil Density on MDC**

25 As stated previously, soil density can affect the MDC of laboratory instrumentation and
26 procedures. Higher density samples, relative to the calibration soil standard, can result in an
27 underestimation of gamma activity, particularly for low-energy gamma emitters.

28 The gamma efficiency for a particular geometry is decreased as the soil density is increased.
29 Figure 8.1 illustrates this effect for three soil calibration geometries with densities of 1.1, 1.54,
30 and 2.02 g/ml. The greatest gamma efficiency deviation in the three samples occurs at the low-
31 energy range.

32 **8.3.3 Effects of High-Z Materials on MDC**

33 Gamma spectrometry analyses to determine the radionuclide concentration in soil samples
34 commonly involves the use of a calibration standard traceable to NIST. The calibration standards
35 used for the analysis of soils should consist of a material similar in composition to that of soil,
36 e.g., a silica-based material. Efficiencies at each gamma energy are then established for each
37 radionuclide energy that is present in the calibration standard. An efficiency vs. energy curve is
38 generated from each of the individual efficiency data points. This efficiency curve is then used to

Table 8.2 Effects of Moisture Content on Gamma Spectrometry Analyses

% Moisture ^a	Radionuclide Concentration (pCi/g)											
	Am-241			Ce-139			Cs-137			Co-60		
	Meas ^b	Corr ^c	%Diff ^d	Meas ^b	Corr ^c	%Diff ^d	Meas ^b	Corr ^c	%Diff ^d	Meas ^b	Corr ^c	%Diff ^d
Dry	125.1	---	---	17.7	---	---	117.3	---	---	133.4	---	---
5%	108.4	115.2	7.92	15.5	16.4	7.39	102.3	108.7	7.32	116.1	123.4	7.51
10%	108.5	121.2	3.09	14.8	16.6	6.53	102.1	114.1	2.75	114.3	127.7	4.27
15%	103.2	121.6	2.83	14.5	17.1	3.59	96.5	113.7	3.07	110.2	129.8	2.70
20%	95.8	119.8	4.25	13.2	16.6	6.71	89.6	112.0	4.51	98.8	123.5	7.42
31%	83.1	120.5	3.68	11.2	16.2	8.75	83.6	121.1	-3.28	93.5	135.6	-1.62
35%	79.5	123.3	1.46	10.7	16.6	6.66	79.4	123.1	-4.93	90.4	140.1	-5.05
38%	73.5	119.5	4.47	9.2	15.0	15.64	69.7	113.3	3.42	79.5	129.3	3.07

^aMoisture content calculated by the following:

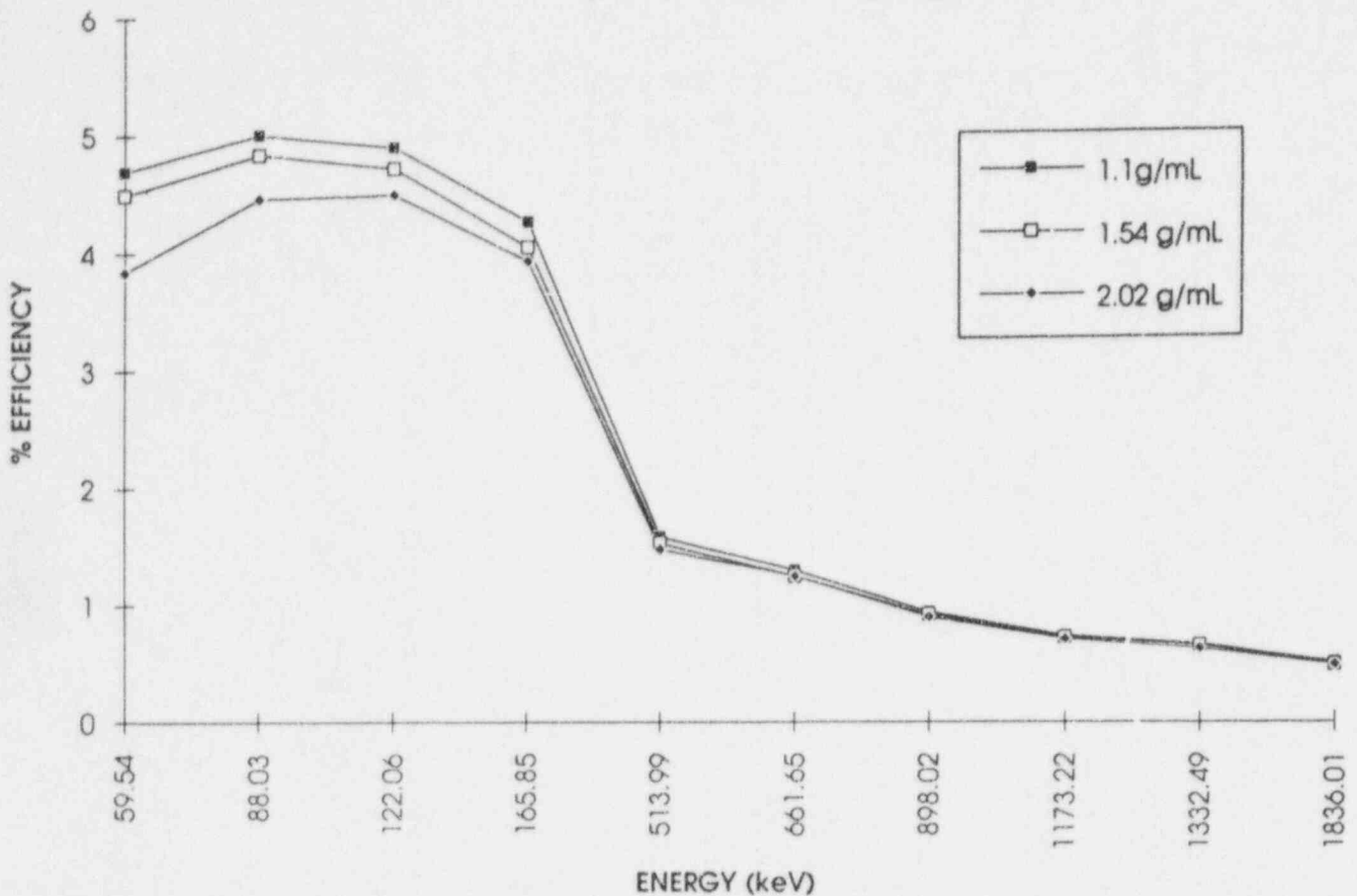
$$\text{Moisture Content} = \frac{\text{Wet Weight} - \text{DryWeight}}{\text{Wet Weight}}$$

^bMeasured radionuclide concentration.

^cRadionuclide concentration corrected for dilution by dividing the measured concentration by one minus the moisture content.

^dPercent difference between the measured and calculated concentrations.

Laboratory Instrumentation Detection Limits



1 **Figure 8.1 Efficiency vs. Energy for Various Densities**

2 assess the radionuclide concentrations in media that may be considered similar in composition to
3 that of soil.

4 A potential deviation from the calibrated geometry described above occurs when a sample
5 contains a measurable quantity of high-Z material, such as metals. The presence of high-Z
6 materials produces attenuation of the gamma radiation (especially the low-energy gamma
7 emissions) in the sample that may not be accounted for in the calibration standard. If no
8 correction is made to account for the absorption of the gamma radiation, use of the standard
9 efficiency curve will underestimate the true radionuclide concentration in the sample. The
10 magnitude of these effects was evaluated by mixing in measurable quantities of metal fines and
11 powder. Specifically, the metals studied were iron, lead, and zirconium, which were mixed in the
12 calibration standards at 1, 5, and 10 weight percents. Table 8.3 presents the results of this
13 experiment. Because the addition of material (i.e., high-Z material) to the soil standard dilutes
14 radionuclide concentration, it is necessary to account for the dilution factor. This was done by
15 increasing the measured concentration by a degree equal to the weight percent of material added
16 to the standard. For example, the measured radionuclide concentration for the sample containing
17 5-percent lead was increased proportionately. The results indicate that in general, the high-Z
18 material effects are most pronounced at the lower gamma energies. Furthermore, the zirconium
19 produces the most significant attenuation losses, followed by lead and then iron.

Table 8.3 Effects of High-Z Content on Gamma Spectrometry Analyses

High-Z Material (%)	Radionuclide Concentration (pCi/g)											
	Am-241			Ce-139			Cs-137			Co-60		
	Meas ^a	Corr ^b	%Diff ^c	Meas ^a	Corr ^b	%Diff ^c	Meas ^a	Corr ^b	%Diff ^c	Meas ^a	Corr ^b	%Diff ^c
Lead												
No Z Material	109.8	---	---	14.6	---	---	112.8	---	---	115.8	---	---
1	108.2	109.3	0.45	13.8	14.0	4.0	109.4	110.5	2.0	111.2	112.3	3.0
5	92.9	97.8	10.9	12.6	13.2	9.2	105.9	111.5	1.2	110.0	115.8	0.01
10	79.7	88.9	19.0	11.3	12.6	13.9	101.5	113.2	-0.4	104.6	116.7	-0.8
Iron												
No Z Material	111.3	---	---	13.6	---	---	108.0	---	---	113.4	---	---
1	113.1	114.2	-2.6	13.5	13.6	-0.4	107.6	108.7	-0.6	110.3	111.4	1.8
5	97.0	102.1	8.3	13.0	13.7	-0.8	102.4	107.8	0.2	106.9	112.5	0.8
10	98.4	109.5	1.6	13.5	15.0	-10.4	102.7	114.4	-5.9	104.6	116.5	-2.7
Zirconium												
No Z Material	121.0	---	---	14.7	---	---	113.4	---	---	115.2	---	---
1	98.8	99.8	17.5	14.3	14.4	1.5	110.2	111.3	1.8	112.2	113.3	0.05
5	80.9	85.2	29.6	13.7	14.4	1.6	109.1	114.8	-1.3	107.7	113.4	0.03
10	62.7	69.6	42.5	12.3	13.7	6.5	100.4	111.6	1.6	100.2	111.3	1.8

^aMeasured radionuclide concentration.

^bRadionuclide concentration corrected for dilution by dividing the measured concentration by one minus the high Z material content.

^cPercent difference between the measured (no Z material) and calculated concentrations.

9 REFERENCES

- 1 2 Altshuler, B., and B. Pasternak. "Statistical Measures of the Lower Limit of Detection of a
3 Radioactivity Counter," *Health Physics* 34(9):293-298. 1963.
- 4 ANSI N13.30. "Performance Criteria for Radiobioassay (Draft)." New York: American National
5 Standards Institute, Inc. 1989.
- 6 ANSI 13.12. "Control of Radioactive Surface Contamination on Materials, Equipment, and
7 Facilities To Be Released for Uncontrolled Use (Draft)." New York: American National
8 Standards Institute, Inc. December 1985.
- 9 Brodsky, A. "Exact Calculation of Probabilities of False Positives and False Negatives for Low
10 Background Counting," *Health Physics* 63(2):198-204. August 1992.
- 11 Brodsky, A. "Standardizing Minimum Detectable Amount Formulations," *Health Physics* 64(4):
12 434-435. April 1993.
- 13 Brodsky, A., and R.G. Gallagher. "Statistical Considerations in Practical Contamination
14 Monitoring," *Radiation Protection Management* 8(4):64-78. July/August 1991.
- 15 Brown, W.S., and D.S. Emmerich. "Auditory Detection of an Increment in the Rate of a Random
16 Process," *Journal of the Acoustical Society of America* 95(5) Part 2:2941. 1994.
- 17 Bruns, L.E. "Capability of Field Instrumentation To Measure Radionuclide Limits," *Nuclear
18 Technology* 58:154-169. August 1982.
- 19 Chambless, D.A., et al. "Detection Limit Concepts: Foundations, Myths, and Utilization," *Health
20 Physics* 63(3):338-340. 1992.
- 21 Chew and Associates, Inc. "Summary of Current Capabilities With Regards to Detection of
22 Radioactivity: A Survey of Commercial Radiochemistry Laboratories and Instrument Suppliers
23 (Interim Report)." August 1993.
- 24 Currie, L.A. "Limits for Qualitative Detection and Quantitative Determination," *Analytical
25 Chemistry* 40(3):586-593. 1968.
- 26 DOE/EP-0100. "A Guide for Radiological Characterization and Measurements for
27 Decommissioning of U.S. Department of Energy Surplus Facilities." Washington, D.C.:
28 Department of Energy. August 1983.
- 29 Egan, J.P. *Signal Detection Theory and ROC Analysis*. New York: Academic Press. 1975.

References

- 1 Egan, J.P., G.Z. Greenberg, and A.I. Schulman. "Operating Characteristics, Signal Detectability,
2 and the Method of Free Response," *Journal of the Acoustical Society of America* 33, 993-1007.
3 1961.
- 4 Goles, R.W., B.L. Baumann, and M.L. Johnson. "Contamination Survey Instrument Capabilities"
5 (PNL-SA-1984, Letter to the U.S. Department of Energy). 1991.
- 6 Green, D.M., and J.A. Swets. *Signal Detection Theory and Psychophysics*. Los Altos, Cal.:
7 Peninsula Publishing. 1988.
- 8 Green, S., R.H. Miller, and R.A. Nelson. "Development and Use of Statistical Survey Criteria for
9 Release of Materials at a Former Uranium Processing Facility," *Health Physics* 61(6):903-911.
10 December 1991.
- 11 HPSR-1/EPA 520/1-80-012. "Upgrading Environmental Radiation Data," Washington, D.C.:
12 Health Physics Society Committee/Environmental Protection Agency. August 1980.
- 13 ISO 7503-1. "Evaluation of Surface Contamination - Part 1: Beta Emitters and Alpha Emitters
14 (first edition)." International Organization for Standardization. 1988.
- 15 ISO 8769. "Reference Sources for the Calibration of Surface Contamination Monitors."
16 International Organization for Standardization. 1988.
- 17 LA-10729. "Alpha RADIAC Evaluation Project." Los Alamos, N.M.: Los Alamos National
18 Laboratory. June 1986.
- 19 Macmillan, N.A., and C.D. Creelman. *Detection Theory: A User's Guide*. Cambridge, England:
20 Cambridge University Press. 1991.
- 21 Maushart, R. "Contamination Monitoring in the Federal Republic of Germany." *Radiation*
22 *Protection Management* 3(2):49-57. January 1986.
- 23 NCRP 50 "Environmental Radiation Measurements." Bethesda, Md.: National Council on
24 Radiation Protection and Measurements. December 27, 1976.
- 25 NCRP 58. "A Handbook of Radioactivity Measurements Procedures." Bethesda, Md.: National
26 Council on Radiation Protection and Measurements. February 1, 1985.
- 27 NCRP 112. "Calibration of Survey Instruments Used in Radiation Protection for the Assessment
28 of Ionizing Radiation Fields and Radioactive Surface Contamination." Bethesda, Md.: National
29 Council on Radiation Protection and Measurements. December 31, 1991.
- 30 NUREG-1500. "Working Draft Regulatory Guide on Release Criteria for Decommissioning:
31 NRC Staff's Draft for Comment." Washington D.C.: Nuclear Regulatory Commission. August
32 1994.

- 1 NUREG-1501. "Background as a Residual Radioactivity Criterion for Decommissioning" (Draft
2 Report for Comment). Washington, D.C.: Nuclear Regulatory Commission. August 1994.
- 3 NUREG-1506. "Measurement Methods for Radiological Surveys in Support of New
4 Decommissioning Criteria" (Draft Report for Comment). Washington, D.C.: Nuclear Regulatory
5 Commission. August 1995.
- 6 NUREG/CR-4007. "Lower Limit of Detection: Definition and Elaboration of a Proposed
7 Position for Radiological Effluent and Environmental Measurements." Washington, D.C.:
8 Nuclear Regulatory Commission. 1984.
- 9 NUREG/CR-5849. "Manual for Conducting Radiological Surveys in Support of License
10 Termination" (Draft 2). Washington, D.C.: Nuclear Regulatory Commission. May 1992.
- 11 NUREG/CR-6062. "Performance of Portable Radiation Survey Instruments." Washington, D.C.:
12 Nuclear Regulatory Commission. December 1993.
- 13 Robbins, H.E. "Estimating the Total Probability of the Unobserved Outcomes of an Experiment,"
14 *Annals of Mathematical Statistics* 39: 256-257. 1968.
- 15 Sommers, J.F. "Sensitivity of G-M and Ion Chamber Beta-Gamma Survey Instruments." *Health*
16 *Physics* 28(6):755-761. June 1975.
- 17 Strom, D.J., and P.S. Stansbury. "Minimum Detectable Activity When Background Is Counted
18 Longer Than the Sample," *Health Physics* 63(3):360-1. September 1992.
- 19 Swinth, K.L., and J.L. Kenoyer. "Evaluation of Draft ANSI Standard N42.17 by Testing."
20 Richland, Wash.: Pacific Northwest Laboratory. July 1984.
- 21 Walker, E. "Proper Selection and Application of Portable Survey Instruments for Unrestricted
22 Release Surveys." Bechtel Environmental, Inc. Presented at 1994 International Symposium on
23 D&D. April 24-29, 1994.
- 24 Watson, C.S., and T.L. Nichols. "Detectability of Auditory Signals Presented Without Defined
25 Observation Intervals, *Journal of the Acoustical Society of America* 59:655-668. 1976.

B
-
P
1

BIBLIOGRAPHIC DATA SHEET

(See instructions on the reverse)

1. REPORT NUMBER
(Assigned by NRC. Add Vol., Supp., Rev.,
and Addendum Numbers, if any.)

NUREG-1507

2. TITLE AND SUBTITLE

Minimum Detectable Concentrations with Typical Radiation Survey
Instruments for Various Contaminants and Field Conditions:
Draft Report for Comment

3. DATE REPORT PUBLISHED

MONTH YEAR

August 1995

4. FIN OR GRANT NUMBER

5. AUTHOR(S)

A.M. Huffert, E.W. Abelquist*, W.S. Brown**
* Environmental Survey and Site Assessment Program
Oak Ridge Institute for Science and Education
**Human Factors and Performance Group
Brookhaven National Lab.

6. TYPE OF REPORT

Draft

7. PERIOD COVERED (Inclusive Dates)

8. PERFORMING ORGANIZATION - NAME AND ADDRESS (If NRC, provide Division, Office or Region, U.S. Nuclear Regulatory Commission, and mailing address; if contractor, provide name and mailing address.)

Division of Regulatory Applications
Office of Nuclear Regulatory Research
U.S. Nuclear Regulatory Commission
Washington, D.C. 20555-0001

9. SPONSORING ORGANIZATION - NAME AND ADDRESS (If NRC, type "Same as above"; if contractor, provide NRC Division, Office or Region, U.S. Nuclear Regulatory Commission, and mailing address.)

Same as above

10. SUPPLEMENTARY NOTES

11. ABSTRACT (200 words or less) This report describes and quantitatively evaluates the effects of various factors on the detection sensitivity of commercially available portable field instruments being used to conduct radiological surveys in support of decommissioning. NRC is currently involved in a rulemaking effort to establish residual contamination criteria for release of facilities for restricted or unrestricted use. In support of that rulemaking, NRC has prepared a draft Generic Environmental Impact Statement (GEIS), consistent with the National Environmental Policy Act. The effects of this new rulemaking on the overall cost of decommissioning are among the many factors considered in the GEIS. The overall cost includes the costs of decontamination, waste disposal, and radiological surveys to demonstrate compliance with the applicable guidelines. An important factor affecting the costs of such surveys is the minimum detectable concentrations (MDCs) of field survey instruments in relation to the residual contamination guidelines. The purpose of this study was two-fold. First, the data were used to determine the validity of the theoretical MDCs used in the draft GEIS. Second, the results of the study, published herein, provide guidance to licensees for (a) selection and proper use of portable survey instruments and (b) understanding the field conditions and the extent to which the capabilities of those instruments can be limited. Such instruments as gas proportional, Geiger-Mueller, zinc sulfide, and sodium iodide detectors were evaluated.

12. KEY WORDS/DESCRIPTORS (List words or phrases that will assist researchers in locating the report.)

Decommissioning
Enhanced Participatory Rulemaking
Instrumentation
Survey Design

13. AVAILABILITY STATEMENT

Unlimited

14. SECURITY CLASSIFICATION

(This Page)

Unclassified

(This Report)

Unclassified

15. NUMBER OF PAGES

16. PRICE



Federal Recycling Program

FIRST CLASS MAIL
POSTAGE AND FEES PAID
USNRC
PERMIT NO. G-67

REGULATORY COMMISSION
WASHINGTON, D.C. 20555-0001

OFFICIAL BUSINESS
PENALTY FOR PRIVATE USE, \$300